



**SELF-ASSEMBLY BASED ON THE 2-UREIDO-4(1H)-PYRIMIDINONE
MOTIF: FROM CYCLIC ARRAYS TO MOLECULAR CAPSULES FOR
FULLERENE SEPARATIONS**
Elisa Huerta Martínez

Dipòsit Legal: T.289-2012

ADVERTIMENT. L'accés als continguts d'aquesta tesi doctoral i la seva utilització ha de respectar els drets de la persona autora. Pot ser utilitzada per a consulta o estudi personal, així com en activitats o materials d'investigació i docència en els termes establerts a l'art. 32 del Text Refós de la Llei de Propietat Intel·lectual (RDL 1/1996). Per altres utilitzacions es requereix l'autorització prèvia i expressa de la persona autora. En qualsevol cas, en la utilització dels seus continguts caldrà indicar de forma clara el nom i cognoms de la persona autora i el títol de la tesi doctoral. No s'autoritza la seva reproducció o altres formes d'explotació efectuades amb finalitats de lucre ni la seva comunicació pública des d'un lloc aliè al servei TDX. Tampoc s'autoritza la presentació del seu contingut en una finestra o marc aliè a TDX (framing). Aquesta reserva de drets afecta tant als continguts de la tesi com als seus resums i índexs.

ADVERTENCIA. El acceso al contenido de esta tesis doctoral y su utilización ha de respetar los derechos de la persona autora. Puede ser utilizada para la consulta o estudio personal, así como en actividades o materiales de investigación y docencia en los términos establecidos en el art. 32 del Texto refundido de la Ley de Propiedad Intelectual (RDL 1/1996). Para otras utilizaciones se requiere la autorización previa y expresa de la persona autora. En cualquier caso, en la utilización de sus contenidos habrá que indicar de forma clara el nombre y apellidos de la persona autora y el título de la tesis doctoral. No se autoriza su reproducción u otras formas de explotación efectuadas con finalidades de lucro ni su comunicación pública desde un sitio ajeno al servicio TDX. Tampoco se autoriza la presentación de su contenido en una ventana o marco ajeno a TDX (framing). Esta reserva de derechos afecta tanto a los contenidos de la tesis como a sus resúmenes o índices.

UNIVERSITAT ROVIRA I VIRGILI
SELF-ASSEMBLY BASED ON THE 2-UREIDO-4(1H)-PYRIMIDINONE MOTIF: FROM CYCLIC ARRAYS TO MOLECULAR CAPSULES
FOR FULLERENE SEPARATIONS
Elisa Huerta Martínez
DL:T.289-2012

UNIVERSITAT ROVIRA I VIRGILI
SELF-ASSEMBLY BASED ON THE 2-UREIDO-4(1H)-PYRIMIDINONE MOTIF: FROM CYCLIC ARRAYS TO MOLECULAR CAPSULES
FOR FULLERENE SEPARATIONS
Elisa Huerta Martínez
DL:T.289-2012

Elisa Huerta Martínez

***Self-assembly Based on the 2-
Ureido-4(1H)-pyrimidinone Motif:
From Cyclic Arrays to Molecular
Capsules for Fullerene Separations***

TESIS DOCTORAL

dirigida por

Javier de Mendoza Sans

Departamento de Química Analítica y Química Orgánica



UNIVERSITAT ROVIRA I VIRGILI

Tarragona

Marzo 2010

UNIVERSITAT ROVIRA I VIRGILI
SELF-ASSEMBLY BASED ON THE 2-UREIDO-4(1H)-PYRIMIDINONE MOTIF: FROM CYCLIC ARRAYS TO MOLECULAR CAPSULES
FOR FULLERENE SEPARATIONS
Elisa Huerta Martínez
DL:T.289-2012

UNIVERSITAT ROVIRA I VIRGILI
SELF-ASSEMBLY BASED ON THE 2-UREIDO-4(1H)-PYRIMIDINONE MOTIF: FROM CYCLIC ARRAYS TO MOLECULAR CAPSULES
FOR FULLERENE SEPARATIONS
Elisa Huerta Martínez
DL:T.289-2012

A mi familia.

UNIVERSITAT ROVIRA I VIRGILI
SELF-ASSEMBLY BASED ON THE 2-UREIDO-4(1H)-PYRIMIDINONE MOTIF: FROM CYCLIC ARRAYS TO MOLECULAR CAPSULES
FOR FULLERENE SEPARATIONS
Elisa Huerta Martínez
DL:T.289-2012

*You don't have yet realized your importance.
You have only begun to discover your power.
Join me and I will complete your training.*
D. V.

Y esta es, sin lugar a dudas, la parte más sencilla y a la vez más complicada de escribir. Sobre todo, si se tiene en cuenta que será la más leída y, posiblemente, la más criticada.

Comenzaré por lo fácil: los formalismos.

El presente trabajo ha sido realizado en el Departamento de Química Orgánica de la Universidad Autónoma de Madrid y en el Instituto Catalán de Investigación Química (ICIQ), bajo la dirección del Dr. Javier de Mendoza Sans. Quisiera agradecer al ICIQ, así como al Ministerio de Educación y Ciencia la concesión de una Beca-Contrato predoctoral que me ha permitido realizar este trabajo.

A las unidades de soporte del ICIQ: Cromatografía, Análisis Térmico y Electroquímica, RMN, Masas, Espectroscopía, Fotofísica, Síntesis en Paralelo y Rayos-X, por su enorme dedicación y su esfuerzo. Gracias por vuestra ayuda, paciencia y consejos.

Javier, es poco lo que se puede agradecer en unas cuantas líneas. Gracias por darme la oportunidad de hacer la tesis en un sitio como este. Los comienzos nunca fueron fáciles y esta no ha sido una excepción. Sin embargo, con tiempo y esfuerzo, ha terminado en esta memoria que hoy tengo entre las manos. Por haberme enseñado y por dejarme aprender, mis más sinceras gracias.

Al Prof. Carles Bo y a Eva Santos por el magnífico trabajo computacional realizado y sobre todo por lo que me han enseñado sobre cálculos y por su ayuda.

Al Prof. Nazario Martín y especialmente a sus colaboradores Emilio y Helena por el trabajo tan estimulante que realizamos con los derivados de TTF y por esas discusiones interminables *via* e-mail. Creo que si los imprimiese todos ocuparían más que la tesis.

Todo este trabajo no habría sido posible sin la colaboración y el apoyo de todos los que, en uno u otro momento, pasaron por el laboratorio: Pilar, Hitos, Curra, Jose, Marieta, Eric, Enrique, Pascal, Jesús, Sandrine, Ruth, Fred, Pili, Vera, Gerald, Juli, Augustin, Berta, Caterina, Joanne, Alla, Matt, Yong-Yang, Sara Pasquale, Sara Sattin, Laura y Ondrej.

Hay dos personas, a las que quiero agradecer de manera especial el apoyo y dedicación desinteresada:

Aritz, muchas gracias por todos tus consejos, por tus "broncas" y por tu *sensatez*. Sabes que siempre he valorado mucho tu opinión.

Margot, muchas gracias por todo lo que has hecho por mi. Hace ya 8 años que nos conocemos y siempre has estado ahí. Sabes que sin tu ayuda y apoyo incondicional, es posible que yo no hubiese seguido con esto. Nunca podré agradecerte lo suficiente la confianza ciega que en mi depositaste un día. Gracias amiga. Por todo.

También quiero agradecer a Danny van Swieten el fantástico trabajo que ha hecho con la cubierta de la tesis. ¡Eres un genio!

I would like also to thank Prof. François Diederich, his assistant Irma Näf, and Prof. Carlo Thilgen for hosting me during three months at their laboratory in Zurich. As well, I would like to thank all the people of their group

who contributed to make my stage easier and really nice, especially Berta, Pablo, Lorenzo, Aga, Petra, Martina, Manuel, Laura, Paolo, Christian, Brian, Shin-ichiro and Michio.

Durante estos años he hecho grandes amigos no solo dentro del grupo, sino también fuera de él. Quiero dar las gracias a todos ellos por esos momentos vividos, especialmente a Patri y a Simo.

Papá, mamá, creo que no erais conscientes de lo que hacíais el día que decidisteis regalarme el "Cheminova-3" por Navidad. Con él hice mis primeras reacciones y tuve mi primer "accidente de laboratorio". Gracias por hacer caso de mi carta a los Reyes Magos, por fomentar mi pasión por la ciencia y por apoyarme en todo momento estos años. Os debo en lo que me he convertido. No me olvido tampoco de mis hermanos Sara, Jesús y Carlos: gracias por vuestro cariño.

Por último, quiero agradecer a Enrique el haber estado siempre ahí, desde el principio, ayudándome constantemente. Por tu contagioso entusiasmo. Por todo lo que me has enseñado de la vida. Por todo lo que hemos compartido y por todo lo que nos queda por compartir. Por tu cariño.



UNIVERSITAT ROVIRA I VIRGILI
SELF-ASSEMBLY BASED ON THE 2-UREIDO-4(1H)-PYRIMIDINONE MOTIF: FROM CYCLIC ARRAYS TO MOLECULAR CAPSULES
FOR FULLERENE SEPARATIONS
Elisa Huerta Martínez
DL:T.289-2012

TABLE OF CONTENTS

UNIVERSITAT ROVIRA I VIRGILI
SELF-ASSEMBLY BASED ON THE 2-UREIDO-4(1H)-PYRIMIDINONE MOTIF: FROM CYCLIC ARRAYS TO MOLECULAR CAPSULES
FOR FULLERENE SEPARATIONS
Elisa Huerta Martínez
DL:T.289-2012

TABLE OF CONTENTS

<i>Contents</i>	<i>Page</i>
Abbreviations and Acronyms	5
CHAPTER I: INTRODUCTION	15
I.1 SUPRAMOLECULAR CHEMISTRY	17
I.2 MULTIPLE HYDROGEN BOND ARRAYS FOR SELF-ASSEMBLY	19
I.2.1 Supramolecular Polymers	22
I.2.2 Hierarchical Self-assembled Structures	27
I.2.3 Self-Assembled Nanocapsules	32
I.3 RECEPTOR FOR FULLERENES	35
I.4 OBJETIVES OF THIS THESIS	43
CHAPTER II: 2D MOLECULAR ARCHITECTURES BASED ON THE 2-UREIDO-4(1H)-PYRIMIDINONE DIMERIC MOTIF	47
II.1 TWO DIMENSIONAL ASSEMBLIES	49
II.2 SYNTHESIS AND INSIGHTS INTO SOLUBILITY OF UPys	52
II.2.1 Synthesis of 2-aminipyrimidin-4-ones	52
II.2.2 Synthesis of 2-Ureidopyrimidiones and Solubility Studies	58
II.2.3 Fullerene Enriched Materials: A "Fullerodendridimer"	65
II.3 CYCLIC AGGREGATES	74
II.3.1 Double Ureidopyrimidinone: A Fully Preorganized Unit for Discrete Cyclic Aggregates.	74
II.3.2 A Rosette Based on an Adamantyl Spacer	90
II.3.3 A Rosette Based on a <i>m</i> -Substituted Aromatic Spacer	93
II.2 CONCLUSIONS	100

CHAPTER III: FULLERENE RECOGNITION AND SEPARATION BY ENCAPSULATION	103
III.1 GENERATION, ISOLATION AND PURIFICATION OF FULLERENES	105
III.2 DESIGN AND SYNTHESIS OF UPy-BASED RECEPTORS FOR FULLERENES	108
III.2.1 Introduction of Ethyl Spacer (S1)	110
III.2.2 Introduction of Propyl Spacer (S2)	111
III.2.3 Introduction of Aryl Spacer (S3)	112
III.2.4 Introduction of Benzylamino Spacer (S4)	113
III.3 COMPLEXATION AND EXTRACTION STUDIES: ISOLATION OF FULLERENES WITHOUT CHROMATOGRAPHY	114
III.3.1 Complexation of C ₆₀ and C ₇₀	114
III.3.2 Stability of Fullerene Complexes	119
III.3.3 Selective Extraction of C ₇₀	125
III.3.4 DFT Calculations	133
III.3.5 Complexation of C ₈₄	140
III.3.6 Selective Extraction of C ₈₄	145
III.3.7 Other Receptors	156
III.4 IMPROVEMENTS IN HIGHER FULLERENES SEPARATION	160
III.4.1 Higher Fullerene Enriched Fullerites	160
III.4.2 A Capsule Soluble in Acetonitrile	162
III.5 HOMOCHIRAL CAPSULES	171
III.5.1 Configurational and Conformational Study of Capsules	171
III.5.2 Stability of Homochiral Capsules	177
III.5.3 Toward Separation of Chiral Fullerenes	180
III.6 CONCLUSIONS	184

CHAPTER IV: FULLERENE RECOGNITION BY DONOR-ACCEPTOR INTERACTIONS	187
IV.1 A RECEPTOR FOR FULLERENES BASED ON EXTENDED TTF SCAFFOLDS	189
IV.1.1 Design, Synthesis and Complexation Studies	190
IV.1.2 Physicochemical and Photophysical Characterization	196
IV.1.2.1 Spectroscopic Characterization of the Complexes	196
IV.1.2.2 Electron Paramagnetic Resonance (EPR) Studies	200
IV.1.2.3 Electrochemical Characterization	201
IV.1.3 DFT Calculations	203
IV.1.4 Homochiral Receptor	210
IV.2 CONCLUSIONS	212
CHAPTER V: CARCERAND FOR FULLERENES: A MOLECULAR MARACA	215
V.1 INTRODUCTION	217
V.2 DESIGN CONSIDERATIONS AND CALCULATIONS	220
V.2.1 Synthetic Approach	223
V.2.2 Stability Studies and Properties of Incarcerated Fullerenes	237
V.3 CONCLUSIONS	245
CHAPTER VI: EXPERIMENTAL PART	247
VI.1 GENERAL PROCEDURES	248
VI.2 SYNTHESIS CHAPTER II	254
VI.3 SYNTHESIS CHAPTER III	287
VI.3.1 Methods for Fullerene Extractions and Extracts Analysis	302
VI.4 SYNTHESIS CHAPTER IV	309
VI.5 SYNTHESIS CHAPTER V	310

CHAPTER VII: APPENDIX	323
Resumen	341

UNIVERSITAT ROVIRA I VIRGILI
SELF-ASSEMBLY BASED ON THE 2-UREIDO-4(1H)-PYRIMIDINONE MOTIF: FROM CYCLIC ARRAYS TO MOLECULAR CAPSULES
FOR FULLERENE SEPARATIONS
Elisa Huerta Martínez
DL:T.289-2012

UNIVERSITAT ROVIRA I VIRGILI
SELF-ASSEMBLY BASED ON THE 2-UREIDO-4(1H)-PYRIMIDINONE MOTIF: FROM CYCLIC ARRAYS TO MOLECULAR CAPSULES
FOR FULLERENE SEPARATIONS
Elisa Huerta Martínez
DL:T.289-2012

A	Acceptor
Ac	Acetyl
Adam	Adamantane
Ar	Aromatic, Aryl
Bn	Benzyl
Boc	<i>tert</i> -Butoxycarbonyl
C	Cytosine
CD	Circular Dichroism
CDI	1,1'-Carbonyldiimidazole
CE	Counter electrode
CM	Crossed Metathesis
COSY	Correlation Spectroscopy
CTV	Cyclotrimeratrylene
CV	Cyclic Voltammetry
D	Donor
DCB	Dichlorobenzene
DCM	Dichloromethane
DFT	Density Functional Theory
DHP	Dihydropyran
DIBAL	Diisobutylaluminum hydride
DMAP	Dimethylaminopyridine
DMF	Dimethylformamide
DMSO	Dimethylsulfoxide
DOSY	Diffusion Ordered Spectroscopy
DPPA	Diphenylphosphoryl azide
DPV	Differential Pulse Voltammetry
DUPy	Double ureidopyrimidinone
E	Potential
EI-MS	Electron Impact Mass Spectrometry
ESI-MS	Electrospray Ionization Mass Spectrometry
EPR	Electronic Paramagnetic Resonance
Et	Ethyl
ex-TTF	Extended Tetrathiafulvalene
FAB-MS	Fast Atom Bombardment Mass Spectrometry
G	Guanine
GPC	Gel Permeation Chromatography
HMBC	Heteronuclear Multiple Bond Correlation
HMQC	Heteronuclear Multiple Quantum Correlation
HPLC	High Performance Liquid Chromatography
HRMS	High Resolution Mass Spectrometry
HSQC	Heteronuclear Single Quantum Correlation
I	Intensity
IR	Infrared
LDA	Lithium diisopropyl amide
MALDI-TOF	Matrix Assisted Laser Desorption/Ionization- Time of Fly

Me	Methyl
MeCN	Acetonitrile
MEM	Methoxyethylmethyl
Mp	Melting point
MW	Molecular weight
n-BuLi	<i>n</i> -Butyl lithium
NMR	Nuclear Magnetic Resonance
NOESY	Nuclear Overhauser Effect Spectroscopy
OCB	<i>o</i> -dichlorobenzene
Ph	Phenyl
PS	Polystyrene
Py	Pyrimidinone
SPS	Solvent purification system
STM	Scanning Tunneling Microscopy
TBAF	Tetrabutylammonium fluoride
TBDMS	<i>tert</i> -Butyldimethylsilyl
^tBu	<i>tert</i> -butyl
RCM	Ring Closing Metathesis
RE	Reference electrode
r.t.	Room temperature
TCE	Tetrachloroethane
TD-DFT	Time Dependent - Density Functional Theory
TFA	Trifluoroacetic acid
THF	Tetrahydrofuran
THP	Tetrahydropyrane
TLC	Thin layer chromatography
UPy	Ureidopyrimidinone
UV-vis	Ultraviolet-visible
VPO	Vapour pressure osmometry
WE	Working electrode

UNIVERSITAT ROVIRA I VIRGILI
SELF-ASSEMBLY BASED ON THE 2-UREIDO-4(1H)-PYRIMIDINONE MOTIF: FROM CYCLIC ARRAYS TO MOLECULAR CAPSULES
FOR FULLERENE SEPARATIONS
Elisa Huerta Martínez
DL:T.289-2012

UNIVERSITAT ROVIRA I VIRGILI
SELF-ASSEMBLY BASED ON THE 2-UREIDO-4(1H)-PYRIMIDINONE MOTIF: FROM CYCLIC ARRAYS TO MOLECULAR CAPSULES
FOR FULLERENE SEPARATIONS
Elisa Huerta Martínez
DL:T.289-2012

Note: Bibliographic citations have been added as footnotes independently at every chapter, so they are duplicated in different chapters when necessary.

CHAPTER I: INTRODUCCION AND OBJECTIVES

UNIVERSITAT ROVIRA I VIRGILI
SELF-ASSEMBLY BASED ON THE 2-UREIDO-4(1H)-PYRIMIDINONE MOTIF: FROM CYCLIC ARRAYS TO MOLECULAR CAPSULES
FOR FULLERENE SEPARATIONS
Elisa Huerta Martínez
DL:T.289-2012

CHAPTER I: INTRODUCTION AND OBJECTIVES

I.1 SUPRAMOLECULAR CHEMISTRY

Supramolecular Chemistry has been defined as "*the chemistry beyond the molecule*",¹ bearing on the organized entities of higher complexity resulting from the association of two or more chemical species held together by intermolecular forces. This new field of chemistry² was born from the pioneering work of Charles Pedersen and Donald Cram on crown ethers and spherands,³ and the additional contribution of Jean-Marie Lehn with the chemistry of cryptands⁴ as a three-dimensional form of crown ethers (Figure 1), the three authors being awarded with the Nobel Prize in 1987.

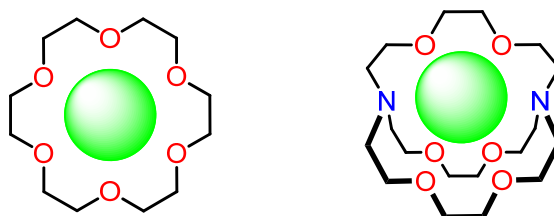


Figure 1: Schematic representation of the complexes formed by a crown ether (left) and a cryptand (right).

Supramolecular chemistry is a young field in chemistry. One of its most important concepts – *recognition*⁵ – had its roots at the first time in the “lock

¹ a) Lehn, J. M. *Science* **1993**, 260, 1762-1763. b) Lehn, J. M. *Supramolecular Chemistry*, Wiley, VCH, Weinheim, Germany, **1995**.

² Lehn, J. M. *Science* **1985**, 227, 849-856.

³ a) Pedersen, C. J. *J. Am. Chem. Soc.* **1967**, 89, 7017-7036. b) Cram, D. J.; Ho, S. P.; Knobler, C. B.; Maverick, E.; Trueblood, K. N. *J. Am. Chem. Soc.* **1986**, 108, 2989-2998.

⁴ Dietrich, B.; Lehn, J. M.; Sauvage, J. P. *Tetrahedron Lett.* **1969**, 2889-2892.

⁵ For a review dealing with molecular recognition see: Lavigne, J. J.; Anslyn E. V. *Angew. Chem. Int. Ed.* **2001**, 40, 3118-3130.

and key" concept introduced by Emil Fisher in 1894 to explain enzyme operating mechanisms. Accordingly, an enzyme recognizes a substrate that is geometrically complementary to its active site, in the same way as a key fixes into its lock. However, molecular recognition requires not only geometrical complementarity but also a chemical interaction (van der Waals forces, hydrogen bonding) and sometimes, a conformational rearrangement.

Unlike molecular chemistry, where structures are based on covalent interactions, supramolecular chemistry assembles aggregates from small molecules through non-covalent interactions, where a close equilibrium between enthalpy (association energy) and entropy (organization penalty) takes place. Compared to simple covalent bonds, whose dissociation energy is about 350 kJ/mol, non-covalent interactions are weaker, having a wide range of interaction energies. Whereas hydrogen bonding is about 4-120 kJ/mol, some electrostatic interactions as ion-pairing can double this value (Table 1). The addition or combination of several non-covalent interactions is thus necessary to form strong assemblies.

Table 1: Non-covalent interactions and related energies. ⁶

Interaction Type	Interaction Energy (kJ/mol)
ion pairing	50-400
ion-dipole	50-200
Dipole-dipole	4-40
hydrogen bonding	4-120
cation- π	5-80
π - π stacking	4-20
dispersion	4-20
Solvent effects	4-40

⁶ Goshe, A. J.; Steele, I. M; Caccrelli, C.; Rheingold, A. L.; Bosnich, B. *Proc. Natl. Acad. Sci. U. S. A.* **2002**, 99, 4823-4829.

I.2 MULTIPLE HYDROGEN BOND ARRAYS FOR SELF-ASSEMBLY

Hydrogen bond plays a very important role in the formation of the three-dimensional structure of a large number of chemical and biological systems due to their specificity and directionality.⁷ The formation of one or more hydrogen bonds in combination with other non-covalent forces (such as ionic or hydrophobic interactions) results in substantial changes in the micro- and macroscopic properties of the supramolecular aggregates formed.⁸ Unlike covalent bonds, hydrogen bonds are formed in a reversible process and their overall strength depends on the chemical environment, solvent or temperature. As a rule, the more polar the solvent is the weaker the hydrogen bonds are, due to the competitive effect of the solvent molecules for the donor (D) or acceptor (A) sites.

Self-association of single molecules (monomer subunits) through multiple hydrogen bonds can result in complex supramolecular aggregates and there are many examples of systems based on the linkage of subunits with complementary donor and acceptor sites. Typical examples are the DD-AA guanidinium-oxoanion pairs (Figure 2A), or the DDA-AAD array of the guanidine-cytosine dimer (Figure 2B), which is more stable than the alternative ADA-DAD array (for instance, in the 2,6-diaminopyridine-imide complex, Figure 2C) due to the increased number of secondary attractive

⁷ a) Lawrence, D. S.; Jiang, T.; Levitt, M. *Chem. Rev.* **1995**, *95*, 2229-2260. b) Philp, D.; Stoddart, J. F. *Angew. Chem. Int. Ed.* **1996**, *35*, 1154-1196. c) Jeffrey, G. A. *An Introduction to Hydrogen Bonding*, 1st ed. Oxford University Press, New York, **1997**.

⁸ a) Whitesides, G. M.; Mathias, J. P.; Seto, C. T. *Science* **1991**, *254*, 1312-1319. b) Bowden, N. B.; Weck, M.; Choi, I. S.; Whitesides, G. M. *Acc. Chem. Res.* **2001**, *34*, 231-238.

interactions in the final structure.⁹

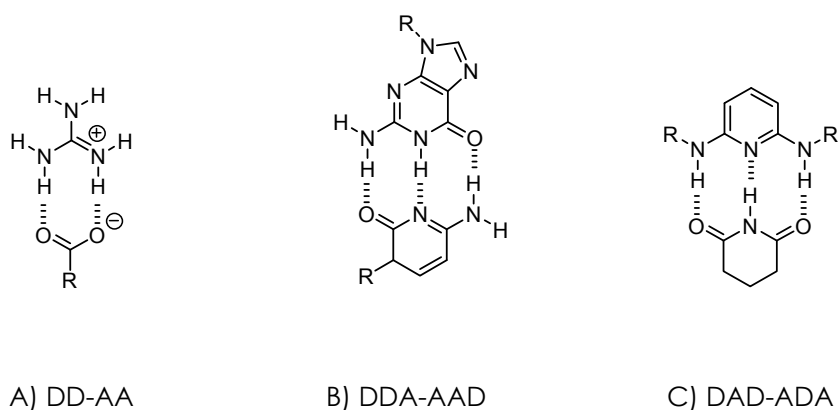


Figure 2: Examples of multiple hydrogen bond contacts in simple molecules.

Quadruple hydrogen bond arrays have been predicted to be much stronger than triple hydrogen bond ones.¹⁰ An additional advantage is that with an even number of hydrogen bonds (four), the construction of self-complementary molecules becomes possible. This is the case of the 2-ureido-4-[1H]-pyrimidinone scaffold (UPy), where the stability of the dimeric aggregate is enhanced, and association constants are in the order of 10^7 M⁻¹.¹¹ The existence of tautomeric equilibria that depend on the polarity of the solvent and the concentration, makes self-assembly more difficult

⁹ a) Jorgensen, W. L.; Pranata, J. *J. Am. Chem. Soc.* **1990**, *112*, 2008-2010. b) Pranata, J.; Wierschke, J. W.; Jorgensen, W. L. *J. Am. Chem. Soc.* **1991**, *113*, 2810-2819.

¹⁰ Sartorius, J.; Schneider, H. *J. Chem. Eur. J.* **1996**, *2*, 1446-1452.

¹¹ a) Beijer, F. H.; Sijbesma, R. P.; Kooijman, H.; Speck, A. L.; Meijer, E. W. *J. Am. Chem. Soc.* **1998**, *120*, 6761-6769. b) Folmer, B. J. B.; Sijbesma, R. P.; Kooijman, H.; Spek, A. L.; Meijer, E. W. *J. Am. Chem. Soc.* **1999**, *121*, 9001-9007. c) Söntjens, S. H. M.; Sijbesma, R. P.; van Genderen, M. H. P.; Meijer, E. W. *J. Am. Chem. Soc.* **2000**, *122*, 7487-7493.

because only two of the possible tautomers (namely 4-[1H]-pyrimidinone and pyrimidin-4-ol) can self-assemble into DDAA-AADD and ADAD-DADA dimers, respectively (Figure 3).

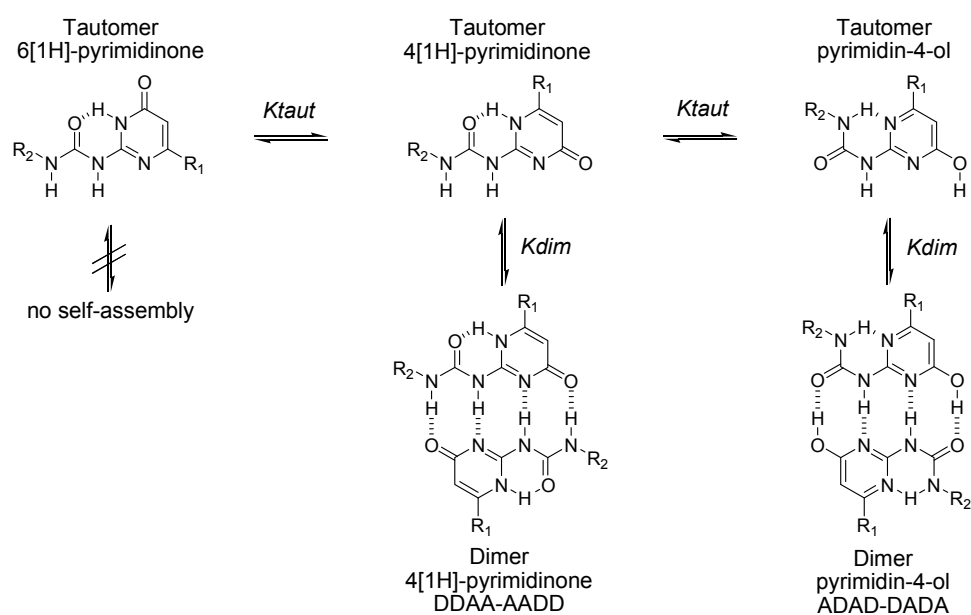


Figure 3: Tautomerism of 2-ureido-4-pyrimidinones.

The presence of an intramolecular hydrogen bond between the pyrimidinone NH and the urea's carbonyl group (or between urea's NH and the nitrogen in the ring in the case of the pyrimidin-4-ol tautomer) preorganizes the structure and facilitates dimerization.

Non-covalent interactions have been widely used in the construction of supramolecular assemblies with a huge variety of properties, such as polymers, organized systems as rosettes and capsules, among others. Some examples of these varieties of assemblies will be showed in the following sections.

1.2.1 Supramolecular Polymers

Supramolecular polymers¹² are composed by several units held together through directional and reversible interactions, whose properties as materials are shown in solution as well as in bulk. Since the first hydrogen-bonded supramolecular polymer was described by Lehn in 1990,¹³ which involved the use of complementary diaminopyridines and uracyl derivatives units in a triple hydrogen bond fashion, many other examples of polymers that take advantage from interactions such as metal coordination, solvophobic effects or hydrogen bonding have been reported. The easy access to different building blocks allows control over molecular weight distribution or cross-linking.¹⁴ Representative cases will be briefly discussed.

Ghadiri's nanotubes constitute a typical example of bio-inspired supramolecular polymers based on hydrogen bonds.¹⁵ They deal with self-assembled stacks of cyclic peptides, made of alternating D- and L-amino acids, so as the side chains point outside of the macrocycle, and hydrogen bonds are formed between the rings like in protein β -sheets (Figure 4).

¹² *Supramolecular Polymers*, 2nd Edition, Ed. Ciferri, A., Taylor and Francis Group, **2005**.

¹³ Fouquey, C.; Lehn, J. M.; Levelut, A. M. *Adv. Mater.* **1990**, *2*, 254-257.

¹⁴ Berl, V.; Schmutz, M.; Kricheldorf, M. J.; Khoury, R. G.; Lehn, J. M. *Chem. Eur. J.* **2002**, *8*, 1227-1244.

¹⁵ a) Ghadiri, M. R.; Granja, J. R.; Milligan, R. A.; McRee, D. E.; Khazanovich, N. *Nature* **1993**, *366*, 324-327. b) Bong, D. T.; Clark, T. D.; Granja, J. R.; Ghadiri, M. R. *Angew. Chem. Int. Ed.* **2001**, *40*, 988-1011.

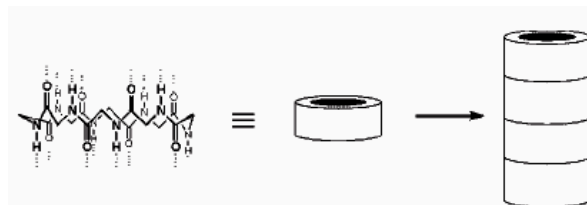


Figure 4: Schematic representation of peptide-based nanotubes.
(Reproduced from ref. 15a).

Meijer *et al.* have made bold contributions to the field. UPy monomers, upon suitable functionalization, can generate lineal polymeric structures of high viscosity,¹⁶ helical and chiral polymers¹⁷ (a topic of interest in sensors). Also, polymers with optoelectronic and photochromic materials¹⁸ have been generated by means of non-covalent interactions. In these materials, polymerization is controlled by the solvent employed: they polymerize in organic solvents, whereas only monomers are present in water (Figure 5).

¹⁶ Sijbesma, R. P.; Beijer, F. H.; Brunsveld, L.; Folmer, B. J. B.; Ky Hirschberg, J. H.; Lange, R. F. M.; Lowe, J. K. L.; Meijer, E. W. *Science* **1997**, *278*, 1601-1604.

¹⁷ a) El-ghayoury, A.; Peeters, E.; Schenning, A. P. H. J.; Meijer, E. W. *Chem. Commun.* **2000**, 1969-1970. b) Ky Hirschberg, J. H.; Brunswald, L.; Ramzi, A.; Vekemans, J. A. J. M.; Sijbesma, R. P.; Meijer, E. W. *Nature* **2000**, *407*, 167-170. c) Schenning, A. P. H. J.; Jonkheijm, P.; Peeters, E.; Meijer, E. W. *J. Am. Chem. Soc.* **2001**, *123*, 409-416. d) Brunsveld, L.; Vekemans, J. A. J. M.; Hirschberg, J. H. K. K.; Sijbesma, R. P.; Meijer, E. W. *Proc. Natl. Acad. Sci. U. S. A.* **2002**, *99*, 4977-4982.

¹⁸ a) Okamoto, Y.; Nakano, T. *Chem. Rev.* **1994**, *94*, 349-372. b) Aimi, J.; Oya, K.; Tsuda, A.; Aida, T. *Angew. Chem. Int. Ed.* **2007**, *46*, 2031-2035. c) Kauranen, M.; Verbiest, T.; Boutton, C.; Teerenstra, M. N.; Clays, K.; Schouten, A. J.; Nolte, R. J. M.; Persoons, A. *Science* **1995**, *270*, 966-969. d) Verbiest, T.; van Elshocht, S.; Kauranen, M.; Helleman, L.; Snauwaert, I.; Nuckolls, C.; Katz, T. J.; Persoons, A. *Science* **1998**, *282*, 913-915. e) Kawauchi, T.; Kumaki, J.; Kitaura, A.; Okoshi, K.; Kusanagi, H.; Kobayashi, K.; Sugai, T.; Shinohara, H.; Yashima, E. *Angew. Chem. Int. Ed.* **2008**, *47*, 515-519.

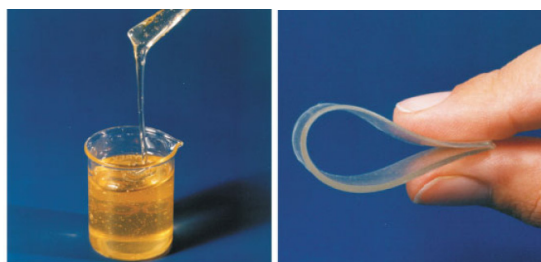


Figure 5: Liquid like poly(ethylene butylene) (left) and UPy functionalized poly(ethylene/butylenes) elastomeric polymer (right). (Reproduced from ref. 19).

An important feature present in helical supramolecular polymers is the possibility of helicity control,²⁰ either introducing chirality in the monomer²¹ or with the help of a chiral regulator.²² The oligophenylenevinylene (OPV) functionalized ureidotriazines (UT) described by Meijer clearly exemplify this property. Intrinsically chiral OPV-UT **I** (Figure 6) forms dimers in a DADA fashion, which polymerize into columnar aggregates through stacking interactions.²³ Aggregate sizes can be controlled by temperature, going from monomers at high temperature, to polymers at low temperature. Helical architectures are induced by the presence of a chiral center in a side chain. Alternatively, achiral OPV-UT **II** forms helicoidal assemblies whose helicity is controlled by the addition of a chiral carboxylic acid, such as *R*-(+)- or *S*-(-)-citronellic acid. The carboxylic acid acts as a chiral regulator,

¹⁹ Folmer, B. J. B.; Sijbesma, R. P.; Versteegen, R. M.; van der Rijt, J. A. J.; Meijer, E. W. *Adv. Mater.* **2000**, *12*, 874-878.

²⁰ Palmans, A. R. A.; Meijer, E. W. *Angew. Chem. Int. Ed.* **2007**, *46*, 8948-8968.

²¹ Yamamoto, T.; Fukushima, T.; Kosaka, A.; Jin, W.; Yamamoto, Y.; Ishii, N.; Aida, T. *Angew. Chem. Int. Ed.* **2008**, *47*, 1672-1675.

²² Hou, J.-Z.; Li, M.; Li, Z.; Zhan, S.-Z.; Huang, X.-C.; Li, D. *Angew. Chem. Int. Ed.* **2008**, *47*, 1711-1714.

²³ Jonkheijm, P.; van der Schoot, P.; Schenning, A. P. H. J.; Meijer, E. W. *Science* **2006**, *313*, 80-83.

attached to the polymer by means of two additional hydrogen bonds; one to the free amine proton not involved in the hydrogen bond array and the second to the triazine-ring nitrogen atom of the UT motif.²⁴

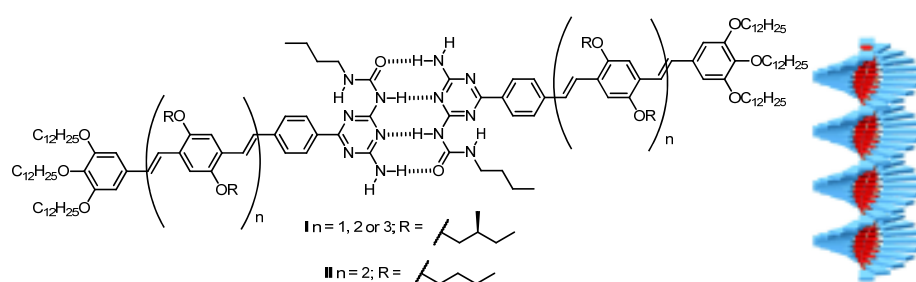


Figure 6: Structure of OPV-UT dimers (left) and schematic self-assembled helical polymer (right). (Reproduced from ref. 24).

There are some other examples in which combined non-covalent interactions are used. In their approximation, Ding and coworkers developed a new polymeric material using two different interactions in the construction of a multitopic ligand with application in asymmetric heterogeneous catalysis.²⁵ On one side, hydrogen bonding through UPy moieties was used as self-recognition motif. The urea moiety was endowed with Feringa's MonoPhos ligand, whose corresponding Rh complexes have been shown to catalyze the hydrogenation of a number of substrates.²⁶ The addition of rhodium over UPy **III** causes polymer precipitation. The catalyst demonstrates excellent asymmetric induction in the catalytic synthesis of optically active α -amino acids and 1-phenylethylamine derivatives, without

²⁴ George, S. J.; Tomovic, Z.; Smulders, M. M. J.; de Greef, T. F. A.; Leclère, P. E. L. G.; Meijer, E. W.; Schenning, A. P. H. J. *Angew. Chem. Int. Ed.* **2007**, *46*, 8206-8211.

²⁵ Shi, L.; Wang, X.; Sandoval, C. A.; Li, M.; Qi, Q.; Li, Z.; Ding, K. *Angew. Chem. Int. Ed.* **2006**, *45*, 4108-4112.

²⁶ van den Berg, M.; Minnaard, A. J.; Schudde, E. P.; van Esch, J.; de Vries, A. H. M.; de Vries, J. G.; Feringa, B. L. J. *Am. Chem. Soc.* **2000**, *122*, 11539-11540.

leaching toxic metal ions into the product. Furthermore, the catalyst was easily recyclable (Figure 7).

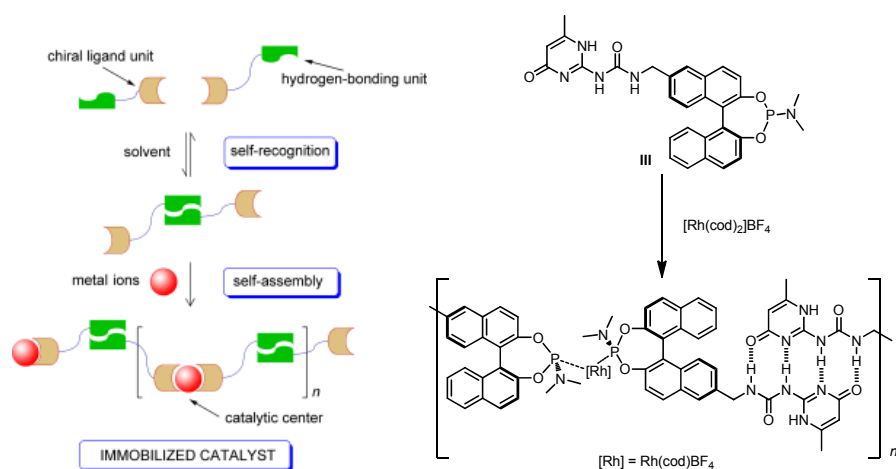


Figure 7: Schematic process for constructing a supramolecular chiral polymer based on hydrogen bonding and metal coordination. (Reproduced from ref. 25).

An analogous strategy was used by Sijbesma and Rutjes in the field of homogeneous catalysis. In their example, a copper(II)-catalyst was assembled by a combination of UPy moieties and a coordinating ligand, and successfully used in a tandem Sonogashira coupling/5-endo-dig cyclization and a Cu-catalyzed [3+2] cycloaddition.²⁷ The catalyst was easily recovered using a resin functionalized with self-complementary UPy units.

²⁷ Gruijters, B. W. T.; Broeren, M. A. C.; van Delft, F. L.; Sijbesma, R. P.; Hermkens, P. H. H.; Rutjes, F. P. J. T. *Org. Lett.* **2006**, *8*, 3163-3166.

I.2.2 Hierarchical Self-Assembled Structures

Significant efforts have been made on controlling the self-assembly of molecules through non-covalent directional bonding to form extended two-dimensional assemblies.²⁸ By carefully selecting the molecular building blocks and guiding the self-assembly process, it is possible to tailor these patterns into specific geometries or chirality.

Nature often builds up complex structures from small fragments by self-assembly in a hierarchical way. This is nicely illustrated by the tobacco mosaic virus (TMV),²⁹ a rod-like structure composed by 2130 identical units coiled around a RNA strand along the structure in a helical fashion. At physiological pH, subunits initially form a disk-shaped structure (Figure 8b), which switches its conformation into a helical shape (Figure 8c) by RNA loop insertion in the central hole of the disk. Then, additional disks, corresponding to two helix turns, are assembled until the structure is completed (Figure 8d).

²⁸ a) De Feyter, S.; De Schryver, F. C. *Chem. Soc. Rev.* **2003**, 32, 139-150. b) Barth, J. V.; Costantini, G.; Kern, K. *Nature* **2005**, 437, 671-679.

²⁹ a) Klug, A. *Angew. Chem. Int. Ed.* **1983**, 22, 565-582. b) Philp, D.; Stoddart, J. F. *Angew. Chem. Int. Ed.* **1996**, 35, 1154-1196. c) Greig, L. M.; Philp, D. *Chem. Soc. Rev.* **2001**, 30, 287-302.

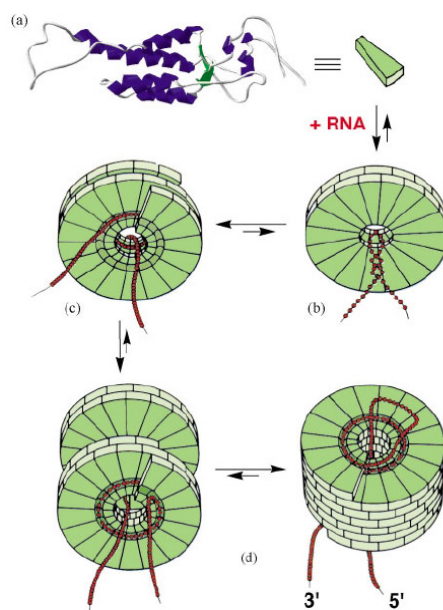


Figure 8: The assembly of the tobacco mosaic virus. Protein subunits (a) associate with viral RNA to form a double disk structure (b). Conformational change results in the formation of a slipped double disk (c) and initiates viral assembly (d). (Reproduced from ref. 29c).

TMV assembly process demonstrates how nature is able to construct large, ordered supramolecular arrays from small units by self-assembly using non-covalent interactions.

An interesting example of hierarchical self-assembly was described in 2005 by Schneider *et al.* in which scanning tunneling microscopy (STM) allows to observe all the stages in the spontaneous self-assembly process of rubrene (5,6,11,12-tetraphenylnaphthacene), going from a single molecule to pentamers and ending with decamers in which each monomeric unit is a former pentamer (Figure 9).³⁰ Moreover, the chirality of rubrene is preserved

³⁰ Blüm, M. C.; Cavar, E.; Pivetta, M.; Patthey, F.; Schneider, W. D. *Angew. Chem. Int. Ed.* **2005**, *44*, 5334-5337.

along all the stages of the self-assembly process.

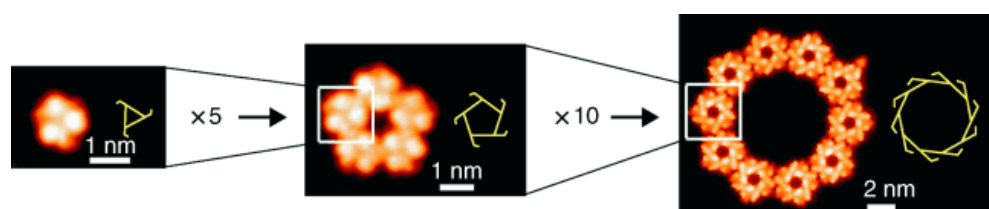


Figure 9: STM images of the nested-self-organized L-type rubrene assemblies. (Reproduced from ref. 30).

Supramolecular chemists have often tried to mimic nature by controlling the size and shape of supramolecular architectures, using either biomolecules such as base pairs or bio-inspired structures. Considerable effort has been devoted to the construction of rosette-like structures, and there are a number of examples in literature such as Reinhoudt and Whitesides' melamine-cyanuric acid hexameric rosettes.³¹ Reinhoudt *et al.* used calixarenes, 1,3-difunctionalized with melamine subunits, leading to double rosettes after addition of the corresponding cyanurate. These double rosettes present supramolecular chirality which involves the non-symmetric arrangement of molecular components in the non-covalent assembly.³² The multiple cooperative hydrogen bonds provide sufficient stability and allowed the isolation of enantiomerically pure assemblies

³¹ a) Whitesides, G. M.; Simanek, E. E.; Mathias, J. P.; Seto, C. T.; Chin, D. N.; Mammen, M.; Gordon, D. M. *Acc. Chem. Res.* **1995**, *28*, 37-44. b) Lawrence, D. S.; Jiang, T.; Levett, M. *Chem. Rev.* **1995**, *95*, 2229-2260. c) Timmerman, P.; Prins, L. J. *Eur. J. Org. Chem.* **2001**, 3191-3205. d) Sherrington, D. C.; Taskinen, K. A. *Chem. Soc. Rev.* **2001**, *30*, 83-93. e) Prins, L. J.; Reinhoudt, D. N.; Timmerman, P. *Angew. Chem. Int. Ed.* **2001**, *40*, 2382-2426.

³² Prins, L. J.; Huskens, J.; de Jong, F.; Timmerman, P.; Reinhoudt, D. N. *Nature* **1999**, *398*, 398-502.

(Figure 10).³³

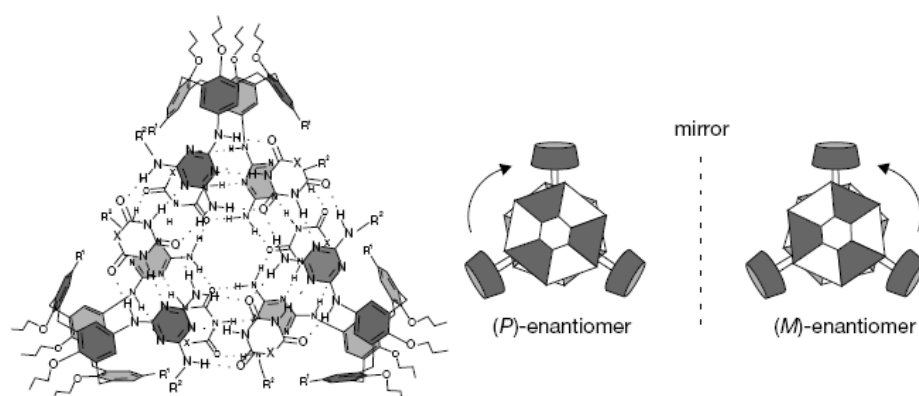


Figure 10: Assembly with D_3 -symmetry is shown (left), with schematic representations for both the (M)- and (P)-enantiomers (right). (Reproduced from ref. 33).

Moreover, the introduction of a linker between two calixarenes leads to the formation of tetra-rosettes capable to recognize saccharides, which constitutes the first example of enantioselective recognition of a carbohydrate by a self-assembled receptor through hydrogen bonds.³⁴

Natural building blocks, such as carbohydrates, amino acids, and nucleic acids, offer a rich source of H-bond donors and acceptors. In this sense, some other bio-inspired two dimensional assemblies have been developed. A typical example is found in the G-quartet tetrameric rosette,³⁵ a hydrogen-bonded macrocycle formed by a cation-templated assembly

³³ Prins, L. J.; Huskens, J.; de Jong, F.; Timmerman, P.; Reinhoudt, D. N. *Nature* **2000**, 408, 181-184

³⁴ Ishi-i, T.; Mateos-Timoneda, M. A.; Timmerman, P.; Crego-Calama, M.; Reinhoudt, D. N.; Shinkai, S. *Angew. Chem. Int. Ed.* **2003**, 42, 2300-2305.

³⁵ Davis, J. F. *Angew. Chem. Int. Ed.* **2004**, 43, 668-698.

of guanosine, first identified in 1962³⁶ as the basis for the aggregation of 5'-guanosine monophosphate. It has been shown that tetramerization of the guanine sequences and subsequent stacking of the tetramers is responsible for the stability of telomeric DNA towards telomerase.³⁷

Related examples are Fenniri's hexameric rosettes that hierarchically self-assemble into nanotubes (Figure 11).³⁸ In water, the hybrid guanine-cytosine (G⁺C⁻) motif forms a six-membered supermacrocycle maintained by 18 hydrogen bonds (a rosette). The resulting and substantially more hydrophobic aggregate self-organizes into a linear stack defining an open central channel, 1.1 nm wide and several micrometers long. Remarkably, the structural integrity of these stacked rosettes survives even in boiling water.³⁹

³⁶ Gellert, M.; Lipsett, M. N.; Davies, D. R. *Proc. Natl. Acad. Sci. U. S. A.* **1962**, *48*, 2013-2018.

³⁷ Schmuck, C. *Chem. Commun.* **1999**, 843-844.

³⁸ a) Fenniri, H.; Mathivanan, P.; Vidale, K. L.; Sherman, D. M.; Hallenga, K.; Wood, K. V.; Stowell, J. G. *J. Am. Chem. Soc.* **2001**, *123*, 3854-3855. b) Fenniri, H.; Deng, B.-L.; Ribbe, A. E. *J. Am. Chem. Soc.* **2002**, *124*, 11064-11072. c) Fenniri, H.; Deng, B.-L.; Ribbe, A. E.; Hallenga, K.; Jacob, J.; Thiyagarajan, P. *Proc. Natl. Acad. Sci. U. S. A.* **2002**, *99*, 6487-6492.

³⁹ Moralez, J. G.; Raez, J.; Yamazaki, T.; Motkuri, R. K.; Kovalenko, A.; Fenniri, H. *J. Am. Chem. Soc.* **2005**, *127*, 8307-8309.

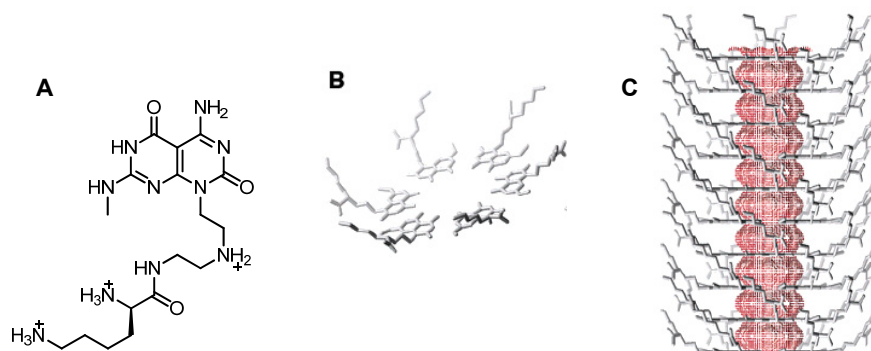


Figure 11: G^{AC} derivative (A), single rosettes (B) obtained from the self-assembly of monomers depicted in A, and rosette nanotubes (C). The inner channel is highlighted in red. (Reproduced from ref. 39).

1.2.3 Self-Assembled Nanocapsules

When the scaffold that holds together self-complementary subunits possesses the appropriate curvature, it is possible to obtain capsule-like structures.⁴⁰ The non-covalent forces that are useful in constructing capsules are primarily hydrogen bonds and metal-ligand interactions. On one side, hydrogen bonds provide plasticity and faster equilibration of the systems, whereas metal coordination provides strength and stability.⁴¹ The first example of self-assembled capsules were the hydrogen-bonded glycoluril-

⁴⁰ Hof, F.; Craig, S. L.; Nuckolls, C.; Rebek, J., Jr. *Angew. Chem. Int. Ed.* **2002**, *41*, 1488-1508.

⁴¹ For capsules based on metal coordination, see: a) Stang, P. J. *Chem. Eur. J.* **1998**, *4*, 19-27. b) Fujita, M. *Chem. Soc. Rev.* **1998**, *27*, 417-425. c) Takeda, N.; Umemoto, K.; Yamaguchi, K.; Fujita, M. *Nature* **1999**, *398*, 794-796. d) Olenyuk, B.; Whiteford, J. A.; Fechtenkötter, A.; Stang, P. J. *Nature* **1999**, *398*, 796-799. e) Caulder, D. L.; Raymond, K. N. *Acc. Chem. Res.* **1999**, *32*, 975-982. f) Fujita, M.; Umemoto, K.; Yoshizawa, M.; Fujita, N.; Kusukawa, T.; Biradha, K. *Chem. Commun.* **2001**, 509-518. g) Mugridge, J. S.; Bergman, R. G.; Raymond, K. N. *J. Am. Chem. Soc.* **2010**, *132*, 1182-1183.

derived described by Rebek and de Mendoza, the so-called "tennis ball" and "softball" (Figure 12). In the first one,⁴² glycoluril units, which give the proper curvature and self-complementarity, were attached to an aromatic spacer, leading to a capsular structure linked through eight hydrogen bonds. The cavity possesses an inner volume of about 50 Å³, large enough to accommodate methane, ethane, ethylene or noble gases. Similarly, when the spacer was changed to a larger one, "softballs" were obtained.⁴³ In this case, the inner volume of the cavity was around 240-320 Å³. Capsule's interior provides to guests an unusual environment, which allows using them as nano-reactors. For example, a Diels-Alder reaction between benzoquinone and cyclohexadiene was accelerated 200-fold within the "softball". However, the entrapped adduct caused product inhibition, preventing turnover.⁴⁴

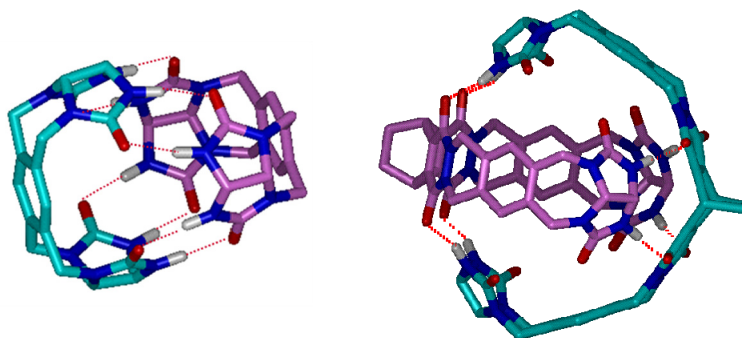


Figure 12: Models of "tennis ball" (left) and "softball" (right).

Since then, many curved scaffolds, such as calixarenes or resorcinarenes, have been used in the construction of supramolecular

⁴² a) Wyler, R.; de Mendoza, J.; Rebek, J., Jr. *Angew. Chem. Int. Ed.* **1993**, 32, 1699-1701. b) Branda, N.; Wyler, R.; Rebek, J., Jr. *Science* **1994**, 263, 1267-1268.

⁴³ Meissner, R. S.; Rebek, J., Jr.; de Mendoza, J. *Science* **1995**, 270, 1485-1488.

⁴⁴ Kang, J.; Rebek, J., Jr. *Nature* **1997**, 385, 50-52.

capsules. For example, 1,3-alternate calix[4]arenes bearing UPy units in two opposite positions were reported by our group to form dimers.⁴⁵ Alternatively, calix[4]arenes,⁴⁶ calix[6]arenes⁴⁷ and calix[4]pyrroles,⁴⁸ decorated with ureas in the upper rim, dimerize into capsules through hydrogen bonding. Rebek has used more rigid structures as resorcinarenes, whose cone conformation is fixed, in which a vase-shaped cavitand structure presents four imide functions around its rim which allowed the formation of cavities suitable for encapsulation of large guests (Figure 13).⁴⁹ These cylindrical nano-containers have also been used to catalyze reactions as the 1,3-dipolar cycloaddition of 1-azidobenzene with 1-ethynylbenzene, which produces selectively 1,3-diphenyl-1,2,3-triazole, the only regioisomer fitting into the cavity.⁵⁰

⁴⁵ González, J. J.; Prados, P.; de Mendoza, J. *Angew. Chem. Int. Ed.* **1999**, *38*, 525-528.

⁴⁶ a) Shimizu, K. D.; Rebek, J., Jr. *Proc. Natl. Acad. Sci. U. S. A.* **1995**, *92*, 12403-12407.
b) Scheerder, J.; van Duynhoven, J. P. M.; Engbersen, J. F. J.; Reinhoudt, D. N. *Angew. Chem. Int. Ed.* **1996**, *35*, 1090-1093. c) Mogck, O.; Böhmer, V.; Vogt, W. *Tetrahedron* **1996**, *52*, 8489-8496.

⁴⁷ González, J. J.; Ferdani, R.; Albertini, E.; Blasco, J. M.; Arduini, A.; Pochini, A.; Prados, P.; de Mendoza, J. *Chem. Eur. J.* **2000**, *6*, 73-80.

⁴⁸ a) Ballester, P.; Gil-Ramírez G. *Proc. Natl. Acad. Sci. U. S. A.* **2009**, *106*, 10455-10459.
b) Gil-Ramírez, G.; Chas, M.; Ballester, P. *J. Am. Chem. Soc.* **2010**, *132*, 2520-2521.

⁴⁹ Heinz, T.; Rudkevich, D. M.; Rebek, J., Jr. *Nature* **1998**, *394*, 764-766.

⁵⁰ Chen, J.; Rebek, J., Jr. *Org. Lett.* **2002**, *4*, 327-329.

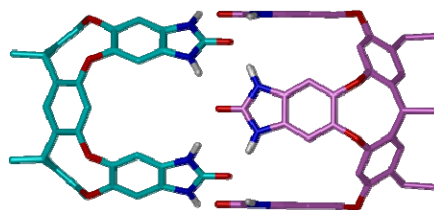


Figure 13: Rebek's cylindrical capsules.

The use of complementary hydrogen-bonded units allows the expansion of Rebek's cylindrical host length just by adding complementary building blocks. Glycoluril spacers provide the proper curvature, and up to 12 units can take part in the assembly allowing the inclusion of lengthly alkane chains. Specifically, *n*-tetradecane was the longest guest accommodated in the original capsule, whereas normal alkanes from C₁₅-C₁₉ were included into expanded assemblies.⁵¹

I.3 RECEPTORS FOR FULLERENES

Designing receptors for specific guests is a challenging topic in supramolecular chemistry.⁵² In the case of fullerenes, the goal is to maximize interactions with the host to obtain complexes with high association constants. For this reason, curved molecules, such as cyclodextrins⁵³ and calixarenes,⁵⁴ have been often employed in the construction of hosts for

⁵¹ a) Ajami, D.; Rebek, J., Jr. *J. Am. Chem. Soc.* **2006**, *128*, 5314-5315. b) Ajami, D.; Rebek, J., Jr. *Supramol. Chem.* **2009**, *21*, 103-106.

⁵² MacGillivray, L. R.; Atwood, J. L. *Angew. Chem. Int. Ed.* **1999**, *38*, 1018-1033.

⁵³ Anderson, T.; Nilsson, K.; Sundahl, M.; Westman, G.; Wennerström, O. *J. Chem. Soc., Chem. Commun.* **1992**, 604-606.

⁵⁴ a) Raston, C. L.; Atwood, J. L.; Nichols, P. J.; Sudria, I. B. N. *Chem. Commun.* **1996**, 2615-2616. b) Atwood, J. L.; Barbour, L. J.; Raston, C. L.; Sundria, I. B. N. *Angew.*

fullerenes.

Calix[8]arenes demonstrated to be efficient tools for C₆₀ precipitation and purification from mixtures,⁵⁵ but examples in which C₇₀ or even higher fullerenes are selectively encapsulated are rare. For example, *p*-homooxacalix[3]arenes reported by Komatsu showed preferential precipitation of C₇₀ over C₆₀, in 1:1 mixtures of fullerenes (Figure 14).⁵⁶

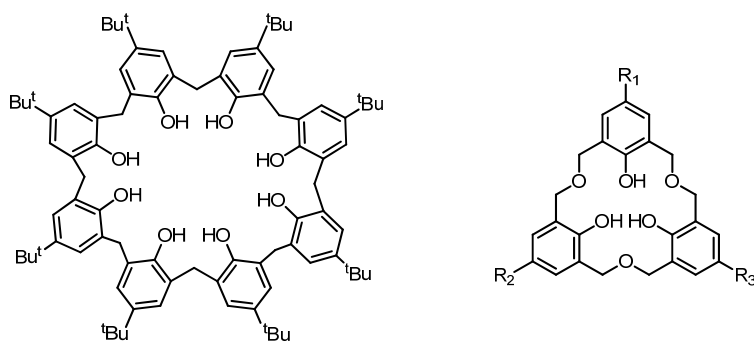


Figure 14: Atwood's calix[8]arene (left) and Komatsu's *p*-homooxacalix[3]arene (right).

Fukazawa *et al.* pointed out the formation of 1:1 complexes in solution between C₆₀ and calix[5]arenes bearing free OH in the lower rim, the strength of the assembly being modulated by the substitution in the upper rim.⁵⁷ However, these complexes exhibit a 1:2 (guest:host) stoichiometry in

Chem. Int. Ed. **1998**, *37*, 981-983. c) Atwood, J. L.; Barbour, L. J.; Heaven, M. W.; Raston, C. L. *Chem. Commun.* **2003**, 2270-2271. d) Atwood, J. L.; Barbour, L. J.; Heaven, M. W.; Raston, C. L. *Angew. Chem. Int. Ed.* **2003**, *42*, 3254-3257.

⁵⁵ a) Suzuki, T.; Nakashima, K.; Shinkai, S. *Chem. Lett.* **1994**, 699-702. b) Atwood, J. L.; Koutsantonis, G. A.; Raston, C. L. *Nature* **1994**, *368*, 229-231.

⁵⁶ Komatsu, N. *Org. Biomol. Chem.* **2003**, *1*, 204-209.

⁵⁷ Haino, T.; Yanase, M.; Fukazawa, Y. *Angew. Chem. Int. Ed.* **1997**, *36*, 259-260.

the solid state,⁵⁸ where two calixarenes were wrapping around the C₆₀ surface. In view of this result, Fukazawa's group designed a number of fullerene receptors based on bis-calix[5]arenes employing different strategies such as hydrogen bonding,⁵⁹ metal coordination,⁶⁰ or covalent linkage.⁶¹ All these receptors showed high affinities for fullerenes. Moreover, receptor size can be modulated by means of the spacer employed, so the selectivity can be shifted towards other fullerenes. For example, a double calix[5]arene container successfully extracts higher fullerenes, especially C₉₄ and C₉₆, from fullerene mixtures.⁶² Raising the temperature to more than 100 °C promotes a conformational *syn-anti* isomerization with release of the captured fullerene (Figure 15).

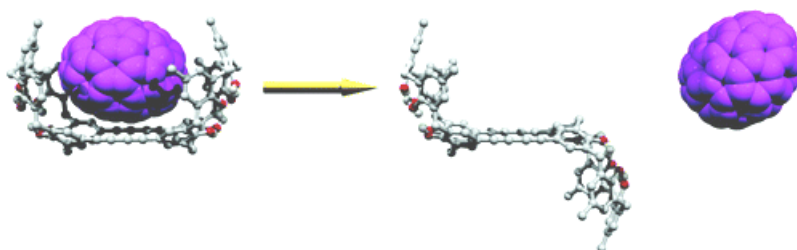


Figure 15: Model of *syn-anti* isomerization process and fullerene releasing of double calix[5]arene container. (Reproduced from ref. 62).

However, complexes presenting a 1:2 stoichiometry in solution are hardly

⁵⁸ Haino, T.; Yanase, M.; Fukazawa, Y. *Tetrahedron Lett.* **1997**, 38, 3739-3742.

⁵⁹ Haino, T.; Fukunaga, C.; Fukazawa, Y. *Tetrahedron Lett.* **1999**, 40, 2781-2784.

⁶⁰ a) Haino, T.; Araki, H.; Yamanaka, Y.; Fukazawa, Y. *Tetrahedron Lett.* **2001**, 42, 3203-3206. b) Haino, T.; Yamanaka, Y.; Haraki, H.; Fukazawa, Y. *Chem. Commun.* **2002**, 402-403.

⁶¹ a) Haino, T.; Yanase, M.; Fukazawa, Y. *Angew. Chem. Int. Ed.* **1998**, 37, 997-998. b) Haino, T.; Matsumoto, Y.; Fukazawa, Y. *J. Am. Chem. Soc.* **2005**, 127, 8936-8937. c) Haino, T.; Yanase, M.; Fukunaga, C.; Fukazawa, Y. *Tetrahedron* **2006**, 62, 2025-2035.

⁶² Haino, T.; Fukunaga, C.; Fukazawa, Y. *Org. Lett.* **2006**, 8, 3545-3548.

found in literature.^{55b,63} Our laboratory recently reported the synthesis of a receptor with an extended cavity based on a C,C-linked biscalix[4]arene.⁶⁴ It showed to form complexes in solution in which two units of the tweezer-like receptor were needed to wrap around fullerenes in a 2:1 “tennis ball” fashion. Moreover, this compound exhibit association constants for C₇₀ around one order of magnitude higher than for C₆₀ (Figure 16).

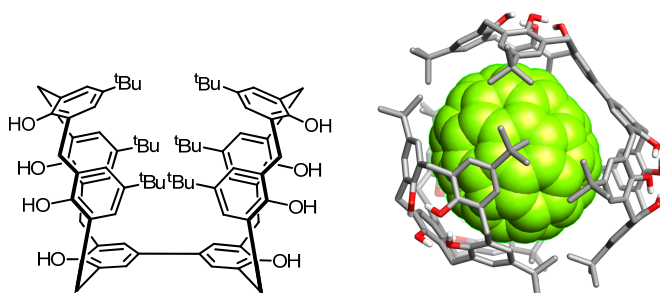


Figure 16: Structure of C,C-linked biscalix[4]arene (left) and molecular model of 1:2 C₇₀ complex (right).

In the early nineties, Atwood *et al.* reported the formation of so-called “ball and socket” complexes between cyclotrimeratrylene (CTV) and C₆₀.⁶⁵ These C₆₀@CTV complexes display a 1:1 stoichiometry in solution and form either 1:1 or 1:1.5 complexes in the crystalline state.⁶⁶ Since then some other

⁶³ a) Ikeda, A.; Yoshimura, M.; Udzu, H.; Fukuhara, C.; Shinkai, S. *J. Am. Chem. Soc.* **1999**, *121*, 4296-4297. b) Atwood, J. L.; Barbour, L. J.; Nichols, P. J.; Raston, C. L.; Sandoval, C. A. *Chem. Eur. J.* **1999**, *5*, 990-996. c) Ikeda, A.; Yoshimura, M.; Udzu, H.; Shinkai, S. *Tetrahedron* **2000**, *56*, 1825-1832. d) Claessens, C. G.; Torres, T. *Chem. Commun.* **2004**, 1298-1299.

⁶⁴ Iglesias-Sánchez, J. C.; Fragoso, A.; de Mendoza, J.; Prados, P. *Org. Lett.* **2006**, *8*, 2571-2574.

⁶⁵ Steed, J. W.; Junk, P. C.; Atwood, J. L. *J. Am. Chem. Soc.* **1994**, *116*, 10346-10347.

⁶⁶ Hardie, M. J.; Raston, C. L. *Chem. Commun.* **1999**, 1153-1163.

receptors based on the CTV scaffold were described, showing to form 1:1 or 1:2 complexes with fullerenes.⁶⁷ Matsubara *et al.* reported a series of CTV derivatives with aromatic pendants.⁶⁸ Although these receptors are able to complex both C₆₀ and C₇₀, they are selective for C₆₀. Indeed, a CTV receptor functionalized with three benzoate moieties was successfully employed in C₆₀ purification from fullerite. Additionally, the same group synthesized a cyclotrimeratrylenophane capsule whose elongated cavity showed to be better suited for C₇₀ encapsulation.⁶⁹

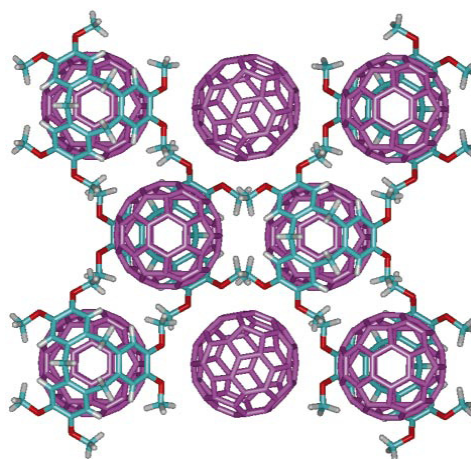


Figure 17: Crystal packing of C₆₀-CTV complex showing a 1:1.5 stoichiometry. (Reproduced from ref. 66).

Besides the classical concave molecules already mentioned, such as calixarenes or CTV, some other bowl-shaped molecules have demonstrated

⁶⁷ a) Felder, D.; Heinrich, B.; Guillon, D.; Nicoud, J.-F.; Nierengarten, J.-F. *Chem. Eur. J.* **2000**, *6*, 3501-3507. b) Nierengarten, J. F. *Fullerenes, Nanotubes and Carbon Nanostruc.* **2005**, *13*, 229-242.

⁶⁸ Matsubara, H.; Hasegawa, A.; Shiwaku, K.; Asano, K.; Uno, M.; Takahashi, S.; Yamamoto, K. *Chem. Lett.* **1998**, 923-924.

⁶⁹ Matsubara, H.; Oguri, S.-Y.; Asano, K.; Yamamoto, K. *Chem. Lett.* **1999**, 431-432.

to form stable complexes with fullerenes in solution, gas phase or in the solid state.⁷⁰ For instance, corannulene, an aromatic system composed of six aromatic rings fused to a central pentagonal ring was one of the first bowl-shaped molecules reported.⁷¹ Thus, its concave shape makes it an interesting candidate to geometrically complement the convex surface of fullerenes.⁷² Consequently, complexes with C₆₀ were observed for the first time in the gas phase in 1993.⁷³ Since then, some corannulene derivatives with extended aromatic surfaces have been reported.⁷⁴

Martín and coworkers have made pioneering contributions in the field of curved receptors for fullerenes using the π -extended tetrathiafulvalene⁷⁵ (ex-TTF) unit. A truxene derivative endowed with 1,3-dithiol subunits resulted in a bowl-shaped molecule that matches C₆₀ and C₇₀ not only in shape but also electronically.⁷⁶ Association constants reported for this receptor were in the range of 10³ M⁻¹. Even with relatively simple tweezers-like designs, composed by two exTTF units linked through an aromatic ring, strong complexes with

⁷⁰ Georghiou, P. E.; Dawe, L. N.; Tran, H.-A.; Strube, J.; Neumann, B.; Stammler, H.-G.; Kuck, D. J. *Org. Chem.* **2008**, *73*, 9040-9047.

⁷¹ Barth, W. E.; Lawton, R. G. *J. Am. Chem. Soc.* **1966**, *88*, 380-381.

⁷² Pérex, E. M.; Martín, N. *Chem. Soc. Rev.* **2008**, *37*, 1512-1519.

⁷³ Becker, H.; Javahery, G.; Petrie, S.; Cheng, P. C.; Schwarz, H.; Scott, L. T.; Bohme, D. K. *J. Am. Chem. Soc.* **1993**, *115*, 11636-11637.

⁷⁴ a) Mizyed, S.; Georghiou, P. E.; Bancu, M.; Cuadra, B.; Rai, A. K.; Cheng, P.; Scott, L. T. *J. Am. Chem. Soc.* **2001**, *123*, 12770-12774. b) Georghiou, P. E.; Tran, A. H.; Mizyed, S.; Bancu, M.; Scott, L. T. *J. Org. Chem.* **2005**, *70*, 6158-6163.

⁷⁵ 2-[9-(1,3-dithiol-2-ylidene)anthracen-10(9H)-ylidene]-1,3-dithiole. a) Yamasita, Y.; Kobayashi, Y.; Miyashi, T. *Angew. Chem. Int. Ed.* **1989**, *28*, 1052-1053. b) Bryce, M. R.; Moore, A. J.; Hasan, M.; Ashwell, G. J.; Fraser, A. T.; Clegg, W.; Hursthouse, M. B.; Karaulov A. I. *Angew. Chem. Int. Ed.* **1990**, *29*, 1450-1452.

⁷⁶ Pérez, E. M.; Sierra, M.; Sánchez, L.; Torres, M. R.; Viruela, R.; Viruela, P. M.; Ortí, E.; Martín N. *Angew. Chem. Int. Ed.* **2007**, *46*, 1847-1851.

C₆₀ were formed.⁷⁷ Very recently, Martín's group pointed out how the macrocyclic effect can increase the stability of fullerene complexes analogous to their tweezer-like receptors (Figure 18).⁷⁸

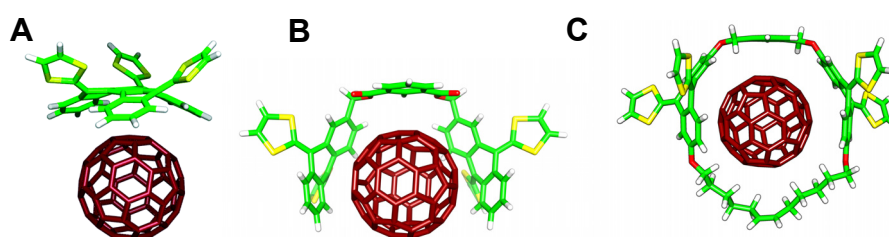


Figure 18: Curved receptors developed by Martín et al. a) Truxene-TTF receptor, b) tweezer-like receptor and c) macrocyclic receptor based on tweezer-like ones. (Reproduced from references 76, 77b and 78, respectively).

In contrast to curved receptors, planar structures, such as porphyrins, bind fullerenes very efficiently by a combination of two porphyrin units, and demonstrated that not always it is necessary to match a concave host with a convex guest. Actually, receptors based on porphyrin-fullerene donor-acceptor interactions have dominated the literature so far.⁷⁹ Thus, Reed and Boyd reported a series of jaw-like receptors that bind C₆₀ and C₇₀.⁸⁰ The X-

⁷⁷ a) Pérez, E. M.; Sánchez, L.; Fernández, G.; Martín, N. *J. Am. Chem. Soc.* **2006**, *128*, 7172-7173. b) Pérez, E. M.; Capodilupo, A. L.; Fernández, G.; Sánchez, L.; Viruela, P. M.; Viruela, R.; Ortí, E.; Bietti, M.; Martín, N. *Chem. Commun.* **2008**, 4567-4569. c) Gayathri, S. S.; Wielopolski, M.; Pérez, E. M.; Fernández, G.; Sánchez, L.; Viruela, R.; Ortí, E.; Guldi, D. M.; Martín, N. *Angew. Chem. Int. Ed.* **2009**, *48*, 815-819.

⁷⁸ Isla, H.; Pérez, E. M.; Gallego, M.; Viruela, R.; Ortí, E.; Martín, N. *J. Am. Chem. Soc.* **2010**, *132*, 1772-1773.

⁷⁹ Tashiro, K.; Aida, T. *Chem. Soc. Rev.* **2007**, *36*, 189-197.

⁸⁰ a) Sun, D.; Tham, F. S.; Reed, C. A.; Chaker, L.; Boyd, P. D. W. *J. Am. Chem. Soc.* **2002**, *124*, 6604-6612. b) Hosseini, A.; Taylor, S.; Accorsi, G.; Armaroli, N.; Reed, C. A.; Boyd, P. D. W. *J. Am. Chem. Soc.* **2006**, *128*, 15903-15913.

ray analysis of some structures revealed that the “double bond” at the 6:6 ring juncture of C_{60} or C_{70} was attracted to the metal or the protic center of the free-base porphyrin. In addition, binding affinities were dictated by the metal employed.

Doubtless, the most efficient porphyrin-based receptors are Aida's cages. These macrocycles are composed of two porphyrin units held together by a flexible chain that allows the macrocyclic host to adapt to the fullerene in the inclusion complex.⁸¹ Moreover, the metal strongly influences the association constant, raising values up to 10^8 M^{-1} when iridium porphyrins were used in the complexation of either C_{60} or C_{70} . Actually, this receptor features the largest association constants with fullerenes reported to date (Figure 19).⁸²

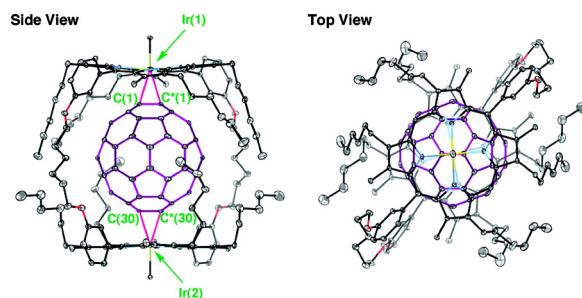


Figure 19: X-ray structure (side and top views) of C_{60} encapsulated into an Ir bis-porphyrin macrocycle. (Reproduced from ref. 82).

Interestingly, Aida's macrocyclic porphyrin host containing zinc as the metal have been employed to successfully extract fullerenes higher than C_{76} directly from fullerite, allowing the enrichment of rare fullerenes (C_{102} –

⁸¹ Tashiro, K.; Aida, T.; Zheng, J.-Y.; Kinbara, K.; Saigo, K.; Sakamoto, S.; Yamaguchi, K. *J. Am. Chem. Soc.* **1999**, *121*, 9477-9478.

⁸² Yanagisawa, M.; Tashiro, K.; Yamasaki, M.; Aida, T. *J. Am. Chem. Soc.* **2007**, *129*, 11912-11913.

C₁₁₀) after several extraction runs.⁸³

I.4 OBJECTIVES OF THIS THESIS

The present work has been divided in two main topics: one concerning the synthesis and aggregation studies of hydrogen-bonded two-dimensional assemblies, and a second one related to self-assembled capsules and receptors for fullerenes.

Within the project involving two dimensional aggregates, 2-ureidopyrimidinones have been chosen as self-complementary hydrogen bonding motif. Thus:

- The synthesis of a number of dimers **1** will be depicted and an insight into its solubility behaviour will be discussed.
- In order to create hydrogen-bonded aggregates of different sizes, the synthesis of bis-ureidopyrimidinones linked through different spacers such as adamantyl **3** and the *m*-disubstituted aromatic ring **4**, as well as a fully preorganized "V-shaped" bis-UPy **2** will be described and the aggregation behaviour in solution will be studied (Figure 20).

⁸³ Shoji, Y.; Tashiro, K.; Aida, T. *J. Am. Chem. Soc.* **2004**, *126*, 6570-6571.

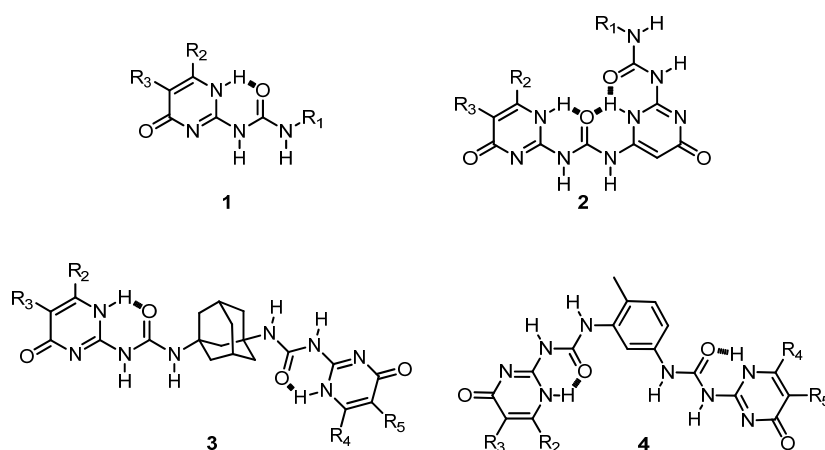


Figure 20: Proposed structures for two dimensional aggregates.

Regarding the second topic, dealing with CTV-based architectures for fullerenes (see Figure 21 for structures):

- The synthesis of a number of CTV-based molecules bearing three hydrogen bonding UPy units (CTV-UPy **5**) able to form capsules for fullerenes will be described.
- Reversible encapsulation of fullerenes in dimers of compound **5** will be studied in solution. On the basis of fullerene recognition and complexation properties, a method for fullerene (C_{70} and C_{84}) separation and purification will be developed.
- A receptor based on a CTV scaffold endowed with three exTTF units (CTV-exTTF, **6**) will be synthesized. Its abilities to bind fullerenes in solution will be studied by techniques such as NMR spectroscopy, mass spectrometry or UV-vis spectroscopy. Additionally, the existence of charge separated states will be studied by EPR techniques.
- Based on the design of CTV-UPy capsules, the synthesis of

Chapter I

carceplexes like compound **7**, containing fullerenes within its interior will be attempted. The properties of incarcerated fullerenes will be studied electrochemically.

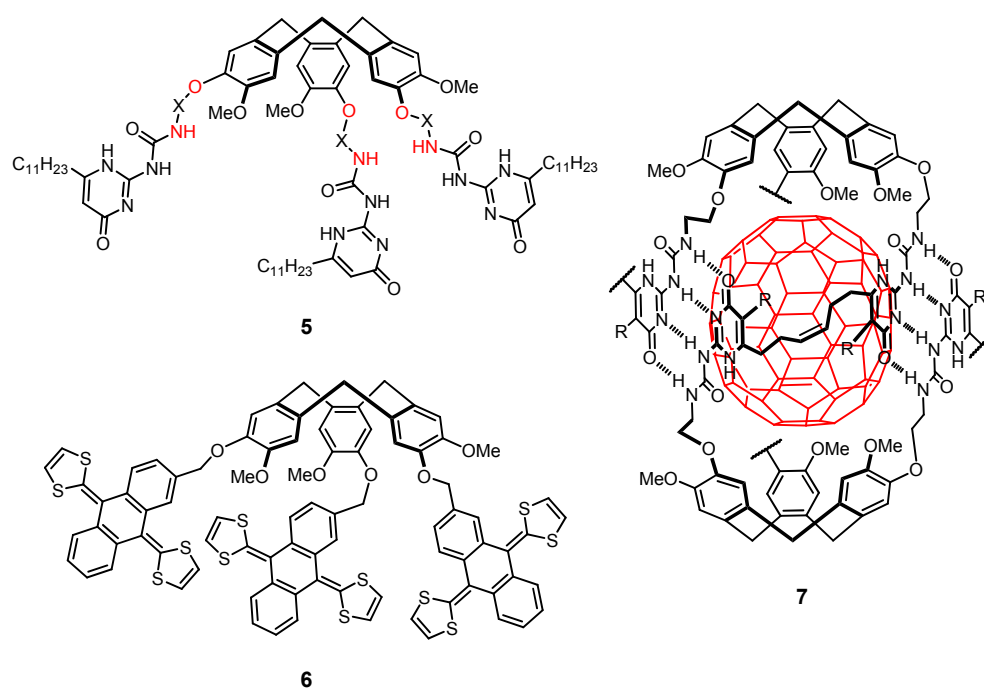


Figure 21: Proposed structures for fullerene recognition and complexation.

UNIVERSITAT ROVIRA I VIRGILI
SELF-ASSEMBLY BASED ON THE 2-UREIDO-4(1H)-PYRIMIDINONE MOTIF: FROM CYCLIC ARRAYS TO MOLECULAR CAPSULES
FOR FULLERENE SEPARATIONS
Elisa Huerta Martínez
DL:T.289-2012

CHAPTER II:

2D MOLECULAR ARCHITECTURES BASED ON THE UP_y DIMERIC MOTIF

Part of this chapter has been published: Hahn, U.; González, J. J.; Huerta, E.; Segura, M.; Eckert, J.-F.; Cardinali, F.; de Mendoza, J.; Nierengarten, J.-F. *Chem. Eur. J.* **2005**, *11*, 6666-6672.

UNIVERSITAT ROVIRA I VIRGILI
SELF-ASSEMBLY BASED ON THE 2-UREIDO-4(1H)-PYRIMIDINONE MOTIF: FROM CYCLIC ARRAYS TO MOLECULAR CAPSULES
FOR FULLERENE SEPARATIONS
Elisa Huerta Martínez
DL:T.289-2012

CHAPTER II: 2D MOLECULAR ARCHITECTURES BASED ON THE UPy DIMERIC MOTIF

II.1 TWO DIMENSIONAL ASSEMBLIES

By a suitable choice of the length, shape and rigidity of the spacer between the two UPy subunits it would be possible to obtain higher aggregates of defined structures such as rosettes, belts or tubes.¹

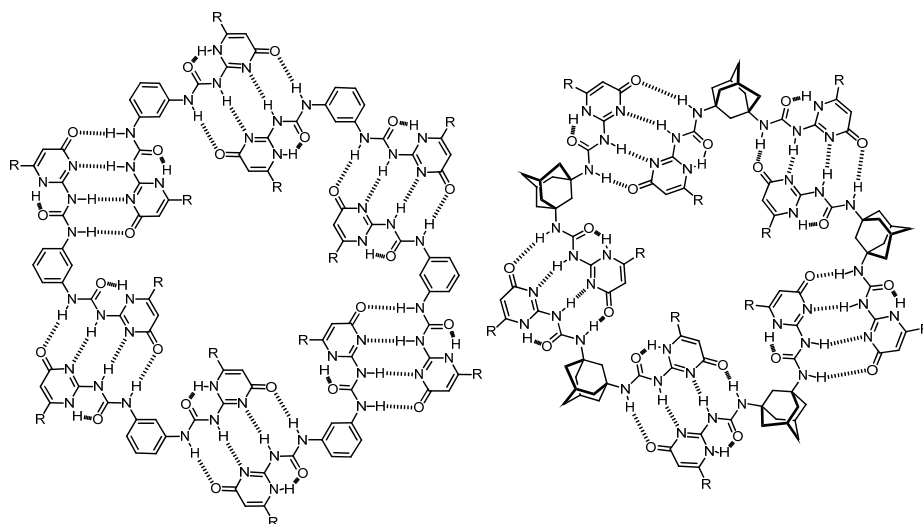


Figure 1: Schematic representation of hexameric and pentameric rosettes.

Thus, use of *m*-disubstituted aromatic spacers would result in hexameric rosettes, induced by the 120° angle between both substituents, whereas pentameric rosettes are likely for 1,3-adamantyl, *cis*-1,3-cyclohexyl, bis-arylmethane or other spacers based on sp³ hybridized carbon scaffolds,

¹ a) Söntjes, S. H. M.; Sijbesma, R. P.; van Genderen, M. H. P.; Meijer, E. W. *Macromolecules* **2001**, *34*, 3815-3818. b) Keizer, H. M.; Ramzi, A.; Sijbesma, R. P.; Meijer, E. W. *Polymer Preprints* **2003**, *44*, 596-597.

where an angle of 109.5° is present (the inner angle of a regular pentagon is 108°) (Figure 1). However, competition with ladder-like, polymeric aggregates is a major concern. In fact, two different linear polymers can be predicted (Figure 2a-b). For cycle formation, the two UPy subunits should be oriented in opposite conformations, and a way to prevent linear self-assembly is to attach a substituent R (such as methyl) in the spacer in the appropriate position (Figure 2c).

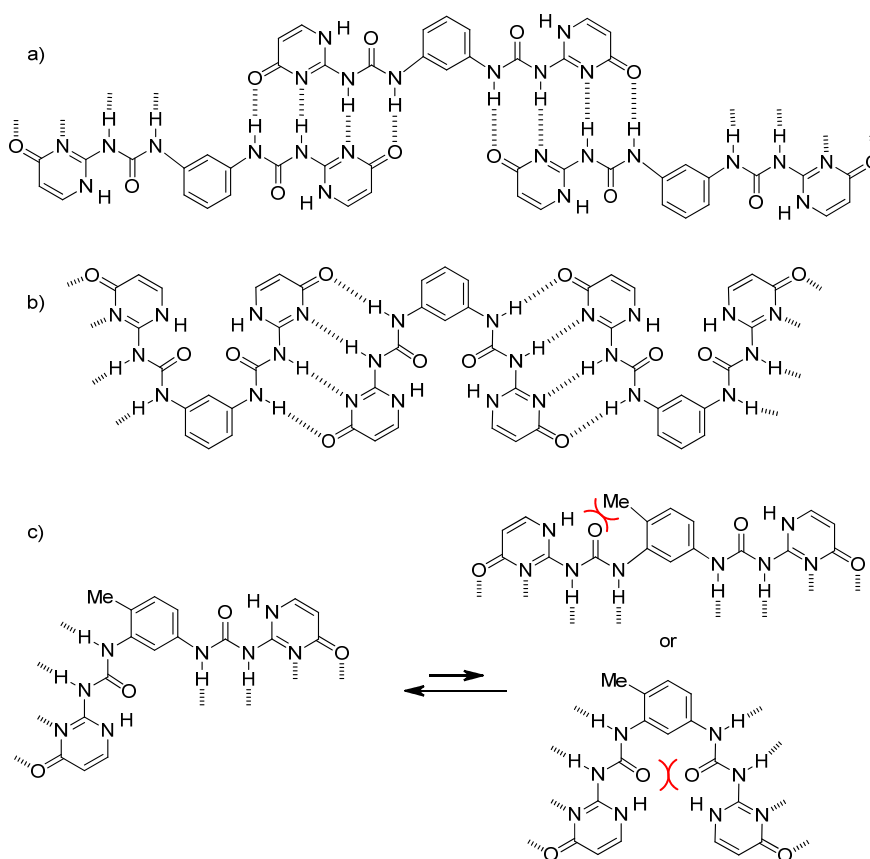


Figure 2: a-b) Predictable linear polymers based on a bis-ureidopyrimidinone with *m*-phenylene spacer. c) A strategy to prevent tapes.

As an initial insight into the self-assembling behaviour of double ureidopyrimidinones we have prepared a number of UPys (**1**) to study their

aggregation into dimers (**1**)₂ and the ideal substituents to optimize solubility. Then, the synthesis of compound **2**, a more rigid structure endowed with two ureidopyrimidinone edges for self-assembly, will be described and its aggregates studied. Additionally, bis-ureidopyrimidinones **3** and **4** with a rigid central 1,3-adamantyl and *m*-phenylene spacer, respectively, will also be prepared and studied. According to the angles, the corresponding rosette-like aggregates should be of type (**3**)₅ and (**4**)₆. In the latter series, substituents at the inner side of the rosette contain additional hydrogen-bonding motifs to stabilize the cyclic form (Figure 3).

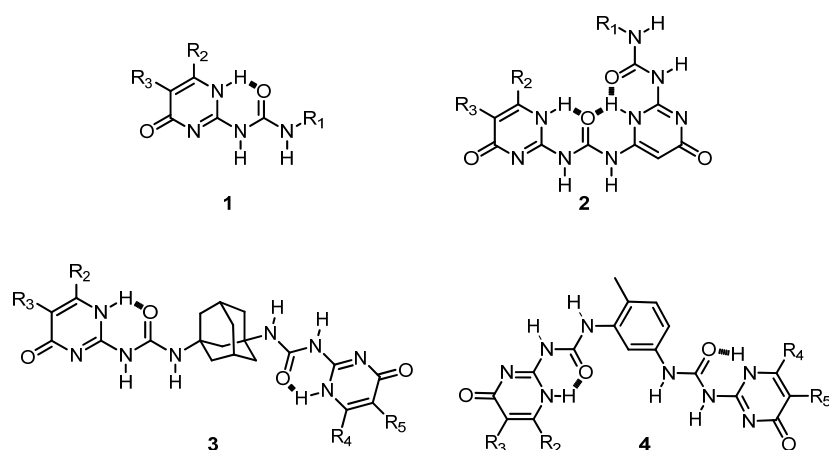
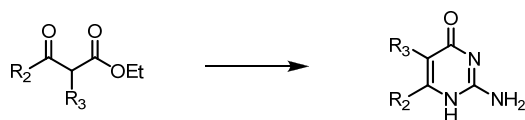


Figure 3: Schematic representation of compounds **1-4** (substituents R₁₋₅ will be shown along the chapter).

II.2 SYNTHESIS AND INSIGHTS INTO SOLUBILITY OF UPys

II.2.1 Synthesis of 2-aminopyrimidin-4-ones

The synthesis of 2-aminopyrimidin-4-ones has been accomplished in all cases by condensation of a β -ketoester with guanidinium carbonate (Scheme 1).² The substitution of the heterocycle is determined by the substituents of the β -ketoester.



Scheme 1: General approach to 2-aminopyrimidin-4-one synthesis.

The corresponding β -ketoesters were obtained by γ - or α -alkylation of ethyl acetoacetate, α -formylation of the appropriate esters or α -esterification of ketones (crossed-Claisen ester condensations). The wide range of reactions that can be carried out with these substrates allowed us to obtain pyrimidinones with a broad range of substituents at either 5 and/or 6 position.³

Thus, γ -alkylation^{4,5} of ethyl acetoacetate led to aminopyrimidinones substituted at position 6 of the ring while 5- or 5,6-disubstituted ones were

² Beijer, F. H.; Sijbesma, R. P.; Kooijman, H.; Speck, A. L.; Meijer, E. W. *J. Am. Chem. Soc.* **1998**, *120*, 6761-6769.

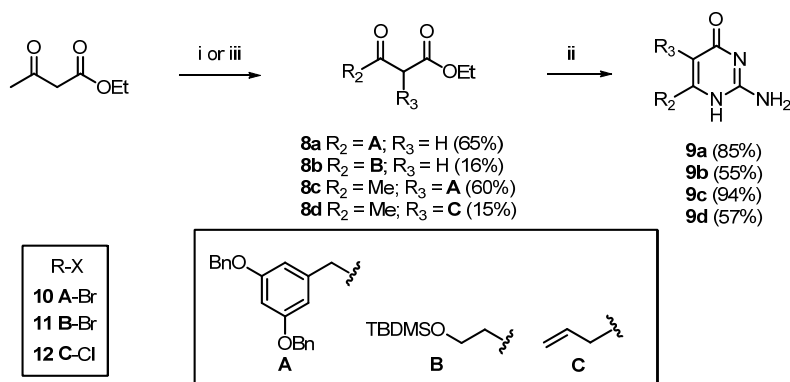
³ Numbers refer to tautomer 4-[1H]-pyrimidinone. See introductory chapter for a discussion on ureidopyrimidinone tautomerism.

⁴ Sum, F. W.; Weiler, L. *Can. J. Chem.* **1979**, *57*, 1431-1441.

⁵ Jamie, J. F.; Rickards, R. W. *J. Chem. Soc., Perkin Trans. 1* **1996**, 2603-2613.

prepared by α -alkylation^{6,7} of the same starting material (Scheme 2).

β -Ketoesters **8a** and **8b** were synthesized by treating ethyl acetoacetate with two equivalents of freshly prepared LDA to get the dienolate, which was subsequently reacted with one equivalent of the appropriate halide **10**⁸ and **11**.⁹ In this way, **8a** and **8b** were obtained in 65% and 16% yields respectively. The low isolated yield of the latter may be caused by the troublesome purification of the compound. The β -ketoesters were then condensed with guanidinium carbonate affording aminopyrimidinones **9a** and **9b** in 85% and 55% yields respectively (Scheme 2).



i) LDA (2eq.), THF, 0 °C, 20 min., then R-X (**10** or **11**), 2 h; ii) guanidinium carbonate, EtOH, 80 °C; iii) NaOEt, THF, r. t., then R-X (**10** or **12**), reflux, 3 h.

Scheme 2: Pyrimidinones obtained by alkylation of ethyl acetoacetate.

⁶ Lee, H.-S.; Park, J.-S.; Kim, B. M.; Gellman, S. H. *J. Org. Chem.* **2003**, *68*, 1575-1578.

⁷ Zhu, J.; You, L.; White, B. J.; Zhao, S. X.; Skonezny, P. M. *patent 6,620,600 B2, US*, **2003**.

⁸ Compound **10** was obtained in 95% yield by bromination of 3,5-bis(benzyloxy)benzyl alcohol with PBr₃ and Et₃N, as described in the literature: a) Forier, B.; Dehaen, W. *Tetrahedron* **1999**, *55*, 9829-9846. b) Andrus, M. B.; Liu, J.; Meredith, E. L.; Nartey, E. *Tetrahedron Lett.* **2003**, *44*, 4819-4822. c) Andrus, M. B.; Meredith, E. L. *patent WO 01/60774 A1*, **2001**.

⁹ Purchased from Sigma-Aldrich.

The β -ketoester precursors of aminopyrimidinones **9c** and **9d** were synthesized via α -alkylation of ethyl acetoacetate (Scheme 2). In this case, an excess of the reagent is necessary to obtain the carbanion under kinetic control (by using sodium ethoxide as a base) and to avoid a double alkylation process in the α -position. The excess ethyl acetoacetate can be recovered by simple distillation. A solution of the appropriate halide (**10** or **12**) was subsequently added to the carbanion and the reaction mixture was refluxed, affording **8c** and **8d**¹⁰ in 60% and 15% yields respectively. Finally, the condensations with guanidinium carbonate led to derivatives **9c** and **9d** in good yields.

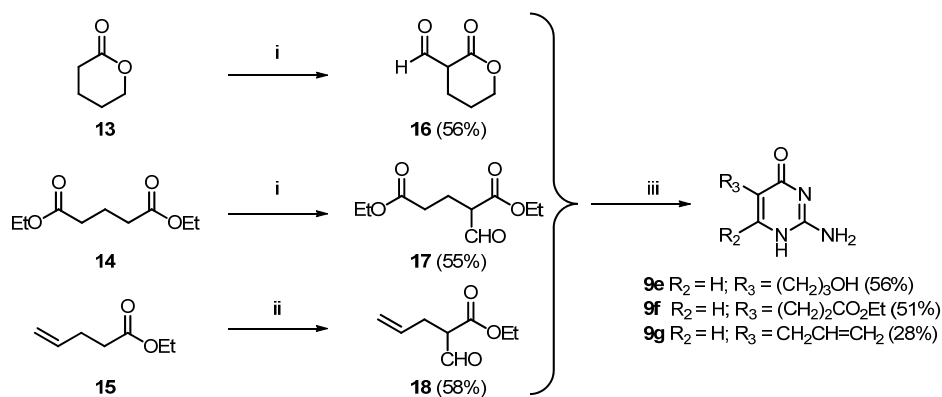
β -Ketoesters could also be obtained through crossed-Claisen ester condensations in two different ways: a crossed-Claisen condensation between an ester and ethyl formate (α -formylation of esters), or a condensation between a ketone and diethyl carbonate (α -esterification of ketones), the former giving rise to aminopyrimidinones substituted only at position 5. The general approach consists of the treatment of the ester with a strong base, followed by the addition of ethyl formate. Acid treatment is required subsequently to obtain the corresponding 3-oxo ester. In this way, β -ketoesters **16**,¹¹ **17**,¹² and **18**¹³ were obtained in moderate yields and used as precursors of aminopyrimidinones **9e-g**, which were obtained by a similar procedure as described before (Scheme 3).

¹⁰ a) Kenji, M.; Masaya, I. *Tetrahedron* **1987**, *43*, 45-58. b) Piva, O. *Tetrahedron* **1994**, *50*, 13687-13696.

¹¹ Harmon, A. D.; Hutchinson, R. J. *Org. Chem.* **1975**, *40*, 3474-3480.

¹² Wrigglesworth, R.; Inglis, W. D.; Livingstone, D. B.; Suckling, C. J.; Wood, H. C. S. *J. Chem. Soc., Perkin Trans. 1* **1984**, 959-963.

¹³ Durrwachter, J. R.; Wong, C.-H. *J. Org. Chem.* **1988**, *53*, 4175-4181.



i) NaH, Et₂O, ethyl formate, r.t., 12 h, then H⁺; ii) LDA (1 eq.), THF, -78 °C; 10 min., then ethyl formate, THF, -78 °C, 1 h; iii) guanidinium carbonate, EtOH, reflux, overnight.

Scheme 3: Aminopyrimidinones obtained by α -formylation of esters.

Compound **9g** constitutes an example for which two tautomeric forms of the pyrimidinone ring are clearly seen and differentiated in the ¹H NMR spectrum (Figure 4). Other complementary experiments, such as ¹³C NMR, COSY, HMBC and HMQC, can be performed in order to correctly assign the corresponding tautomers. In this case, the 6-[1H] tautomer - the major compound (70%) - and the enol tautomer - the minor one (30%) - were thought to be the most probable structures according to the signals found in the spectra.

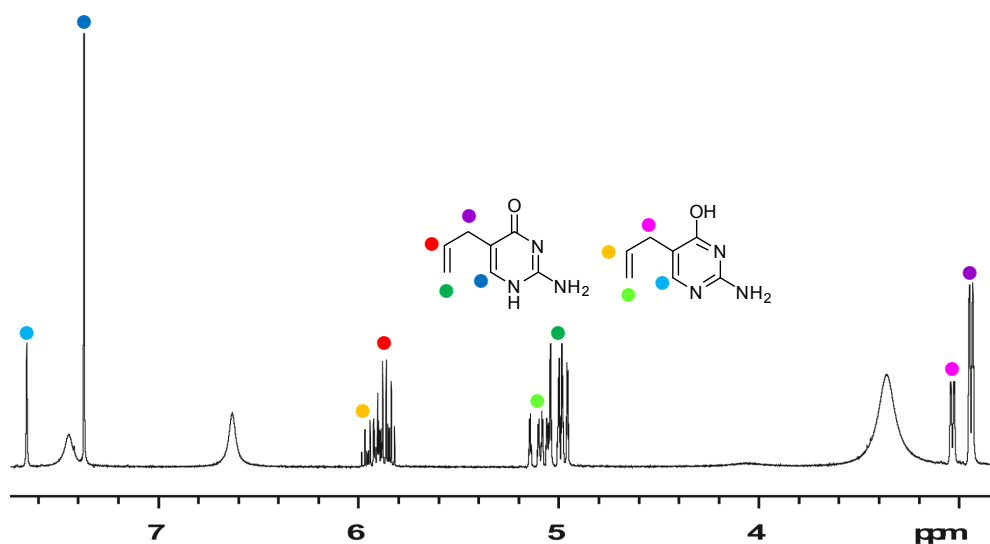


Figure 4: ^1H NMR ($\text{DMSO-}d_6$, 400 MHz) spectrum of compound **9g**.

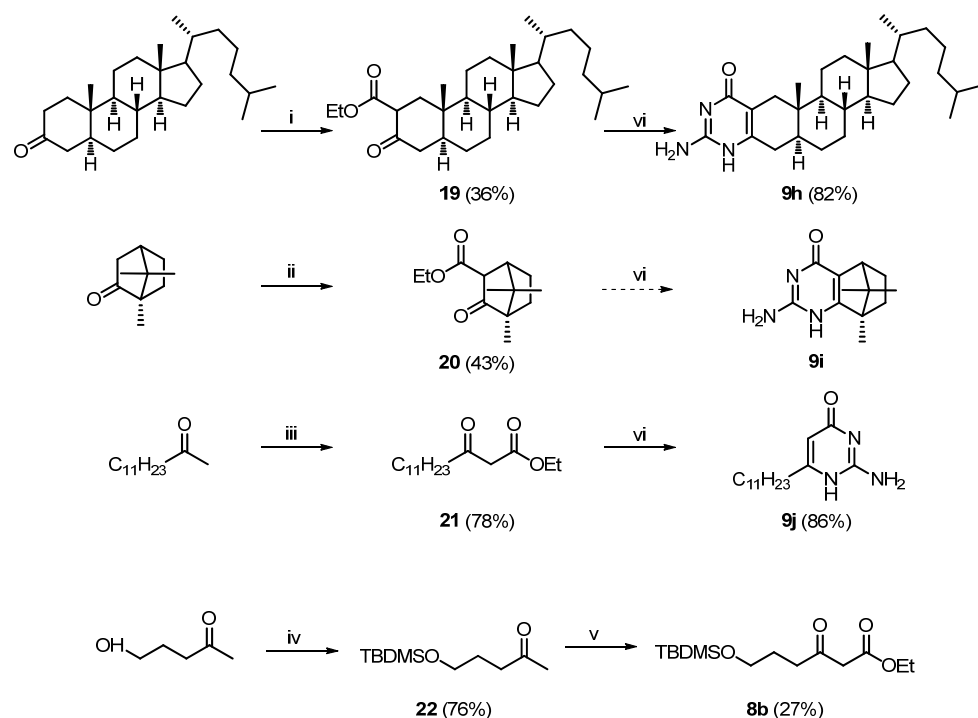
In a similar way as described above, the Claisen condensation between ketones and diethyl carbonate was employed to obtain β -ketoesters such as **19**,¹⁴ **20**,¹⁵ and **21**¹⁶ in yields ranging from moderate to good (Scheme 4). In all cases, sodium hydride was used as base for the α -deprotonation of the ketone. Similarly, the corresponding pyrimidinones **9h** and **9j** were obtained in good yields.¹⁷

¹⁴ Mikulás, M.; Möller, C.; Rust, S.; Wierchem, F.; Armhein, P.; Rück-Braun, K. *J. Prakt. Chem.* **2000**, *342*, 791-803.

¹⁵ a) Paquette, L. A.; Dahnke, K.; Doyon, J.; He, W.; Wyant, K.; Friedrich, D. *J. Org. Chem.* **1991**, *56*, 6199-6205. b) Shumway, W. W.; Kent Dalley, N.; Birney, D. M. *J. Org. Chem.* **2001**, *66*, 5832-5839.

¹⁶ Keizer, H. M.; González, J. J.; Segura, M.; Prados, P.; Sijbesma, R. P.; Meijer, E. W.; de Mendoza, J. *Chem. Eur. J.* **2005**, *11*, 4602-4608.

¹⁷ Compound **9i** could not be obtained after condensation reaction with guanidinium carbonate, probably due to the highly tensioned bonds.



i) NaH, diethyl carbonate, benzene, reflux, 4 h, then H⁺; ii) NaH, THF, reflux, 30 min., then diethyl carbonate, THF, reflux, 12 h; iii) NaH, diethyl carbonate, THF, reflux, 2 h; iv) TBDMSCl, imidazole, DMF, 70 °C, 24 h; v) NaH, THF, reflux, 30 min., then diethyl carbonate, THF, reflux, 12 h; vi) guanidinium carbonate, EtOH, reflux, overnight.

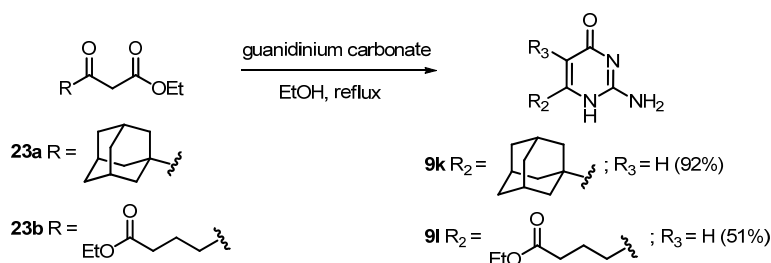
Scheme 4: Pyrimidinones obtained by α -esterification of ketones.

In order to improve the yield of the isolated compound, **8b** was also synthesized following this approach (Scheme 4). The hydroxy group of commercially available 5-hydroxy-2-pentanone was first protected as *tert*-butyldimethylsilyl ether following a procedure described in the literature.¹⁸ Ketone **22** was subsequently treated with diethyl carbonate in the presence of NaH to afford compound **8b** in 27% yield. However, this yield was only slightly higher than the one obtained by direct γ -alkylation of ethyl

¹⁸ Chiarello, J.; Joullié, M. M. *Tetrahedron* **1988**, *44*, 41-48.

acetoacetate (16%, Scheme 2), due again to difficulties in the purification.

Other pyrimidinones such as **9k**¹⁹ and **9l** have also been obtained, in good yields, from commercially available β -ketoesters **23a-b** (Scheme 5).



Scheme 5: Synthesis of pyrimidinones **9k-l**.

In summary, pyrimidinones with a wide scope of substituents in positions 5 and/or 6 can be prepared, as the result of the large number of reactions available to obtain the β -ketoester precursors.

II.2.2 Synthesis of 2-Ureidopyrimidiones and Solubility Studies

A major problem with ureidopyrimidinones (as well as with their aminopyrimidinone precursors), aimed at forming higher order aggregates, is their poor solubility in aprotic apolar solvents such as dichloromethane or chloroform, which requires the introduction of suitable substituents.² However, the design of discrete aggregates, such as cyclic rosettes, does not allow the use of lengthy or highly branched substituents in the inner part of the aggregate, and this makes the selection of the proper substituent a challenging choice. Thus, a number of 2-ureidopyrimidinone dimers, properly functionalized, were synthesized from aminopyrimidinones **9c**, **9k**, and **9l**

¹⁹ Orzeszko, B.; Kazimierczuk, Z.; Maurin, J. K.; Laudy, A. E.; Starosciak, B. J.; Vilpo, J.; Vilpo, L.; Balzarini, J.; Orzeszko, A. *Il Farmaco* **2004**, *59*, 929-937.

(Scheme 2 and 5 respectively).

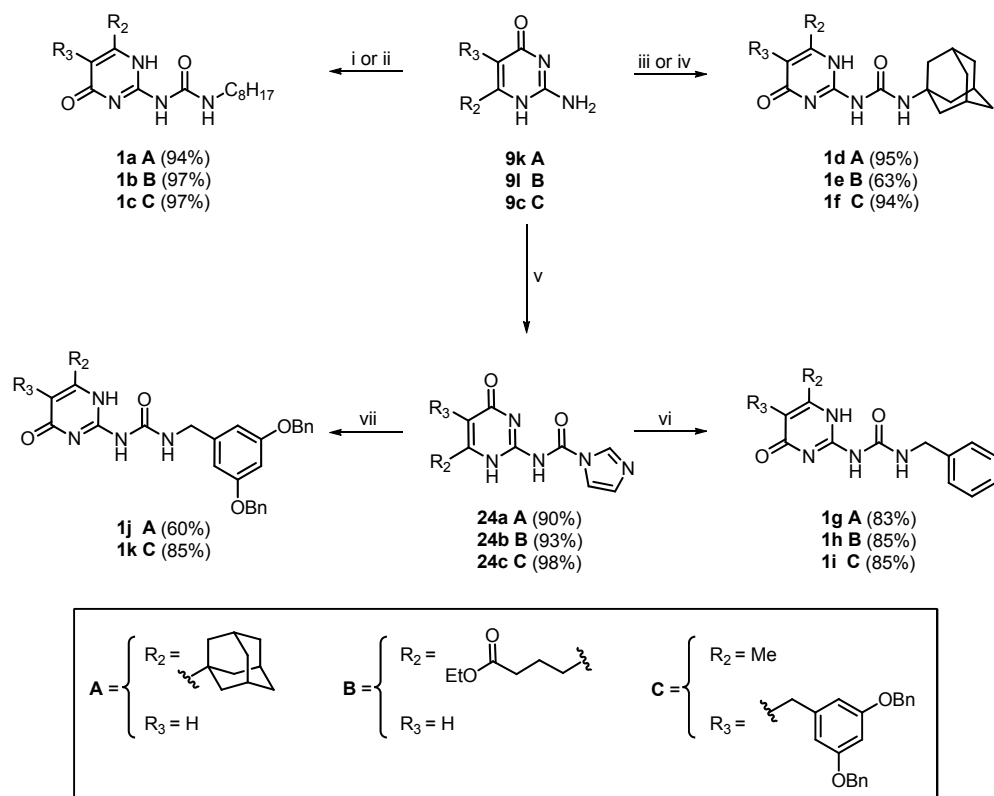
Two different approaches were used for the synthesis. For instance, aminopyrimidinones **9k** and **9c** were reacted with octyl isocyanate, in the presence of an excess of triethylamine, affording compounds **1a** and **1c** respectively, in yields higher than 90% (Scheme 6). In the same way, when **9k** and **9c** reacted with adamantyl isocyanate, ureidopyrimidinones **1d** and **1f** were obtained, also in high yields. Finally, compound **9l** was reacted with both isocyanates in a THF/DMF mixture in the absence of base, to yield octyl- (**1b**) and adamantyl-urea (**1e**) derivatives in 97% and 63% yields respectively (Scheme 6).

The synthesis of the remaining ureidopyrimidinones proceeded through the corresponding isocytosines **24a-c**, which were prepared from aminopyrimidinones **9k**, **9l** and **9c**, suspended in a small amount of dry THF or CH₂Cl₂, and 1,1'-carbonyldiimidazole (CDI) as activating agent.²⁰ The intermediate imidazolides **24a-c** were obtained in good yields (Scheme 6), and these compounds were able to react with amines to form the desired ureidopyrimidinones.

Thus, benzylamine was reacted with **24a-c** in dichloromethane, and the corresponding ureidopyrimidinones **1g-i** were obtained in good yields after 4 hours at 50 °C. However, for the sterically hindered amine **26**,²¹ synthesized from the phthalimide derivative **25** (Scheme 7), the reaction required 12 hours at the same temperature and yields were slightly lower. Finally, ureidopyrimidinones **1j** and **1k** were obtained in 85% and 60% yields respectively (Scheme 6).

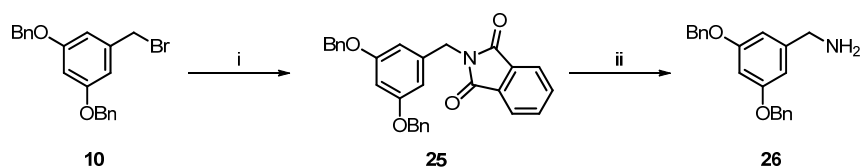
²⁰ Keizer, H. M.; Sijbesma, R. P.; Meijer, E. W. *Eur. J. Org. Chem.* **2004**, 2553-2555.

²¹ van Bomel, K. J. C.; Metselaar, G. A.; Verboom, W.; Reinhoud, D. N. *J. Org. Chem.* **2001**, *66*, 5405-5412.



i) octyl isocyanate, toluene, Et₃N, 80 °C, overnight; ii) octyl isocyanate, THF/DMF (2:1), 60 °C, 2 days; iii) adamantyl isocyanate, toluene, Et₃N, 80 °C, overnight; iv) adamantyl isocyanate, THF/DMF (2:1), 60 °C, 2 days; v) CDI, THF or CH₂Cl₂, r.t., 3 h to 8 h; vi) benzylamine, CH₂Cl₂, 50 °C, 4 h; vii) **26**, CH₂Cl₂, 50 °C, 12 h.

Scheme 6: Synthesis of ureidopyrimidinones **1a-k**.



i) potassium phthalimide, DMF, 80 °C, 2 h; ii) hydrazine monohydrate, EtOH, reflux, 2 h, then KOH 20%.

Scheme 7: Synthesis of amine derivative **26**.

These new ureidopyrimidinones formed dimers in apolar organic solvents, as indicated the ^1H NMR spectra in chloroform (Figure 5). Thus, signals corresponding to the NH protons were downfield shifted, accounting for the formation of strong hydrogen bonds in the dimer.

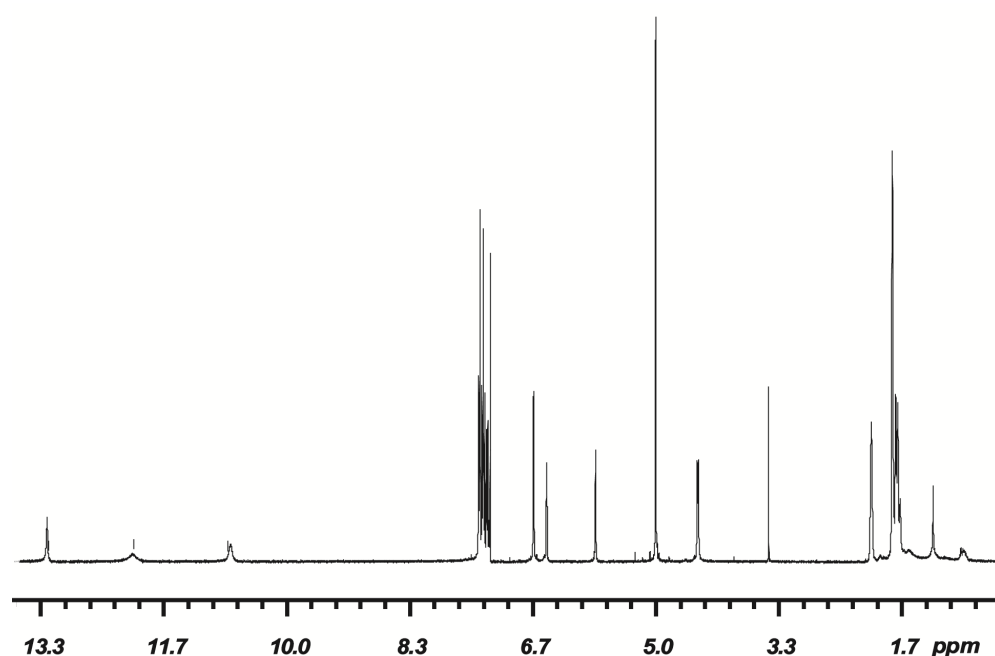


Figure 5: ^1H NMR (CDCl_3 , 400 MHz) spectrum of compound **1j·1j**.

Furthermore, MALDI-TOF and even ESI mass spectra (only at high concentration, for the most soluble favorable cases) showed both the molecular masses of the monomer, at m/z 561.2 $[(\text{M}+\text{H})^+]$ and the dimer at m/z 1121.5 $[(\text{M}+\text{H})^+]$.

It has to be noted that all dimers with an adamantyl substituent at the urea showed a significant content of the tautomeric ureidopyrimidin-4-ol dimer in chloroform. Figure 6 shows the NH signals for a mixture of *keto* and *enol* forms for UPy **1d·1d**. This behavior was also observed in dimers **1e·1e** and **1f·1f**, but not in the ones where the adamantyl group was on the

pyrimidinone ring (*i.e.* compounds **1a-1a**, **1g-1g**, and **1j-1j**).

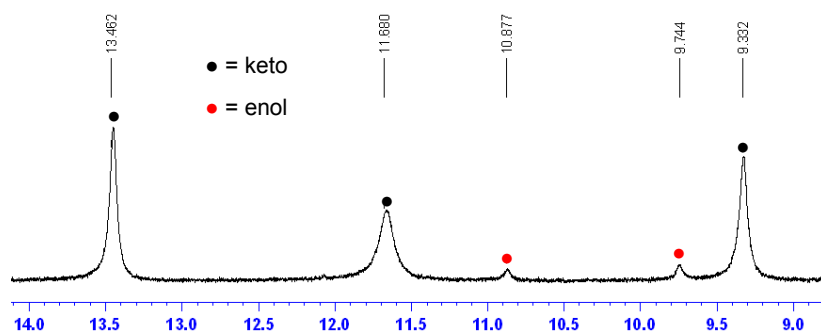
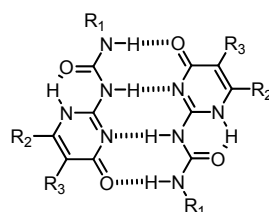


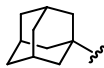
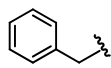
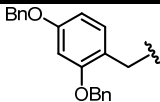
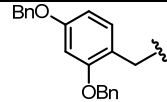
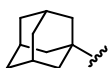
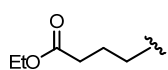
Figure 6: Partial ¹H NMR (400 MHz, CDCl₃) spectrum of **1d·1d** showing the NH's region.

Once all ureidopyrimidinones were synthesized, their solubility in aprotic apolar solvents was determined. The solvent of choice for this solubility study was dichloromethane that fulfills the requirements previously indicated.

To evaluate solubilities, saturated solutions of each ureidopyrimidinone were prepared. After filtration, a known volume was taken and evaporated to dryness. The residue was dried under vacuum for two days and then weighted in an analytical balance. The results (expressed in molar concentration) are shown in Table 1.

Table 1: Solubility (mol/L) of ureidopyrimidinone dimers in dichloromethane.



		R ₁ →			
R ₂	R ₃	C ₈ H ₁₇ -			
Me		0.0948	0.0045	0.0336	0.0275
	H	0.2132	0.0059	0.0240	0.0673
	H	0.2742	0.064	0.1013	--

Long alkyl chains attached to the urea provide very good solubilities, whereas adamantyl substituents decrease the solubility by at least a factor of ten. Moreover, this substituent at R₁ favors the presence of the undesired *enol* dimer. On the other hand, in the pyrimidinone moiety, the ester group gives rise to the most soluble compounds, even in the case of the adamantyl urea, which is more than ten times more soluble than the other adamantyl ureidopyrimidinones.

From this study it is possible to establish an order in the different substituents used that helps to predict the best combination for optimal solubility (Figure 7).

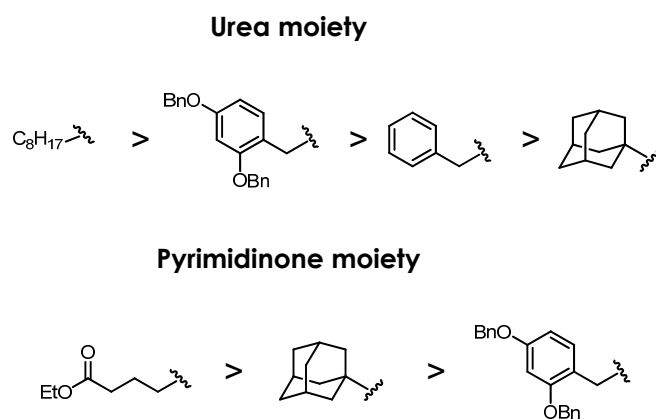
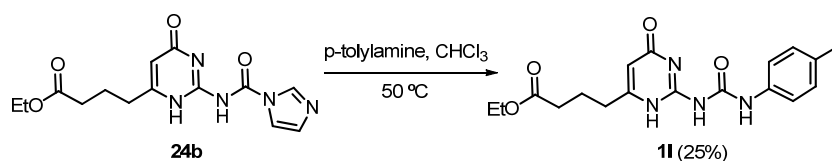


Figure 7: Substituents in decreasing order of solubility.

Since one of the goals was the synthesis of a planar hexameric rosette, which requires an aromatic linker in the urea moiety between the two pyrimidinones to form the bis-UPy (see Figure 1), a new urea substituent was tested on the light of the results obtained so far.

The available space inside the rosette restricts the size of the substituents at the pyrimidinone inner part of the aggregate, whereas those at the outer part and at the spacer (except at the position between the two UPy moieties) should contain longer or even branched chains. Thus, we decided to synthesize a new collection of ureidopyrimidinones using *p*-tolylamine as the urea substituent.

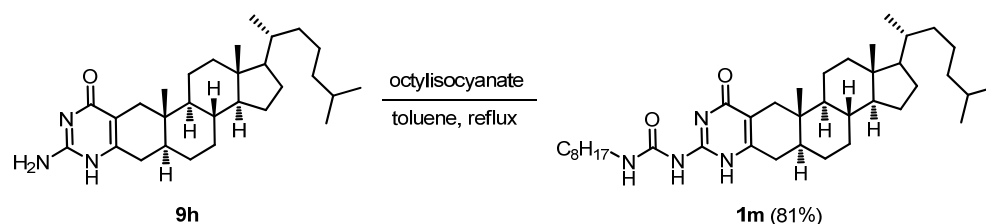
Imidazolid **24b** was reacted with *p*-tolylamine to form ureidopyrimidinone **11** in a 25% yield (Scheme 8).



Scheme 8: Synthesis of compound **11**.

In addition, other ureidopyrimidinones have been synthesized and their solubility tested, such as pyrimidinones with a cholesteryl substituent (Scheme 9) which may form interesting aggregates.

Cholesteryl-derived aminopyrimidinone **9h**, was reacted with octyl isocyanate, to afford derivative **1m** in 81% yield. These dimers are very soluble in apolar aprotic solvents and good candidates for 2D-aggregates.



Scheme 9: Synthesis of compound **1m**.

II.2.3 Fullerene Enriched Materials: A “Fullerodendridimer”

This section deals with the synthesis and characterization of two supramolecular dendrimers resulting from the dimerization of fullerene-functionalized dendrons (“fullerodendridimers”) through an ureidopyrimidinone motif (Figure 8). This project was developed in collaboration with Prof. J.-F. Nierengarten (Toulouse and Strasbourg, France).

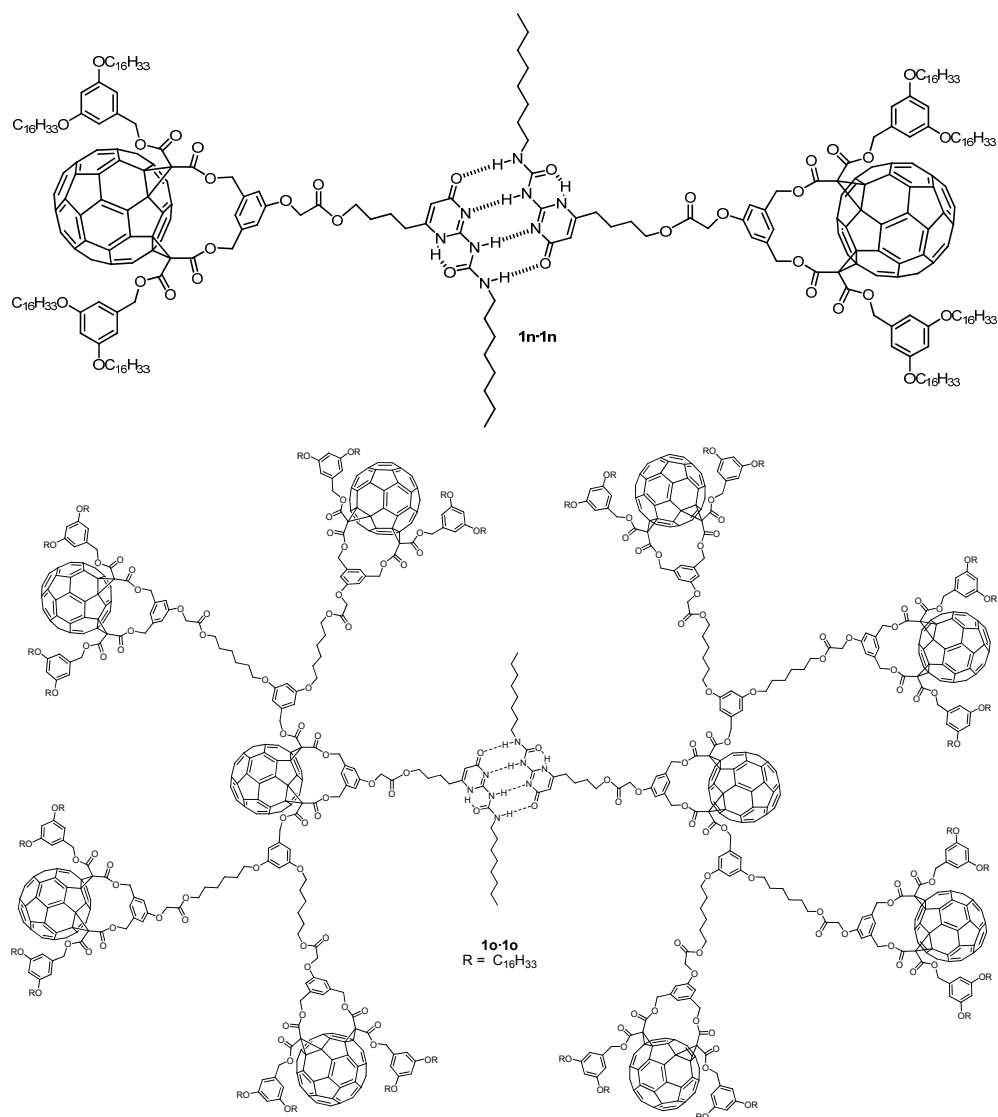


Figure 8: Supramolecular dendrimers based on ureidopyrimidinone motifs.

In recent years, the rapid advances in dendrimer synthetic chemistry have focused on the creation of functional systems, with increased attention

being given to potential applications.²² Among the large number of molecular subunits used for dendrimer chemistry, C₆₀ has proven to be a versatile building block and fullerene-functionalized dendrimers, that is, fullerodendrimers,²³ have generated significant research activities in the past few years.²⁴ In particular, the peculiar physical properties of fullerene derivatives make fullerodendrimers attractive candidates for a variety of interesting features in supramolecular chemistry and materials science.²⁵ C₆₀ itself is a convenient core for dendrimer chemistry,^{24a} and the functionalization of C₆₀ with a controlled number of dendrons improves dramatically the solubility of the fullerenes.²⁶

In this context supramolecular dendrimers **1n·1n** and **1o·1o** (Figure 8) were synthesized, which resulted from the dimerization of fullerene-functionalized dendrons through the quadruple ureidopyrimidinone hydrogen bonding motif. The self-assembly of dendritic macromolecules through hydrogen bonding interactions²⁷ is particularly well suited for the

²² *Dendrimers and other Dendritic Polymers* (Eds.: J. M. J. Fréchet, D. A. Tomalia), Wiley, Chichester, **2001**.

²³ Nierengarten, J.-F. *Chem. Eur. J.* **2000**, *6*, 3667-3670.

²⁴ a) Hirsch, A.; Vostrowsky, O. *Top. Curr. Chem.* **2001**, *217*, 51-93; b) Nierengarten, J.-F. *Top. Curr. Chem.* **2003**, *228*, 87-110.

²⁵ Nierengarten, J.-F. *New J. Chem.* **2004**, *28*, 1177-1191.

²⁶ a) Wooley, K. L.; Hawker, C. J.; Fréchet, J. M. J.; Wudl, F.; Srdanov, G.; Shi, S.; Li, C.; Kao, M. *J. Am. Chem. Soc.* **1993**, *115*, 9836-9837. b) Hawker, C. J.; Wooley, K. L.; Fréchet, J. M. J. *J. Chem. Soc., Chem. Commun.* **1994**, 925-926. c) Nierengarten, J.-F.; Habicher, T.; Kessinger, R.; Cardullo, F.; Diederich, F.; Gramlich, V.; Gisselbrecht, J.-P.; Boudon, C.; Gross, M. *Helv. Chim. Acta* **1997**, *80*, 2238-2276. d) Brettreich, M.; Hirsch, A. *Tetrahedron Lett.* **1998**, *39*, 2731-2734. e) Rio, Y.; Nicoud, J.-F.; Rehspringer, J.-L.; Nierengarten, J.-F. *Tetrahedron Lett.* **2000**, *41*, 10207-10210.

²⁷ a) Zeng, F.; Zimmerman, S. C. *Chem. Rev.* **1997**, *97*, 1681-1712. b) Smith, D. K.; Diederich, F. *Chem. Eur. J.* **1998**, *4*, 1353-1361. c) Newkome, G. C.; He, E.; Moorefield,

preparation of fullerene-rich molecules. Indeed, the synthesis itself is restricted to the preparation of dendrons, and self-aggregation leads to the dendritic structure. This avoids tedious final synthetic steps with precursors incorporating potentially reactive functional groups, such as C₆₀.

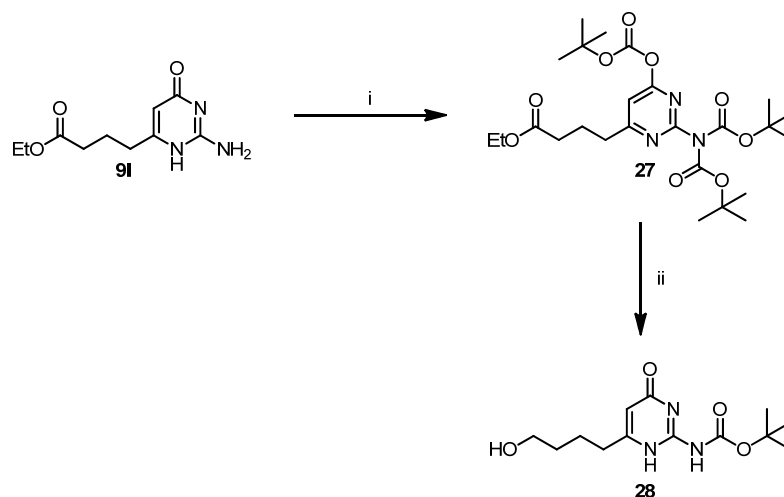
The synthetic route envisaged for the preparation of supramolecular dendrimer **1o·1o** (and its analogous **1n·1n**) relies upon esterification of the UPy precursor **28** bearing an alcohol function with a fullerodendron possessing a carboxylic acid group at the focal point.

To this end, precursor **28** was prepared in two steps from aminopyrimidinone **9I** (Scheme 10). Treatment of **9I** with an excess di-*tert*-butyl dicarbonate in THF at 40 °C for two days, in the presence of triethylamine and a catalytic amount of 4-dimethylaminopyridine, yielded the triply Boc-protected derivative **27**.²⁸

Reduction of the ester function in **27** by treatment with diisobutylaluminum hydride in CH₂Cl₂ at -78 °C caused simultaneously the cleavage of two Boc protecting groups, affording the pyrimidinone derivative **28** with a residual Boc-protected amine function in position 2 and a 4-hydroxybutyl chain in position 6.

C. N. *Chem. Rev.* **1999**, *99*, 1689-1746. d) Kaifer, A. E. *Acc. Chem. Res.* **1999**, *32*, 62-71.

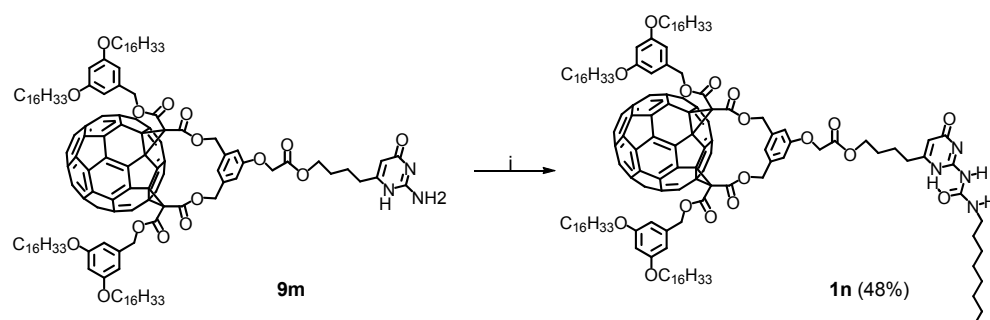
²⁸ Controlling mono-protection of the amino group was not possible and **27** was obtained in 47% yield as the major component of a mixture of mono-, di-, and tri-Boc-protected compounds.



i) Boc_2O , Et_3N , DMAP, THF, reflux, 2 days; ii) DIBAL-H, CH_2Cl_2 , -78°C , 5 h, then r. t. overnight.

Scheme 10: Synthesis of ureidopyrimidinone **28**.

Coupling of compound **28** with the corresponding fullerene moiety, followed by Boc deprotection with TFA, resulted in compounds **9m** and **9n** as trifluoroacetate salts, which are the precursors in the synthesis of **1n** and **1o**. Washing with base followed by coupling with octyl isocyanate, yielded **1n** (Scheme 11) in 48% yield - after purification by flash chromatography - and **1o** (Scheme 12) in 87% yield - after precipitation with cold ethanol.



i) octyl isocyanate, Et_3N , toluene, 40°C , overnight.

Scheme 11: Synthesis of dendrimer **1n**.

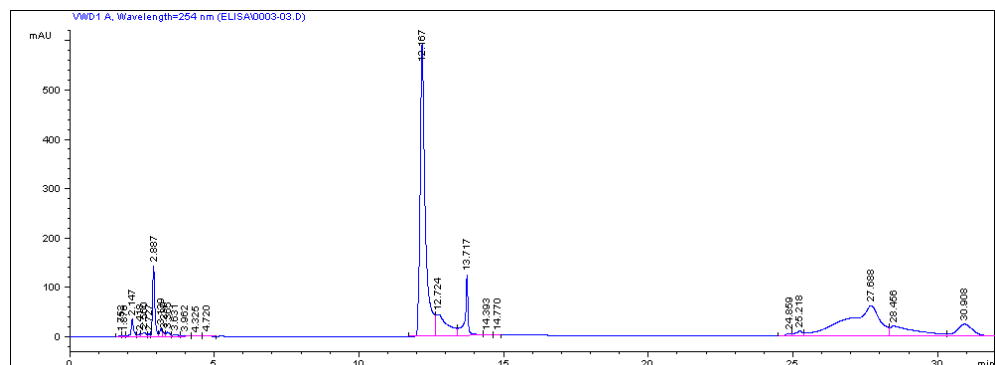


Figure 9: HPLC ($\text{CH}_2\text{Cl}_2/\text{MeOH}$; gradient of MeOH 0.1 to 2%) chromatogram of compound **1n**.

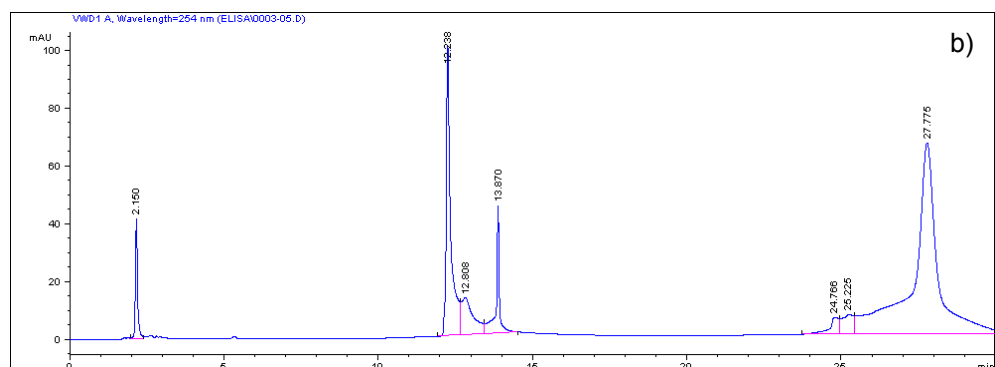
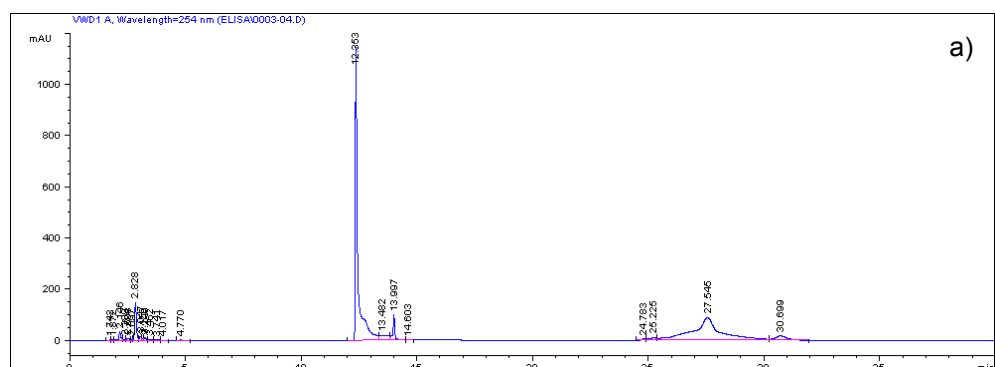


Figure 10: HPLC ($\text{CH}_2\text{Cl}_2/\text{MeOH}$; gradient of MeOH 0.1 to 2%) chromatogram of a) second fraction of peaks; b) third fraction of peaks.

Owing to the presence of the four hexadecyloxy substituents per peripheral fullerene subunit, compounds **1n** and **1o** were highly soluble in common organic solvents, such as CH₂Cl₂, CHCl₃, toluene or THF, so the spectroscopic characterization was relatively easy. Both **1n** and **1o** were also characterized in the gas phase by using MALDI-TOF mass spectrometry, a well-suited tool for the characterization of such high-molecular-weight compounds because of its mild ionization process prevents extensive fragmentation.²⁹ Even if the mass spectrum of **1n** is dominated by the ion peak corresponding to the monomer at m/z 2564.7 (m/z calculated for C₁₇₁H₁₈₁N₄O₁₇ = 2564.3), the molecular ion peak of the dimer **1n·1n** was clearly detected at m/z 5126.0 (m/z calculated for C₃₄₂H₃₆₁N₈O₃₄ = 5127.6) (Figure 11). Similarly, the MALDI-TOF mass spectrum of fullerodendrimer **1o** was characterized by two peaks corresponding to the supramolecular dimer **1o·1o** at m/z 21932 ([2M+H]⁺, m/z calculated for C₁₄₉₄H₁₄₀₁N₈O₁₅₄ = 21932.1) and to the monomer at m/z 10964 ([M+H]⁺, m/z calculated for C₇₄₇H₇₀₁N₄O₇₇ = 10966.5). As for **1n**, the spectrum of **1o** is largely dominated by the ion peak corresponding to the monomer, and the relative intensity of the signal attributed to the supramolecular dimer is quite low (5%). Finally, no peaks corresponding to defected dendrons were observed in the MALDI-TOF mass spectrum of **1o**, providing clear evidence for its monodispersity.

²⁹ Rio, Y.; Accorsi, G.; Nierengarten, H.; Bourgoigne, C.; Strub, J.-M.; Van Dorselaer, A.; Armaroli, N.; Nierengarten, J.-F. *Tetrahedron* **2003**, *59*, 3833-3844.

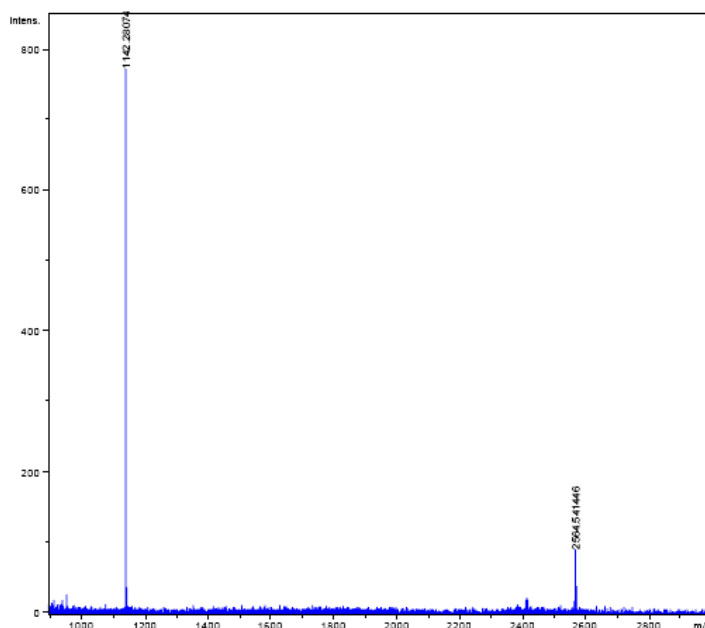


Figure 11: MALDI-TOF spectrum of compound **1n**.

Conclusive evidence for the dimer structure of **1n** and **1o** came from the results of ^1H NMR measurements conducted in CDCl_3 . Characteristic, diagnostic large downfield shifts were observed for the protons involved in the hydrogen bonding motif. For compound **1o** the signals of the urea NH protons were observed at $\delta = 11.81$ and 10.06 ppm and the intramolecularly chelated pyrimidinone NH at $\delta = 13.23$ ppm. As shown in Figure 12, the ^1H NMR spectrum of **1n** recorded in CDCl_3 also displayed the characteristic signals for the hydrogen bonding protons ($\delta = 11.84$ and 10.12 ppm for urea NH protons and $\delta = 13.22$ ppm for the pyrimidinone NH), thus providing conclusive evidence for the dimeric structure in solution.

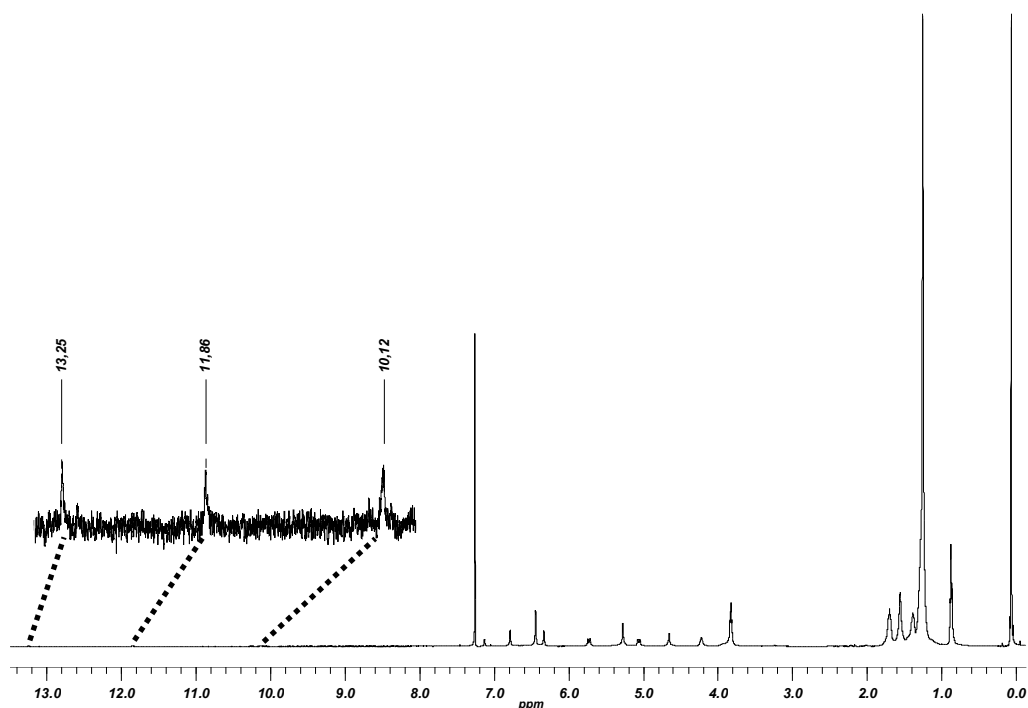


Figure 12: ^1H NMR (500 MHz, CDCl_3) spectrum of fullerodendrimer dimer **1n·1n** highlighting the hydrogen-bonded protons.

II.3 CYCLIC AGGREGATES

II.3.1 Double Ureidopyrimidinone: A Fully Preorganized Unit for Discrete Cyclic Aggregates.

To get discrete, cyclic bidimensional aggregates based on H-bonded bis-ureidopyrimidinones (bis-UPy), both units have to be properly oriented, since the geometry of the aggregate will be determined by the type of spacer employed in the design.

Alternatively, a highly preorganized bis-UPy not based on the choice of the appropriate spacer could be envisaged, and we describe herein the design, synthesis and aggregation studies of such a bis-ureidopyrimidinone (Figure 13). The design is based on the direct linkage of two

ureidopyrimidinones through a urea group. This approach leads to a double-UPy (DUPy) which is able to form an intramolecular hydrogen-bonded array leading the molecule with a "V" shape in which each UPy is oriented in the same direction. The number of monomers involved in the most stable aggregate is hard to predict since it depends on the strength of the intramolecular array of hydrogen bonds which dictates the angle formed between the two ureidopyrimidinone edges. Thus, if the angle between the edges is 90° the rosette would be tetrameric, but a pentamer would result from an angle around 72° .

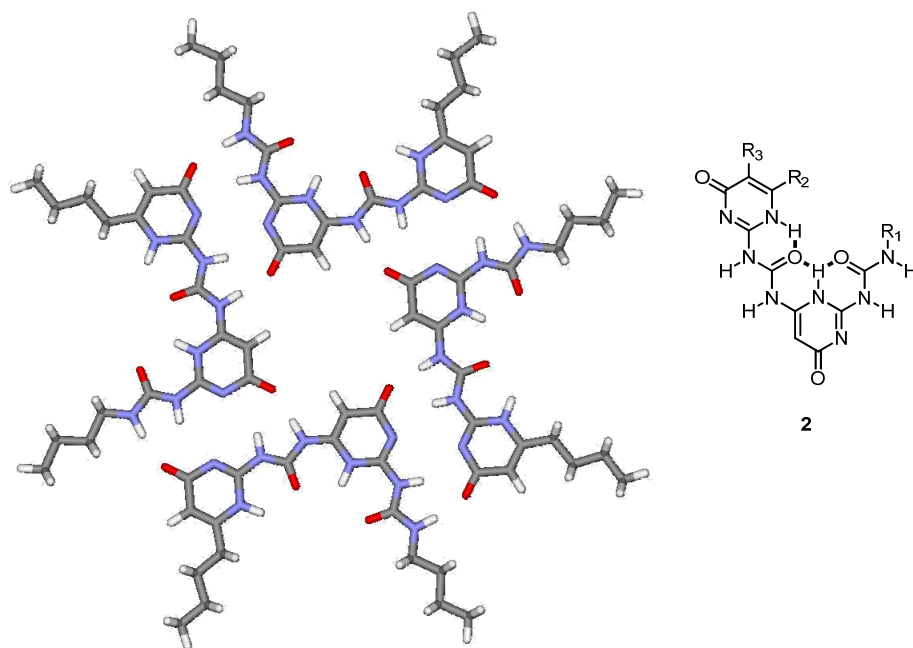
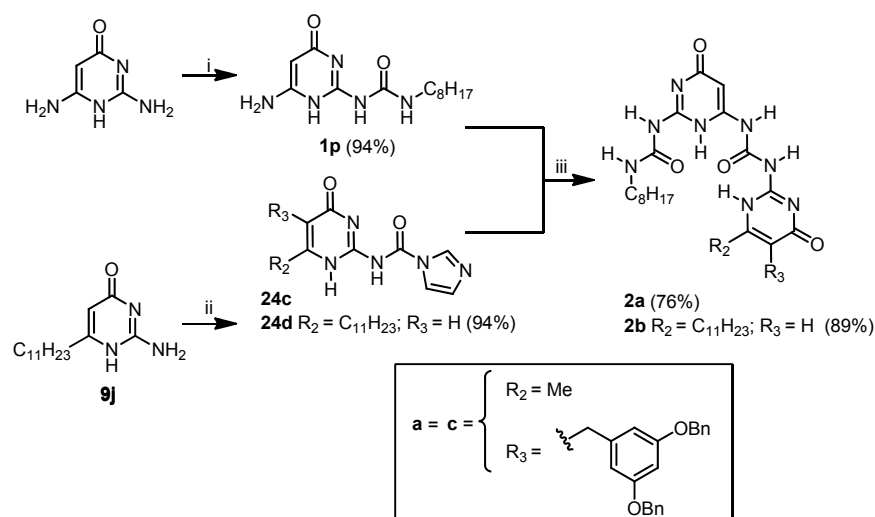


Figure 13: Tetrameric aggregate based on a preorganized bis-ureidopyrimidinone type **2**.

The synthesis of compounds **2a-b** was performed from the commercially available 2,4-diamino-6-hydroxypyrimidine, which possesses two amino groups of different reactivity. Since the amino group of the *guanidine* part of the molecule should be less reactive due to its more delocalized electronic

structure and the enamine character of the other amino group,³⁰ the formation of a urea from this side should require additional protection and deprotection steps of the remaining amine. However, the unprotected compound reacted with isocyanates to directly form ureas at position 2 in high yields (Scheme 13).³¹



i) octyl isocyanate, toluene, 80 °C, 2 days; ii) CDI, THF, r.t., 3 h; iii) DCM/DMF, 60 °C, 3h.

Scheme 13: Synthesis of bis-ureidopyrimidinones **2a-b**.

³⁰ For examples of reactions of 2,4-diamino-6-hydroxypyrimidine (enamine part), see: a) Gangjee, A.; Zeng, Y.; McGuire, J. J.; Mehraein, F.; Kisliuk, R. L. *J. Med. Chem.* **2004**, *47*, 6893-6901. b) Sanders, W. J.; Nienaber, V. L.; Lerner, C. G.; McCall, J. O.; Merrick, S. M.; Swanson, S. J.; Harlan, J. E.; Stoll, V. S.; Stamper, G. F.; Betz, S. F.; Condroski, K. R.; Meadows, R. P.; Severin, J. M.; Walter, K. A.; Magdalinos, P.; Jakob, C. G.; Wagner, R.; Beutel, B. A. *J. Med. Chem.* **2004**, *47*, 1709-1718. c) Klepper, F.; Polborn, K.; Carell, T. *Helv. Chim. Acta* **2005**, *88*, 2610-2616.

³¹ To the best of our knowledge, there is only one precedent of a reaction of isocyanates with 2,4-diamino-6-hydroxypyrimidine involving the amino group in position 2: Zimmerman, S. C.; Witmer, M. J.; Zill, A. T. *Polymer Preprints* **2003**, *44*, 572-573.

Since long alkyl chains are in general necessary to provide solubility, as was shown in the previous section, octyl isocyanate was selected to form the first moiety of the final molecule. In this way compound **1p** was obtained in excellent yield (94%) without further purification.³²

The reaction of **1p** with the blocked isocytosine **24d** afforded **2b** in 89% yield. Unfortunately, despite the two long alkyl chains, the product was poorly soluble, even in a polar solvent such as DMSO. This limited solubility did not allow a NMR study to characterize the compound, nor to have an insight into its aggregation behavior, although the mass spectrum (MALDI-TOF) showed peaks for the monomeric as well as for the dimeric species.

A wide range of non-polar and polar solvents (such as chloroform, dichloromethane, carbon tetrachloride, carbon disulfide, DMSO, pyridine, water, benzene, toluene, *p*-xylene, tetrahydrofuran, or hexane) and also some solvent mixtures (such as water/TFA, DMSO/TFA...) were tested unsuccessfully for optimal solubility to allow a complete analysis of the structure and its properties. Although long alkyl chains have demonstrated to be a good choice to obtain soluble compounds they do not always fit well the space occupied by the intramolecular net of hydrogen bonds, making it difficult to solubilize the compound.

To avoid this problem the C₁₁-pyrimidinone (**9j**) was replaced for another one designed to better fit this space. Even though bis-benzyloxybenzyl-pyrimidinones showed the lowest values for solubility, as pointed out in

³² As described in Section II.2.2, addition of triethylamine was necessary to increase yields and to improve reaction times in the reaction of aminopyrimidinones with isocyanates. However, in this case, addition of triethylamine promoted the reaction of octyl isocyanate with both amines and the corresponding bis-urea was obtained as the major compound.

previous section, they were selected due to its dendrimeric shape.

Reaction of **1p** with imidazolidone **24c** as for other examples described before, afforded bis-UPy **2a** in 76% yield, and this compound was soluble enough in chloroform or dichloromethane to be fully characterized. Figure 14 shows the ¹H NMR spectrum in DMSO-*d*₆. The signal corresponding to the UPy proton (green) was downfield shifted ($\Delta\delta = 1.6$ ppm) with respect to the same signal in compound **1p**, probably due to the effect of the urea's carbonyl.

When the NMR spectrum was registered in CDCl₃ (Figure 15), a number of signals were observed at the range between 9 and 14 ppm, which were found to be concentration-dependent. At higher concentration than 12 mM more than ten signals for NH protons were present, indicating a slow equilibrium between different species and/or aggregates. However, at ten times more diluted samples, the number of signals was reduced to only six, which is consistent with the formation of a discrete aggregate with a defined form. The rest of the signals of the spectrum were in agreement with this hypothesis: in the concentrated sample the signals for the aromatic and aliphatic proton broadened, indicative of a polymeric aggregate, while in the diluted sample the signals were sharp, indicating that a defined aggregate was formed.³³

³³ a) Söntjens, S. H. M.; Sijbesma, R. P.; van Genderen, M. H. P.; Meijer, E. W. *Macromolecules* **2001**, *34*, 3815-3818. b) Folmer, B. J. B.; Sijbesma, R. P.; Meijer, E. W. *J. Am. Chem. Soc.* **2001**, *123*, 2093-2094. c) ten Cate, A. T.; Sijbesma, R. P.; Meijer, E. W. *Polymer Preprints* **2002**, *43*, 333-334. d) ten Cate, A. T.; Sijbesma, R. P. *Macromol. Rapid Commun.* **2002**, *23*, 1094-1112. e) Keizer, H. M.; Sijbesma, R. P.; Jansen, J. F. G. A.; Pasternack, G.; Meijer, E. W. *Macromolecules* **2003**, *36*, 5602-5606. f) Ligthart, G. B. W. L.; Ohkawa, H.; Sijbesma, R. P.; Meijer, E. W. *J. Am. Chem. Soc.* **2005**, *127*, 810-811.

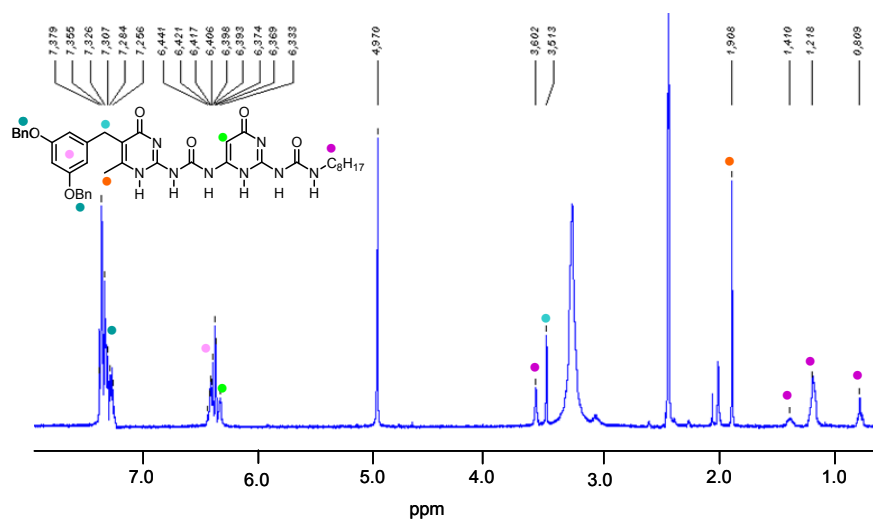


Figure 14: ^1H NMR ($\text{DMSO}-d_6$, 400 MHz) spectrum of **2a**.

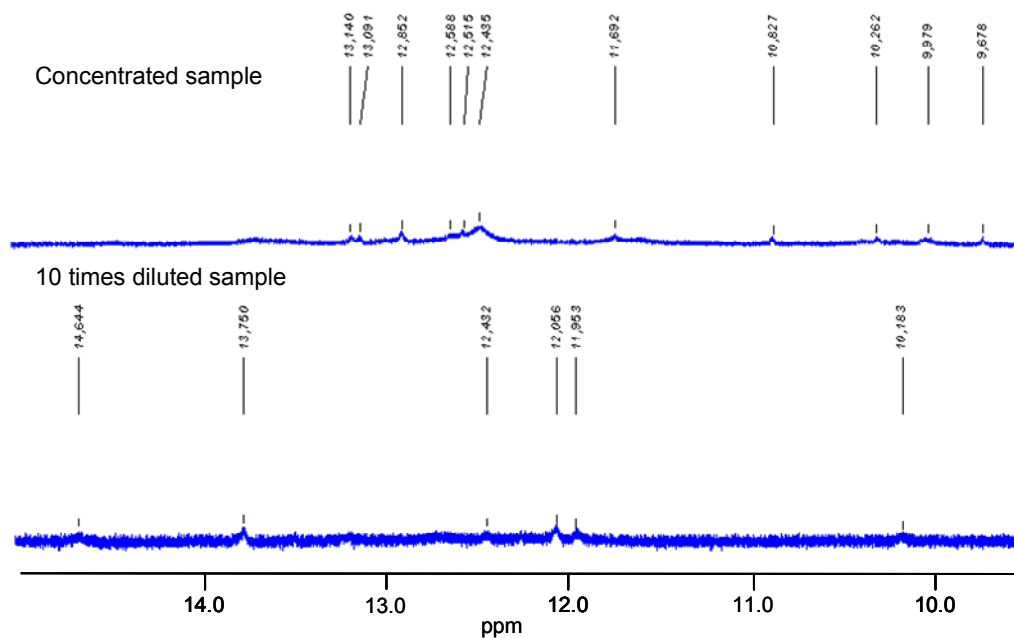


Figure 15: Partial ^1H NMR spectra (CDCl_3 , 400 MHz) of compound **2a** showing NH's region at two different concentrations.

Figure 16 shows cyclic and linear aggregates for this double ureidopyrimidinone. Although the molecule is substantially preorganized, it is

able to form a number of aggregates, depending on tautomerism, chelation angle, etc.

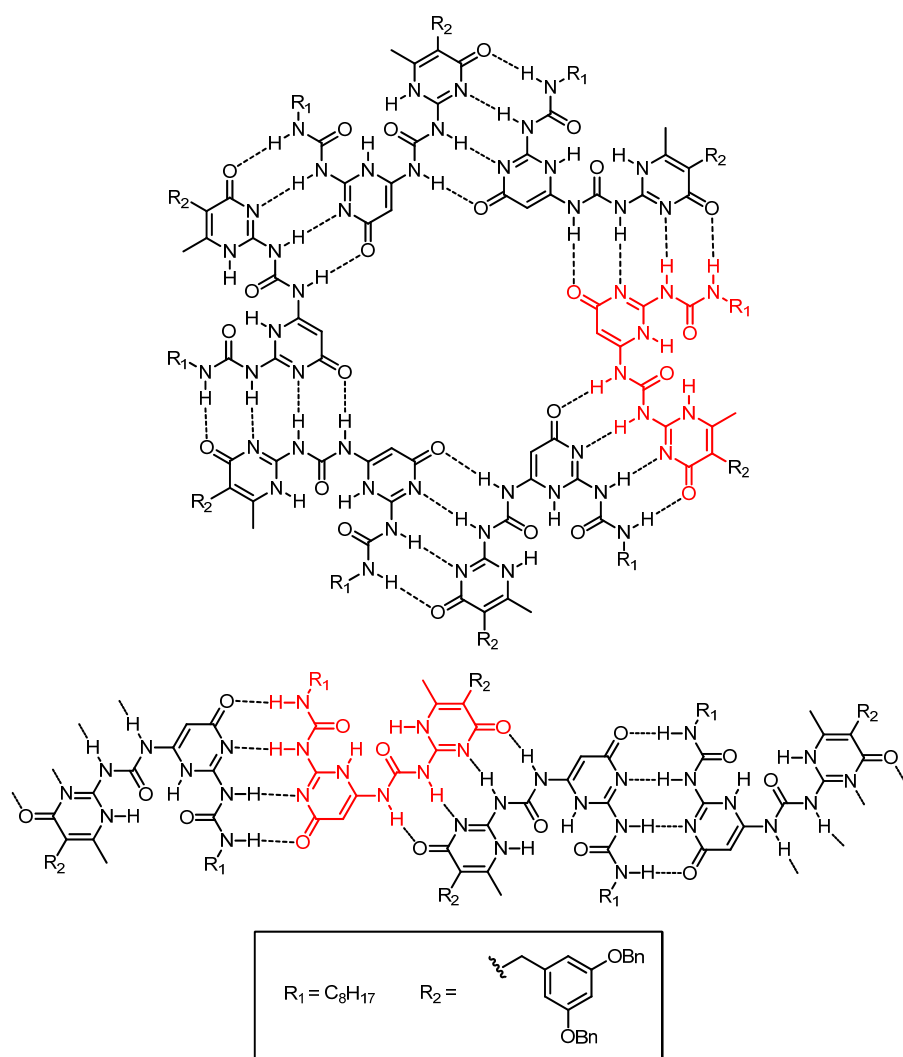


Figure 16: Two [discrete (**2a**)₆ and polymeric (**2a**)_n] aggregates of compound **2a** (the monomer unit highlighted in red).

In order to determine the critical concentration that favors formation of the cyclic aggregate, as well as the aggregation number for the rosette, ^1H NMR experiments at different concentrations and Diffusion Ordered ^1H NMR Spectroscopy (DOSY) dilution experiments were performed in CDCl_3 .^{16, 34}

As shown in Figure 17 top, the signals, although still broad, became sharper at lower concentration.

Changes were also observed in the NH's region, but resolution of the spectra was low (Figure 17, bottom). From this dilution experiment, it was not possible to determine a concentration where compound **2a** forms a discrete cyclic aggregate.

³⁴ DOSY measurements have been applied for the characterization of supramolecular aggregates and provide useful information about their size: a) Olenyuk, B.; Levin, M. D.; Whiteford, J. A.; Shield, J. E.; Stang, P. J. *J. Am. Chem. Soc.* **1999**, *121*, 10434-10435. b) Keresztes, I.; Williard, P. G. *J. Am. Chem. Soc.* **2000**, *122*, 10228-10229. c) Timmerman, P.; Weidmann, J.-L.; Jolliffe, K. A.; Prins, L. J.; Reinhoudt, D. N.; Shinkai, S.; Frish, L.; Cohen, Y. *J. Chem. Soc., Perkin Trans. 2* **2000**, 2077-2089. d) Cohen, Y.; Avram, L.; Frish, L. *Angew. Chem. Int. Ed.* **2005**, *44*, 520-554.

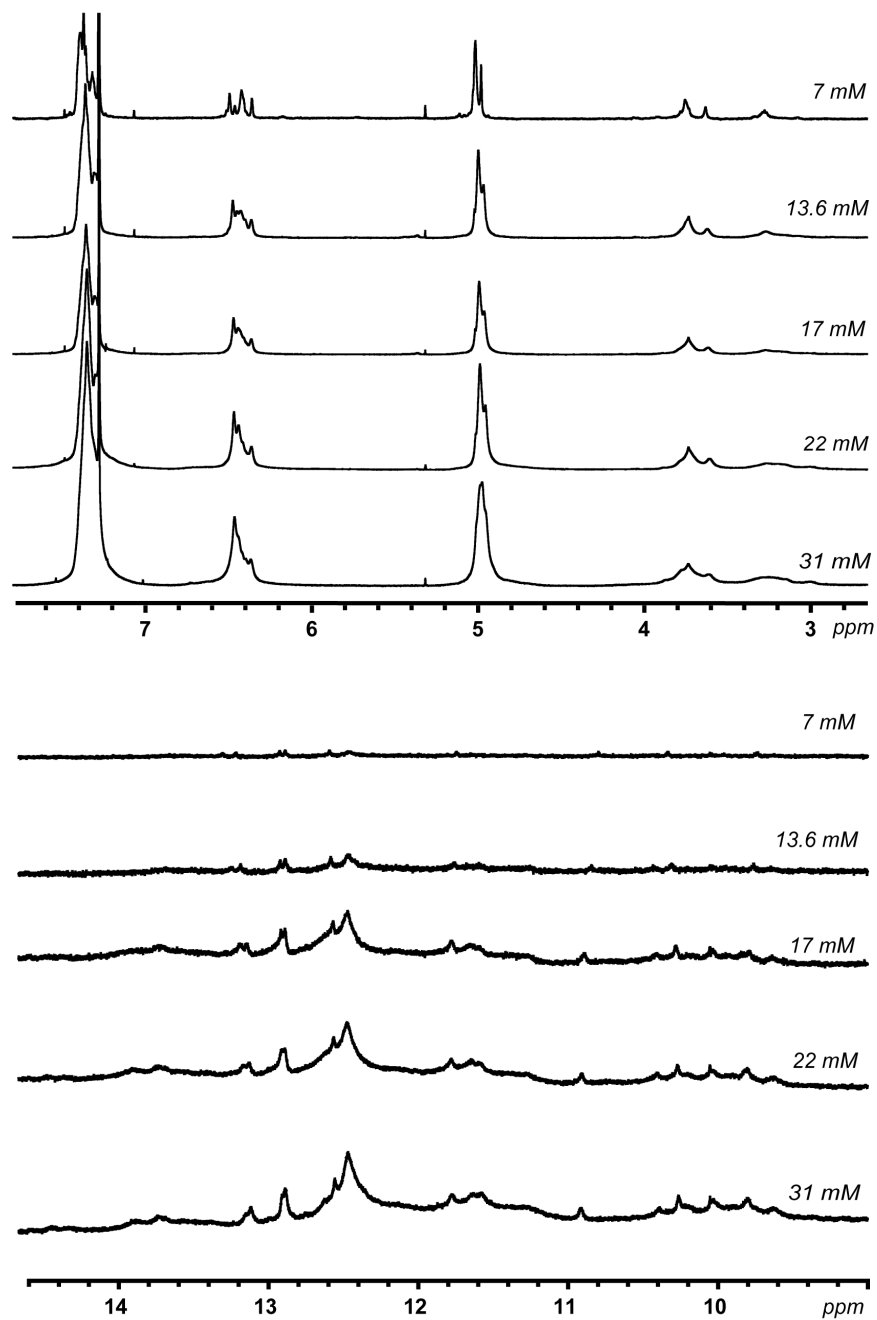


Figure 17: Partial ¹H NMR (CDCl₃, 400 MHz) spectra of compound **2a** at different concentrations: (top) 3.0-7.3 ppm region (aromatic and pyrimidinone CH protons); (bottom) 9.0-14.5 ppm region (NH protons).

Preliminary DOSY experiments were performed to determine how the diffusion coefficient changed with the size of the molecule/aggregate: the smaller the measured compound the higher the diffusion coefficient should be (Figure 18).

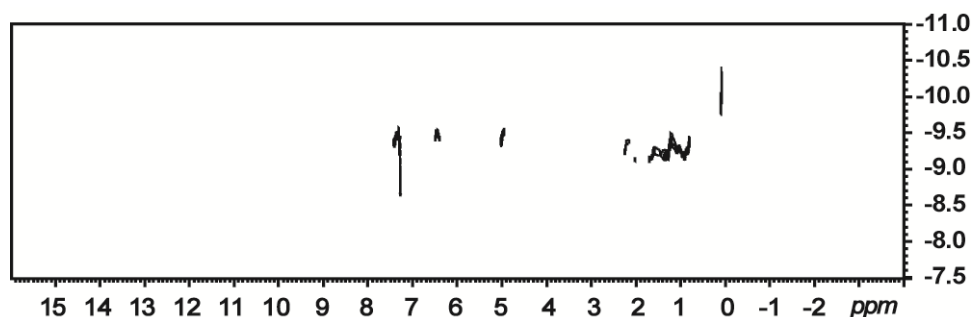


Figure 18: DOSY NMR spectrum (CDCl_3 , 13.6 mM) of compound **2a**.

As aggregation was shown to be concentration-dependent, the DOSY experiments were done on solutions of **2a** in CDCl_3 at different concentrations, using the solvent as internal standard (Table 2). Two concentration regimes could be distinguished for **2a** in a double logarithmic plot of the relative diffusion coefficient vs. concentration (Figure 19). In the higher concentration region (> 17 mM), the relative diffusion coefficient decreases with an exponent $\alpha_D = -0.007$ in CDCl_3 , whereas in the lower concentration region the relative diffusion coefficient decreases as the concentration increases ($\alpha_D = -0.001$). The existence of two concentration regimes for **2a** suggests the presence of different types of aggregates. However, with these data alone it is not possible to conclude unequivocally about the aggregation number and the shape of the aggregate.

Table 2: Diffusion coefficients (absolute and relative to the solvent value) measured for **2a** at different concentrations.

Concentration (mM)	D (m ² /s)	D _{rel} (D/D _{chloroform})
31	3.365 x 10 ⁻¹⁰	0.023
22	1.914 x 10 ⁻¹⁰	0.057
17	4.046 x 10 ⁻¹⁰	0.121
13.6	3.126 x 10 ⁻¹⁰	0.147
7	4.046 x 10 ⁻¹⁰	0.154

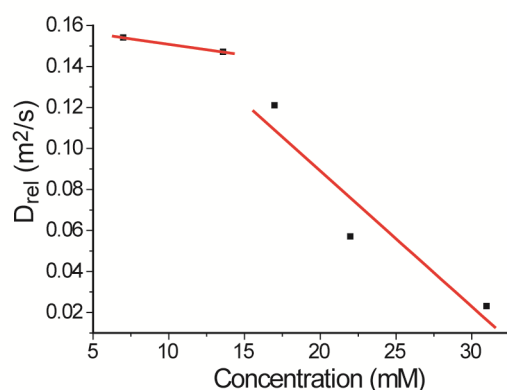


Figure 19: Concentration-dependent diffusion ¹H NMR spectroscopy measurements of **2a** in CDCl₃ (solvent used as internal standard).

In addition to the above experiments, molecular weight determinations were performed for **2a** by vapour pressure osmometry (VPO), in chloroform at 35 °C in a concentration range from 2-30 mM. For calibration, polystyrene PS1000 and benzyl were used as standards, giving an average molecular weight of 2911.9 and 2715.6 g/mol respectively, which is consistent with a tetrameric assembly (**2a**)₄ (calculated MW = 2937.4 g/mol).

A computational study aimed at predicting the aggregation behaviour was undertaken. Since the design of a DUPy is based on the direct linkage of two pyrimidinones through a urea group, leading to a V-shaped compound,

the number of monomers involved in the aggregate is not easily predictable, since the angle between the edges will depend on the intramolecular hydrogen bond net strength (Figure 20).

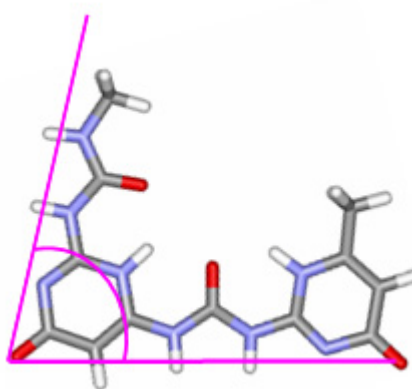


Figure 20: Optimized geometry (B3P86/6-311G**) of a DUPy monomer.

Therefore, DFT calculations were performed. The geometry optimization of the different systems was done using the JAGUAR V5.5 program. In all cases, the B3P86³⁵ functional was employed and 6-311G** was used as basis set. To determine the angle between the edges, the geometry of one single monomer was optimized. The resulting monomer is fully planar with an angle between the edges of 82°, which is too large for a pentameric assembly and a bit too short to form a cyclic tetramer (Figure 23E).

Optimization of a DUPy dimer resulted also into a planar geometry (Figure 21F). Then, a cyclic tetramer was constructed and optimized (Figure 21A-D) and the calculated assembly resulted in a concave structure. The hydrogen bond distances were measured and compared with those obtained for the DUPy monomer and with the distances of an UPy monomer and dimer, at the same calculation level. These distances were also

³⁵ Becke, A. D. *J. Chem. Phys.* **1993**, *98*, 5648-5652.

compared with crystallographic experimental values obtained for an UPy dimer¹³ (Table 3).

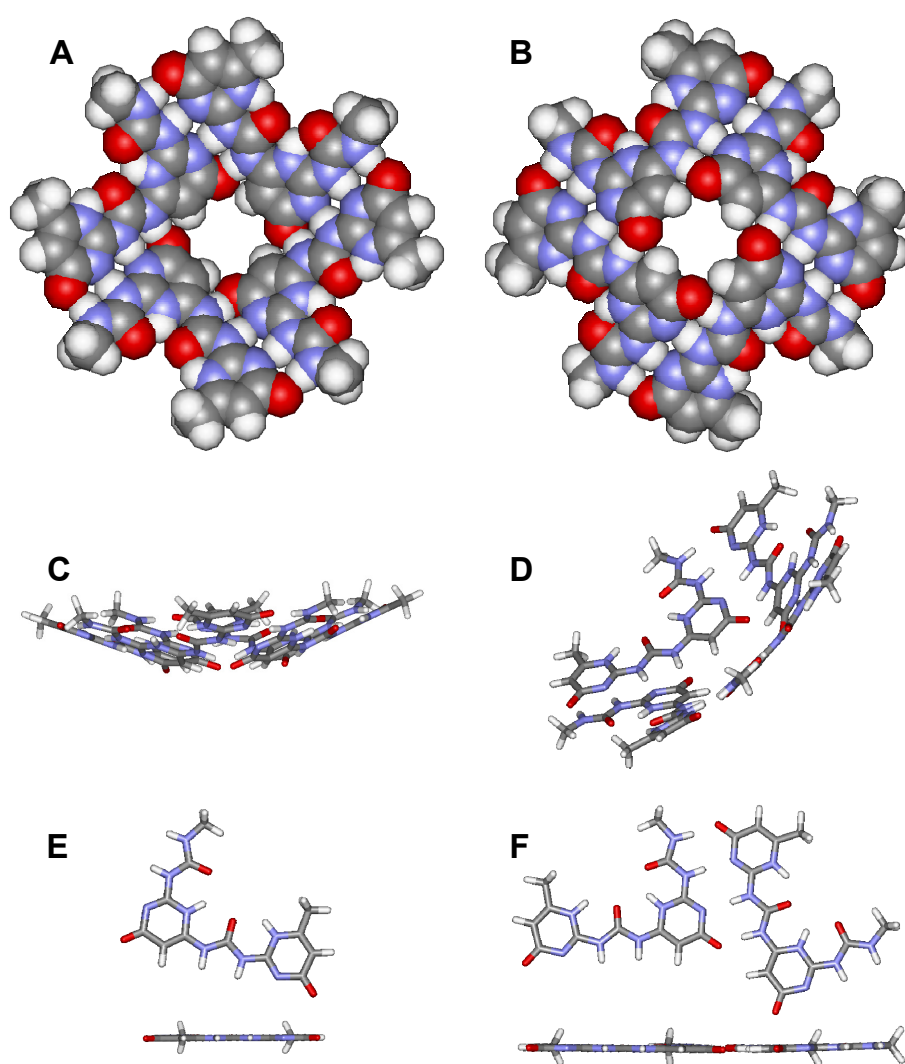
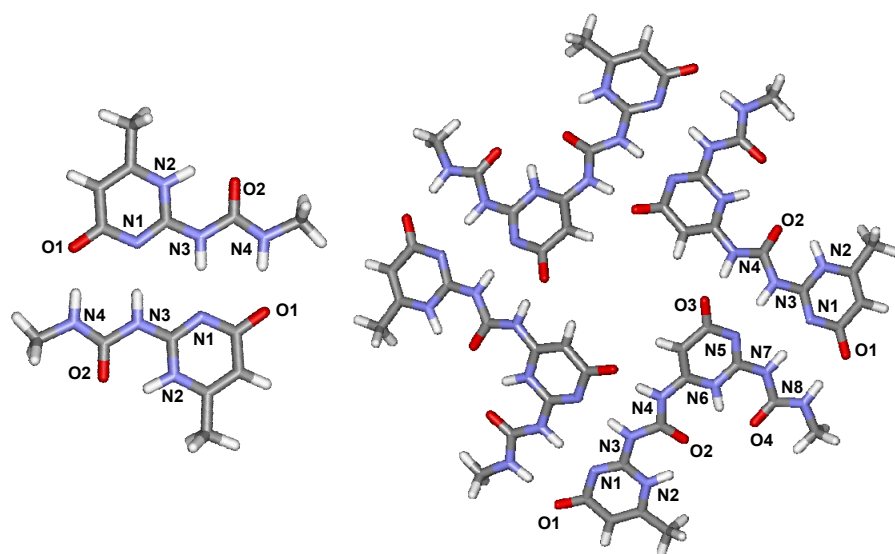


Figure 21: Optimized geometry of a tetrameric aggregate based on fully preorganized DUPys A-D; different views of the optimized tetramer. E) top and side view of the optimized monomer. F) top and side view of the optimized dimer.

Table 3: Bond distances (Å).



	Intramolecular H-Bond			Intermolecular H-Bond					
	N2-O2	O2-N6	N6-O4	O1-N4	N1-N3	O1-N8	N1-N7	N3-N5	N4-O3
UPy Monomer	2.646	--	--	--	--	--	--	--	--
UPy Dimer^a	--	--	--	2.757	2.966	--	--	--	--
UPy Dimer	2.547	--	--	2.732	2.916	--	--	--	--
DUPy Monomer	2.689	2.725	2.688	--	--	--	--	--	--
DUPy Tetramer	2.592	2.742	2.597	--	--	2.786	2.972	2.894	2.578

^aExperimental values.¹³

In general, calculated bond distances correspond quite well with the

experimental values. In the case of the UPy, the distance calculated for the intramolecular H-bond (N2-O2) was shorter in the dimer than in the UPy monomer, indicating that dimerization affects to the intramolecular hydrogen bond strength. This behaviour was also observed in the DUPy molecule where the distances N2-O2 and N4-O6 are shorter in the tetramer's geometry. On the other hand, calculated distances for the intermolecular hydrogen bonds in the UPy dimer were in agreement with the experimental values, but in the case of the tetrameric aggregate the distances N3-N5 and N4-O3 are shorter than expected, probably due to the curved geometry of the DUPy monomer in the tetrameric assembly (Figure 22).

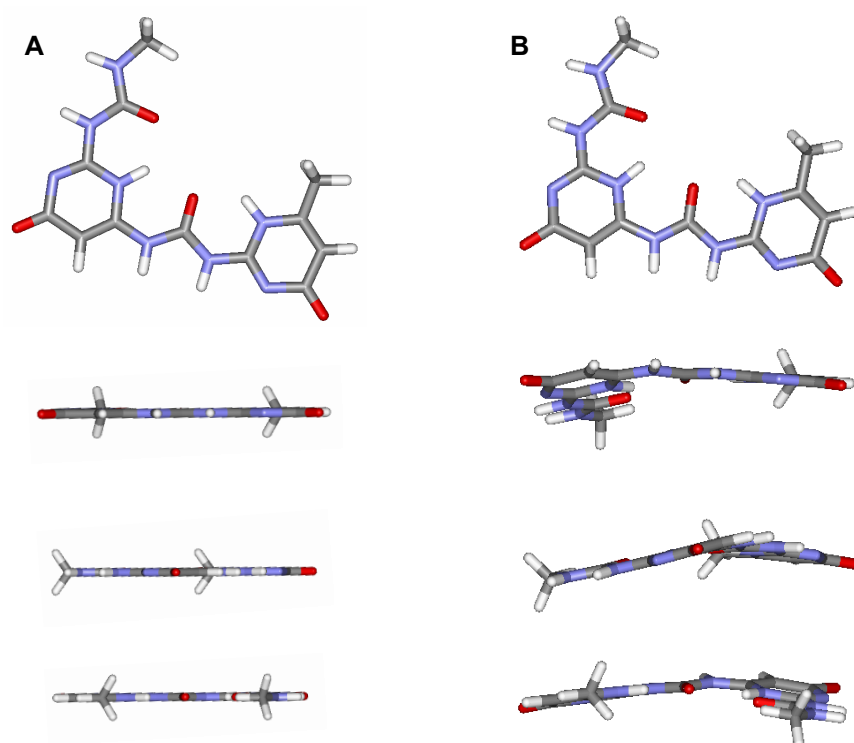


Figure 22: A) top and different side views of the optimized monomer. B) top and different side views of the optimized monomer in the tetramer's geometry.

Additionally, dimerization/tetramerization energies of each aggregate were calculated. As shown in Table 4, the DUPy dimer dimerization energy is more favorable than the one obtained for the UPy dimer. This can be explained by the lower value of the deformation energy in the DUPy molecule. In the case of the tetrameric assembly, the highly favorable values for the tetramerization energy - the most stable geometry - highlight the cooperativity of these systems.

Remarkably, the deformation energy, i.e., the enthalpic penalty that the DUPy monomer has to pay to adopt the proper geometry to form the tetramer, was quite high, about 10 kcal·mol⁻¹, which represents the double of the energy needed to form a single UPy or DUPy dimer.

Table 4: Dimerization energies (kcal·mol⁻¹) for a simple UPy dimer compared with the ones for a DUPy dimer and for the DUPy tetramer.

	^a E _{intSp}	^b E _{defor}	^c E _{dim}
UPy Dimer	-58.8	5.54	-47.7
DUPy Dimer	-60.1	4.48	-51.2
DUPy Tetramer	-246.9	9.64	-208.3

^aDifference between the energy of the optimized dimer (tetramer) and the energy of the monomers in the dimer's (tetramer) geometry.

^bEnergy needed in the deformation of the monomer to form the dimer.

^cDimerization energy calculated as the subtraction of the energy of the optimized monomers from the dimer's (or tetramer) energy. The BSSE has not been taken into account.

Thus, calculations indicate that formation of discrete oligomeric aggregates is unlikely. The difference in deformation energy (E_{defor}) of approximately 5 kcal·mol⁻¹ in favor of linear arrays should promote polymeric or oligomeric aggregates over the desired rosettes.

II.3.2 A Rosette Based on an Adamantyl Spacer

This part of the chapter deals with the synthesis of a bis-ureidopyrimidinone self-assembling structure endowed with an adamantyl spacer. In 2005, a pentameric rosette based on a 1,3-adamantyl spacer and C₁₁ chains in the pyrimidinone ring (**3a**, Scheme 14) was reported by our group in collaboration with E. W. Meijer *et al.*¹⁶

For a bis-UPy derivative with a 1,3-adamantyl spacer and also an adamantane as substituent at position 6 of the pyrimidinone ring, molecular modelling (Figure 23) indicates that the best packing of the inner adamantanes is achieved in an hexameric aggregate, where the adamantyl residues inside the rosette can adopt a chair-like structure.

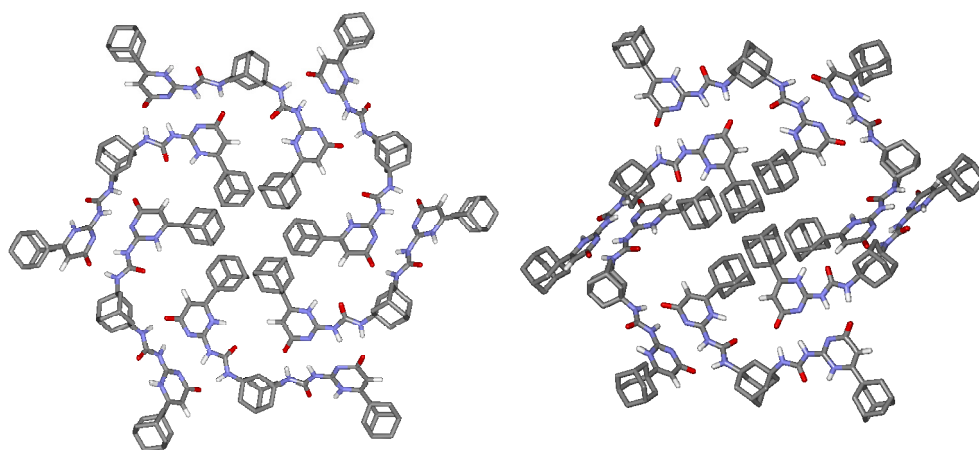
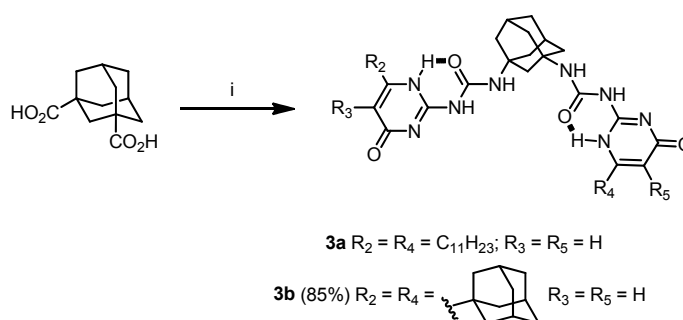


Figure 23: Two views of the molecular modelling (*Insight II/Discover, cvff calculations*) of the hexameric rosette (**3b**)₆ based on adamantyl spacer. Adamantane hydrogens have been removed for clarity.

The synthesis of this bis-ureidopyrimidinone is based in the Curtius rearrangement.³⁶ Thus, 1,3-adamantane dicarboxylic acid was reacted with diphenylphosphoryl azide (DPPA) at 40 °C to form an acyl azide that rearranged to the corresponding bis-isocyanate upon increasing the reaction temperature to 80 °C, along with the release of molecular nitrogen. Isolation of the bis-isocyanate was not necessary, as it reacted *in situ* with aminopyrimidinone **9k** to form the target bis-UPy **3b** in 85% yield (Scheme 14).



i) a) DPPA, Et₃N, toluene, 40 °C, 1 h; then, 80 °C, 3 h; b) **9k**, 80 °C, 2 days.

Scheme 14: Synthesis of compound **3b**.

Despite aggregation was observed by ¹H NMR spectroscopy, **3b** was poorly soluble in CDCl₃ and did not allow studies at higher concentrations. The signals for the associated NH's were downfield shifted and split, and the aggregate formed from dimers of the pyrimidin-4-ol tautomer was also observed in the NMR spectrum (Figure 24). Moreover, the splitting observed for the NH signals suggests the presence of at least two different aggregates in solution, making it more difficult to study.

³⁶ a) Shioiri, T.; Ninomiya, K.; Yamada, S. *J. Am. Chem. Soc.* **1972**, *94*, 6203-6205. b) Ninomiya, K.; Shioiri, T.; Yamada, S. *Tetrahedron* **1973**, *30*, 2151-2157.

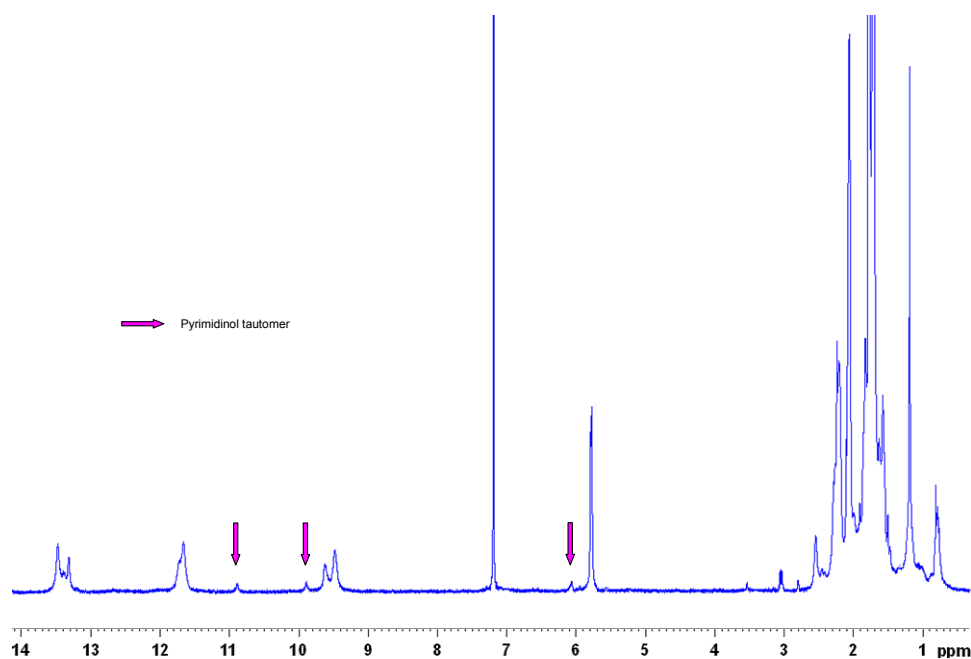


Figure 24: ¹H NMR (CDCl₃, 400 MHz) spectrum of compound **3b**.

The product was slightly more soluble in dichloromethane than in chloroform so a variable temperature ¹H NMR experiment was performed in the former solvent at saturation. Unfortunately, only ill-defined aggregates were observed in the temperature range of the experiment (290 K-190 K).

On the contrary, a defined aggregate was observed by MALDI-TOF mass spectrometry, as peaks corresponding to monomeric up to pentameric species were detected.³⁷

Since **3b** was poorly soluble, the number and quality of experiments that could be carried out with this compound was limited, mass spectrum being the only evidence for the formation of a discrete aggregate, although pentamers were seen but not hexamers as calculations had predicted.

³⁷ See appendix, Section VII.1

II.3.3 A Rosette Based on an *m*-Substituted Aromatic Spacer

Our goal in this case was the synthesis of bis-ureidopyrimidinones with an appropriate geometry to self-assemble only into rosette-type cyclic hexamers. To achieve this, a *m*-substituted aromatic ring,³⁸ bearing a methyl group in position 2 to prevent tape formation, was chosen as spacer. Additionally, the new bis-UPy should contain a lipophilic chain for the outer part of the rosette - to allow solubilization in apolar solvents (such as chloroform or toluene) - and a hydrophilic chain of appropriate dimensions to accommodate in the inner part of the aggregate - to provide an additional hydrogen bonding network that should further stabilize the cyclic form (Figure 25). The hydrophilic substituent could be located in positions 5 or 6 of the pyrimidinone ring in order to evaluate its influence in the aggregate formation and the possibility of having channels derived from rosette stacking.³⁹

³⁸ a) Corbin, S. P.; Lawless, L. J.; Li, Z.; Ma, Y.; Witmer, M. J.; Zimmerman, S. C. *Proc. Natl. Acad. Sci. U. S. A.* **2002**, *99*, 5099-5104. b) Ma, Y.; Kolotuchin, S. V.; Zimmerman, S. C. *J. Am. Chem. Soc.* **2002**, *124*, 13757-13769. c) Todd, E. M.; Zimmerman, S. C. *J. Am. Chem. Soc.* **2007**, *129*, 14534-14535. d) Yang, Y.; Xue, M.; Xiang, J.-F.; Chen C.-F. *J. Am. Chem. Soc.* **2009**, *131*, 12657-12663.

³⁹ Jonkheijm, P.; Miura, A.; Zdanowska, M.; Hoeben, F. J. M.; De Feyter, S.; Schenning, A. P. H. J.; De Schryver, F. C.; Meijer E. W. *Angew. Chem. Int. Ed.* **2004**, *43*, 74-78.

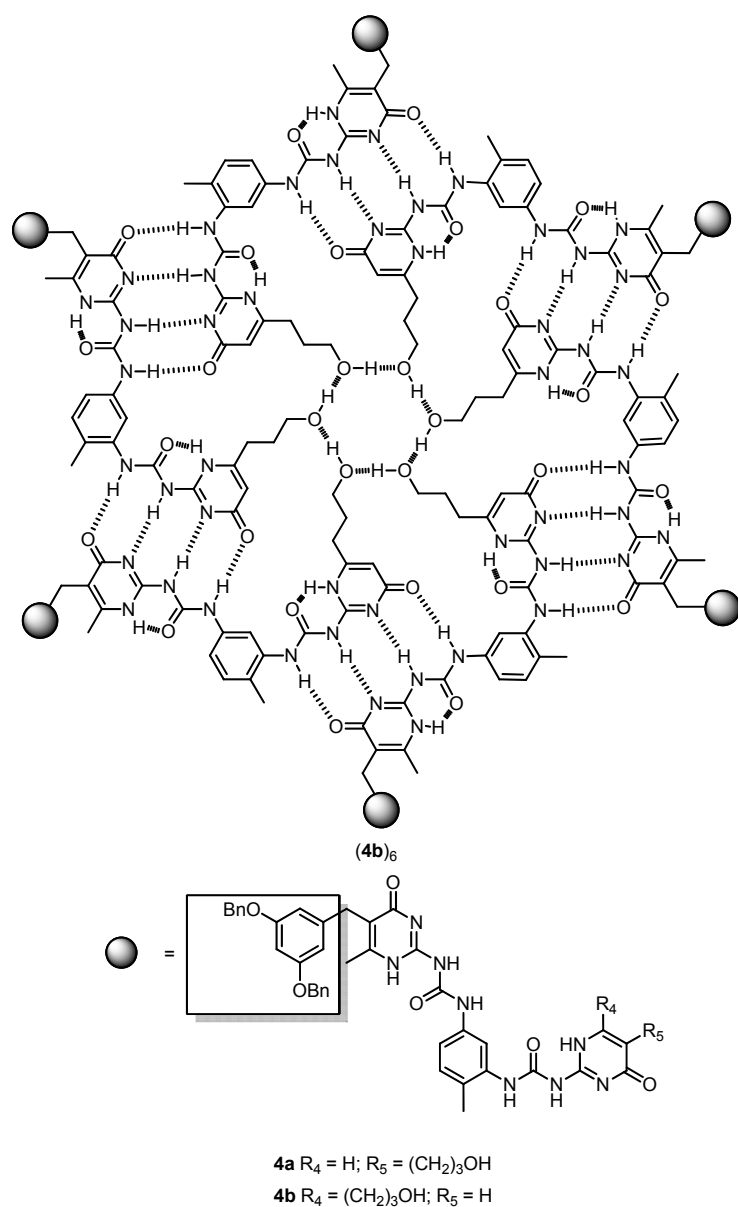
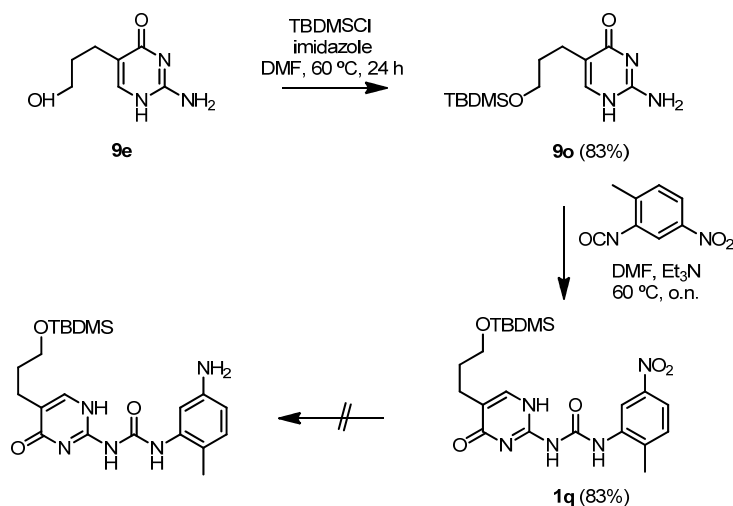


Figure 25: Hexameric aggregate $(4b)_6$ and structure of bis-ureidopyrimidinones **4a-b**.

Consequently, in the synthesis of these disymmetric bis-UPys, a modular approach was adopted. The inner ureidopyrimidinone, which must contain a free hydroxyl group in the final structure, was synthesized following two

strategies: one with a silyl protected alcohol and the other one bearing an ester function whose reduction in the final step would yield the desired alcohol.

Silyl protected aminopyrimidinone **9o** was obtained in good yields by treatment of aminopyrimidinone **9e** with *tert*-butyldimethylsilyl chloride in basic medium (see Scheme 15). **9o** was then reacted with commercially available 2-methyl-5-nitrophenyl isocyanate giving ureidopyrimidinone **1q**. Subsequent attempts to reduce the nitro group to an amino function failed, only partially reduced and/or partially deprotected compounds being detected under all tested conditions. For this reason, attempts to prepare 6-substituted aminopyrimidinone **9b**, analogous to **9o**, were not pursued following this synthetic strategy.

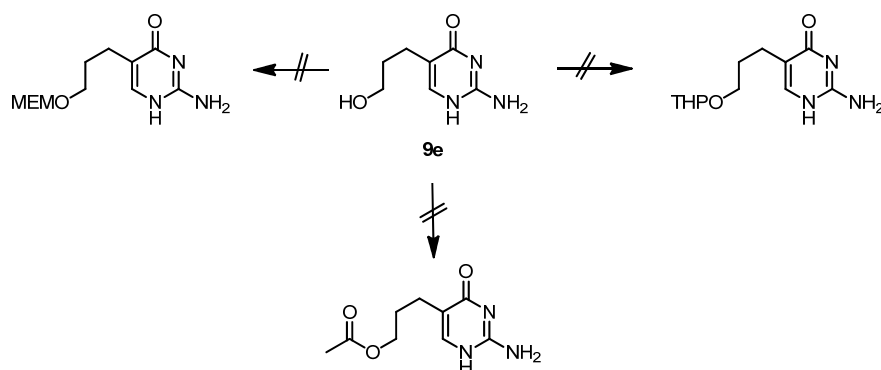


i) TBDCMSCl, imidazole, DMF, sealed tube, 60 °C, 24 h. ii) DMF, Et₃N, sealed tube, 60 °C, overnight.

Scheme 15: Synthesis of inner part of bis-Upy **4a**.

It was then decided to change the protecting group and pyrimidinone **9e** was selected as a model to test various reagents. Initially, protection of

the hydroxyl group as methoxyethylmethyl (MEM) ether, using MEMCl and NaH (60%) at room temperature⁴⁰ or imidazole at reflux,⁴¹ was attempted (Scheme 16). Since in no case the desired products were isolated, acetylation of the hydroxyl group was then attempted with acetyl chloride in the presence of acetic anhydride,⁴² as well as protection as 2-tetrahydropyranyl (THP) derivative (with DHP) but, once again, no products were isolated.



Scheme 16: Attempts of protection of the hydroxyl group of **9e**.

The failure in the synthesis of amino-functionalized precursor and the difficulties in the protection of the hydroxy function in pyrimidinone **9e**, led us to attempt the synthesis of aminopyrimidinones with an ester group at the end of the chain.⁴³

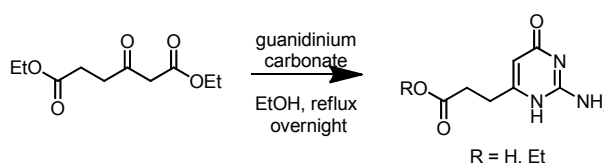
⁴⁰ Xiao, Z.; Timberlake, J. W. *Heteroatom Chem.* **2000**, *11*, 65-72.

⁴¹ Richter, F.; Bauer, M.; Perez, C.; Maichle-Mössmer, C.; Maier, M. E. *J. Org. Chem.* **2002**, *67*, 2474-2480.

⁴² Streitwieser, Jr., A.; Berke, C. M.; Robbers, K. J. *Am. Chem. Soc.* **1978**, *100*, 8272-8273.

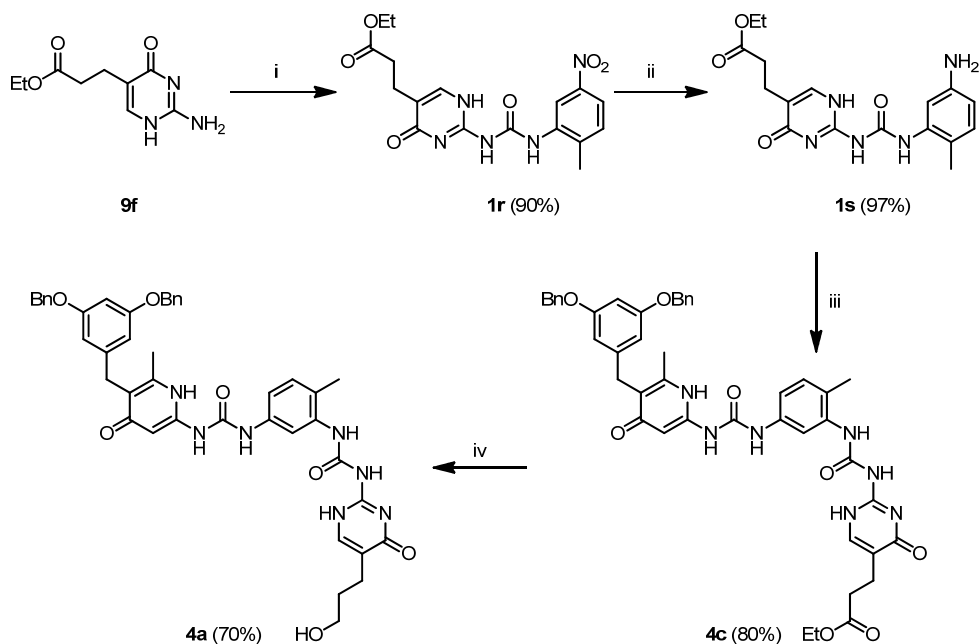
⁴³ The synthesis of 5-ester substituted pyrimidinone (**9f**) is described above.

For the 6-substituted pyrimidinone the synthesis started with commercially available diethyl 3-oxopimelate (Scheme 17). Treatment with guanidinium carbonate under standard conditions afforded the desired pyrimidinone although the ester group was partly hydrolyzed (acid/ester in a 3:1 ratio). Hydrolysis did not occur when the ester chain was at position 5. The hydrolysis could be facilitated by the formation of an intramolecular hydrogen bond between the carbonyl group of the ester group and the NH of the pyrimidinone, which cannot form when the substituent was at position 5 (compound **9f**). Use of dry solvents and drying agents such as magnesium or sodium sulfate, or molecular sieves did not prevent hydrolysis.



Scheme 17

Currently, the synthesis of these 6-substituted aminopyrimidinones has been postponed due to the synthetic problems above described. Work then concentrated in the synthesis of non-symmetric, 5-substituted bis-ureidopyrimidinones. Thus, **9f** was reacted with the corresponding isocyanate in the presence of triethylamine. UPy **1r** was obtained in good yield. Unlike for 6-substituted derivatives, reduction of the nitro function proceeded in excellent yield with hydrogen and palladium black to give product **1s**, which was subsequently reacted with blocked isocytosine **24c** to afford bis-UPy **4c** in good yield (Scheme 18).



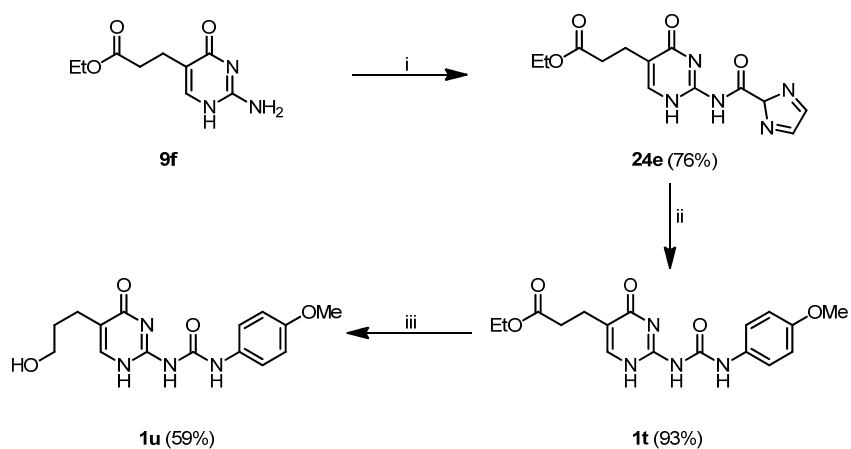
i) 2-methyl-nitrobenzyl isocyanate, DMF, 60 °C, overnight; ii) H₂, Pd black, DMF, r.t., overnight; iii) **24c**, DMF, 60 °C, overnight; iv) DIBAL-H, CH₂Cl₂, -78 °C, 5 h; then r.t., overnight.

Scheme 18: Synthesis of disymmetric bis-UPy **4a**.

4c was very soluble in solvents such as chloroform or dichloromethane. The ¹H NMR spectrum recorded in chloroform showed broad signals accounting from a poorly defined aggregate. The spectrum signals remained broad even in the presence of 30% (v/v) of a competitive solvent such as MeOH. Sharp signals were obtained only when the NMR was run in DMSO. MALDI-TOF as well as ESI (positive mode) mass spectrometry analysis of **4c** allowed the observation of species composed up to three monomers.

For 5-substituted pyrimidinones, model **1t** was synthesized to optimize the reduction conditions (Scheme 19). Reaction of pyrimidinone **9f** with CDI according to Meijer's approach,²⁰ gave the blocked isocytosine **24e** in 76% yield. For the synthesis of **1u**, compound **24e** was heated overnight in dry

chloroform with *p*-anisidine and ureidopyrimidinone **1t** was obtained in excellent yield (93%).



i) CDI, THF, r.t., 3 h; ii) *p*-anisidine, CHCl₃, 50 °C, overnight; iii) DIBAL-H, CH₂Cl₂, -78 °C, 5 h; then r.t., overnight.

Scheme 19: Synthesis of ureidopyrimidinone **1u**.

Then, ester reduction was studied with model compound **1t**, which was treated with DIBAL-H at low temperature (-78 °C) in dry dichloromethane. After quenching, only a few milligrams of **1u** were isolated. Due to its insolubility, the crude was continuously extracted DCM in a liquid-liquid extractor and the compound was isolated in a 59% yield.

Accordingly, reduction of **4c** was carried out under identical conditions and **4a** was obtained in 70% yield. Since **4a** is much more soluble than **1t**, no continuous extraction was needed.

Mass spectrometry analysis of **4a** showed monomeric and dimeric species using the MALDI-TOF technique, whereas trimers were observed in ESI. However, **4a** was only partially soluble in chloroform and broad signals, as in the case of its precursor **4c**, were observed in the ¹H NMR spectrum (Figure 29). Addition of some MeOH caused complete dissolving of the

sample in chloroform, although the signals remained broad. The poor solubility did not allow further characterization of the aggregate. For this reason, new compounds with improved solubilities are currently under preparation in our laboratories.

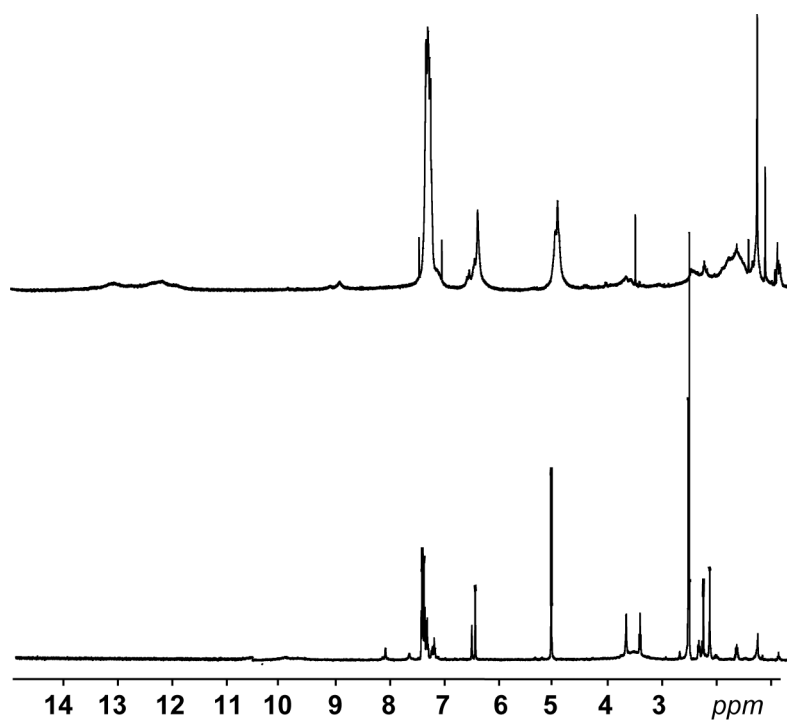


Figure 26: ^1H NMR (400 MHz) of **4a** in $\text{DMSO-}d_6$ (bottom) and CDCl_3 (top).

II.4 CONCLUSIONS

Due to the easy access to their precursors, a large variety of ureidopyrimidinones, bearing different functionalities have been synthesized and studied. Strong self-assembled dimers based on ureidopyrimidinones can be formed efficiently even from highly crowded fullerodendrons.

Fullerodendrons were obtained by following a synthetic strategy based

on the esterification of a Boc-protected UPy precursor possessing an alcohol function with a carboxylic acid bearing the functional unit. In this way, it was possible to prepare new ureidopyrimidinone derivatives substituted by one or by five fullerene subunits.

As demonstrated by MALDI-TOF mass spectrometry and ^1H NMR spectroscopy, both compounds form self-assembled dimers spontaneously through hydrogen bonding interactions, thus leading to supramolecular structures containing two or ten fullerene moieties. The highly directional four-fold hydrogen bonding motif based on ureidopyrimidinone is, therefore, well suited for stable, non-covalent dendritic supramolecular arrays.

In order to create two dimensional aggregates, a series of bis-ureidopyrimidinones were synthesized, the size and shape of these aggregates being defined by the spacer employed between the UPy units.

Thus, a double-UPy, composed by two UPy units held together through a urea function leads to a V-shape molecule. Aggregates accounting from this product have demonstrated to be concentration dependent, and defined aggregates most likely form at low concentrations. VPO experiments accounted for a tetrameric aggregate, and calculations predicted that these oligomeric species are energetically favored. Even though, the angle between the edges of the DUPy molecule predicted that tetramers are the only cyclic aggregate that could be constructed. Further experiments are thus necessary to envisage the most stable structure of these aggregates. These will include new DOSY measurements and Gel Permeation Chromatography (GPC) analysis.

An adamantyl spacer leads to pentameric aggregates when bulky substitution as with another adamantane was used, although the compound was initially predicted to form hexamers due to a better packing. However, the low solubility of this compound did not allow a

Chapter II

complete characterization in solution.

When *m*-disubstituted aromatic rings were used, hexameric aggregates were predicted to form. However, none of the bis-ureidopyrimidinones so far synthesized in our laboratory exhibit this behaviour, being only oligomeric, ill defined species as found by ¹H NMR spectroscopy. Once again, the poor solubility of bis-UPy **4a** limited the number of experiments that could be carried out for characterization.

CHAPTER II: RECOGNITION AND SEPARATION OF FULLERENES

Part of this chapter has been published: a) Huerta, E.; Metselaar, G. A.; Fragoso, A.; Santos, E.; Bo, C.; de Mendoza, J. *Angew. Chem. Int. Ed.* **2007**, 46, 202-205. b) Huerta, E.; Cequier, E.; de Mendoza, J. *Chem. Commun.* **2007**, 5016-5018. c) de Mendoza, J.; Huerta, E.; Metselaar, G. A. US patent US 2008/0025904 A1.

UNIVERSITAT ROVIRA I VIRGILI
SELF-ASSEMBLY BASED ON THE 2-UREIDO-4(1H)-PYRIMIDINONE MOTIF: FROM CYCLIC ARRAYS TO MOLECULAR CAPSULES
FOR FULLERENE SEPARATIONS
Elisa Huerta Martínez
DL:T.289-2012

CHAPTER III: RECOGNITION AND SEPARATION OF FULLERENES

III.1 GENERATION, ISOLATION AND PURIFICATION OF FULLERENES

Resistive heating of graphite – a method based on the technique for the production of amorphous carbon films in a vacuum evaporator – generates macroscopic quantities of fullerenes. The apparatus (Figure 1) consists of a chamber as a recipient, connected to a pump system and a gas inlet. In the interior, a thin graphite rod of about 3 mm diameter, guided by a copper sleeve, with a sharpened tip is located on a flat thick graphite rod (12 mm). To produce soot, the apparatus is repeatedly evacuated and purged with helium; after several cycles, the chamber is finally filled with *ca.* 100 Torr of helium. After applying a current of about 40-60 A, only the material of the thin rod evaporates. The electric current passing through the rods dissipates most of the Ohmic power heating at the narrow point of contact. This leads to a bright glowing in this area at 2500-3000 °C. The smoke generated condenses in the coolest zones of the chamber and is collected as a black fluffy dust composed by the soot and the slag. Based on evaporated graphite, 5-10% yields of fullerenes are obtained.

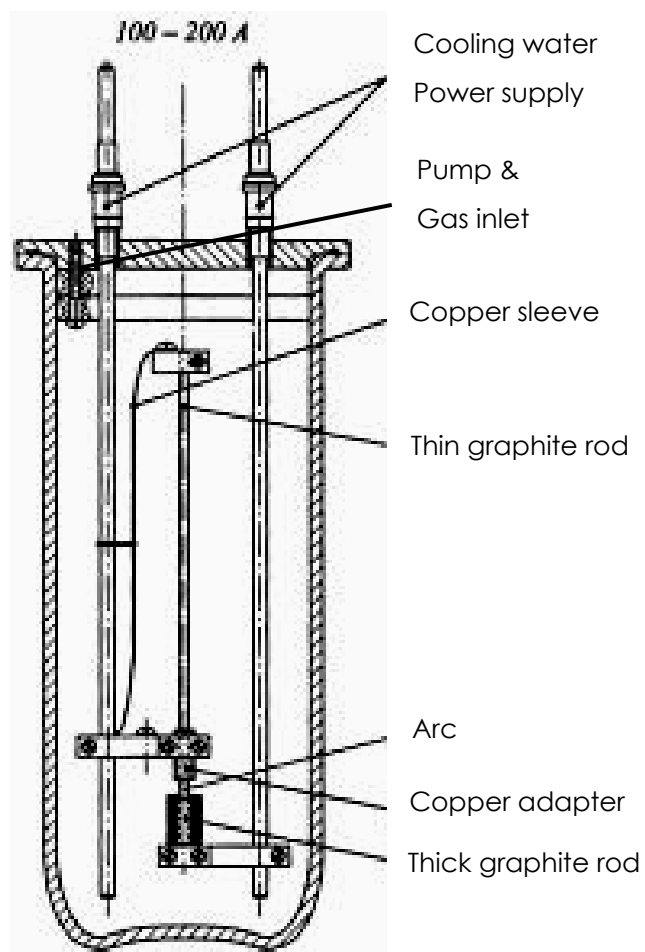


Figure 1: Arc discharge apparatus.

The ratio of C_{60} to higher fullerenes is typically 8:2. The relative yields of higher fullerenes can be improved when graphite containing light elements such as B, Si or Al is used and the buffer gas helium is mixed with small amounts of N_2 .¹

¹ Tohji, K.; Paul, A.; Moro, L.; Malhotra, R.; Lorents, D. C.; Ruoff, R. S. *J. Phys. Chem.* **1995**, *99*, 17785-17788.

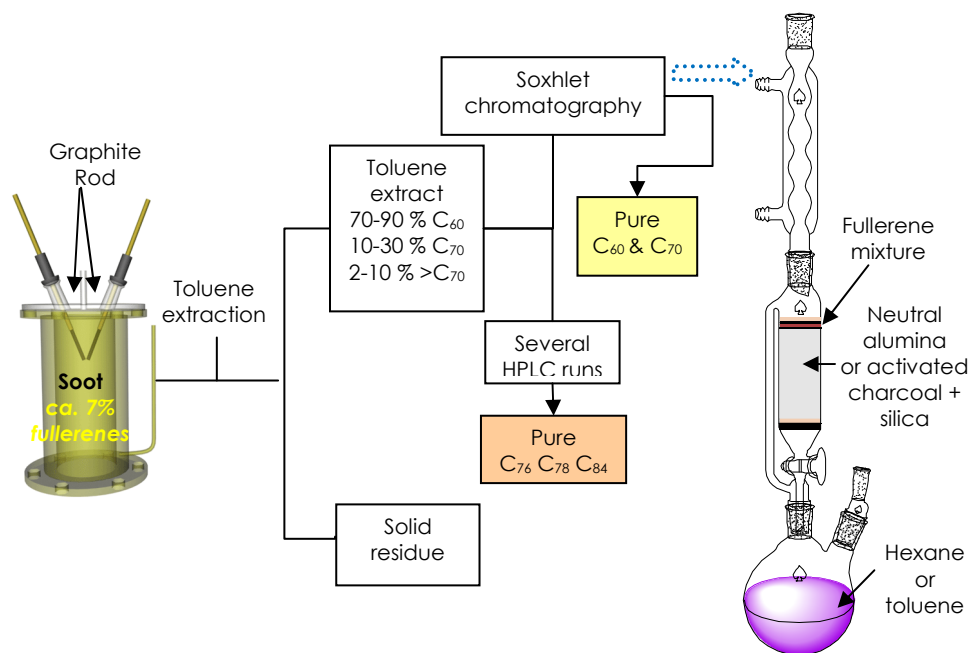


Figure 2: Protocol for fullerene generation, separation and isolation. (Adapted from ref. 5).

The most common method for the isolation of fullerenes from soot is by continuous extraction in a Soxhlet apparatus with organic solvents (Figure 2). In general, the preferred solvent is toluene since it provides enough solubility and is less toxic than benzene or carbon disulfide. The toluene extract is typically red to reddish brown and contains higher fullerenes such as C₇₆, C₇₈, C₈₄, C₉₀, and C₉₆, in addition to C₆₀ and C₇₀.

For the isolation of pure C₆₀ and C₇₀ Soxhlet-chromatography² is typically used. This method combines distillation or Soxhlet extraction with chromatography and does not require large amounts of solvent. In this way,

² a) Chatterje, K.; Parker, D. H.; Wurz, P.; Lykke, K. R.; Gruen, D. M.; Stock, L. M. *J. Org. Chem.* **1992**, *52*, 3253-3254. b) Khemani, K. C.; Prato, M.; Wuldi, F. *J. Org. Chem.* **1992**, *52*, 3254-3257.

gram quantities of C₆₀ can be obtained in relatively short time. After eluting C₆₀, a fresh hexane-containing flask is used to collect eluting C₇₀. With chromatography on graphite, higher amounts of toluene can be used, improving the solubility of the material. A major improvement, which allows the use of pure toluene as mobile phase, was achieved using a mixture of charcoal and silica gel as stationary phases.³ Although chromatography and Soxhlet-chromatography are very efficient and simple methods for the separation of C₆₀ and C₇₀, the fullerenes partly decompose or remain irreversibly adsorbed to the stationary phases. Especially, higher fullerenes hardly elute from charcoal columns. C₁₈-reverse phase HPLC is the preferred method for the separation of the higher fullerenes.⁴ Typically, (1:1) MeCN/toluene mixtures are used and several runs are required to obtain pure samples of C₇₆, C₇₈ and C₈₄. Currently, the most efficient columns for the HPLC separations of parent fullerenes, including endohedral fullerenes, are the commercially available COSMOSIL columns (Nalcalai Tesque, Japan). These columns allow the use of pure toluene as mobile phase maintaining a good resolution.⁵

III.2 DESIGN AND SYNTHESIS OF UPy-BASED RECEPTORS FOR FULLERENES

As shown in the introductory chapter, cyclotrimeratrylene (CTV) has the appropriate size and shape for the complexation of fullerenes.⁶ The present

³ a) Scrivens, W. A.; Bedworth, P. V.; Tour, J. M. *J. Am. Chem. Soc.* **1992**, *114*, 7917-7919. b) Isaacs, L.; Wehrsig, A.; Diederich, F. *Helv. Chim. Acta* **1993**, *76*, 1231-1250.

⁴ a) Ettl, E.; Diederich, F.; Whetten, R. L. *Nature* **1991**, *353*, 149-153. b) Diederich, F.; Thilgen, C.; Whetten, R. L.; Ettl, E.; Chao, I.; Álvarez, M. M. *Science* **1991**, *254*, 1768-1770.

⁵ Thilgen, C.; Diederich, F.; Whetten R. L. *Buckminsterfullerenes* **1993**, 59-81.

⁶ Steed, J. W.; Junk, P. C.; Atwood, J. L.; Barnes, M. J.; Raston, C. L.; Burkhalter, R. S. *J. Am. Chem. Soc.* **1994**, *116*, 10346-10347.

work is based on the synthesis of a hydrogen-bonded self-assembled capsule for fullerene complexation, based on a combination of a CTV functionalized with three ureidopyrimidinone (UPy) subunits that, as was shown, self-assemble into dimers through the formation of four hydrogen bonds (Figure 3).

We selected amino pyrimidinone **9j**,⁷ endowed with an eleven-carbon chain to facilitate solubility in apolar solvents suitable for hydrogen bonding, to be attached on the CTV scaffold. As was pointed out in Chapter II, the activated isocytosine derivative **24d**⁸ can be subsequently reacted with an amino group anchored on the CTV platform to promote UPy formation.

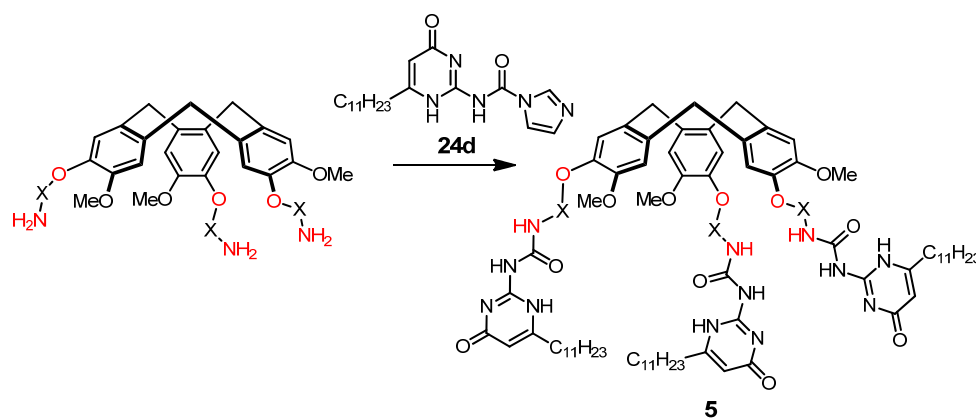


Figure 3: General synthesis of CTV-UPy monomer **5**.

Herein we discuss the synthesis of different receptors whose size can be modulated by introducing different spacers (-X-) between the CTV scaffold and the UPy units.

Selected spacers were divided into two groups: those based on alkyl

⁷ Keizer, H. M.; González, J. J.; Segura, M.; Prados, P.; Sijbesma, R. P.; Meijer, E. W.; de Mendoza, J. *Chem. Eur. J.* **2005**, 4602-4608.

⁸ Synthesis of **24d** has been described in Chapter II.

chains and those based on rigid aromatic spacers. In the first group, the alkyl chains are flexible enough to allow the capsule to adapt to the fullerene guest. However, too long alkyl chains may cause collapse of the self-assembled structure. For this reason, ethyl (S1) and propyl (S2) chains were selected (Figure 4).

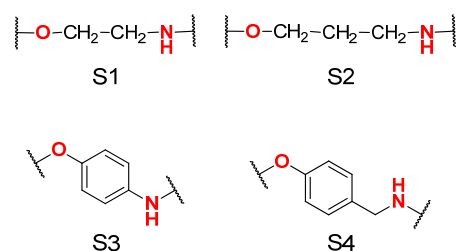


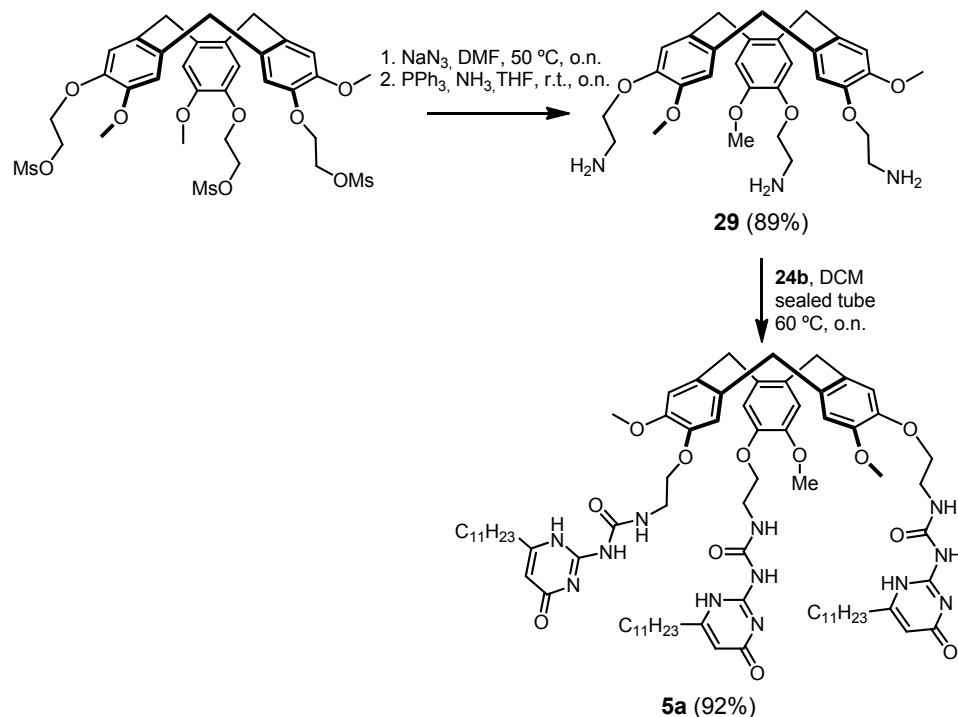
Figure 4: Proposed spacers.

Spacers S3 and S4 constitute the second group. The electron-rich aromatic rings should strongly contribute to interact with the electron deficient fullerene guest. The introduction of these spacers not only modifies the size of the capsule but also its shape. For example, spacer S3 should give rigidity to the molecule while spacer S4 introduces an angle in the final structure, making the aggregate slightly wider.

III.2.1 Introduction of Ethyl Spacer (S1)

CTV-triamine **29** was prepared in two steps from the known CTV-tris-mesyate⁹ (Scheme 1). Nucleophilic substitution of the mesyl group with NaN₃ in DMF afforded the corresponding CTV-tris-azide, which was subsequently reduced with triphenylphosphine to give **29** in 89% overall yield. The ureidopyrimidinone attached to the CTV scaffold, referred to as CTV-UPy **5a** was obtained by stirring **29** with **24d** at 60 °C overnight.

⁹ Vériot, G.; Dutasta, J. P.; Matouzenko, G.; Collet, A. *Tetrahedron* **1995**, *51*, 389-400.



Scheme 1

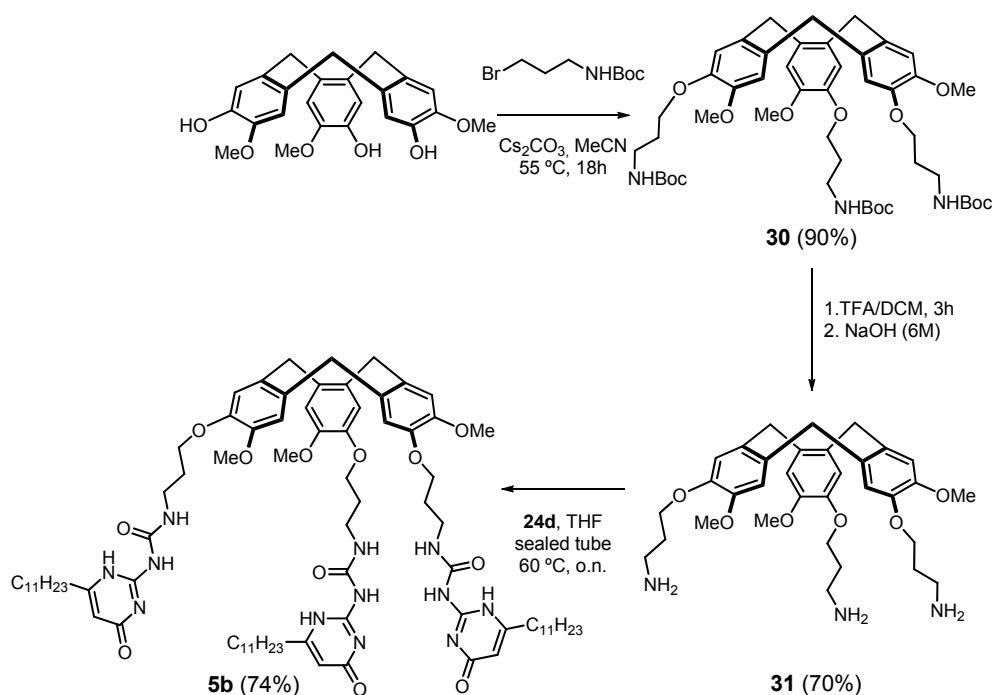
III.2.2 Introduction of Propyl Spacer (S2)

The synthesis of compound **5b** was easily accomplished following the procedure described by Reinhoudt *et al.*¹⁰ Alkylation of the known cyclotrimer derivative¹¹ with the commercially available Boc-aminopropyl bromide in a basic medium afforded compound **30** in excellent yield as a foam (Scheme 2). Deprotection of the amino groups with trifluoroacetic acid, followed by hydrolysis of the resulting salts, gave the free amino compound **31** in good yield, which was subsequently reacted with imidazole **24d** to get the enlarged CTV-UPy molecule **5b** after

¹⁰ Dam, H. H.; Reinhoudt, D. N.; Verboom, W. *New J. Chem.* **2007**, 31, 1620-1632.

¹¹ Canceill, J.; Gabard, J.; Collet, A. *J. Chem. Soc., Chem. Commun.* **1983**, 122-123.

precipitation.



Scheme 2

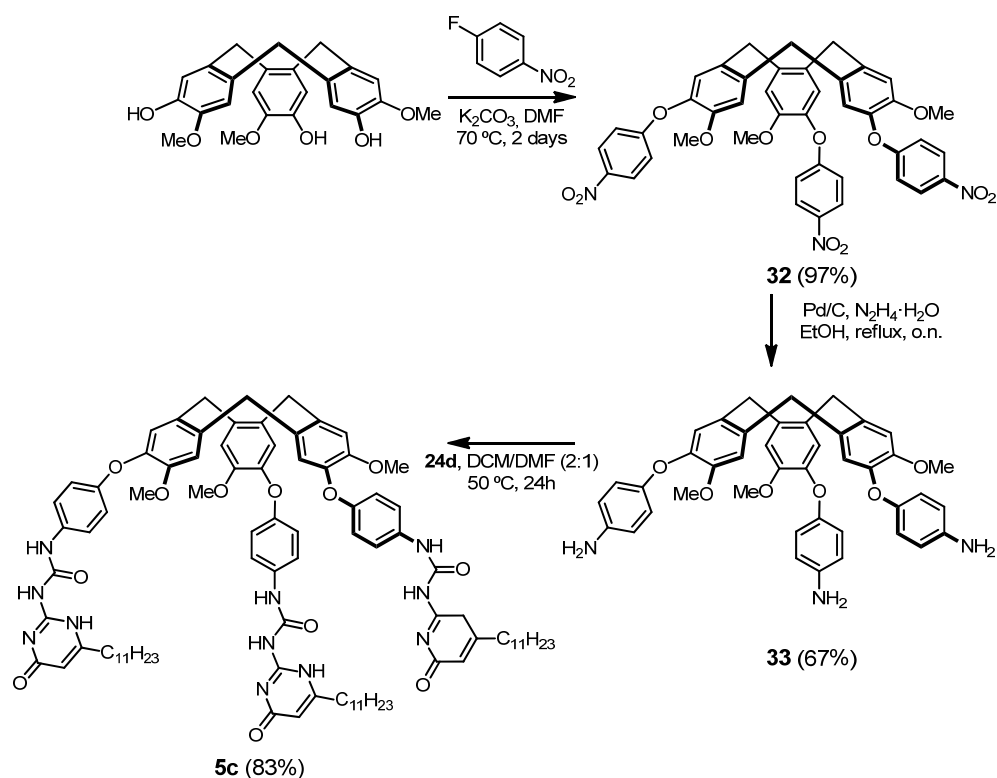
III.2.3 Introduction of Aryl Spacer (S3)

The formation of the diaryl ether on the CTV-triphenol scaffold was also carried out via nucleophilic substitution. Cyclotriguaiacylene was treated with base in DMF and 4-nitrofluorobenzene¹² was added. Compound **32** was obtained in high yield, after precipitation. Reduction of the nitro function was performed in the presence of Pd/C and hydrazine, giving triamine **33** in moderate yield (Scheme 3).

Due to the low solubility of triamine **33**, it was reacted with imidazolidine

¹² Arduini, A.; Calzavacca, F.; Demuru, D.; Pochini, A.; Secchi, A. *J. Org. Chem.* **2004**, *69*, 1386-1388.

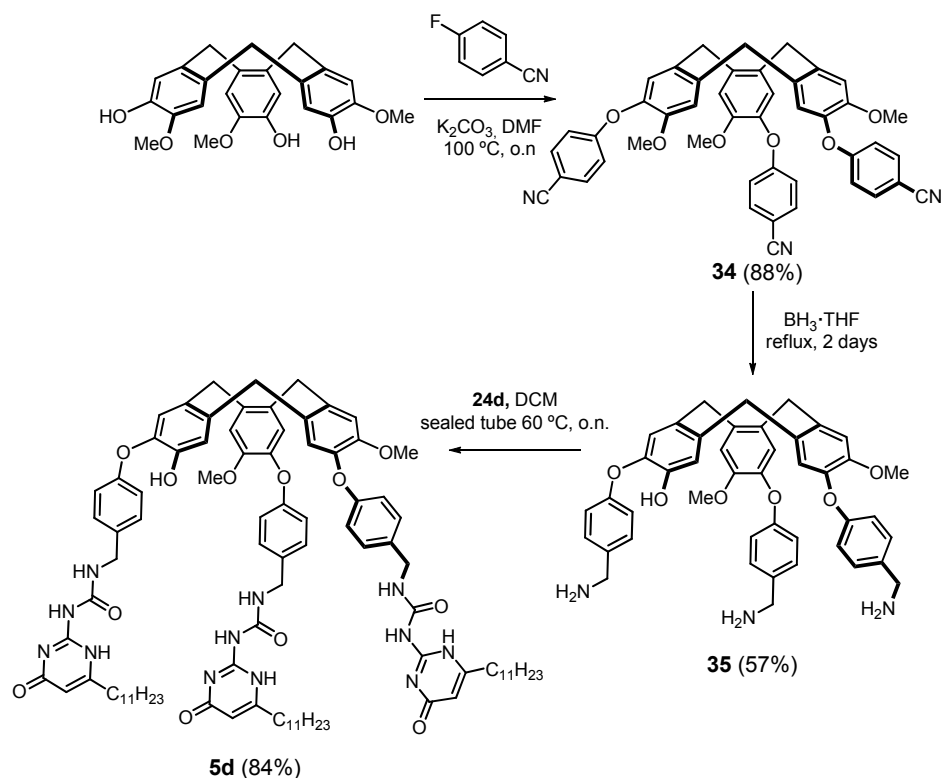
24d in a DCM/DMF mixture, and CTV-UPy **5c** obtained in good yield.



Scheme 3

III.2.4 Introduction of Benzylamino Spacer (S4)

The introduction of the aromatic spacer was performed, as previously described, *via* nucleophilic aromatic substitution of cyclotriguaiacylene with 4-fluorobenzonitrile in basic medium (Scheme 4). Compound **34**, obtained in 88% yield, was then treated with $\text{BH}_3 \cdot \text{THF}$ to get the CTV-triamine **35** in moderate yield. The reaction of the triamine with imidazolide **24d** afforded the desired CTV-UPy **5d** in a good yield.



Scheme 4

III.3 COMPLEXATION AND EXTRACTION STUDIES: SEPARATION OF FULLERENES WITHOUT CHROMATOGRAPHY

III.3.1 Complexation of C_{60} and C_{70}

CTV-UPy **5a**, insoluble in toluene, could be solubilized by sonication in a toluene solution containing C_{60} , as was demonstrated by IR-spectroscopy (Figure 5). This suggests a specific interaction between the fullerene and **5a** resulting into a soluble entity. This increased solubility could be tentatively explained by the formation of relatively apolar capsules involving two molecules of **5a** around the fullerene, where the polar UPy groups are all participating in the hydrogen-bonded network. The NH-stretching vibrations at $\nu = 3200\text{ cm}^{-1}$ indicated the presence of hydrogen-bonded urea protons

of the ureidopyrimidinone units, whereas in the absence of the C_{60} , the host-concentration in the solution was below the detection limit of IR-spectroscopy.

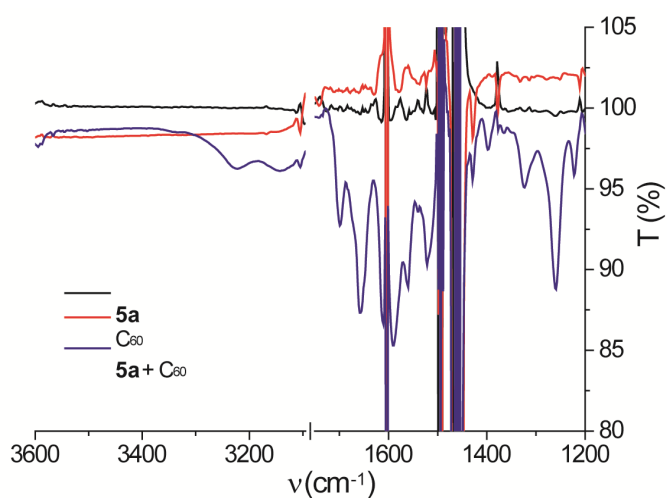


Figure 5: IR-spectra in toluene of **5a** (black), C_{60} (red) and **5a**+ C_{60} (blue).

The 1H NMR spectrum of **5a** in tetrachloroethane showed only broad signals (Figure 6, top),¹³ presumably caused by poorly defined H-bonded aggregates formed. Addition of 0.5 equivalents of C_{60} to this solution resulted in a significant sharpening of the 1H NMR spectrum (Figure 6, bottom).

¹³ [**5a**] = 5 mM.

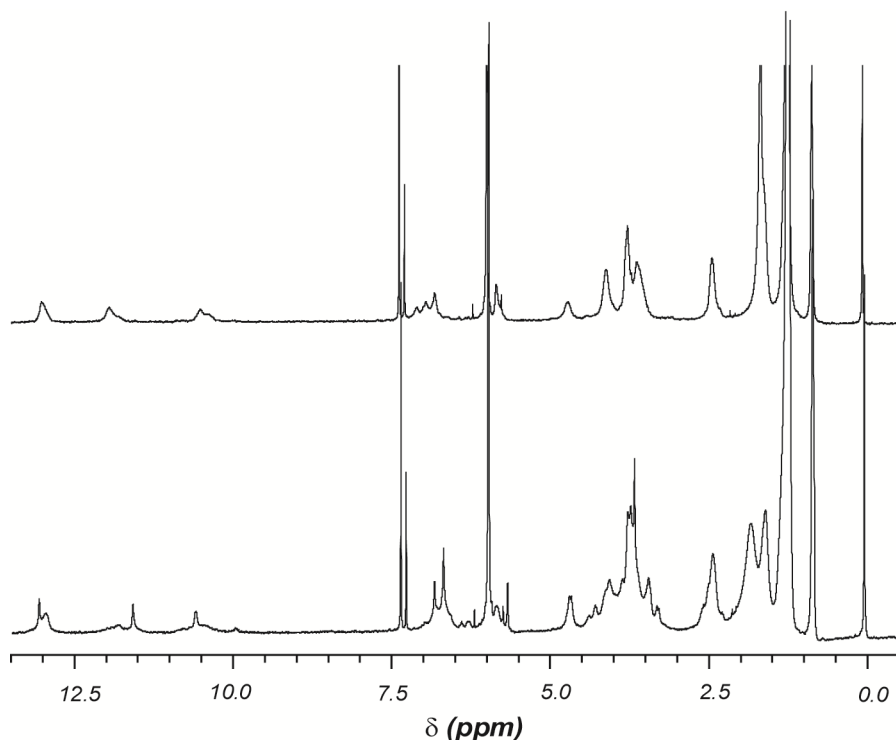


Figure 6: ¹H NMR spectra of 5 mM solution of **5a** in C₂D₂Cl₄ with (bottom) and without (top) C₆₀.

Apparently, the added C₆₀ acts as a template for the formation of well-defined complexes with **5a**, in which the fullerene is most likely encapsulated by two equivalents of **5a** as was indicated by the Job's plots (see Section III.3.2). When this solution was subjected to a VT-¹H NMR experiment (Figure 7), the dynamic nature of the host-guest system was evident. At 100 °C, **5a** is present only in its monomeric form as can be observed by the absence of downfield-shifted signals for the NH-protons and the sharpness of the remaining signals. Upon cooling to 80 °C the downfield signals, characteristic for the UPy amide protons, appeared at $\delta = 13.12, 11.61$ and 10.58 ppm. Their intensity increased as the temperature was further decreased and the signals were more pronounced around room temperature. Upon further cooling, the spectrum broadened once again which could be attributed to

a hindered mobility of the long aliphatic tails, resulting in kinetically trapped conformations.

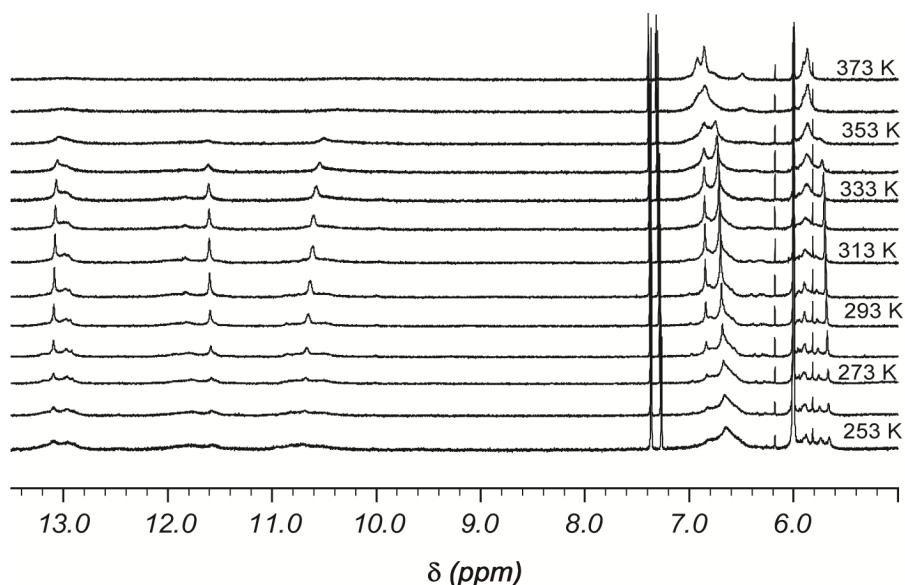


Figure 7: VT NMR spectra of **5a** with 0.5 equivalents of C_{60} in $C_2D_2Cl_4$.

The ¹H NMR spectrum of free **5a** in tetrachloroethane had relatively broad signals but, upon addition of fullerene, the signals sharpened significantly. Besides C_{60} , the complex formed with C_{70} was also investigated by ¹H NMR spectroscopy. However, it is clear from these spectra that not only one discrete complex was formed, but a mixture of aggregates instead.

The influence of the solvent on the aggregates and complexes was also studied. Figure 8 shows the ¹H NMR spectra of C_{70} with CTV-UPy **5a** in three different solvents. With the exception of carbon disulfide, where only one complex was observed, more than one species apparently were formed regarding multiple signals observed for the UPy NH-protons. Considering that C_{70} is a unique isomer of D_{5h} symmetry, it can be stated that the splitting of signals is due mainly to the presence of different diastereoisomeric capsules

(homochiral or *meso*) resulting from the racemic CTV employed (see section III.5 for a detailed discussion).

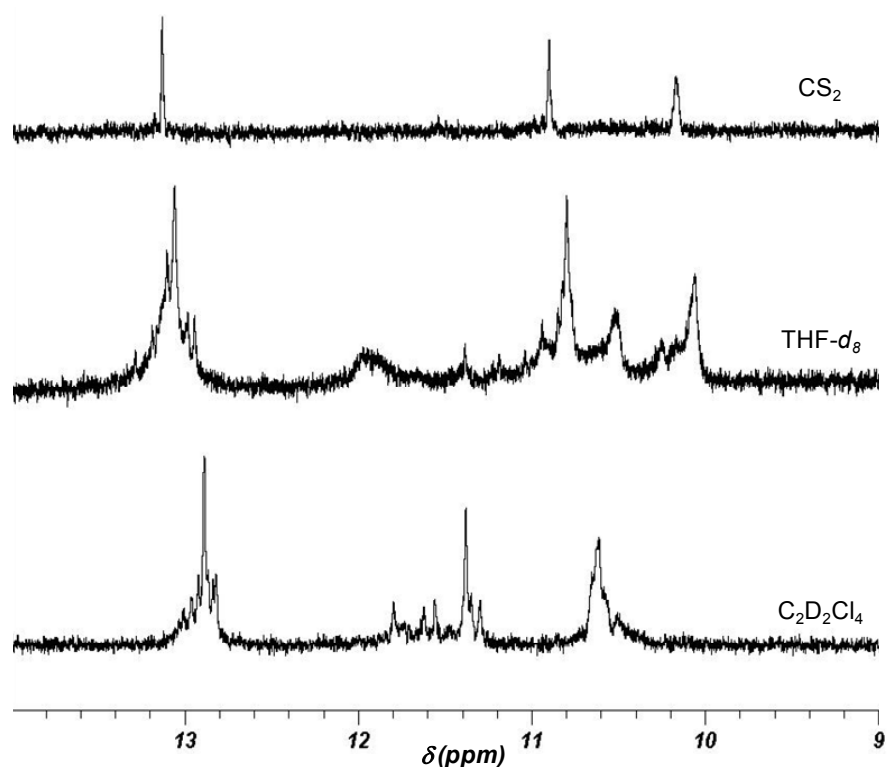


Figure 8: ^1H NMR-spectra of complexes of C_{70} :**5a-5a** in CD_2Cl_4 (bottom), $\text{THF-}d_8$ (middle) and CS_2 ($\text{MeOH-}d_4$ was placed into an inset tube for locking)(top).

A solution of the C_{70} complex was also studied by VT- ^1H NMR (Figure 9). Interestingly, at 100 °C the characteristic downfield signals corresponding to the hydrogen-bonded NH protons are still visible, which indicates that the complex is thermodynamically more stable than the one with C_{60} . At room temperature, the signals became sharper and more intense and, like for the C_{60} complex, further cooling resulted in broader signals.

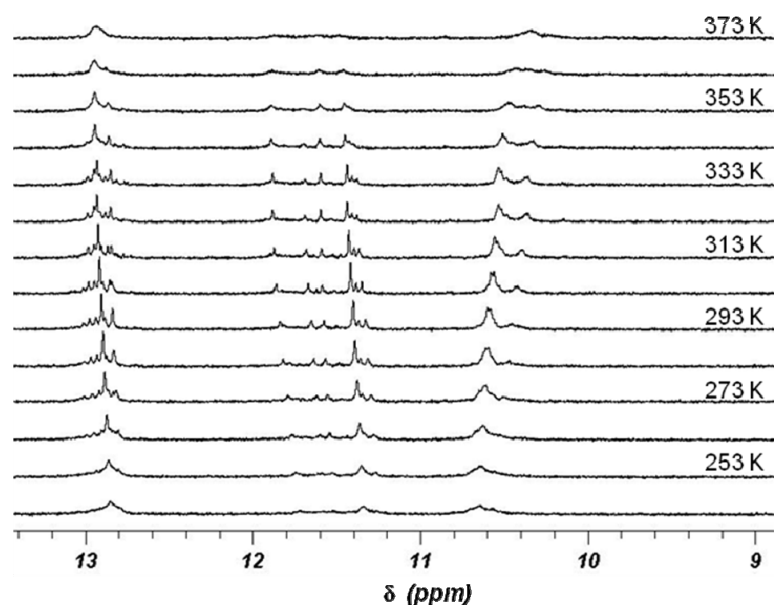


Figure 9: VT NMR spectra of **5a** with 0.5 equivalents of C_{70} in $C_2D_2Cl_4$.

III.3.2 Stability of the Fullerene Complexes

The stoichiometry of the complexation between **5a** and both C_{60} and C_{70} at different concentrations was determined by Job plots measured in tetrachloroethane (Figure 10). For C_{60} , at a concentration of 1.5×10^{-5} M, the complexation by **5a** was negligible, as evidenced by the lack of correlation between the points in the plot. At 1.5×10^{-4} M, the curve showed a maximum at 0.4 which can be attributed to the presence of both 1:1 and 1:2 (C_{60} :**5a**) complexes in solution. However, upon increasing the concentration to 1.5×10^{-3} M, the stoichiometry of C_{60} :**5a** complexes changes to 1:2, likely by dimeric capsule formation, driven by the strong quadruple H-bonds between the ureidopyrimidinone moieties.

When C_{70} was used as the guest for **5a** instead of C_{60} , a 1:2 stoichiometry for C_{70} :**5a** was found at all studied concentrations. This suggests again that the association constant for C_{70} is significantly higher than that for C_{60} .

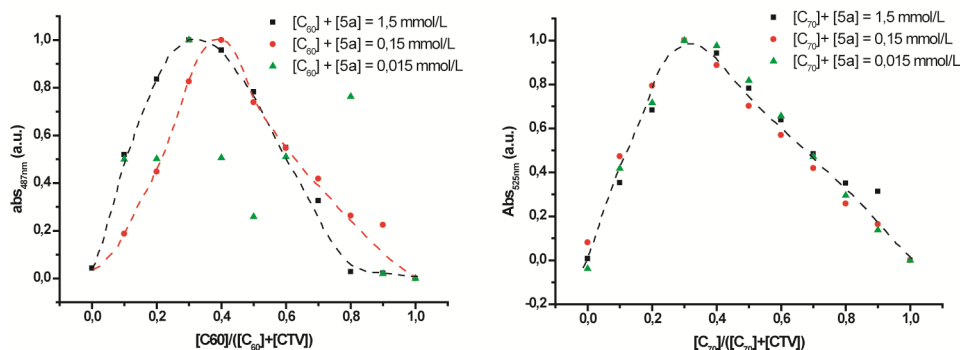


Figure 10: Job's plots for **5a**:fullerene complexes at different concentrations.

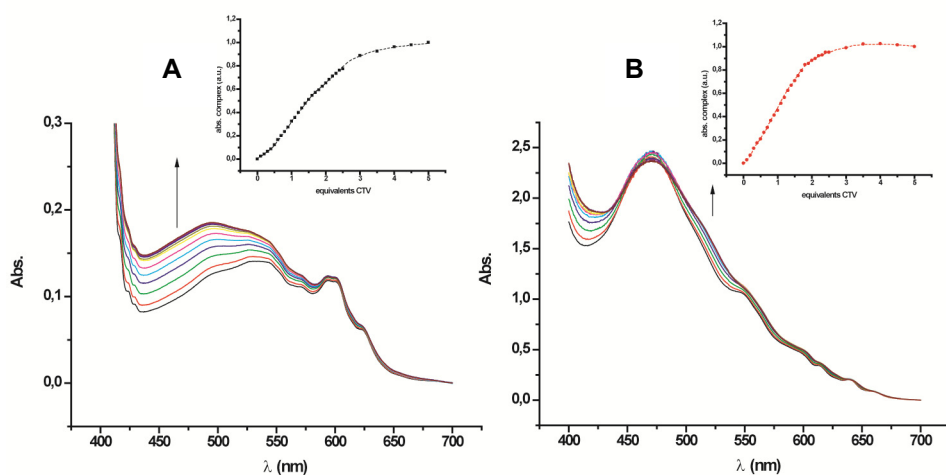


Figure 11: UV-spectra of the titration of **5a** (0.5 eq. steps) with: A) C_{60} and B) C_{70} . Inner plots: UV-titration curves for the binding of C_{60} (black squares) and C_{70} (red circles) to **5a**.

In order to calculate the strength of the binding, the association constants (K_a) of the 1:2 complexes of **5a** with both C_{60} and C_{70} in tetrachloroethane were determined by UV-spectroscopic titrations, adding **5a** to a guest solution, *i.e.* C_{70} or C_{60} , keeping the guest concentration constant at 1.5 mM (Figure 11).

The complexes could be formed by the two encapsulation mechanisms depicted in Figure 12. Both accurately describe the cooperative process, but they must be considered to calculate the association constant.

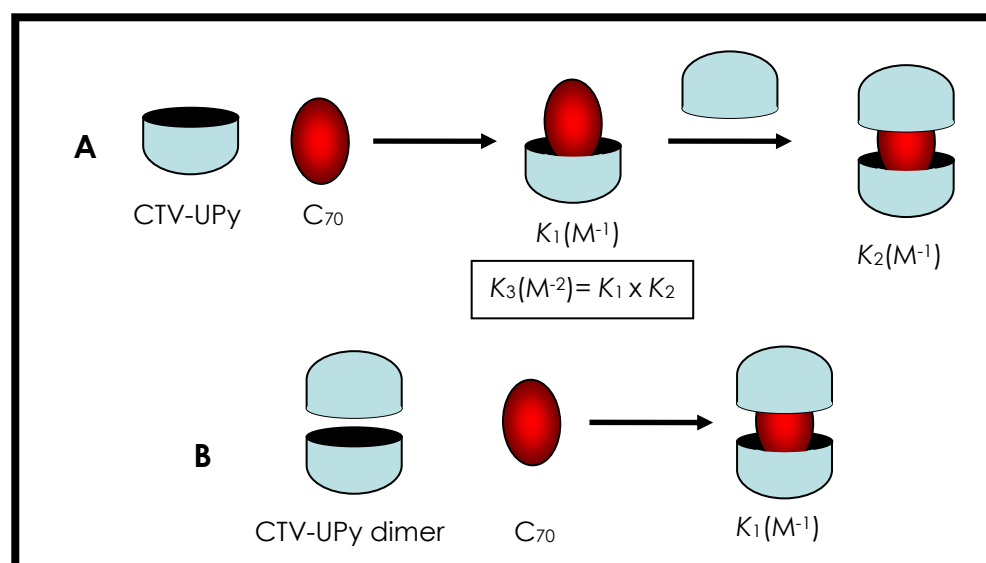
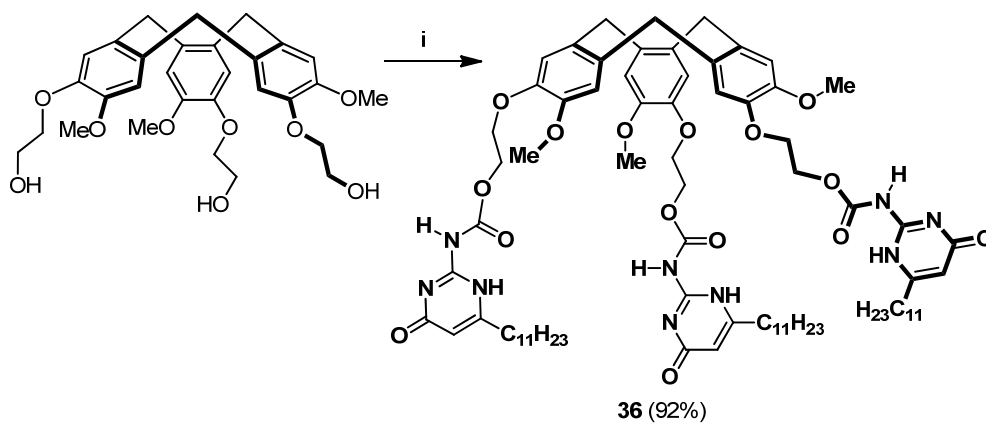


Figure 12: A) 1:2 binding model in which fullerene is first bound by one CTV-host, after which a second CTV-host completes the encapsulation of the fullerene. B) 1:1 binding model of fullerene to a preformed CTV-capsule.

The *termolecular* model A proceeds in two steps and involves two binding constants. The first one would be the association of one CTV-UPy moiety with the fullerene (K_1) and the second step (K_2) the association of a second CTV-UPy subunit through hydrogen bonding. The global constant (K_3) would be the product of both constants and would have units M^{-2} . According to this model, the association constants can be estimated as $K_a(C_{60}) = (1.93 \pm 0.13) \times 10^6 M^{-2}$ and $K_a(C_{70}) = (7.4 \pm 1.5) \times 10^7 M^{-2}$, which confirms the higher stability of the C_{70} complex.

We tried to evaluate the contribution of K_1 to the global association constant. For this purpose the receptor model **36**, which cannot dimerize

since it contains carbamates instead of ureas, was synthesized (Scheme 5). The synthesis proceeds through the reaction of the already described CTV with hydroxyethoxy chains⁹ with the imidazolide of the undecyl amino pyrimidinone **24d**. The product was obtained in a 92% yield after precipitation and employed without further purification.



i) **24d**, THF, DMF (5:1), sealed tube, 60 °C, overnight.

Scheme 5

Then, C₆₀ and C₇₀ were titrated separately by UV with a solution of **36** in tetrachloroethane. The titrations (Figure 13) revealed that no substantial binding with either C₆₀ or C₇₀ was taking place, so the binding is likely due to a partial disruption of an initial **5a 5a** capsule or a dimeric aggregate to accommodate the guest, in good agreement with model B.

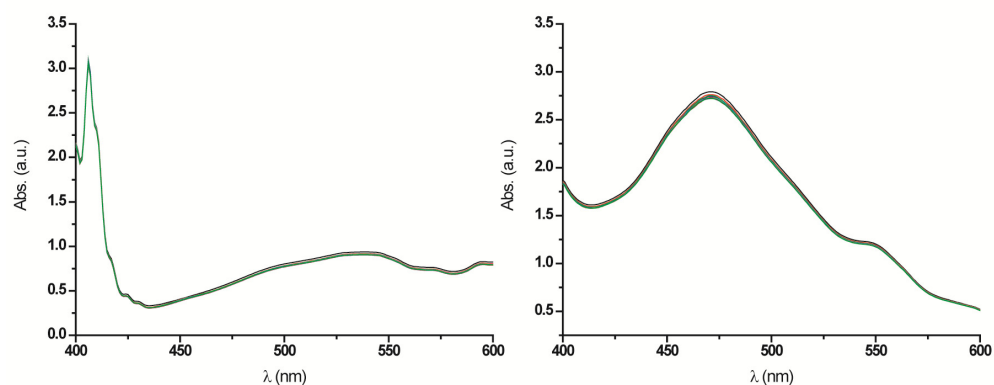


Figure 13: UV-titration of CTV **36** with C_{60} (left) and C_{70} (right).

Indeed, the *bimolecular* model B considers that encapsulation occurs through partial disruption of a previously formed dimeric capsule. In this case, the association constant involves only the encapsulation of the fullerene. For this 1:1 binding model, the calculated values for the association constants were $1.82 \times 10^3 \text{ M}^{-1}$ for C_{60} and $3.89 \times 10^4 \text{ M}^{-1}$ for C_{70} .

Table 1 summarizes the values obtained from UV-titrations for the binding of the fullerenes by **5a**.

Table 1: Binding constants of fullerenes to **5a** determined by UV-titrations.

Fullerenes	K_a 1:1 model (M^{-1})	K_a 1:2 model (M^{-2})
C_{60}	1.82×10^3	1.93×10^6
C_{70}	3.89×10^4	7.94×10^7

Additionally, the results obtained by UV-titrations were confirmed by isothermal titration calorimetry (ITC), in which a 3.5 mM solution of **5a** in tetrachloroethane was added to a 0.5 mM solution of fullerene in the same solvent. For C_{60} a quite high binding constant of $K_a = 1.2 \pm 0.3 \times 10^6 \text{ M}^{-1}$ was obtained. This could be tentatively ascribed to the heat effect caused by the dilution, which is accompanied by a substantial disruption of the

hydrogen bonding network. These heat effects cannot entirely be ruled out by blank experiments in which a concentrated solution of **5a** is added to pure tetrachloroethane, since the presence of the fullerene influences the non-hydrogen-bonded CTV-hosts. Consequently, we designed an alternative experiment in which a 5 mM solution of fullerene in tetrachloroethane was added to a 1.42 mM solution of **5a** (or 0.71 mM of the corresponding dimeric capsules of **5a**) in tetrachloroethane. This approach circumvents the undesired heat-effects related with the dilution-induced disruption of the hydrogen bonds between the two halves of the CTV-UPy molecules. The resulting titration curves are depicted in Figure 14 and the corresponding binding constants and thermodynamic parameters are summarized in Table 2.

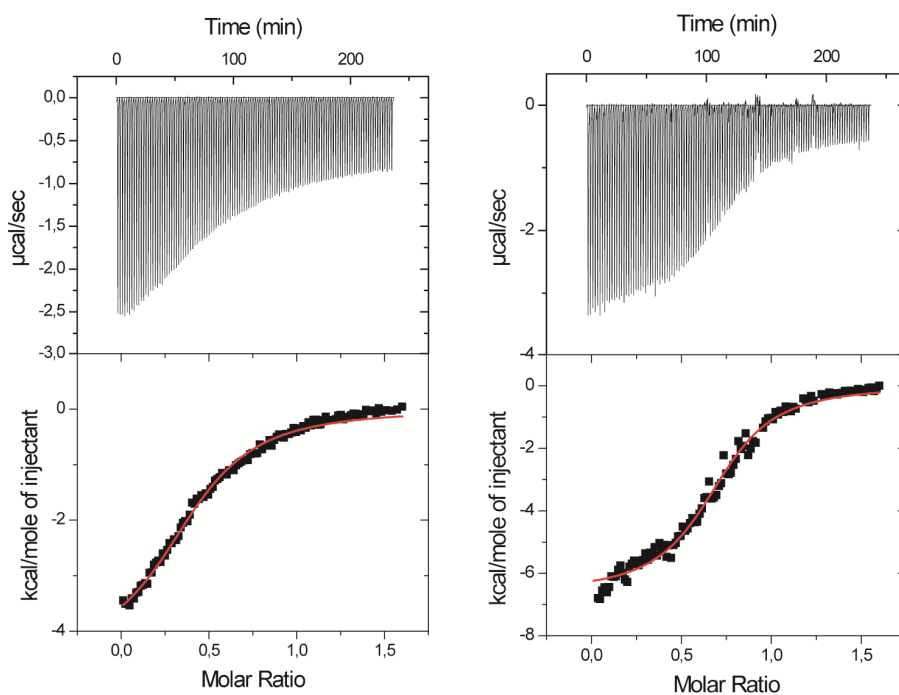


Figure 14: ITC-curves for titration of a 5 mM solution of fullerene in tetrachloroethane to a 1.42 mM solution of **5a** in tetrachloroethane.

Table 2: Results of the ITC.

	C₆₀	C₇₀
<i>N</i>	0.49	0.86
<i>K_a</i> (M ⁻¹)	1.06 x 10 ⁴	4.45 x 10 ⁴
ΔH (kcal·mol ⁻¹)	-4.1	-6.0
ΔS (cal·mol ⁻¹ ·K ⁻¹)	5	1.5

In this case, the curve obtained for the encapsulation of C₆₀ could not be correctly fitted for a 1:1 binding process, as it is apparent from the found *N* = 0.49 value. Nevertheless, the ITC results confirm the stronger binding of C₇₀ over C₆₀.

III.3.3 Selective Extraction of C₇₀

In view of the differences in the strength of fullerene binding found for CTV-UPy receptor **5a**, a method for the selective separation of C₇₀ from complex mixtures was developed. For an accurate quantification of the extracts, HPLC was the selected technique.

Chromatographic separations of C₆₀ and C₇₀ have been widely described in literature.¹⁴ Octadecylsilane (ODS) reverse phase HPLC columns are typically employed for analytical separations. Usually, toluene (to ensure fullerene solubilization) mixed with another solvent such as hexane, methanol or acetonitrile (to reduce the eluting force of toluene) is used as mobile phase. Taking into account the literature data, we have optimized a chromatographic method, which allowed not only the separation and quantification of C₆₀ and C₇₀ but also of mixtures containing

¹⁴ a) Saito, Y.; Ohta, H.; Jinno, K. *Anal. Chem.* **2004**, 267A-272A. b) Ohta, H.; Saito, Y.; Nagae, N.; Pesek, J. J.; Matyska, M. T.; Gino, K. *J. Chrom. A* **2000**, 883, 55-66. c) Xie, S.-Y.; Deng, S.-L.; Yu, L.-J.; Huang, R.-B.; Zheng, L.-S. *J. Chrom. A* **2001**, 932, 43-53.

receptor **5a** without causing interferences in the measurement (Figure 15).

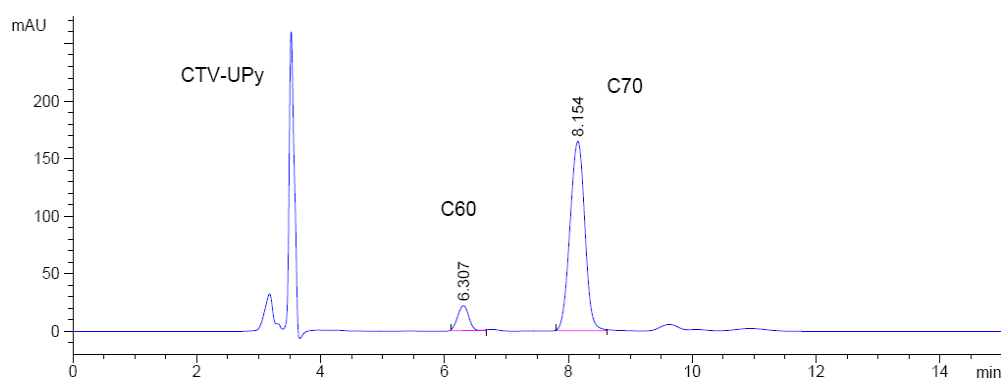


Figure 15: Mobile phase: toluene/CH₃CN/MeOH/TFA 80:20:20:0.1 (v/v); flow 1 mL/min; detection λ : 325 nm.

For quantification, fullerene response factors were calculated through a calibration curve, plotting the areas vs. concentrations for each fullerene. Hence, standards of C₆₀ and C₇₀ of different concentrations were prepared in toluene and injected according to the described chromatographic method.¹⁵

A preliminary set of extractions on C₆₀/C₇₀ mixtures of different ratios, was performed in dry THF¹⁶ (Table 3). In a typical procedure, solid fullerenes were mixed with a THF solution of **5a** and stirred at room temperature for 30 minutes. No sonication was used since it could cause precipitation of fullerenes if sonicated for more than 10 minutes.¹⁷ The mixture was filtered or centrifuged and to 200 μ L of this solution containing fullerene@**5a** **5a**, as a result of the extraction, 10 μ L of TFA and 500 μ L of toluene (to maintain the

¹⁵ See Appendix, Section VII.2 for correlation.

¹⁶ THF was suitable for receptor solubilization and H-bonding. Moreover, fullerenes were reported to be poorly soluble in this solvent: Ruoff, R. S.; Tse, D. S.; Malhotra, R.; Lorents, D. C. *J. Phys. Chem.* **1993**, *97*, 3379-3383.

¹⁷ Beck, M. T. *Pure Appl. Chem.* **1998**, *70*, 1881-1887.

fullerenes dissolved) were added. The composition of the extracts was measured by the optimized HPLC method. The concentration obtained for each fullerene was measured taking into account the dilution and values were corrected according to the inherent solubility of fullerenes in THF (blank)¹⁸. This value was subtracted from the concentration value obtained before dilution. For example, a 1:1 mixture of C₆₀ and C₇₀, extracted with two equivalents of **5a**, gave a selectivity of 1:6.85 (Table 3, entry 1). When the amount of host was reduced by 50%, selectivity was increased from 87% to more than 96% (Table 3, entry 2). Under these conditions, fullerenes are competing for the capsule and selectivity increases as C₇₀ fits better into the cavity.

Table 3: Extraction results ([x:y:z] = [C₆₀:C₇₀:**5a**] ratio).

Entry	Mixture	% C ₇₀	% C ₆₀	Corrected Ratio
1	[1:1:2]	87.26	12.74	6.85
2	[1:1:1]	96.38	3.62	26.60
3	[6:1:2]	92.47	7.53	12.28
4	[1:12:12]	99.31	0.69	144.51
5	Fullerite	85.36	14.64	5.83
6	Soot	45.85	54.15	0.85
7	Soot	53.69	46.31	1.16

Other experiments were additionally performed: *i.e.* a 6:1 mixture of C₆₀ and C₇₀, (the approximate ratio of both fullerenes in fullerite), was treated

¹⁸ The blank experiment consisted of a suspension of fullerenes in THF that was stirred in the same way as in the extractions, and the resulting saturated solution was quantified by HPLC.

with one equivalent of CTV-UPy dimer, enough to encapsulate most of the C₇₀. Under these conditions, the selectivity was very good: 92% for C₇₀ (Table 3, entry 3). If a mixture of fullerenes is prepared in the same ratio that the one obtained in the previous experiment (1:12) and extracted with enough CTV-UPy **5a** (12 equivalents), selectivity was improved until more than 99% (Table 3, entry 4).

In addition, CTV-UPy **5a** was also tested as extractant for fullerite and soot, which contains large amounts of polycyclic aromatic hydrocarbons (PHA), in addition to some fullerenes.

Initially, 1 mg of fullerite¹⁹ was completely dissolved in toluene and analyzed by HPLC (Figure 16, red chromatogram). The relative composition of the batch was 79% C₆₀ and 21% C₇₀. High order fullerenes were also detected by HPLC, whose quantification was not attempted at this stage.

¹⁹ Purchased from Sigma Aldrich. Typically 70-90% C₆₀, 10-30% C₇₀ and less than 2% of high order fullerenes.

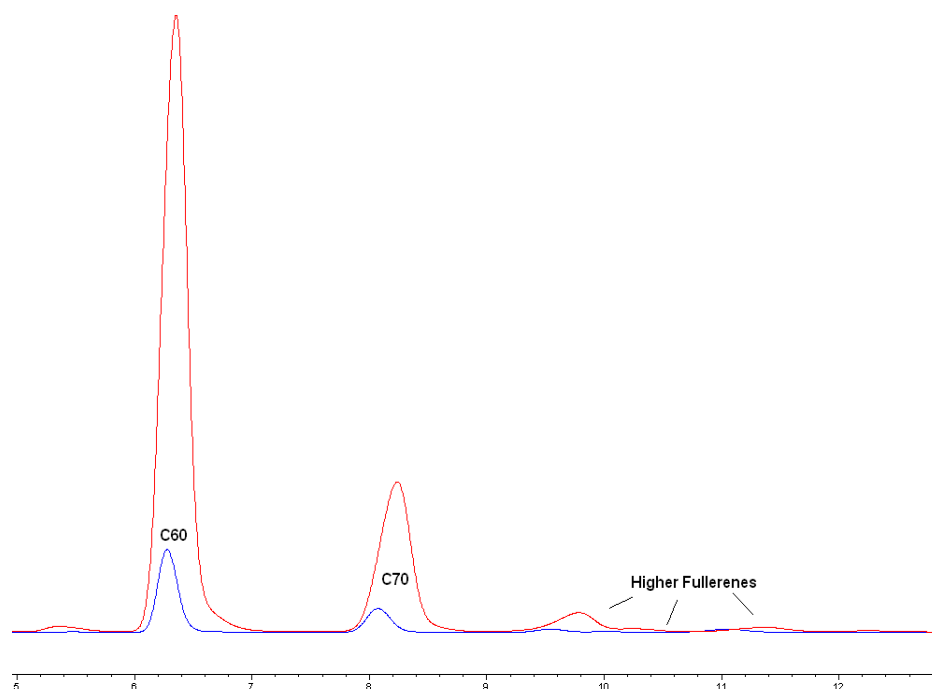


Figure 16: Chromatogram of fullerite dissolved in toluene (red line) and fullerite in THF (blue line).

When fullerite (1.08 g) was treated with enough amount of **5a** (0.72 mg) to extract most of the C_{70} , C_{60}/C_{70} ratios were inverted respect to the initial ratios in fullerite: 85% C_{70} and 15% C_{60} in just one extraction (Table 3, entry 5).

In addition, extractions of soot were carried out. In a first attempt, 10.05 mg of soot were extracted with 0.55 mg (5.5% w/w) of **5a**. The extract contained 45% C_{70} (Table 3, entry 6, Figure 17, red chromatogram). Moreover, a small enhancement of the higher fullerenes area was observed. To increase the selectivity toward C_{70} in soot extractions, the amount of **5a** employed was reduced to the half (Table 3, entry 7 and Figure 17, green chromatogram). Although selectivity was not substantially improved (53.7%), the higher fullerenes content was clearly increased.

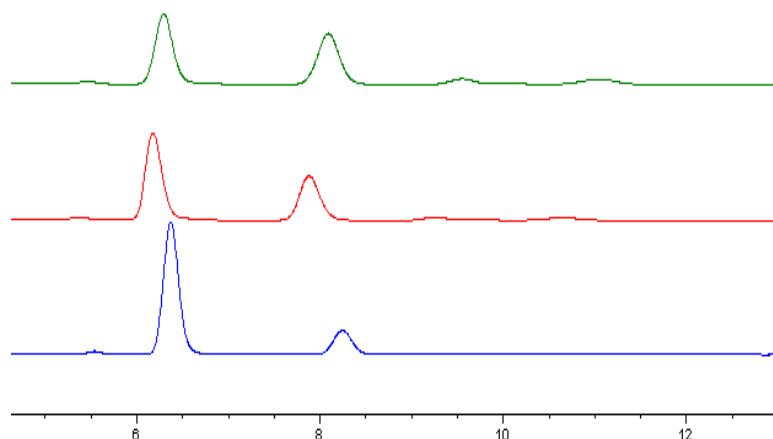


Figure 17: HPLC profiles of soot blank experiment in THF (blue) and soot extractions with 5.5% (red) and 2.8% (green) by weight of **5a**.

The use of other solvents to perform extractions was evaluated since the main obstacle to overcome is the remaining solubility of both fullerenes in THF. A number of ethers - either linear, branched, or cyclic - were tested (Figure 18).

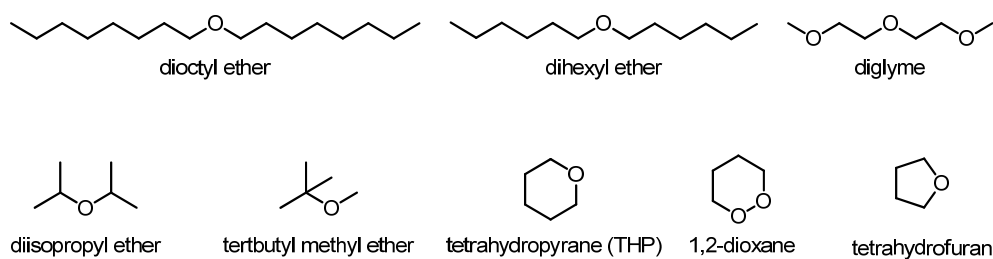


Figure 18: Structures of the ethers tested for extractions.

The host was soluble or partially soluble in all the ethers except the branched ones: *tert*-butyl methyl ether and diisopropyl ether. Therefore, to measure the inherent solubility of C₆₀, 1 mg was suspended in 1 mL of each solvent and stirred for two hours at room temperature, avoiding warming or sonicating the samples (Table 4, *blank* column). C₆₀ was found to be more soluble in any of the ethers tested than in THF. Linear hexyl and octyl ethers

provided good solubility for C₆₀ while cyclic ethers and polyethers were less efficient. Interestingly, tetrahydropyran was a better solvent for C₆₀ than tetrahydrofuran (>80 µg/mL), whereas dioxane showed values only slightly higher. Indeed, C₆₀ solubility was lower in polyethers (diglyme and dioxane), as expected, due to their higher polarity.

Table 4: C₆₀ solubility in ethers in the presence or absence of **5a**.

Entry	Solvent	Blank (µg/mL)	Extraction (µg/mL)	Solubility enhancement
1	Dihexyl ether	145,34	305,80	2,10
2	Diocetyl ether	124,83	146,99	1,18
3	Diglyme	48,64	62,00	1,27
4	Dioxane	33,40	362,94	10,87
5	THP	85,72	367,35	1,74
6	THF	17,99	44,30	2,46

Additionally, C₆₀ extractions with two equivalents of **5a** were performed using these solvents (Table 4). Interestingly, 1,2-dioxane provided the highest solubility enhancement. The efficiency of C₆₀ complexation seems to be better in this solvent than in THF, which was demonstrated not to be very efficient for C₆₀ encapsulation (*vide infra*).

Once the selectivity of the system was studied, the efficiency of the extraction in dry THF was evaluated. A new series of extractions of artificial mixtures of fullerenes as well as fullerite were performed. Taking into account the amount of fullerenes employed and the amount extracted, the yields of the extractions were calculated (Table 5).

Table 5: Yields of extractions in THF.

Entry	Experiment	Initial Ratio	% of C ₇₀ Extracted
1	C ₆₀ / 5a 5a	[1:0,1]	4,43 ^a
2	C ₆₀ / 5a 5a	[1:1]	12,66 ^a
3	C ₇₀ / 5a 5a	[1:0,1]	8,94
4	C ₇₀ / 5a 5a	[1:1]	78,71
5	C ₆₀ /C ₇₀ / 5a 5a	[1:1:1]	67,49
6	C ₆₀ /C ₇₀ / 5a 5a	[4:1:1]	54,95
7	C ₆₀ /C ₇₀ / 5a 5a	[4:1:5]	98,21
8	C ₆₀ /C ₇₀ / 5a 5a	[1:4:5]	79,95
9	Fullerite		84,61

^a yield is referred to C₆₀.

Extractions were performed adding a solution of CTV-UPy **5a** in THF over the solid fullerenes in the way described previously. When one equivalent of C₆₀ was treated with 0.1 or 1 equivalents of CTV-UPy dimer (Table 5, entries 1 and 2), the amount of fullerene extracted was quite low, especially considering that there was no competition of other fullerenes for the capsule. In similar conditions, extractions of C₇₀ gave yields around 80% (Table 5, entries 3 and 4).²⁰ These results are consistent with the association constant, as C₇₀ fits better than C₆₀ in the cavity. The efficiency of C₇₀ extraction was tested in the presence of other fullerenes as competitors (entries 5 to 9). When the ratio C₆₀/C₇₀ was 1:1 (entry 5), the yield of the extraction was near 70% and, even in the presence of a large excess of C₆₀, the yield of C₇₀ extracted was still good (entry 6). When an excess of **5a** was used, it was possible to extract almost all the C₇₀ present (entries 7 and 8). In

²⁰ For entry 3 it must be taken into account that around 8% of C₇₀ was extracted from a maximum value of 10%, considering the amount of extractant employed.

extractions performed with fullerite, CTV-UPy **5a** was able to encapsulate more than 84% of the C₇₀ present, reaching >80% purity in a single extraction.

Finally, it was possible to purify C₇₀ from fullerite by using an extraction-precipitation-reextraction protocol without chromatography. Releasing of fullerenes from the capsule was exceedingly simple. Addition of a few drops of trifluoroacetic acid (TFA) to the THF solutions of the complexes caused the hydrogen-bonded network to break and the fullerenes to precipitate. The host could then be recycled by evaporation. Indeed, two consecutive extractions yielded an initial 84:16 C₇₀/C₆₀ mixture (from 20.9 mg fullerite and 3.8 mg of host **5a** in 2.0 mL THF), which turned into a 97:3 mixture upon addition of TFA, centrifugation and re-extraction with 1.6 mg of **5a** (Table 6).

Table 6: C₇₀ purification protocol.

Sample	%C ₇₀	%C ₆₀
Fullerite 1 st extraction	84	16
Fullerite 2 nd extraction	97	3

III.3.4 DFT Calculations

To rationalize the differences in binding affinities among the different fullerenes, we carried out a computational study in collaboration with Prof. Carles Bo (ICIQ). The geometries of the complexes were determined by a density functional method (DFT),²¹ which was accurate enough to

²¹ a) Te Velde, G.; Bickelhaupt, F. M.; Baerends, E. J.; Fonseca Guerra, C. S.; van Gisbergen, J. A.; Snijders, J. G.; Ziegler, T. J. *Comput. Chem.* **2001**, *22*, 931-967. b) Fonseca Guerra, C.; Snijders, J. G.; Te Velde, G.; Baerends, E. J. *Theor. Chem. Acc.* **1998**, *99*, 391-403.

reproduce fairly well the geometry of the UPy dimer in the solid state,²² and chosen as a compromise between accuracy and computational effort. Geometry minimizations were performed using ADF 2005 code. In all calculations, the BP86 functional was employed.²³ A DZP Slater type basis set, as included in the ADF2005 library, was used for the geometry optimizations, whereas energy values were evaluated by single point calculations using a TZP basis set.

A number of variables have to be considered in order to construct and evaluate the relative stabilities of the different complexes: on one hand, cyclotrimeratrylene is a relatively rigid nine-membered ring. When substituted with OMe and OR groups (Figure 19), it displays a C_{3v} symmetry.²⁴ Thus, two enantiomeric forms could be isolated in the absence of ring inversion. The enantiomers are stable at room temperature, which indicates that the inversion barrier is greater than 23 kcal mol⁻¹. However, the “crown to crown” interconversion, leading to racemization, occurs readily upon heating.²⁵ Dimeric capsules generated from a racemic monomer could be in principle homochiral if formed by two monomers of identical chirality (a pair of *M-M* and *P-P* capsules) or heterochiral (an optically inactive) *meso* dimer, if arising from the combination of two monomers of opposite chirality (*P-M*).

²² Beijer, F. H.; Sijbesma, R. P.; Kooijman, H.; Spek, A. L.; Meijer, E. W. *J. Am. Chem. Soc.* **1998**, *120*, 6761-6769.

²³ a) Becke, A. D. *Phys. Rev. A* **1988**, *38*, 3098-3100. b) Perdew, J. P. *Phys. Rev. B* **1986**, *33*, 8822-8824.

²⁴ a) Canceill, J.; Collet, A.; Gottarelli, G. *J. Am. Chem. Soc.* **1984**, *106*, 5997-6003. b) Canceill, J.; Collet, A.; Gabard, J.; Gottarelli, G.; Spadat, J. P. *J. Am. Chem. Soc.* **1985**, *107*, 1299-1308.

²⁵ a) Collet, A.; Jacques, J. *Tetrahedron Lett.* **1978**, 1265-1268. b) Collet, A.; Gabard, J. *J. Org. Chem.* **1980**, *45*, 4500-4501. c) Collet, A.; Gottarelli, G. *J. Am. Chem. Soc.* **1981**, *103*, 204-205.

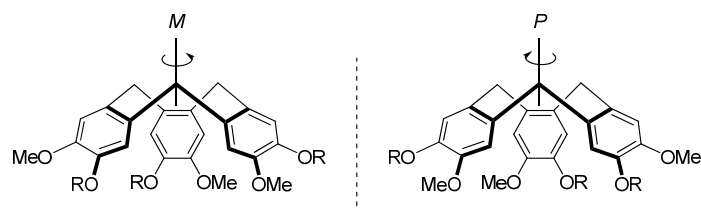


Figure 19: The two enantiomers of chiral cyclotrimeratrylene (CTV).

On the other hand, ureidopyrimidinones are involved in tautomeric equilibria (see the introductory section), so capsules arising from either the *keto* or the *enol* forms should also be taken into account.

Moreover, UPys are linked to the CTV scaffold through an O-CH₂CH₂-N linker. *Antiperiplanar* vs. *gauche* conformations have thus to be considered. In the presence of a fullerene, this conformation must be *gauche* to provide the required curvature to wrap around the convex, almost spherical guest, since an *anti* conformation would project the hydrogen-bonded platform away from the fullerene surface. Finally, the UPy-UPy planar surface cannot freely rotate in the presence of a fullerene guest: the NH protons of each urea should point either away from the OCH₃ group of the CTV scaffold - A or *anti* orientation - or, on the contrary, to the same side - referred to as S or *syn* orientation (Figure 20). Regarding the remaining possible rotations, inspection of CPK models in the presence of the fullerene guest indicates that, in all cases, the dihedral angle C(OMe)-C-O-CH₂ can be either *ca.* 90° - the chain points away from the capsule surface, we name this orientation α - or *ca.* 180° - the chain lies in the plane of the capsule surface, named β - but it can not be 0° for steric reasons (not shown in Figure 20).

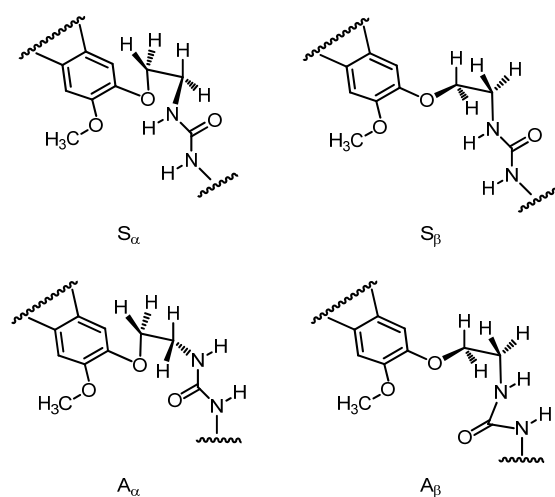


Figure 20: Most favorable conformations of the chain linking the CTV and UPy moieties in homochiral capsules (see text for definitions).

Taking into account these restrictions, all the possible assemblies were constructed and calculated for C_{60} and C_{70} (Figure 21).

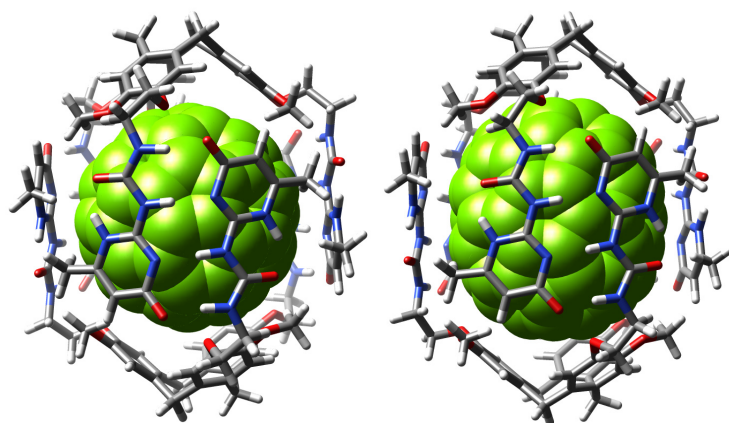


Figure 21: Models of C_{60} (left) and C_{70} (right) complexes both in $A_\alpha A_\alpha$ conformation.

Table 7 summarizes the values obtained for the total interaction energies of the complexes. In all cases, the energy for the C_{70} complex is significantly more favorable than for C_{60} . For the three most stable assemblies, the

interaction energies were also calculated for larger fullerenes as C_{76} , C_{78} , C_{84} and C_{90} (Figure 22). As can be seen, calculations predicted that the most favorable conformation has an *anti* orientation and a β angle in the linker. Furthermore, the most stable complexes are those formed with C_{84} .

Table 7: Interaction energies fullerene-cage.²⁶

ΔE_{tot}	$A_{\beta}A_{\beta}$	$A_{\alpha}A_{\alpha}$	$A_{\beta}S_{\alpha}$	$S_{\alpha}S_{\alpha}$	$S_{\beta}S_{\beta}$	$A_{\alpha}S_{\alpha}$	$A_{\alpha}S_{\beta}$
$C_{60}@5a-5a$	-227.1	-212.8	-215.4	-197.1	-216.4	-201.5	-206.8
$C_{70}@5a-5a$	-256.8	-244.3	-242.2	-227.0	-242.8	-230.3	-236.0
$C_{76}@5a-5a$	-269.6	-253.6	-250.6	--	--	--	--
$C_{78}@5a-5a$	-274.4	-257.0	-256.6	--	--	--	--
$C_{84}@5a-5a$	-280.1	-264.2	-270.3	--	--	--	--
$C_{90}@5a-5a$	-276.6	-255.6	-265.4	--	--	--	--

Based on the above results, the following scale of fullerenes affinity can be established: $C_{60} < C_{70} < C_{76} < C_{78} < C_{90} < C_{84}$.

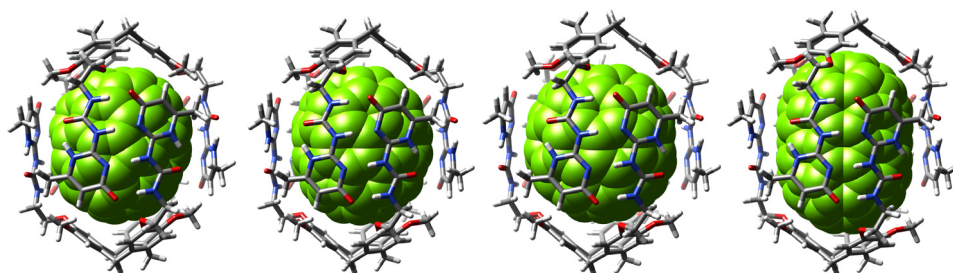


Figure 22: Models of complexes formed with (from left to right): C_{76} , C_{78} , C_{84} , and C_{90} .

Regarding geometric parameters, the best values ($A_{\beta}A_{\beta}$ assembly) for

²⁶ The total energy (ΔE_{tot}) was calculated as the difference of the energy of dimeric **5a** minus twice the energy of monomeric **5a** plus the electronic host-guest interaction plus the dispersion of the host-guest interaction (see Eva Santos, PhD. Thesis, Tarragona 2008).

different fullerenes were compared, using an isolated UPy dimer as a reference model (Figure 23).

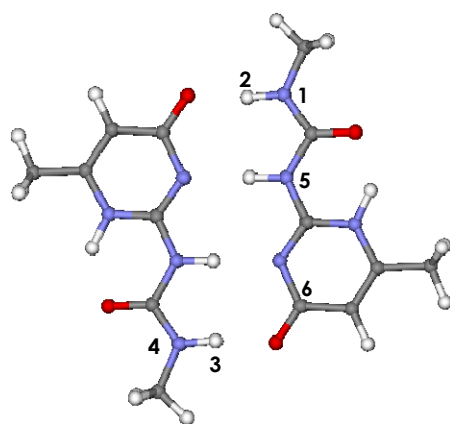


Figure 23: UPy dimer.

In all cases (Table 8), there is a deviation from planarity in the UPy dimers in the capsule with respect to the ideal UPy dimer because of the round-shaped guest (**dih** and **angleCurv**). However, the hydrogen bonding distances are maintained. The CTV scaffold is also adapting its shape to the guest (**angleCTV**). Thus, it is slightly "opened" or "closed" as a function of the guest curvature.

Table 8: Geometry parameters measured from an ideal UPy dimer and $A_{\beta}A_{\beta}$ capsules with several fullerenes as guests.

	$A_{\beta}A_{\beta}$						
	UPy dimer	C ₆₀	C ₇₀	C ₇₆	C ₇₈	C ₈₄	C ₉₀
dNH--O^a	1.680	1.678	1.674	1.673	1.673	1.687	1.680
dNH--N^a	1.843	1.834	1.843	1.853	1.852	1.883	1.854
Dih^b	179.7	160.1	163.7	164.3	165.2	159.0	160.7
angle1^c	172.7	164.7	168.7	169.6	170.1	170.6	174.2
angle2^d	179.2	164.1	172.9	174.0	174.0	172.5	173.6
angleCurv^e	180	174.5	174.5	175.0	175.0	171.5	175.1
distDomes^f	-	15.9	15.9	16.1	16.1	15.9	17.0
angleCTV^g	-	109.9	111.6	114.0	115.7	113.7	118.8
distUPy^h	-	11.6	11.7	11.8	11.8	12.4	11.6
AvrgMinDⁱ	-	4.561	4.338	4.143	4.105	3.841	3.690
StandardDevⁱ	-	0.767	0.728	0.743	0.712	0.631	0.577

^a Hydrogen bonding distances.

^b Torsion angle between atoms 1, 2, 3 and 4.

^c Angle in the hydrogen bond of N-H...O type. (Angle in N-H...O type hydrogen bond)

^d Angle in the hydrogen bond of N-H...N type.

^e Angle formed by the atoms 1, 5 and 6.

^f Distance between the two domes of the CTV-3UPys.

^g Angle formed by the centroid of consecutive CTV aromatic rings and the carbon linking them.

^h Average distance from centroids of the bonds linking the pyrimidinone ring to the ureido group in consecutive UPys of a CTV-3UPy molecule.

ⁱ Average minimum host-guest distance.

ⁱ Standard deviation for (i).

In general, the geometry of the capsules tries to adapt to the guest by either increasing its width, its height or modifying the relative orientation of the UPy dimers. It seems that the size and shape of C₈₄ is the most appropriate for this assembly, since it enables a homogeneous folding of the capsule around the fullerene. Therefore, experimental studies on the complexation of C₈₄ were undertaken.

III.3.5 Complexation of C₈₄

The higher fullerene C₈₄ was reported as the third most abundant fullerene after C₆₀ and C₇₀.²⁷ A total of 24 isomers, obeying the isolated pentagon rule, can be predicted by calculations.²⁸ The analysis of ¹³C NMR spectra of C₈₄, obtained by the standard graphite arc procedure, is consistent with a 2:1 thermodynamic mixture of isomers with the isoenergetic D₂ and D_{2d} symmetry. Due to the quite limited availability of pure C₈₄, only a few reactions have been tested so far on this fullerene at a very small scale with the goal to separate the different isomers or to evaluate their reactivity.²⁹ Consequently, no much is known regarding possible applications. A C₈₄-based field effect transistor was developed by Shibata *et al.*³⁰ and some pioneering work has been done in the field of nonlinear optics and superconductivity.³¹ Hummelen *et al.*³² have developed organic

²⁷ a) Krätschmer, W.; Lamb, L. D.; Fostiropoulos, K.; Huffman, D. R. *Nature* **1990**, *347*, 354-358. b) Diederich, F.; Ettl, R.; Rubin, Y.; Whetten, R. L.; Beck, R.; Alvarez, M.; Anz, S.; Sensharma, D.; Wudl, F.; Khemani, K. C.; Koch, A. *Science* **1991**, *252*, 548-551.

²⁸ Manolopoulos, D. E.; Fowler, P. W. *J. Chem. Phys.* **1992**, *96*, 7603-7614.

²⁹ a) Wang, G. W.; Saunders, M.; Khong, A.; Cross, R. J. *J. Am. Chem. Soc.* **2000**, *122*, 3216-3217. b) Nuffer, R.; Bartl, A.; Dunsch, L.; Mathis, C. *Synth. Met.* **2001**, *121*, 1151-1152. c) Wakahara, T.; Han, A. H.; Niino, Y.; Maeda, Y.; Akasaka, T.; Suzuki, T.; Yamamoto, K.; Kako, M.; Nakadaira, Y.; Kobayashi, K.; Nagase, S. *J. Mater. Chem.* **2002**, *12*, 2061-2064. d) Darwish, A. D.; Martsinovich, N.; Taylor, R. *Org. Biomol. Chem.* **2004**, *2*, 1364-1367.

³⁰ Shibata, K.; Kubozono, Y.; Kanbara, T.; Hosokawa, T.; Fujiwara, A.; Ito, Y.; Shinohara, H. *Appl. Phys. Lett.* **2004**, *84*, 2572-2574.

³¹ a) Harigaya, K. *J. Lumin.* **1998**, *76-77*, 652-654. b) Denning, M. S.; Dennis, T. J. S.; Rosseinsky, M. J.; Shinohara, H. *Chem. Mater.* **2001**, *13*, 4753-4759. c) Koudoumas, E.; Konstantaki, M.; Mavromanolakis, A.; Michaut, X.; Couris, S.; Leach, S. *J. Phys. B: At. Mol. Opt. Phys.* **2001**, *34*, 4983-4996.

³² a) Kooistra, F. B.; Mihailetchi, V. D.; Popescu, L. M.; Kronholm, D.; Blom, P. W. M.;

transistors based on the newly synthesized solution-processable methanofullerene [6,6]-phenyl-C₈₄-butyric acid methyl ester ([84]PCBM), the higher analogue of [60]PCBM and [70]PCBM derivatives, with good electron-transporting properties. Unlike its lower analogues, [84]PCBM-based transistors are stable to air and light, and are capable of functioning even after exposure to ambient air for long-standing periods of time.

In the previous section, we described the selective complexation of C₇₀. However, it was observed that at low host concentration higher fullerenes were also extracted in small quantities. Since DFT calculations predicted better interaction energy for C₈₄ complexes, the development of a new methodology for C₈₄ purification was therefore investigated.

Thus, the complex was first studied by NMR spectroscopy. ¹H NMR experiments of C₈₄@**5a** revealed that, in carbon disulfide, NH signals were split (Figure 24), probably due to the presence of at least two C₈₄ isomers in addition to the different isomers arising from the capsule. Interestingly, in tetrachloroethane, splitting of downfield signals was less pronounced than in the case of the C₇₀ complex.

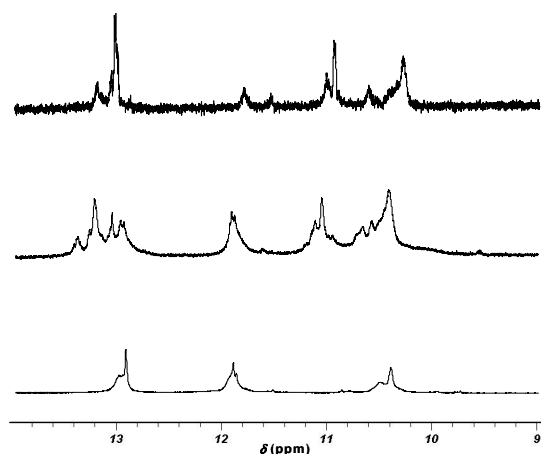


Figure 24: ¹H NMR spectra of complexes of C₈₄@**5a-5a** in CD₂Cl₄ (bottom), THF-d₈ (middle) and CS₂ (MeOH-d₄ was placed into an inset tube for locking) (top).

Additionally, variable temperature experiments were recorded using deuterated TCE as the solvent. The spectra were compared with those at variable temperature recorded for the C₆₀ and C₇₀ complexes (Figures 7 and 9). For receptor **5a** and C₈₄, sharp downfield NH signals for the dimer were observed, even beyond 100 °C, indicating that this assembly is stronger than those with C₆₀ and C₇₀ (Figure 25). From these experiments, a stability order for the different fullerene complexes could be established as follows: C₈₄ > C₇₀ > C₆₀

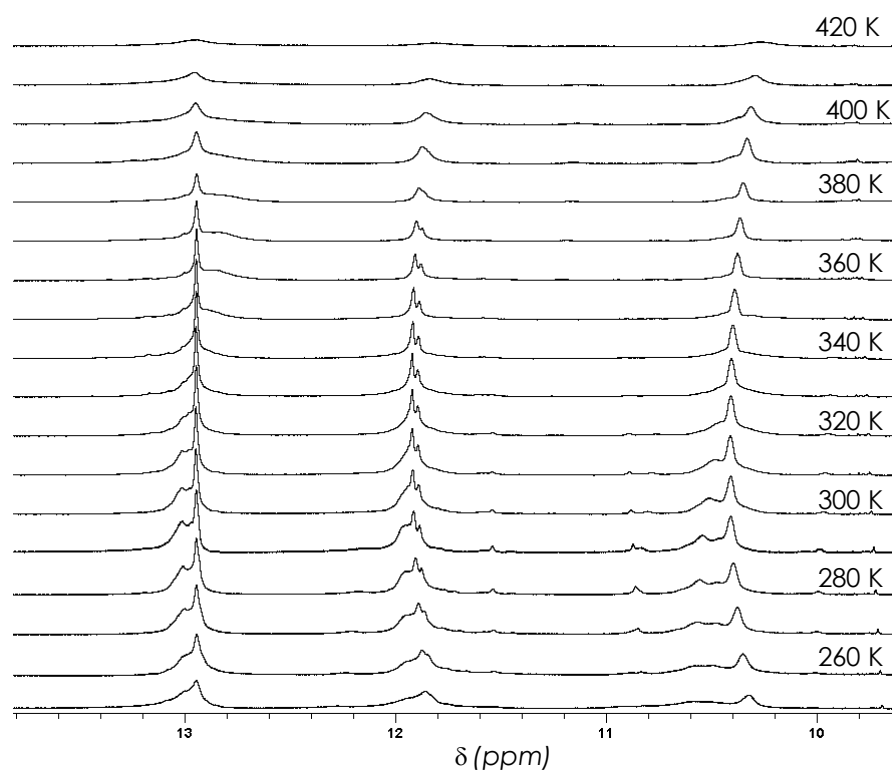


Figure 25: Variable temperature ^1H NMR spectra performed in d_2 -TCE of a 1:2 mixture of C_{84} and **5a**.

The stoichiometry of the complex formed by **5a** and C_{84} was determined by the continuous variation method (Job plot). Solutions with different host/guest ratios at 0.015 mM were measured by UV-vis spectroscopy. The complex corresponded to a 1:2 stoichiometry (Figure 26).

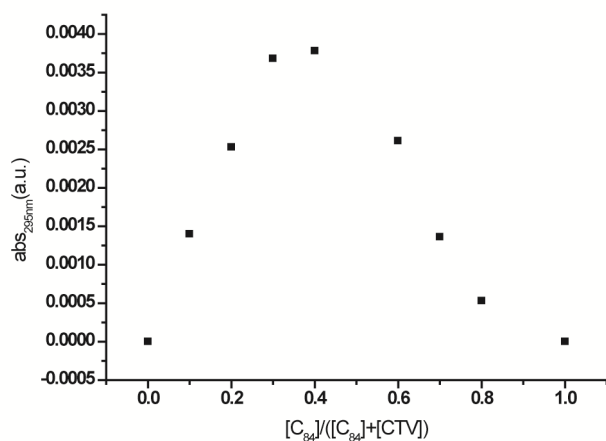


Figure 26: Job plot for the C₈₄@**5a-5a** complex.

Furthermore, the association constant for the C₈₄@**5a-5a** complex was established. A UV-titration was carried out in tetrachloroethane using a 0.017 mM solution of C₈₄ and a 0.051 mM solution of **5a**. The concentration of fullerene was kept constant (Figure 27).⁹

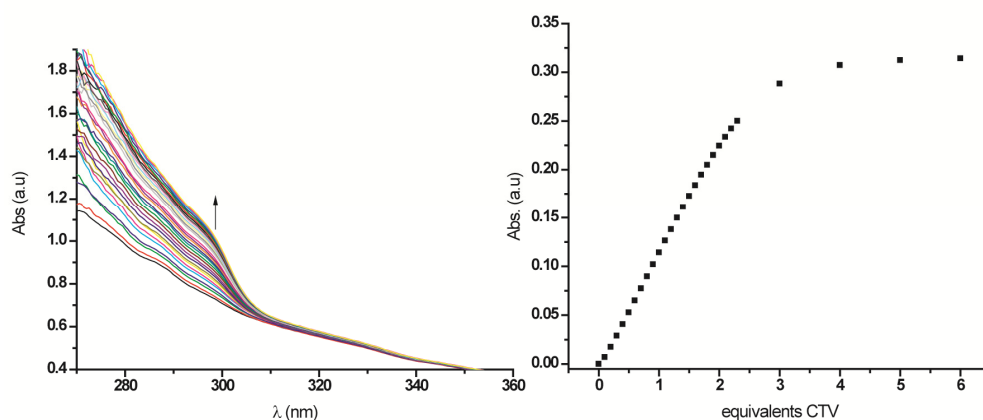


Figure 27: UV titration (left) and binding isotherm (right) for C₈₄@**5a-5a** complex in tetrachloroethane at room temperature.

The association constant calculated for the C₈₄ complex was one order of magnitude higher than those for the C₆₀ and C₇₀ complexes according to a 1:1 binding model, whereas fitting the titration data for a 1:2 binding model the observed constant was around 10¹⁰ M⁻² (Table 9).

Table 9: Association constants for fullerene@**5a**-**5a** complexes.

Complex	K _{ass} 1:2 model (M ⁻²)	K _{ass} 1:1 model (M ⁻¹)
C ₆₀ @ 5a - 5a	1,93 x 10 ⁶	1,82 x 10 ³
C ₇₀ @ 5a - 5a	7,40 x 10 ⁷	3,89 x 10 ⁴
C ₈₄ @ 5a - 5a	2,63 x 10 ¹⁰	3,70 x 10 ⁵

III.3.6 Selective Extraction of C₈₄

In order to establish the optimal conditions for the selective extraction of C₈₄ from fullerite, a fast and reliable technique for fullerene detection is required, in addition to HPLC. Mass spectrometry, in particular MALDI-TOF, has been reported as a useful tool for this aim.³³ Moreover, when appropriately calibrated, this technique can be used for the quantification³⁴ of these mixtures. Indeed, a test with fullerite was carried out using 67% w/w of **5a** in the extraction. The C₆₀/ C₇₀ ratio extracted was then calculated by both HPLC and mass spectrometry. By HPLC, the ratio was 13:87. The initial C₇₀ content, relative to C₆₀, was 26% (Table 10). The same mixtures were then quantified using MALDI-TOF mass spectrometry. The calibration curve (Figure 28) showed a linear behavior at the concentration employed. However, a direct data interpolation on each sample in the curve was not possible, and the standard addition was selected as the analytical method. An internal

³³ Kraetschmer, W.; Fostiropoulos, K.; Huffman, D. R. *Chem. J Phys. Lett.* **1990**, *170*, 167-170.

³⁴ Haino, T.; Fukunaga, C.; Fukazawa, Y. *Org. Lett.* **2006**, *8*, 3545-3548.

standard, usually a fullerene close in molecular weight to the analyzed one, is necessary in order to correct deviations in the signal intensity promoted by the laser impact.³⁵

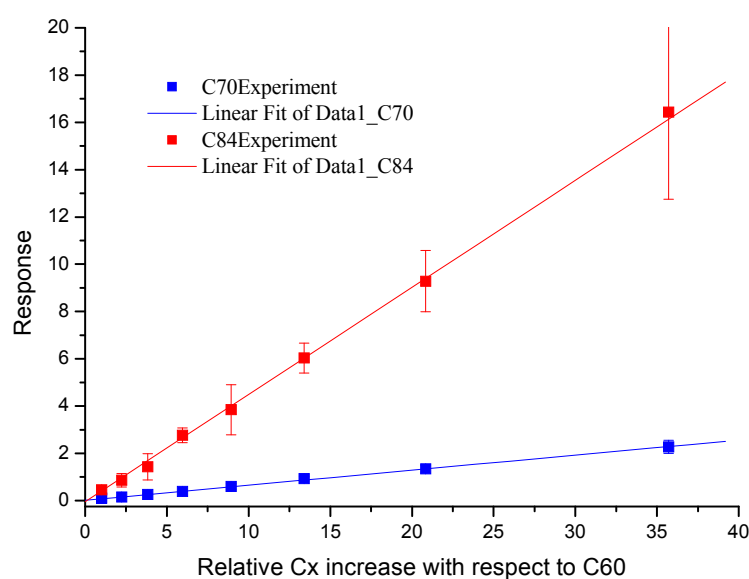


Figure 28: Calibration curves for C₇₀ (blue) and C₈₄ (red).

Figure 29 shows the mass spectra obtained for fullerite (Figure 29a) and for the extract (Figure 29b). Although the intensity of each signal is not directly proportional to the concentration, an increment of the intensity of the C₇₀ signal with respect to the C₆₀ one was observed after the extraction. A small intensity increment was also observed for the signals corresponding to higher fullerenes with respect to the C₆₀ signal. Quantitatively C₇₀ recovery was 86% calculated with this technique (Table 10), almost the same value obtained by HPLC, which demonstrates that mass spectrometry is accurate

³⁵ Mass analyses and method development were designed by Dr. J. Barr (ICIQ's Mass Spectrometry Unit Manager 2004-2007)

enough and can be used as an alternative to HPLC.

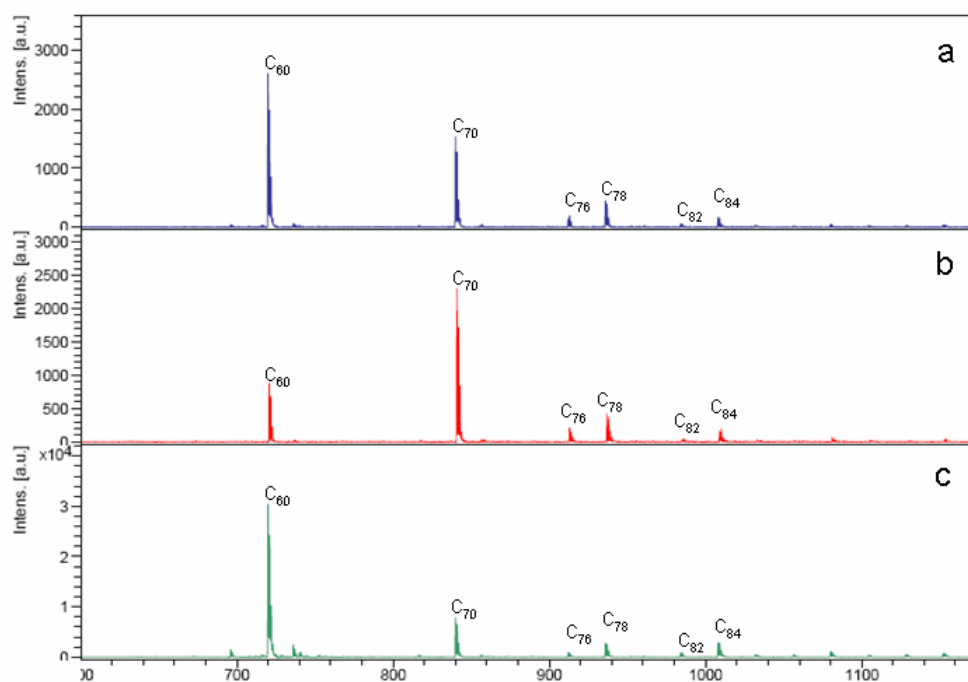


Figure 29: MALDI-TOFF (-ve) spectra of a) fullerite; b) extract of fullerite extracted with 67% by weight of CTV-UPy **5a** with respect to the fullerite amount; c) residue of the extraction.

Table 10: Comparison of quantifications by MALDI-TOF and HPLC techniques.

Sample	%C ₇₀ (MALDI-TOF)	%C ₇₀ (HPLC)
Fullerite	30	26
Extraction	86	87

Besides the ratio, also the efficiency of C₈₄ extraction using 2 equivalents of **5a** was determined. When 201 µg of C₈₄ were extracted with 536 µg of **5a**, the yield by mass spectrometry was 98%.

Although accurate, the mass spectrometry technique only allows quantification of one fullerene per experiment, which means that simultaneous quantification of C₆₀, C₇₀ and C₈₄ from a single extraction would require at least three experiments with their corresponding standard additions, which is very time-consuming. However, as was pointed out above, this technique is useful for a fast qualitative analysis of extractions.

For example, extractions of fullerite were performed using variable concentrations of receptor **5a**. In all cases, 15 mg fullerite samples were extracted with 1, 2, 5, 10, 15, 20, 40 and 60% w/w of **5a** (Figure 30).

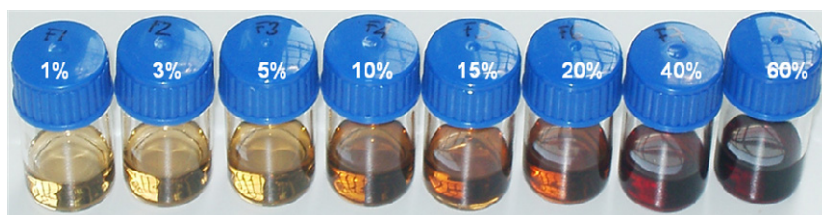


Figure 30: Extractions of fullerite with variable amounts of **5a**.

The samples were stirred at room temperature and aliquots were taken at different times. Qualitative analysis by mass spectrometry (Figure 31) showed how the intensity of the signals (from C₇₀ to C₁₀₀), relative to C₆₀ intensity, varied as a function of the amount of receptor employed.

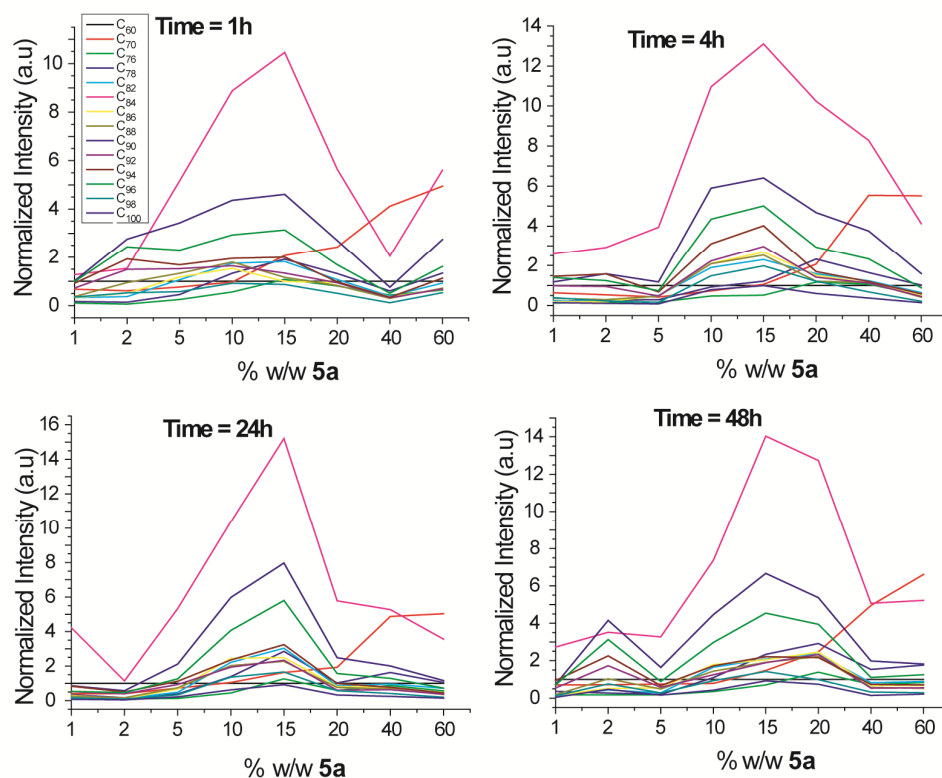


Figure 31: Qualitative analysis by MALDI-TOF spectrometry of the extractions (all signals normalized to C_{60} signal).

After single extractions, a general trend could be observed: the receptor extracts selectively C_{84} , especially at concentrations of **5a** below 15% by weight. In addition, the equilibration time seemed to be an important factor to take into account. Even though, after one hour stirring, the major component in the mixtures was C_{84} and its ratio relative to the other fullerenes was maximal after 24h. There were almost no variations if the mixtures were stirred additionally for 24h. Comparison of all mass spectra at different times for an extraction using 1% w/w, showed that almost only C_{84} was extracted (Figure 32).

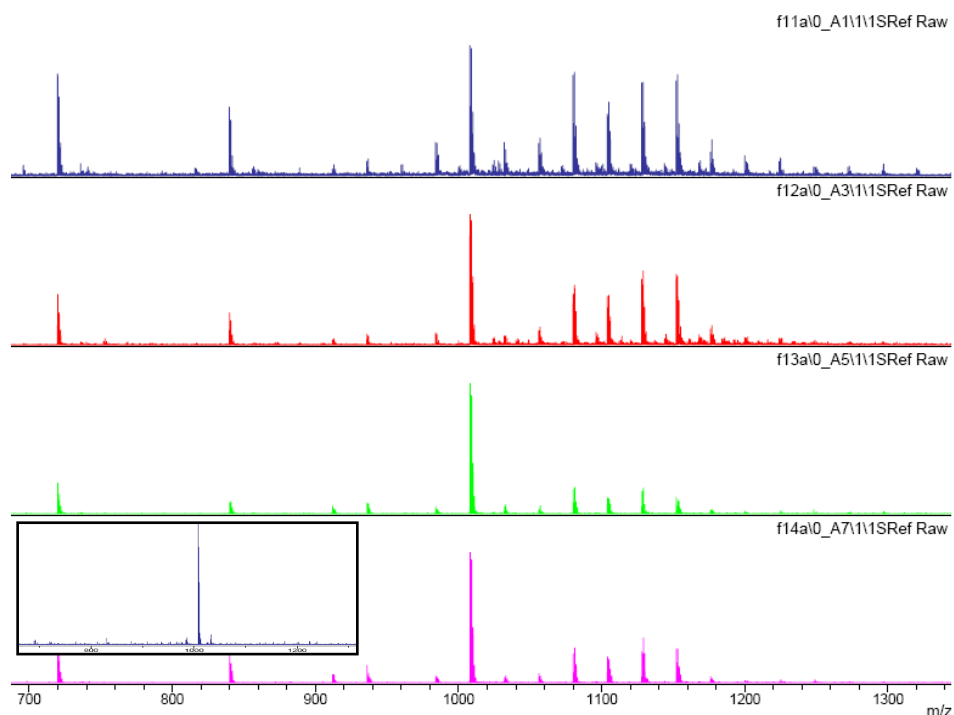


Figure 32: Mass spectra of a fullerite extraction with 1% w/w of **5a** after 1h (blue), 4h (red), 24h (green) and 48h (pink) and mass spectrum of a 99% pure C₈₄ (inner square, light blue) purchased from Bucky-USA.

As was observed, a decrease in receptor concentration was translated in an increment of the higher fullerenes concentration, likely as the result of the competition of the different fullerenes for the cavity. As well, the signals corresponding to fullerenes higher than C₉₀ were also increased. Since they are too large to fit into the capsules, the increase of these signals might be a consequence of their inherent solubility in THF.

Extractions done from soot, under the same conditions described above for fullerite samples, were also qualitatively analyzed by mass spectrometry (Figure 33).

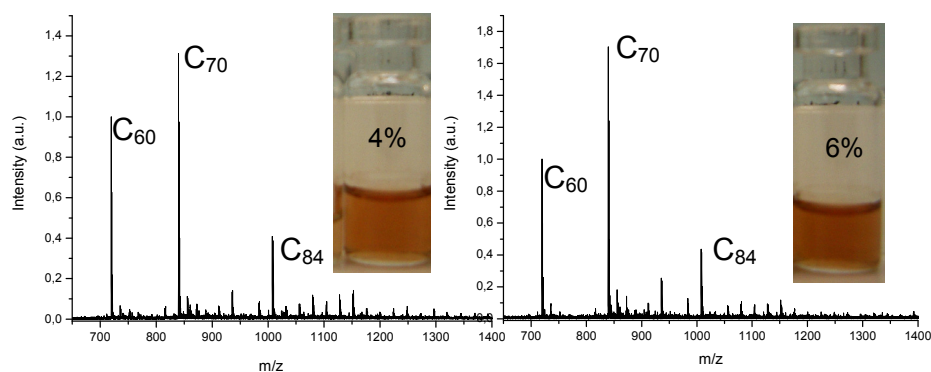


Figure 33: MALDI-TOF mass spectra of soot extractions.

Only when high concentrations of extractant were used – from 2% to 6% by weight respect to the soot³⁶ - solutions became reddish, indicating the presence of encapsulated fullerenes. Based on the signal intensity for each fullerene in the MALDI-TOF spectra, a significant enrichment of the samples in C₇₀ and C₈₄ occurred. Figure 34 represents the normalized intensities of each fullerene respect to the C₆₀ signal, at a given concentration of compound **5a**.

³⁶ Since soot contains about 7% fullerenes, a 6% **5a** by weight should suffice to extract all the C₇₀ and/or the higher fullerenes present in the mixture.

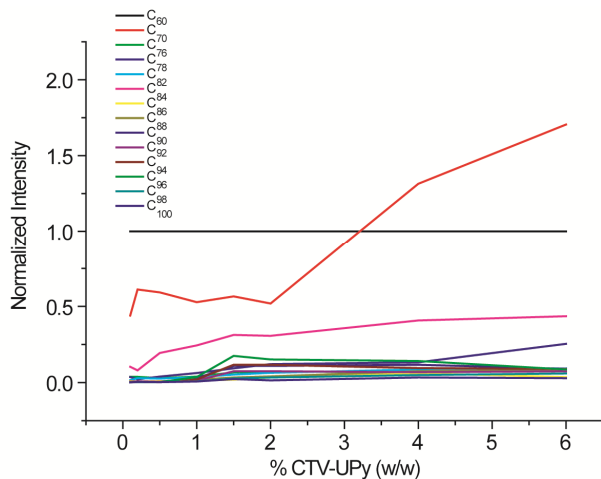


Figure 34: Plot of the normalized intensity of fullerenes extracted vs. amount of receptor **5a** used (% w/w with respect to the soot).

Compound **5a** was also applied in a practical case to purify a commercially available sample of C₇₈ provided by Bucky-USA (>98% purity based on HPLC analysis, Figure 35, inner square).

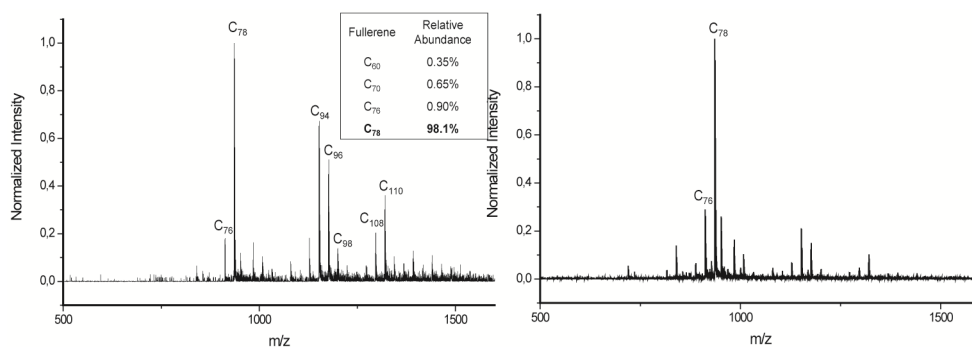


Figure 35: Mass spectrometry analysis of a commercially available sample of C₇₈ before (left) and after (right) treatment with **5a**. Inner square: HPLC analysis of same sample provided by the manufacturer.

The mass spectrometry analysis revealed that other fullerenes higher than C₇₈ (Figure 35, left) were present in substantial amounts, so this material could hardly be used as a standard for quantification.

A small amount of this material was thus extracted in THF with **5a**, and the resulting extract was considerably enriched in C₇₈ with respect to the original sample (Figure 35, right). The residual signals for higher fullerenes observed likely arises from their inherent solubility in THF, because they are too big to fill the cavity of the capsule.

Quantitative analysis of C₈₄ extractions could not be carried out by HPLC in the same way as for C₆₀ and C₇₀, since C₁₈ reverse phase columns do not have enough resolution for higher fullerenes. Therefore, a specific column for fullerenes was employed, namely Cosmosil Buckyprep-M from Nalcalai Tesque (Japan). This column contains phenothiazinyl residues anchored to the silica to maximize the interactions with fullerenes. When a fullerite solution was injected, a quite good resolution was obtained using toluene as the mobile phase for C₆₀ and C₇₀, although the signals for some higher fullerenes (including C₈₄) were hardly resolved. However, addition of 20% methanol to the mobile phase retained fullerenes long enough to allow signal integration.³⁷ Thus, calibration curves were registered using solutions of C₆₀ and C₇₀ in toluene, and C₈₄ in 1-chloronaphthalene.¹⁵

Extractions were performed as usual with some post-treatment modifications, because the column used did not allow a correct separation of fullerenes and receptor during the analysis. Consequently, after the extraction, samples were treated with TFA and the solvent was eliminated. Fullerenes were then recovered from the solid residue by solubilization in carbon disulfide (CS₂), causing the receptor to precipitate. This solution was directly injected for analysis.

Subsequently, solid-liquid extractions of fullerite were performed in THF

³⁷ Enrique Cequier (ICIQ's Chromatography, Thermal Analysis and Calorimetry Unit Manager) Master Thesis, Tarragona 2009.

using, as in the previous example, variable concentrations of **5a** (1-60%), in order to optimize the ratio of C₈₄ extracted (Table 11 entries 1-9). It was found that high receptor/fullerite ratios (ca. 50-60%) are better suited for a selective extraction of C₇₀, whereas the selectivity for C₈₄ was maximized for ca. 5-15% receptor/fullerite ratios (Figure 36).

Table 11: Composition of fullerene mixtures upon extraction of fullerite with variable amount of receptor **5a**.

Entry	Ratio (fullerene:5a)			Composition ^a			Recovery ^b		
	C ₆₀	C ₇₀	C ₈₄	(%)			(%)		
	C ₆₀	C ₇₀	C ₈₄	C ₆₀	C ₇₀	C ₈₄	C ₆₀	C ₇₀	C ₈₄
1	1:0.01	1:0.03	1:0.13	54	16	30	0.8	0.8	7
2	1:0.02	1:0.08	1:0.40	43	13	44	0.8	0.9	14
3	1:0.04	1:0.14	1:0.66	26	9	65	0.7	0.9	31
4	1:0.06	1:0.22	1:1.06	17	10	73	0.6	1.2	44
5	1:0.08	1:0.28	1:1.32	14	8	77	0.6	1.2	53
6	1:0.12	1:0.41	1:1.98	13	20	67	0.7	4.2	66
7	1:0.16	1:0.55	1:2.64	12	30	58	0.8	6.9	64
8	1:0.32	1:1.10	1:5.29	11	51	38	1.2	19.1	69
9	1:0.47	1:1.65	1:7.93	15	59	26	2.0	28.3	60
10	1:0.00	1:0.00	1:0.00	48	16	36	0.5	0.6	7
11	1:0.04	1:0.14	1:0.66	19	6	75	0.6	0.7	40
12	1:0.08	1:0.28	1:1.32	12	11	76	0.6	2.0	64
13	1:0.12	1:0.41	1:1.98	10	21	69	0.6	4.6	72

^a Composition of extracted fullerenes

^b Percentage of each fullerene with respect to the amount of C₆₀, C₇₀ and C₈₄

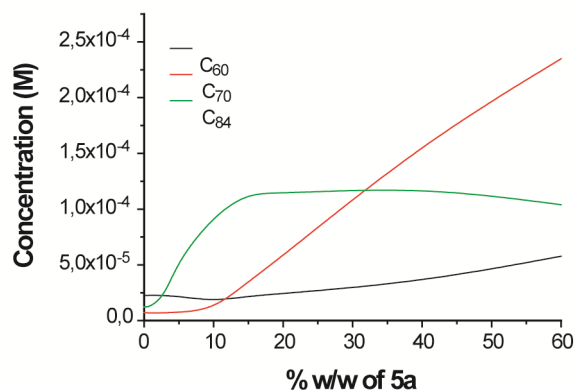


Figure 36: Plot of concentration of fullerenes extracted against amount of receptor **5a** used (percentage by weight with respect to the solid fullerite).

In addition, the amount of solvent employed (concentration of the extraction) was investigated for the best extractions found. In the initial screening, the ratio fullerite/solvent was around 3 mg/mL. When this ratio was increased to 5 mg/mL (Table 11, entries 11-13), selectivity achieved was slightly better, since a reduction of solvent amount decreased the quantity of undesired fullerenes inherently solubilized. Indeed, the HPLC profiles (Figure 37) indicate that beyond 10% any improvement in C₈₄ extraction was accompanied by an exceedingly amount of C₇₀. It should be noted that the amount of C₆₀ extracted remained constant at all ratios of extractant, indicating that this represents the inherent solubility of C₆₀ in THF.

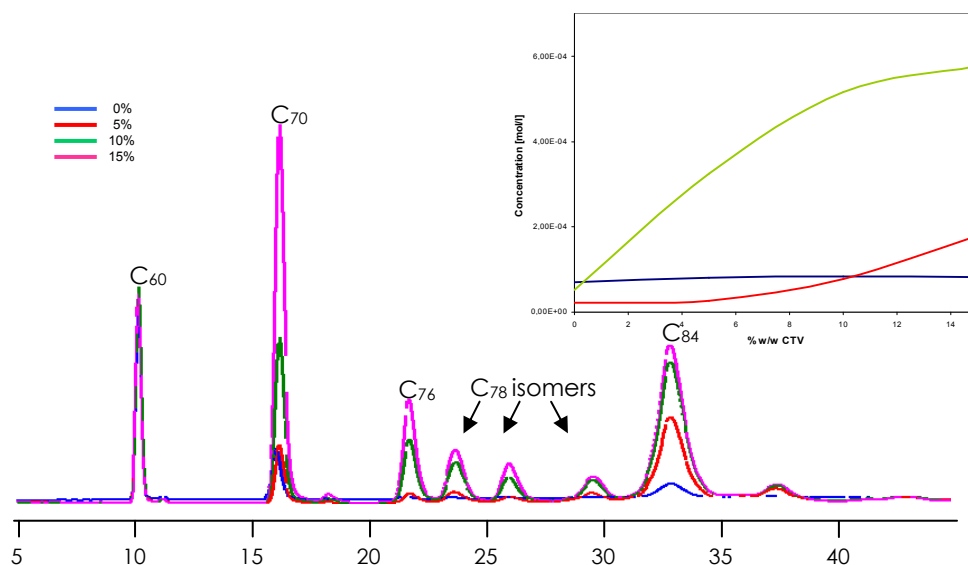


Figure 37: HPLC profiles of extractions with different amounts of **5a**. Cosmosil Buckyprep-M column 4.6x250 mm; mobile phase: toluene-methanol (80:20); flow rate: 1 mL/min; λ : 290 nm. Inner square: plot of concentrations of C₆₀ (blue), C₇₀ (red) and C₈₄ (green) vs. amount of receptor used.

Enrichment in C₈₄ up to 76% was thus achieved after one single extraction, and recoveries were up to about 75%. Further extractions of the resulting C₈₄-enriched mixture did not improve C₈₄ purity due to the inherent solubility of residual C₆₀ and C₇₀. However, washing out with some THF allowed the purity of C₈₄ to rise up to 85%.

III.3.7 Other Receptors

The remaining three receptors (**5b-d**) synthesized in section III.2 were also tested as extractants for fullerenes.

Receptor **5b**, who has an aliphatic three-carbon chain as linker, showed the typical downfield-shifted signal for the hydrogen-bonded UPy when the ¹H NMR spectrum was collected in chloroform (Figure 38).

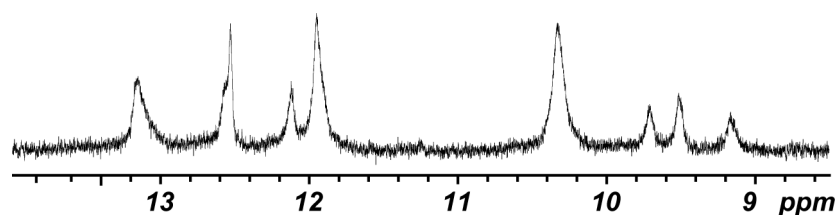


Figure 38: NHs region of the ¹H NMR spectrum of compound **5b** (CDCl₃, 400 MHz)

The number of downfield-shifted signals exceeded the expected number of three for a well-defined UPy dimer. This, and the observed splitting and broadening of signals over the whole spectrum, accounts for the formation of ill defined aggregates, as a consequence of a more flexible spacer.

Fullerite was extracted with **5b** using the protocol described for **5a**. Variable amounts of extractant were used (1%, 3% and 5%). The resulting chromatogram (Figure 39) showed that the peak corresponding to C₈₄ (12.5 min) increased significantly, and there was as well a small increment in the intensity of the peaks corresponding to fullerenes higher than C₈₄. These peaks became apparent even when only 1% by weight of CTV-UPy **5b** was added.

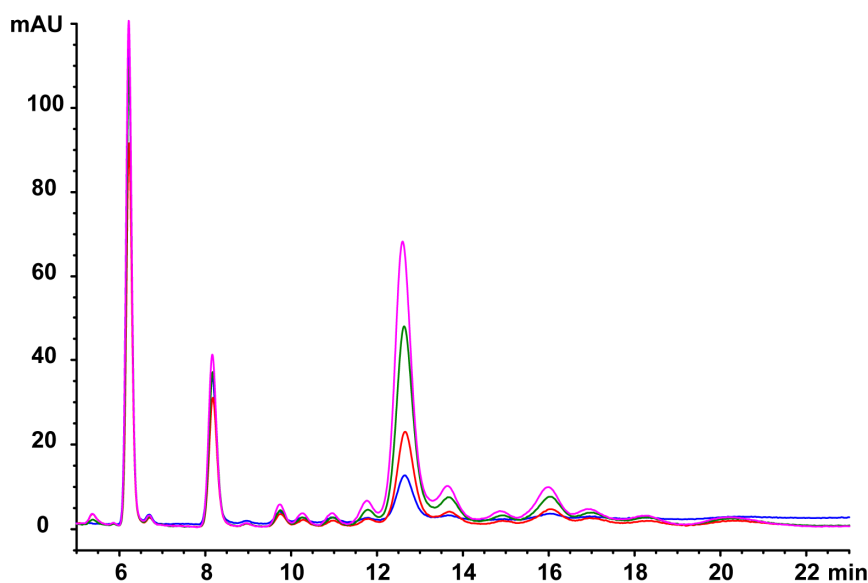


Figure 39: HPLC profiles of extractions of fullerite using 5% (pink line), 3% (green line) and 1% (red line) of **5b**. Blank experiment: blue line. (Cosmosil Buckyrep-M column 4.6x250 mm; mobile phase: toluene (100%); flow rate: 1 mL/min; λ : 290 nm).

On the other hand, compound **5c** (bearing an aromatic spacer) was almost insoluble in the solvent selected for the extractions, even in the presence of fullerenes. No extraction studies were thus performed.

On the contrary, compound **5d** (bezylamino spacer) resulted to be quite soluble in a variety of common solvents, such as dichloromethane, chloroform or THF. The ^1H NMR spectrum showed the typical well-defined set of three signals for the hydrogen-bonded NHs (Figure 40). For this more rigid spacer no splitting was observed. Even though, the remaining signals were quite broad, indicating formation of oligomeric assemblies.

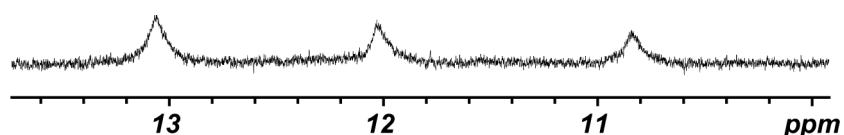


Figure 40: NHs region of the ¹H NMR spectrum of compound **5d** (CDCl₃, 400 MHz).

An extraction experiment was attempted using CTV-UPy **5d** and fullerite. Once again, THF was used as solvent for the extraction and variable amounts of capsule were employed. However, no fullerenes were extracted by encapsulation (Figure 41) and the observed peaks accounted only from the solubility of fullerenes in THF. Likely, the self-assembled cavity is, in this case, too large for light fullerenes.

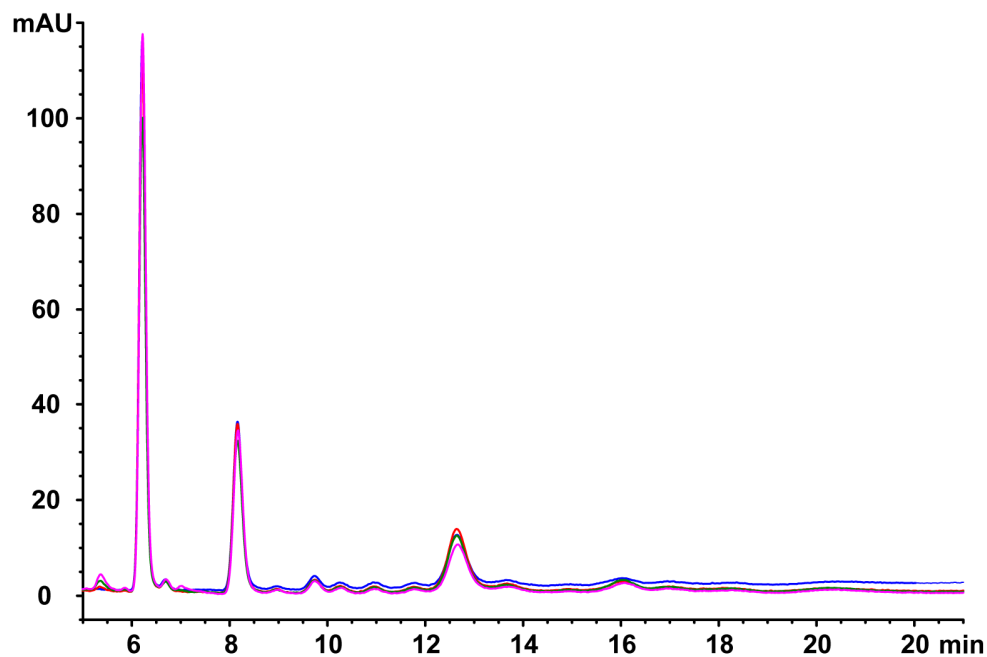


Figure 41: HPLC profiles of extractions of fullerite using variable amounts of **5d**. Cosmosil Buckyprep-M column 4.6x250 mm; mobile phase: toluene (100%); flow rate: 1 mL/min; λ: 290 nm.

Indeed, compound **5d** was tested as extracting agent for a mixture of C₆₀ and C₁₂₀³⁸ but nothing was extracted. Although the size of the capsule seems appropriate, it is probably too wide to match the shape of C₁₂₀.

III.4 IMPROVEMENTS IN HIGHER FULLERENES SEPARATION

III.4.1 Higher Fullerene Enriched Fullerites

A major interest of this part of the project was to study arc discharge conditions to produce fullerenes and to develop new extraction protocols to maximize higher fullerenes content in fullerites. This study was performed at the ETH laboratories in Zürich under the supervision of Prof. F. Diederich.

Generation of carbon soot was accomplished under the conditions described in Section III.1. Soot was then collected and placed into a cellulose thimble and extracted continuously using different solvents.

In polar and/or H-bonding competitive solvents such as acetone, tetrahydrofuran or methanol, C₆₀ is essentially insoluble. It is sparingly soluble in alkanes, and solubility increases with the number of carbon atoms of the solvent. Aromatic solvents and carbon disulfide provide the higher values in solubility. The increment in solubility going from benzene to naphthalene is remarkable. Although there are trends for the solubility behavior, there is no direct dependence of the solubility on several solvent parameters.^{16, 39}

³⁸ This C₆₀ dimer was kindly provided by Professor K. Komatsu (University of Kyoto): Wang, G.-W.; Komatsu, K.; Murata, Y.; Shiro, M. *Nature* **1997**, 387, 583-586.

³⁹ For a recent study of light fullerene solubility see: Semenov, K. N.; Charykov, N. A.; Keskinov, V. A.; Piartman, A. K.; Blokhin, A. A.; Kopyrin, A. A. *J. Chem. Eng. Data* **2010**, 55, 13-36.

During extraction experiments, it was observed that solubility of C₈₄ in THF was considerably higher than that of C₆₀ or C₇₀. For this reason, some unusual solvents were selected to carry out the separation of fullerenes from soot. These solvents were THF, 1,4-dioxane and hexane. Toluene was also used as a control experiment. Compositions of the fullerenes mixture obtained after the continuous extraction were evaluated by HPLC and mass spectrometry (MALDI-TOF).

As shown in Figure 42, a remarkable enrichment in higher fullerenes was obtained after 24 hours of continuous extraction with THF (*THF-1*), due to the differences in solubility of the higher fullerenes with respect to C₆₀ and C₇₀. The resulting mixture is not only significantly enriched in C₈₄ but also even in higher fullerenes, which could allow their isolation by chromatography or by selective encapsulation. Increasing the time of the continuous extraction to two (*THF-2*) or three days (*THF-3*), resulted in an increase of the total amount of C₆₀ and C₇₀ dissolved. That meant a decrease in the ratio C₆₀-C₇₀/higher fullerenes. Another advantage of using THF is that at high concentrations fullerenes precipitate and they can be collected directly by filtration.

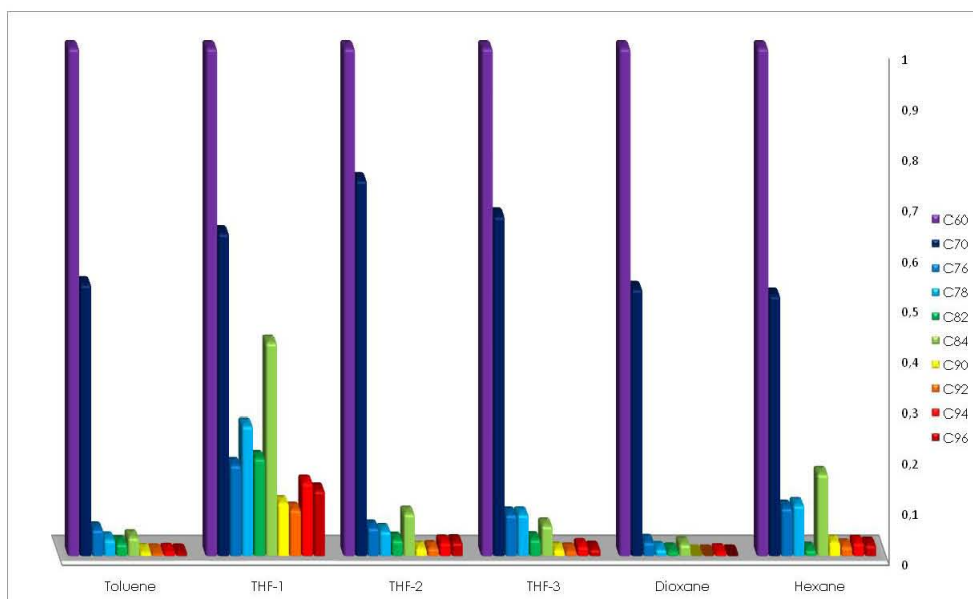


Figure 42: Plot of the normalized intensity in MALDI-TOF mass spectra of fullerenes extracted vs. solvent used.

The case of hexane was also significant. Although the resulting mixture was not as rich in higher fullerenes as with THF, this solvent showed preference for C_{76} , C_{78} and C_{84} and this new fullerite could be useful for improving the C_{84} purification process. Further re-extractions of these materials did not result in a significant enrichment of the samples.

III.4.2 Acetonitrile Soluble Capsule

PATENT PENDING

PATENT PENDING

PATENT PENDING

PATENT PENDING

PATENT PENDING

PATENT PENDING

PATENT PENDING

PATENT PENDING

PATENT PENDING

III.5 HOMOCHIRAL CAPSULES

III.5.1 Configurational and Conformational Study of Capsules

A number of variables have to be considered to evaluate the relative stabilities of the different conformers. As was pointed out in Section III.3.4, the capsule could adopt several different conformations, depending on the relative position of the UPy moiety respect to CTV platform, and the angle adopted by the linker chain. The prevalence of homochiral capsules over the heterochiral (*meso*) ones and the preferred conformation anti- β were demonstrated experimentally by ^1H NMR spectroscopy.

Although C_{84} provides the optimal binding, the study should be performed with C_{60} and C_{70} complexes, which are unique species and not isomeric mixtures.⁴² Since C_{70} fits better than C_{60} into the complex cavity, it was selected as the guest for the conformational analysis.

Racemic **5a** was resolved into its enantiomers⁴³ using semi-preparative chiral HPLC (Figure 46, left), the compounds giving rise to two major peaks in the HPLC chromatogram (fractions I and II), which showed mirror image

⁴² a) Kroto, H. W. *Nature* **1991**, 329, 529-531. b) Fowler, P. W.; Batten, R. C.; Manolopoulos, D. E. *J. Chem. Soc., Faraday Trans.* **1991**, 87, 3103-3104. c) Henrich, F. H.; Michel, R. H.; Fischer, A.; Richard-Schneider, S.; Gilb, S.; Kappes, M. M.; Fuchs, D.; Bürk, M.; Kobayashi, K.; Nagase, S. *Angew. Chem. Int. Ed.* **1996**, 35, 1732-1734. d) Kikuchi, K.; Nakahara, N.; Wakabayashi, T.; Suzuki, S.; Shiromaru, H.; Miyake, Y.; Saito, K.; Ikemoto, I.; Kainosho, M.; Achiba, Y. *Nature* **1992**, 357, 142-145. e) Taylor, R.; Langley, G. J.; Dennis, T. J. S.; Kroto, H. W.; Walton, D. R. M. *J. Chem. Soc., Chem. Commun.* **1992**, 1043 – 1046.

⁴³ a) Canceill, J.; Collet, A.; Gabard, J.; Gottarelli, G.; Spadat, J. P. *J. Am. Chem. Soc.* **1985**, 107, 1299-1308. b) Lesot, P.; Merlet, D.; Sarfati, M.; Courtieu, J.; Zimmermann, H.; Luz, Z. *J. Am. Chem. Soc.* **2002**, 124, 10071-10082.

circular dichroism (CD) spectra corresponding to both enantiomers (Figure 46, right).

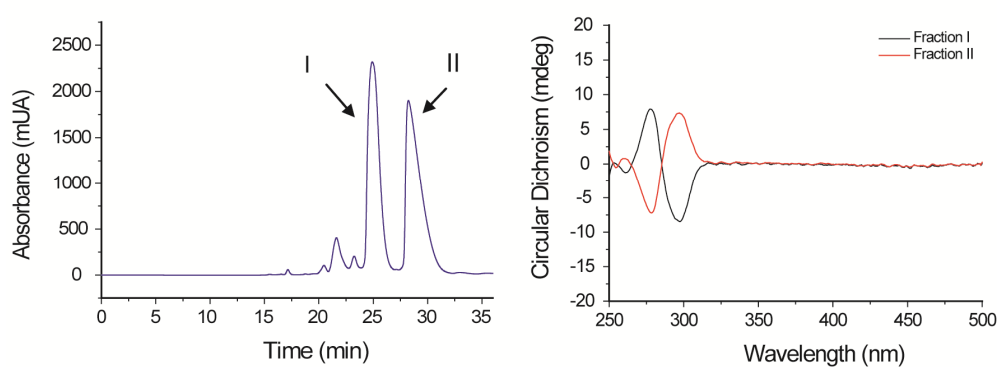


Figure 46: Left: HPLC Profile of enantiomeric separation of **5a** (Daicel, Chiralpack-IC 250 x 7.8mm, 5 μ m, mobile phase: DCM/MeOH (90:10 v/v) + 0.1% TFA, flow rate = 0.95 mL/min, λ = 254 nm). Right: CD Spectra of 10^{-4} M solutions of each enantiomer in chloroform.

^1H NMR spectra were registered for the racemic mixture, each pure enantiomer and a 1:1 mixture of both enantiomers, always in the presence of 0.5 equivalents of C_{70} to ensure capsule formation (Figure 47).

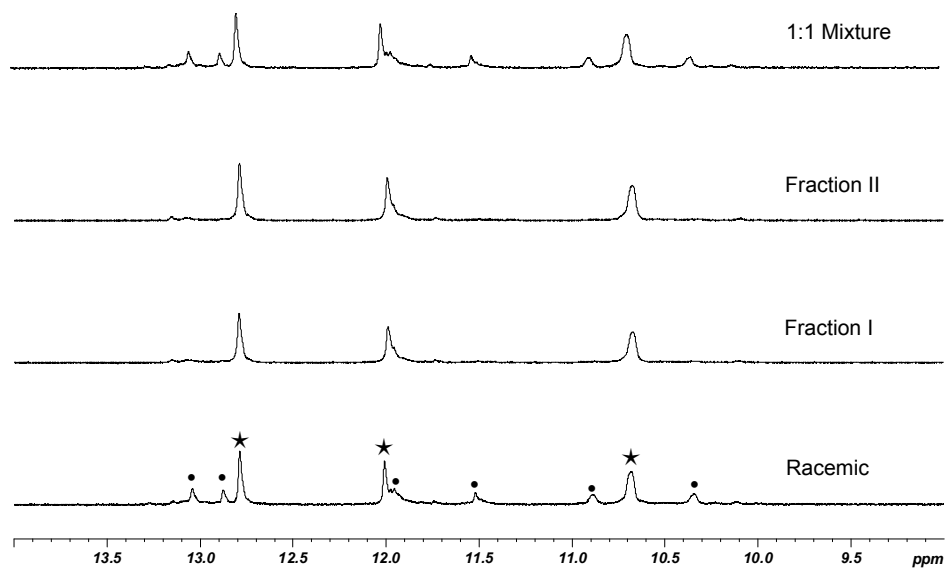


Figure 47: ^1H NMR spectra (NH region) of racemic, both homochiral and the 1:1 mixture of enantiomeric **5a** capsules in the presence of C_{70} . (★) NH signals corresponding to homochiral capsules. (•) NH signals corresponding to meso self-assembled capsules.

The NH's region of the homochiral capsules showed only three signals at the typical strongly deshielded chemical shifts of the DDAA keto tautomers of UPy dimers. As expected, both spectra were identical. The absence of additional signals accounted for the presence of only one tautomeric dimer. The spectrum of the capsule formed from racemic **5a** displays six minor peaks, in addition to the three signals observed for the pure enantiomers. Mixing the two solutions arising from the pure enantiomers remarkably reproduced the spectrum arising from racemic CTV. This proved conclusively that the minor signals are due to the presence of meso capsules of lower symmetry. The ratio homochiral/meso capsules from the racemic **5a** and from mixing both enantiomerically pure solutions was 7:3, as determined by integration of the spectrum.

Experimentally, conformation $A_{\beta}A_{\beta}$ prevails in solution, as was clearly shown by the NMR data. All signals were unequivocally assigned by a complement of 2D and 3D (COSY, NOESY and HSQC) NMR techniques.⁴⁴ Apart from the typical deshielding of the three NH signals (Figure 47) of each monomer, the central part of the NMR spectrum is diagnostic for the observed conformation. Several signals were upfield- or downfield-shifted upon encapsulation (Figure 48). This effect was significant for the signals corresponding to the O-CH₂-CH₂-N linker.

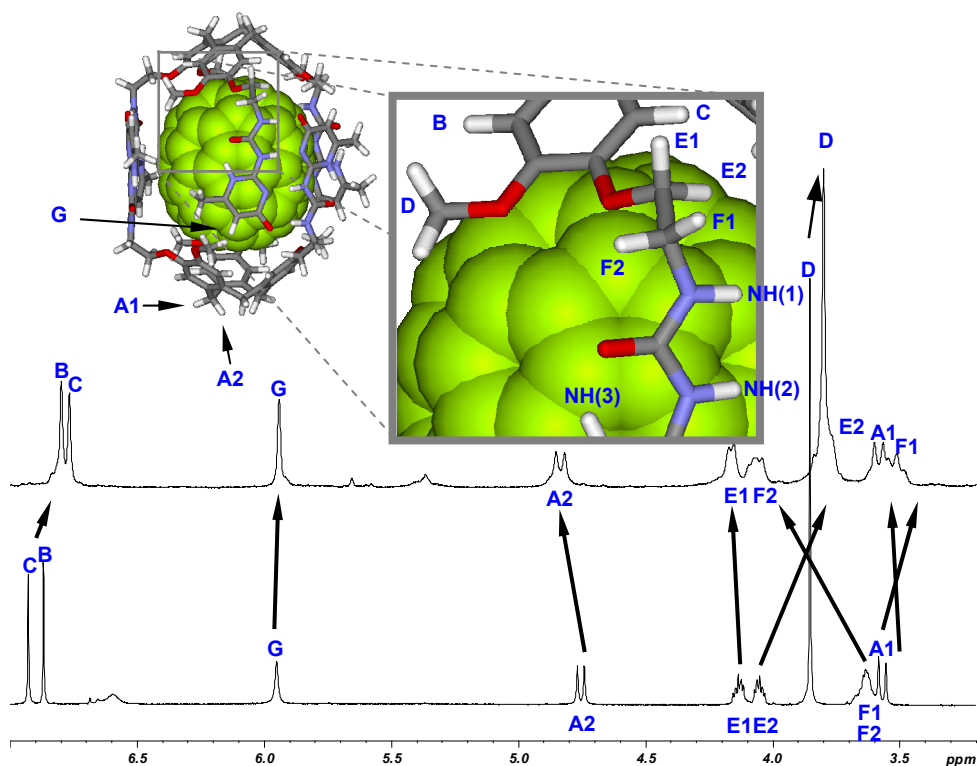


Figure 48: ¹H NMR spectra (CDCl₃, 400 MHz, 3.2-7.0 ppm region shown). Bottom: free monomeric host (**5a** + TFA). Top: dimeric capsule C₇₀@**5a-5a**.

⁴⁴ See appendix, Section VII.2.

Coupling is mediated by the interaction of orbitals within the bonding framework. It is therefore dependent of overlap, and hence of dihedral angle. The relationship between the dihedral angle and the vicinal coupling constant 3J (as observed from ^1H NMR spectra) is given theoretically by the Karplus equations.⁴⁵ One of the protons of the CH_2 next to the nitrogen (namely F2), showed an intense vicinal coupling with the proton of the urea, compatible with their mutual *anti* orientation (see Figure 49) where the coupling constant reaches a maximum value, and was also strongly deshielded due to its proximity to the carbonyl group. On the contrary, protons C, D, E2, and F1, close to the fullerene surface, were shielded. E1, pointing away, is not affected. These anisotropic effects are fully compatible with a β conformation of the linker.

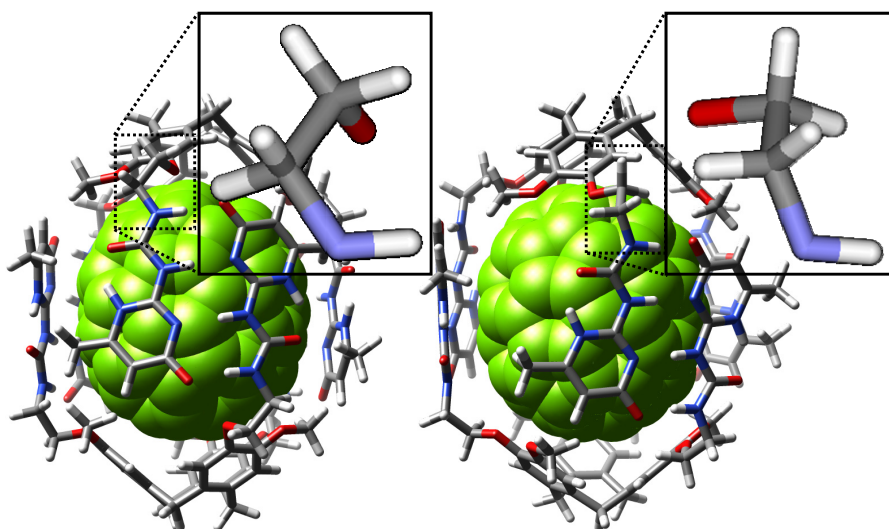


Figure 49: Comparison between molecular models of the C_{70} capsule in conformations $\text{A}_\alpha\text{A}_\alpha$ (left) and $\text{A}_\beta\text{A}_\beta$ (right).

⁴⁵ a) Karplus, M. J. *Chem. Phys.* **1959**, 30, 11-15. b) Karplus, M. J. *Am. Chem. Soc.* **1963**, 85, 2870-2871.

On the other hand, *anti* (A) orientation of the UPy was determined by means of NOESY experiments. A comparison between $A_{\beta}A_{\beta}$ and $S_{\beta}S_{\beta}$ models showed that, for an *anti* orientation, a coupling through the space must be detected between pyrimidinone CH (named G) and the first CH₂ of the eleven-carbon chain (named H) with the methoxy group (D) in the CTV scaffold, which are spatially closed. Whereas in a *syn* (S) orientation, only proton G is spatially close to methoxy group D, but not the aliphatic chain. NOESY experiment for a homochiral C₇₀ complex revealed coupling between the spin of these signals, indicating the presence of *anti* orientation (Figure 50).

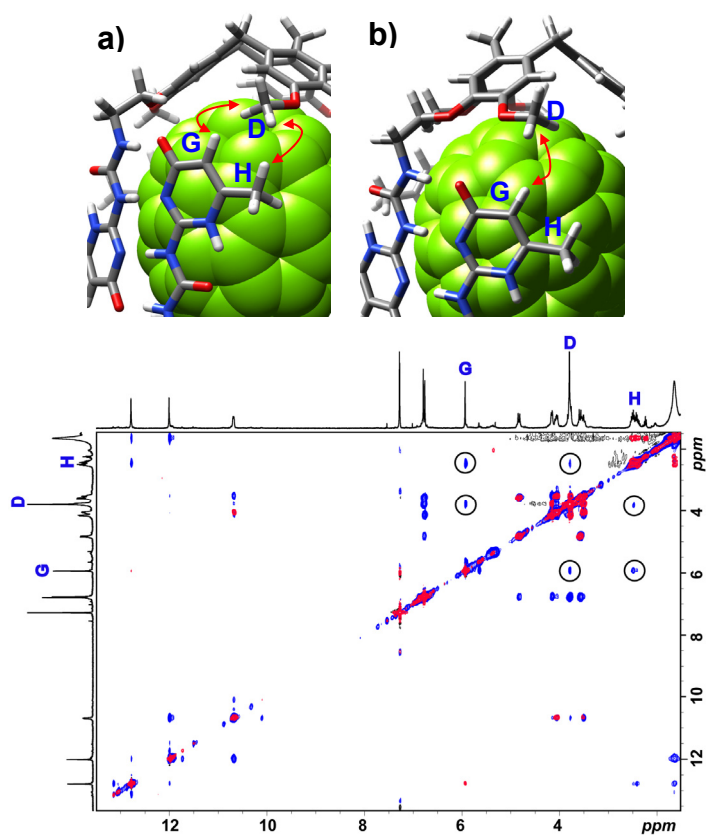


Figure 50: Detail of a) $A_{\beta}A_{\beta}$ and b) $S_{\beta}S_{\beta}$ models showing the spatial proximity of D, G and H protons; and partial NOESY (400 MHz, CDCl₃) spectrum of homochiral C₇₀@**5a**·**5a** complex (bottom).

The experimental NMR results nicely match the predictions made by calculations, in which all the geometric alternatives were evaluated, and concluded that the $A_{\beta}A_{\beta}$ conformation was the most stable.²⁶

III.5.2 Thermal Stability of Homochiral Capsules

In above sections, we described the stereochemical aspects of cyclotriveratrylene derivatives and the separation of the two enantiomers of CTV-UPy **5a**. Herein, the thermal stability of the homochiral assembly and, consequently, the CTV enantiomers, will be studied.

Racemization of CTV occurs through a “crown to crow” interconversion, whose rate is sensitive to temperature.^{24, 25} The following study evaluates how the inclusion of a given fullerene inside the capsule affects its stability.

Racemization of empty receptor **5a** and the 1:2 complexes formed with C_{60} , C_{70} , and C_{84} as guest was monitored at three different temperatures by circular dichroism (CD) (Figure 51). Spectra were collected every ten minutes until total racemization.

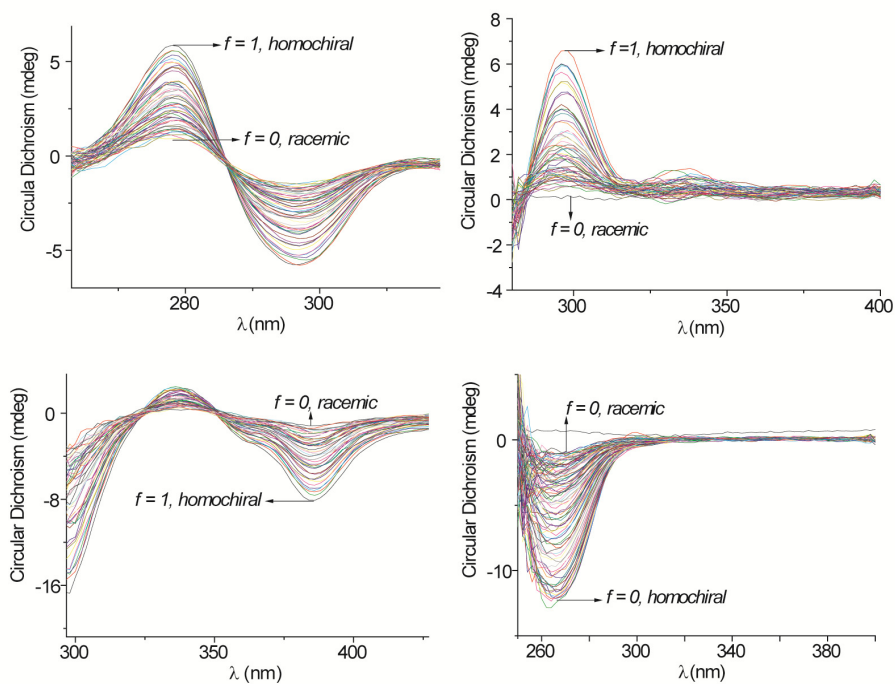


Figure 51: Racemization profiles of compound **5a** (top left), C_{60} (top right), C_{70} (bottom left) and C_{84} (bottom right) complexes in tetrachloroethane at 47 °C.

In all cases, racemization followed first order kinetics. The data⁴⁶ were fitted by using Eyring plot (Figure 52) to calculate the thermodynamic parameters (Table 15).

⁴⁶ See appendix for details about kinetics.

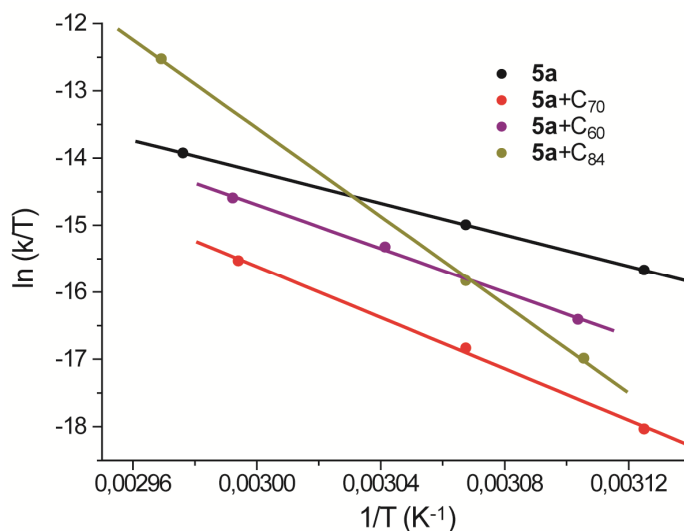


Figure 52: Eyring Plots for the different complexes.

Table 15: Thermodynamic transition state parameters of cyclotrimeratrylene derivatives (E_a values calculated by Arrhenius equation, ΔG^\ddagger given at 298 K).

Compound	E_a (Kcal/mol)	ΔH^\ddagger (Kcal/mol)	ΔS^\ddagger (cal/mol K)	ΔG^\ddagger (Kcal/mol)
Collet ⁴⁷	26.5	25.9	-1.9	26.5
5a	23.9	23.3	-5.6	25.0
C ₆₀ @ 5a 5a	33.0	32.4	20.8	26.2
C ₇₀ @ 5a 5a	38.5	37.9	35.4	27.4
C ₈₄ @ 5a 5a	66.0	65.6	121.8	29.0

For compound **5a**, the racemization thermodynamic parameters were very similar to those obtained by Collet⁴⁷ for the racemization of (+)-10, 15-dihydro-3, 8, 13-trimethoxy-2, 7, 12-tris(trimethoxy-2, 7, 12-tris(methoxy-*d*₅-5H-tribenzo[a,d,g]cyclononene (Figure 53).

⁴⁷ Collet, A.; Gabard, J. J. *Org. Chem.* **1980**, *45*, 5400-5401.

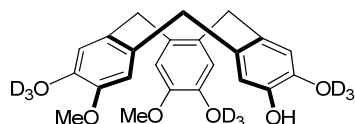


Figure 53: Collet's cyclotrimeratrylene.

Even though compound **5a** forms hydrogen-bonded oligomers, it displayed similar degrees of freedom allowing racemization in a similar manner as Collet's CTV.

For filled capsules, the racemization rates depended on the size of the encapsulated fullerene. The bigger it was, the bigger the enthalpic barrier was. However, the free energy (ΔG^\ddagger) was similar in all cases due to the entropic gain. The increase in entropy in the transition state might result from the increase of degrees of freedom with respect to the initial capsule geometry, which are more restricted with bigger fullerenes.

III.5.3 Toward Separation of Chiral Fullerenes

Separation and characterization of chiral fullerenes has been a hot topic in the field for many years. Higher fullerenes as C_{76} , C_{78} and C_{84} are present as mixtures of isomers, some of them chiral.⁴⁸ Up to date, the most effective way for their isolation is the use of recycling HPLC coupled with chiral columns.^{4a} In 1999, Diederich and coworkers were able to isolate three constitutional isomers of C_{84} and separate the enantiomers of the optically active D_2 -isomer, by means of a novel methodology based on Bingle and

⁴⁸ a) Thilgen, C.; Diederich, F. *Top. Curr. Chem.* **1999**, *199*, 135-171. b) Goto, H.; Harada, N.; Crassous, J.; Diederich, F. *J. Chem. Soc., Perkin Trans. 2* **1998**, *8*, 1719-1723. c) Hawkins, J. M.; Nambu, M.; Meyer, A. *J. Am. Chem. Soc.* **1994**, *116*, 7642-7645.

retro-Bingle reactions.⁴⁹ Therefore, design of host molecules for recognizing asymmetrically distorted π -electronic surfaces of carbon nanoclusters is one of the most challenging issues. Unlike ordinary asymmetric compounds, carbon nanoclusters are devoid of suitable functionalities for point recognition so that chiral recognition requires a different strategy.

In literature, there are just a few examples of chiral discrimination of carbon nanostructures. Osuka *et al.* developed chiral porphyrin tweezers able to differentiate and extract chiral single-walled carbon nanotubes.⁵⁰ In 2006 Aida *et al.*⁵¹ proposed the synthesis of a novel heterocyclic porphyrin dimer containing an asymmetrically distorted *N*-alkylporphyrin. This was the first host molecule capable of sensing (but not isolating) chiral fullerene C₇₆^{4a} by ¹H NMR spectroscopy (Figure 54).

⁴⁹ Crassous, J.; Rivera, J.; Fender, N. S.; Shu, L.; Echegoyen, L.; Thilgen, C.; Herrmann, A.; Diederich, F. *Angew. Chem. Int. Ed.* **1999**, *38*, 1613-1617.

⁵⁰ a) Peng, X.; Komatsu, N.; Kimura, T.; Osuka, A. *J. Am. Chem. Soc.* **2007**, *129*, 15947-15953. b) Peng, X.; Komatsu, N.; Bhattacharya, S.; Shimawaki, T.; Aonuma, S.; Kimura, T.; Osuka, A. *Nature Nanotech.* **2007**, *2*, 361-365.

⁵¹ a) Shoji, Y.; Tashiro, K.; Aida, T. *J. Am. Chem. Soc.* **2006**, *128*, 10690-10691. b) Shoji, Y.; Tashiro, K.; Aida, T. *Chirality* **2008**, *20*, 420-424.

$C_{76}@(M)\text{-}5\mathbf{a}$ $5\mathbf{a}$], should translate into splitting of all signals, as observed in Aida's porphyrins cage, but this behavior was not detected in CTV-UPy capsules.

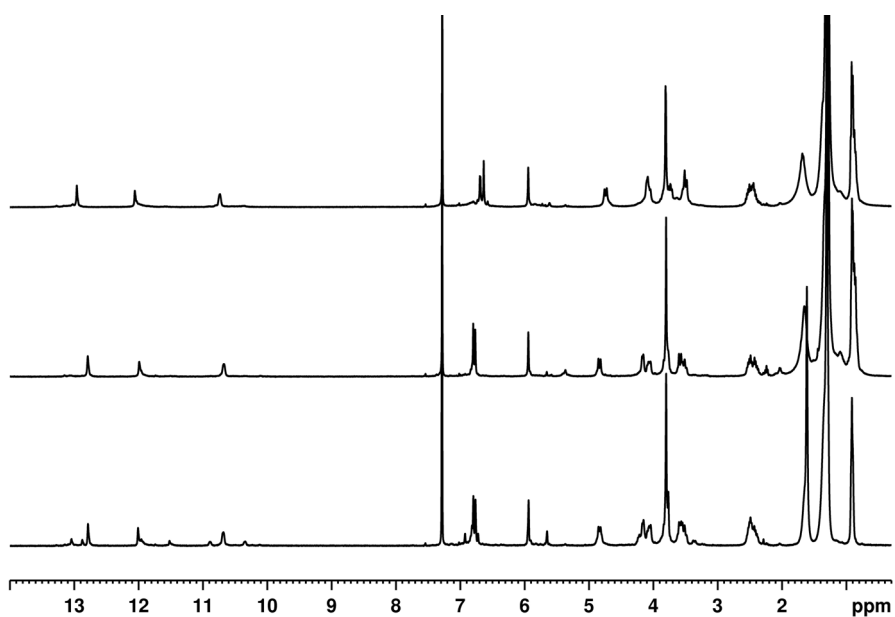


Figure 55: ¹H NMR profile of 2:1 mixtures in CDCl₃ (400 MHz) of: racemic **5a** and C₇₀ (bottom); homochiral **5a** and C₇₀ (middle) and racemic **5a** plus racemic C₇₆ (top).

Furthermore, addition of one equivalent of (\pm)-C₇₆ to two equivalents of homochiral **5a** did not result in a well-defined spectrum but in a mixture of broad bands instead, likely due to oligomeric species arising from the mismatched diastereomeric combination.

The observations made in the ¹H NMR spectrum of a 1:2 mixture of racemic C₇₆ and racemic **5a** could either account for a perfect match between homochiral capsule and the right C₇₆ enantiomer or for no anisotropic effect of the chiral guest over the chiral host. Further experiments must be carried out in order to discard one theory or the other.

Nevertheless, some C_{76} extractions were attempted. As expected, racemic C_{76} showed no CD-signal (Figure 56), but unfortunately, extractions with one equivalent of C_{76} and one equivalent of **5a** in THF did not yield any CD signal, indicating that no substantial enrichment in one of the C_{76} enantiomers had occurred.

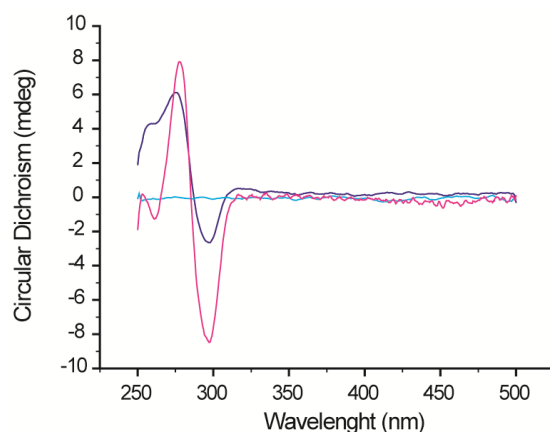


Figure 56: CD profile of homochiral **5a** (pink) and C_{76} @**5a** **5a** complex (blue). Extracted C_{76} (turquoise) shows no CD signal.

III.6 CONCLUSIONS

The combination of a concave cyclotrimertrilene host molecule, capable of complexing fullerenes, with the strongly quadruple hydrogen bonding ureidopyrimidinone resulted in a new host molecule that forms well-defined dimeric hydrogen-bonded assemblies encapsulating a fullerene molecule into its large cavity.

Additionally, compound **5a** displays a remarkable selectivity for the encapsulation of C_{70} over C_{60} . By simple solid-liquid extractions, 97% purity C_{70} could be obtained from fullerite after only two runs. Fullerenes were purified avoiding the use of chromatography and moreover, the host molecule resulted to be easily recyclable.

Chapter III

The selectivity of the host towards C₇₀ or C₈₄ was easily tuneable by playing with concentrations. At high receptor/fullerite ratios, C₇₀ is selected, whereas C₈₄ is preferred at low ratios. In this way, C₈₄ was isolated from fullerite up to 85% purity in a single extraction in THF. Additionally, by changing solubility properties of CTV-UPy receptors towards more polar solvents, the purity of extracted C₈₄ was raised up to 93% in only one round.

DFT calculation demonstrated to be a powerful tool predicting complex stability and structure.

Racemization of CTV-UPy homochiral complexes involves the disruption of H-bonds and consequently, the capsule. Thus, the stronger the capsule is, the better the H-bonds are and the higher is the energetic barrier (ΔH^\ddagger).

Neither enantioselective extraction nor enrichment of racemic mixtures of C₇₆ was obtained upon preliminary extractions with enantiopure **5a** host.

UNIVERSITAT ROVIRA I VIRGILI
SELF-ASSEMBLY BASED ON THE 2-UREIDO-4(1H)-PYRIMIDINONE MOTIF: FROM CYCLIC ARRAYS TO MOLECULAR CAPSULES
FOR FULLERENE SEPARATIONS
Elisa Huerta Martínez
DL:T.289-2012

CHAPTER IV: FULLERENE RECOGNITION BY DONOR- ACCEPTOR INTERACTIONS

Part of this chapter will be published: Huerta, E.; Isla, H.; Pérez, E. M.; Bo, C.; Martín, N.; de Mendoza, J. *J. Am. Chem. Soc.*, submitted.

UNIVERSITAT ROVIRA I VIRGILI
SELF-ASSEMBLY BASED ON THE 2-UREIDO-4(1H)-PYRIMIDINONE MOTIF: FROM CYCLIC ARRAYS TO MOLECULAR CAPSULES
FOR FULLERENE SEPARATIONS
Elisa Huerta Martínez
DL:T.289-2012

CHAPTER IV: FULLERENE RECOGNITION BY DONOR-ACCEPTOR INTERACTIONS

IV.1 A RECEPTOR FOR FULLERENES BASED ON EXTENDED TTF SCAFFOLDS

A key feature in the design of efficient receptors for fullerenes is to use a combination of large aromatic surfaces and shape complementarity to the curved, convex surface of the guests. In this way, the curvature and the aromaticity of the π -extended tetrathiafulvalenes (exTTF)¹ (Figure 1, left) make them almost perfect candidates to be attached to suitable platforms.² In addition, the exTTF fragment becomes aromatic and planar after gaining two electrons.

New tweezer-like receptors based on two exTTF units held together through an aromatic (isophthalic or phthalic) spacers have been recently reported by Prof. Martín and co-workers.³

The receptor forms 1:1 complexes with C₆₀ ($K_s = 2.98 \times 10^3 \text{ M}^{-1}$, chlorobenzene).

¹ Pérez, E. M.; Sierra, M.; Sánchez, L.; Torres, M. R.; Viruela, R.; Viruela, P. M.; Ortí, E.; Martín, N. *Angew. Chem. Int. Ed.* **2007**, *46*, 1847-1851.

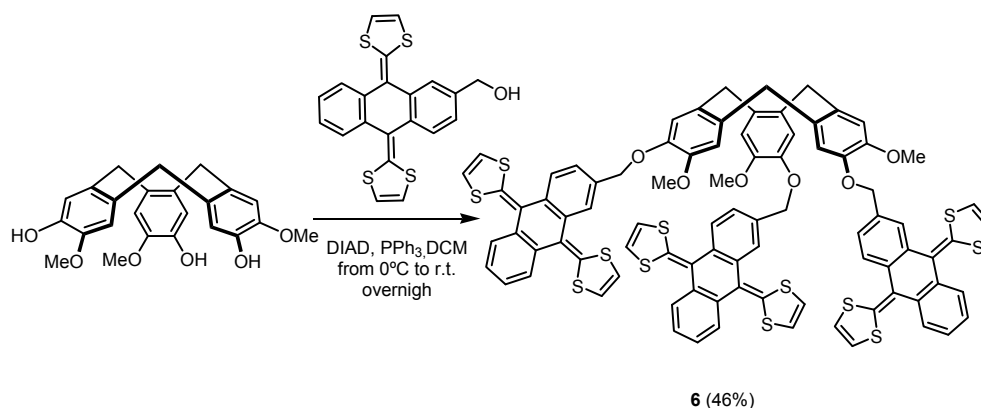
² Pérez, E. M.; Martín, N. *Chem. Soc. Rev.* **2008**, *37*, 1512-1519.

³ a) Pérez, E. M.; Sánchez, L.; Fernández, G.; Martín, N. *J. Am. Chem. Soc.* **2006**, *128*, 7172-7173. b) Gayathri, S. S.; Wielopolski, M.; Pérez, E. M.; Fernández, G.; Sánchez, L.; Viruela, R.; Ortí, E.; Guldi, D. M.; Martín, N. *Angew. Chem. Int. Ed.* **2009**, *48*, 815-819.

IV.1.1 Design, Synthesis and Complexation Studies

Based on these precedents, a new host, in which three units of exTTF are linked to a CTV scaffold through short ether linkages, has been designed and synthesized in collaboration with Prof. Martín's group. The concave surfaces of both the CTV and the exTTF subunits should nicely wrap around the entrapped fullerene guest.

Host **6** was readily synthesized from known fragments via a simple Mitsunobu⁴ coupling (Scheme 1).



Scheme 1: Synthesis of receptor **6**.

Its purity and identity was unambiguously established by HPLC-MS, ¹H and ¹³C NMR and UV-vis spectroscopy.

An early indication of the ability of **6** to bind fullerenes came from the MALDI-TOF spectrum (negative mode in pyrene matrix). When 1:1 mixtures of **6** and either C₆₀ or C₇₀ were analyzed, peaks at *m/z* 2306.3 and 2426.2, corresponding to C₆₀@**6** (calculated 2306.1) and C₇₀@**6** (calculated 2426.1),

⁴ Swamy, K. C. K.; Kumar, N. N. B.; Balaraman, E.; Kumar, K. V. P. P. *Chem. Rev.* **2009**, *109*, 2551-2651.

respectively, were observed, in perfect agreement with their calculated isotopic mass distribution (Figure 1). No peaks corresponding to aggregates of other stoichiometries were found, even when mixtures of different fullerene/receptor ratios were analyzed.

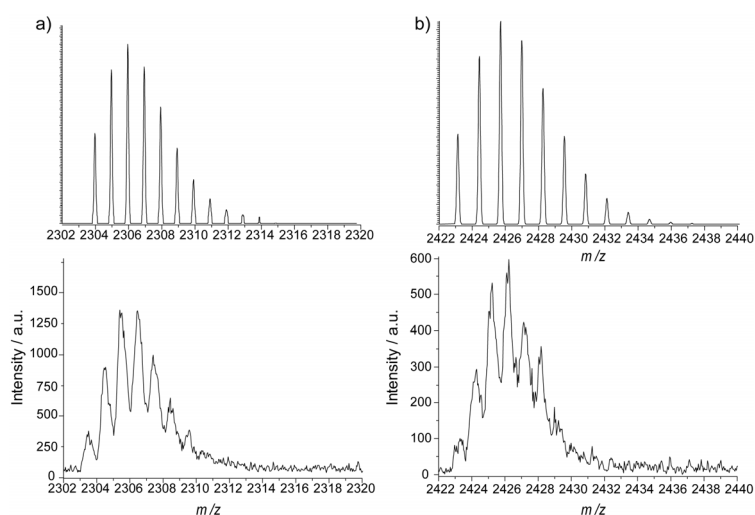


Figure 1: Simulated (top) and found (MALDI-TOF, bottom) isotopic pattern for a) C₆₀@**6** and b) C₇₀@**6**.

After isolation, compound **6** was studied by ¹H-NMR spectroscopy. Initially, the sample was dissolved in a CDCl₃/CS₂ (5:2 v/v) mixture. The host shows rather complex ¹H-NMR spectra (500 MHz) at room temperature, indicative of the coexistence of several stable conformations in solution, in slow chemical exchange (Figure 2).

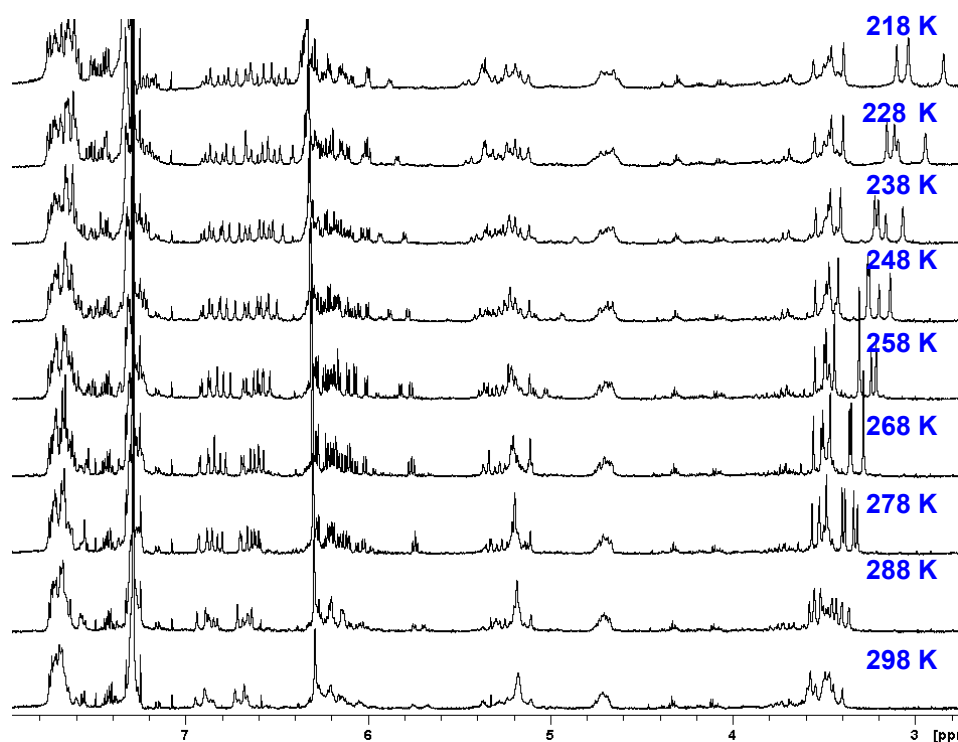


Figure 2: Variable temperature ¹H-NMR experiment (298 - 218 K) of compound **6** in a (5:2) mixture of CDCl₃/CS₂ (500 MHz).

The solvent was then replaced for deuterated toluene to carry out a high temperature experiment (Figure 3). The sample was heated from room temperature to 378 K. Heating caused the spectrum to significantly simplify, and despite some signals were still splitted (such as the CH₂ linking the CTV and the exTTF at ~ 5 ppm or the OMe group at ~ 3.5 ppm) some others were resolved, such as the methylene bridges of the CTV scaffold, although still not matching with a C₃ symmetric molecule.

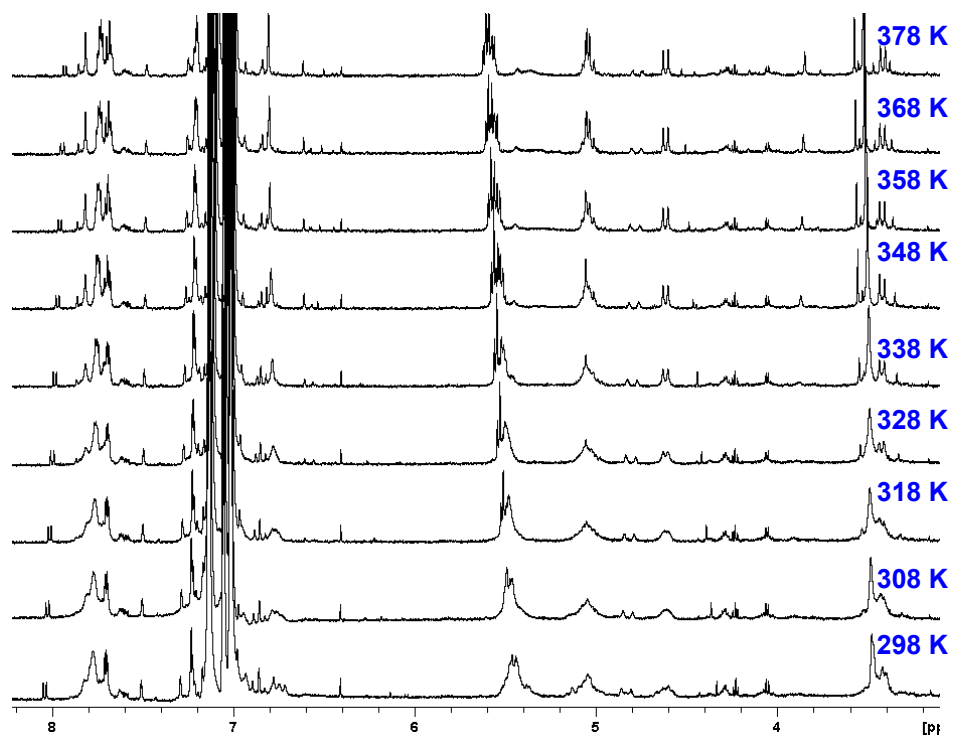


Figure 3: Variable temperature ¹H-NMR experiment (298 - 378 K) of compound **6** in toluene-*d*₈ (500 MHz).

In toluene, unlike in a chloroform-carbon disulfide mixture, the signal became broader and no splitting was observed when cooling down to 198 K (Figure 4), probably because the aromatic solvent tends to stack with the receptor **6**.

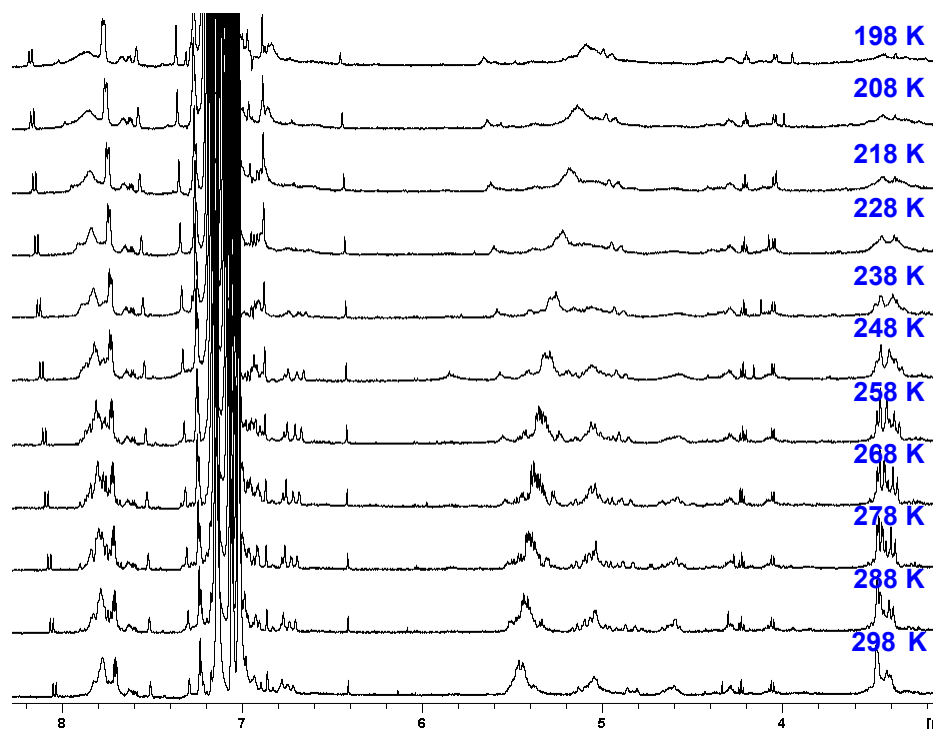


Figure 4: Variable temperature $^1\text{H-NMR}$ experiment (298 - 198 K) of compound **6** in toluene- d_8 (500 MHz).

Due to the complexity of the spectra in these solvents, no distinguishable changes were observed when C_{60} was added to the receptor in a 1:1 ratio, so the effect produced by the complexation could not be evaluated.⁵

When the solvent was changed to chlorobenzene- d_5 , the spectrum showed a single set of broad signals at room temperature, which is fully resolved at 353 K. Moreover, the binding event produced slight, though reproducible changes in the $^1\text{H NMR}$ spectrum of **6** (Figure 5).

⁵ See appendix, section VII.3

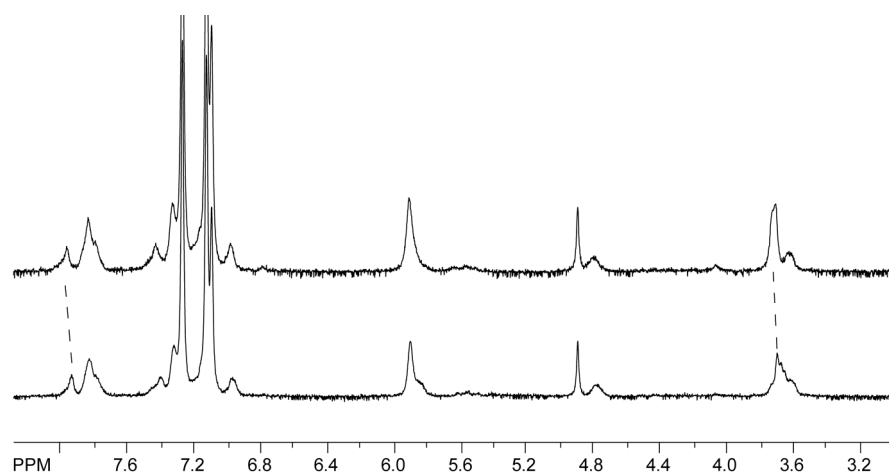


Figure 5: ¹H NMR (chlorobenzene-*d*₅, 500 MHz, 298 K) spectra of C₆₀@6 (top) and 6 (bottom).

Additionally, the C₆₀ ¹³C NMR signal was upfield shifted and broadened in C₆₀@6 (Figure 6), both processes being more evident upon cooling (Figure 7).

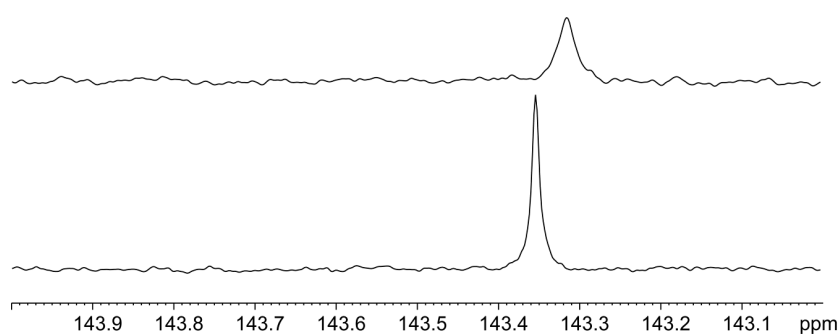


Figure 6: ¹³C NMR (chlorobenzene-*d*₅, 125 MHz, 298 K) spectra of C₆₀@6 (top) and C₆₀ (bottom).

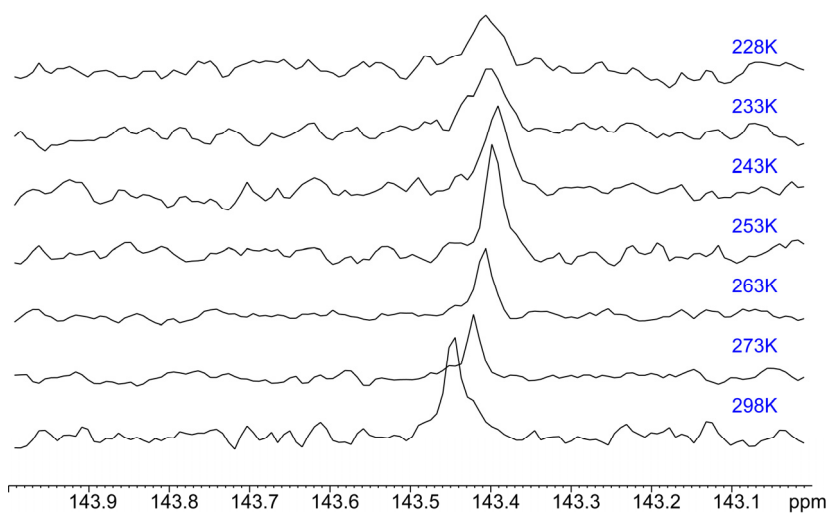


Figure 7: VT-¹³C NMR experiment (chlorobenzene-d₅, 75 MHz, 298 - 228 K) of C₆₀@6.

IV.1.2 Physicochemical and Photophysical Characterization

IV.1.2.1 Spectroscopic Characterization of the Complexes

The 1:1 stoichiometry of the complexes in solution was confirmed spectroscopically (UV-vis) by means of the method of continuous variations (Job's plot). The experiments were carried out using chlorobenzene as solvent at 0.3 mM concentration for both the fullerene (C₆₀ or C₇₀) and the receptor **6** (Figures 8 and 9).

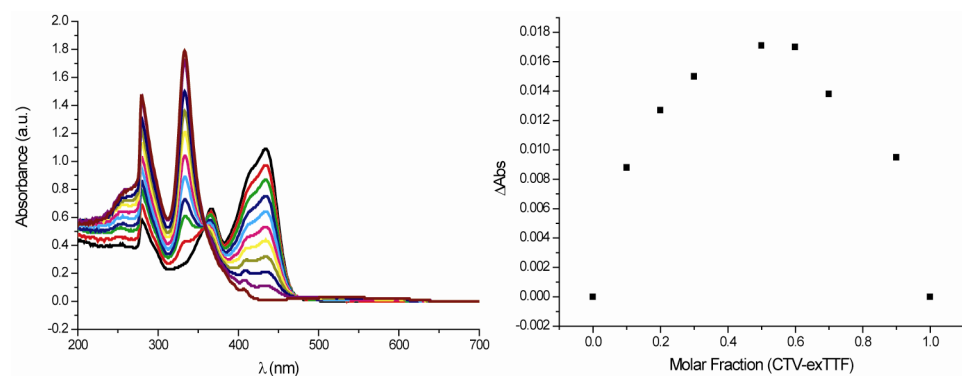


Figure 8: Job's Plot for complex $C_{60}@6$. $[CTV] = [C_{60}] = 0.3$ mM in chlorobenzene ($\lambda = 436$ nm).

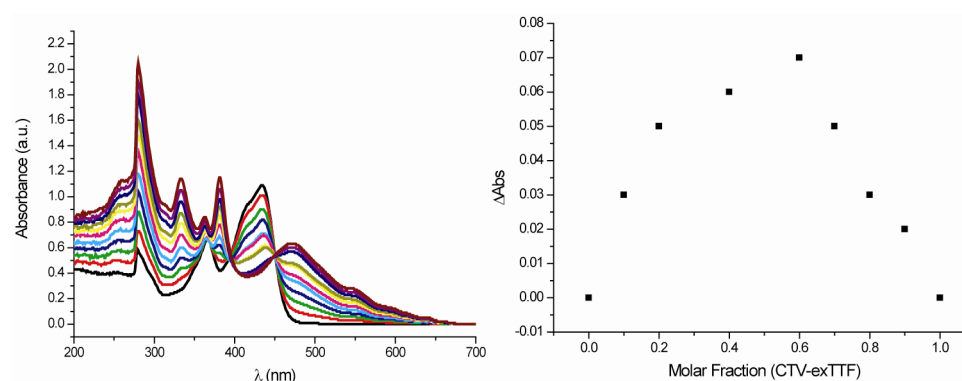


Figure 9: Job's Plot for complex $C_{70}@6$. $[CTV] = [C_{70}] = 0.3$ mM in chlorobenzene ($\lambda = 436$ nm).

The stability of the complexes was estimated through three independent UV-vis titrations. In a typical experiment, aliquots of 0.1 equivalents of the fullerene were added (0.0 - 3.3 equivalents) to a constant concentration of the **6** host (10^{-4} M, chlorobenzene).

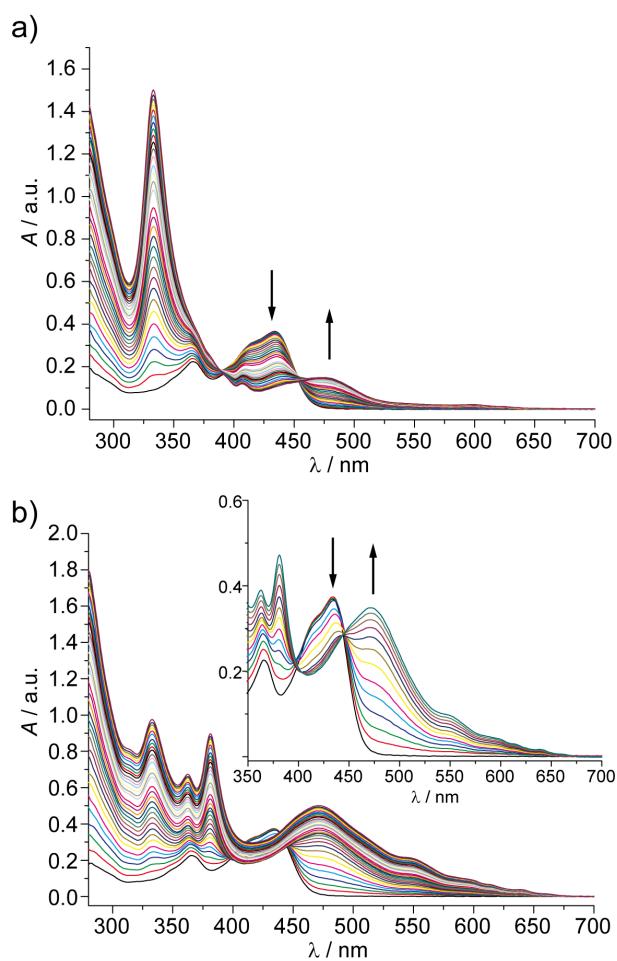


Figure 10: UV-vis spectra as recorded during the titration of a) **6** vs C₆₀ and b) **6** vs C₇₀ (inset shows the first twelve additions) in chlorobenzene at 298 K.

Upon addition of either C₆₀ or C₇₀ a significant decrease in intensity of the exTTF band at $\lambda_{\text{max}} = 434$ nm was observed (Figure 10), accompanied by the emergence of an intense charge-transfer band centered at $\lambda = 478$ nm for C₆₀ and at $\lambda = 472$ nm for C₇₀. During the early steps of the titration (after addition of 1.0 - 1.2 equivalents of guest), well defined isosbestic points at 452 nm (C₆₀) and 445 nm (C₇₀) were observed. The changes in the electronic absorption spectra are fully consistent with those found for previously

reported tweezer-like exTTF receptors and constitute a typical signature of the exTTF-fullerene interaction.⁶

An accurate determination of the binding constants is somewhat troublesome, due to the extensive band overlap with the increasing fullerene absorption during the titration. Indeed, data analysis for C₆₀ titration (using Specfit software), was unable to provide a reliable value for the binding constant. Nevertheless, analysis taking into account only those fits with chemically meaningful predicted absorbances for the complex, allowed unambiguously concluding that log K_a should be higher than 5 M⁻¹. Alternatively, using Origin software and fitting the data to the equation commonly employed,⁷ afforded a value of log K_a = 5.3 ± 0.2 M⁻¹. This value is two orders of magnitude higher than the one calculated for tweezer-like receptors. With regard to C₇₀, analysis of the binding constant with Specfit satisfactorily produced a value of log K_a = 6.3 ± 0.6 M⁻¹, 10-fold higher than that found for C₆₀. The values of the binding constants are the highest reported to date for a non metalloporphyrin containing host, and comparable to those reported by the groups of Boyd, Reed and Armaroli for bisporphyrin tweezers⁸ and by Aida for bisporphyrin cages, with the exception of the Ir(III) metalloporphyrin derivative, in which the metal is coordinatively bound to a 6,6 junction of the fullerene in a η² fashion.⁹

⁶ Jones, A. E.; Christensen, C. A.; Perepichka, D. F.; Batsanov, A. S.; Beeby, A.; Low, P. J.; Bryce, M. R.; Parker, A. W. *Chem. Eur. J.* **2001**, *7*, 973-978.

⁷ Schalley, C., *Analytical Methods in Supramolecular Chemistry*, **2007**, 17-54.

⁸ Hosseini, A.; Taylor, S.; Accorsi, G.; Armaroli, N.; Reed, C. A.; Boyd, P. D. W. *J. Am. Chem. Soc.* **2006**, *128*, 15903-15913.

⁹ Yanagisawa, M.; Tashiro, K.; Yamasaki, M.; Aida, T. *J. Am. Chem. Soc.* **2007**, *129*, 11912-11913.

IV.1.2.2. Electron Paramagnetic Resonance (EPR) Studies

Besides the very high binding constants, one of the most significant features of the $C_{60}@6$ complex is the combination of shape and electronic complementarity between exTTF and C_{60} . It has been previously shown that photoinduced electron transfer (PET) from the electron donor exTTF to the electron acceptor C_{60} occurs readily in the tweezers-like receptors reported by Martín *et al.*^{3b} This is also the case of the $C_{60}@6$ complex, as demonstrated by preliminary light-induced electron spin resonance measurements at 298 K (Figure 11).

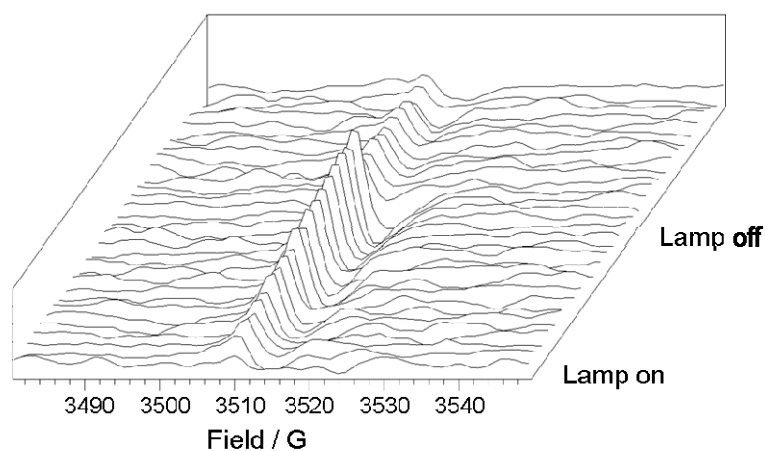


Figure 11: ESR spectra of $C_{60}@6$ (chlorobenzene, 298 K) taken at 45 s intervals. The sample was irradiated with a broadband Hg lamp.

When a 1:1 mixture of C_{60} and **6** in degassed chlorobenzene - ESR silent in the dark - was irradiated with a broadband Hg lamp, a clearly visible, albeit weak signal ($g = 2.0014$; $\Delta H = 5.9$ G) was observed, which increases in intensity with irradiation time, and decreases rapidly upon switching the lamp off. To unambiguously establish the PET origin of this ESR signal, control LESR experiments were carried out with both C_{60} and **6** separately, which remained ESR silent under light irradiation.

Nevertheless, unequivocal assignment of this signal is not straightforward. It could be attributed to the photogenerated $C_{60}^{\bullet-}$ encapsulated in the **6** receptor: the free $C_{60}^{\bullet-}$ shows an ESR signal with $g = 1.9984$ and $\Delta H = 30.9$ G at 213K. Both the increase in g value and the decrease in ΔH correspond to a lowering of the symmetry of $C_{60}^{\bullet-}$, as would be the case in $C_{60}^{\bullet-}$ @**6**.¹⁰ Alternatively, it could also be due to $exTTF^{\bullet+}$ since similar compounds show ESR signals with $g = 2.0028 - 2.0034$,¹¹ although it is likely caused by overlapping of signals.

1.V.1.2.3. Electrochemistry of the Complexes

The electrochemical characterization of **6** and its fullerene complexes was carried out by cyclic voltammetry (CV). Considering supporting electrolyte and fullerene solubility, it was established that 15-20 % (v/v) acetonitrile in toluene was the best solvent composition (under these conditions, at low temperature and under vacuum, it has been possible to observe up to the sixth reduction wave of C_{60} and C_{70}).¹² Thus, experiments were carried out using 10^{-5} M solutions of fullerenes, **6** and complexes in chlorobenzene/acetonitrile (5:1 v/v) (scan rates: 25, 50, 100 and 200 mV/s). To perform the experiments, solutions were bubbled with argon to eliminate the oxygen present. To avoid sample concentration, the argon flow was passed through a reservoir flask containing the solvent mixture which was placed before the working cell.

¹⁰ Fukuzumi, S.; Mori, H.; Suenobu, T.; Gao, X.; Kadish, K. M. *J. Phys. Chem. A* **2000**, *104*, 10688-1694.

¹¹ Perepichka, D. M.; Bryce, M. R.; Perepichka, I. F.; Lyubchik, S. B.; Christensen, C. A.; Godbert, N.; Batsanov, A. S.; Levillain, E.; McInnes, E. J. L.; Zhao, J. P. *J. Am. Chem. Soc.* **2002**, *124*, 14227-14238.

¹² a) Xie, Q.; Perez-Cordero, E.; Echegoyen, L. *J. Am. Chem. Soc.* **1992**, *114*, 3978-3980. b) Echegoyen, L.; Echegoyen, L. E. *Acc. Chem. Res.* **1998**, *31*, 593-601.

In this solvent mixture the cyclic voltammogram of a solution of fullerenes (C_{60} and C_{70} , respectively) showed four of their characteristic cathodic waves, corresponding to their first, second, third and fourth reduction processes, respectively¹³ (Figure 12, black lines). In all cases, the third and the fourth waves were electrochemically reversible when the scan rate was increased.

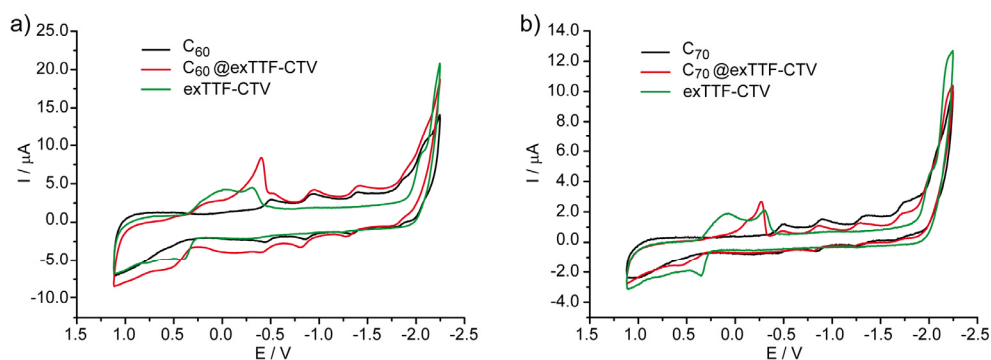


Figure 12: Cyclic voltammetry measurements of solutions 10^{-5} M of free fullerenes and their complexes in chlorobenzene with 0.1 M Bu_4NClO_4 as supporting electrolyte. Working electrode: glassy carbon; Counter electrode: Pt wire; Reference electrode Ag/AgCl; Scan rate: 50 mV/s.

The voltammogram of **6** shows the presence of the characteristic electrochemically irreversible oxidation wave of exTTF at 0.36 V, with a weak shoulder at 0.74 V, most probably due to weak adsorption processes of the sample over the working electrode (Table 1). Upon complexation with either fullerene, a significant shift of the oxidation potential to 0.54 V was observed. With regard to the reduction waves, the first four reduction processes for fullerene complexes were recorded. The changes to the first and second reduction potential upon complexation were about 10-50 mV, while the

¹³ Allemand, P. M.; Koch, A.; Wudl, F.; Rubin, Y.; Diederich, F.; Alvarez, M. M.; Anz, S. J.; Whetten, R. L. *J. Am. Chem. Soc.* **1991**, *113*, 1050-1051.

third reduction process was affected to a greater extent, up to 100 mV in the case of C₇₀@**6**.

Table 1: Redox potentials (V) of fullerenes and their complexes.

	E^1_{red}	E^2_{red}	E^3_{red}	E^4_{red}	E^1_{ox}
6	–	–	–	–	0.36
C ₆₀	-0.50	-0.92	-1.41	-1.87	–
C ₆₀ @ 6	-0.49	-0.91	-1.37	–	0.54
C ₇₀	-0.51	-0.92	-1.37	-1.77	–
C ₇₀ @ 6	-0.48	-0.87	-1.27	-1.74	0.54

Even though the complex formation, the process is still reversible as is indicated by the presence of anodic waves in the cyclic voltammogram independently of the scan rate (Figure 13).

IV.1.3 DFT Calculations

The structure of the complexes was investigated computationally in the gas phase. Geometry optimizations were performed with a Density Functional Theory (DFT) methodology as implemented in the ADF v.2008 code.¹⁴ For structure optimization, BP86 functional and DZP basis set were applied in both cases.¹⁵ Final energies were evaluated by single point calculations at the BP86/TZP and BH&H/TZ2P levels. Despite the intrinsic limitations of pure DFT methods for evaluating non-bonding interaction energies, a related study previously developed by Ortí *et al.*^{3b} showed that

¹⁴ a) Baerends, E. J.; Ellis, D. E.; Ros, P. *Chem. Phys.* **1973**, *2*, 41-51. b) Baerends, E. J.; Ros, P. *Chem. Phys.* **1973**, *2*, 52-59.

¹⁵ See experimental part.

this hybrid method was suitable to qualitatively evaluate the interaction strength of this sort of species in the gas phase.¹⁶

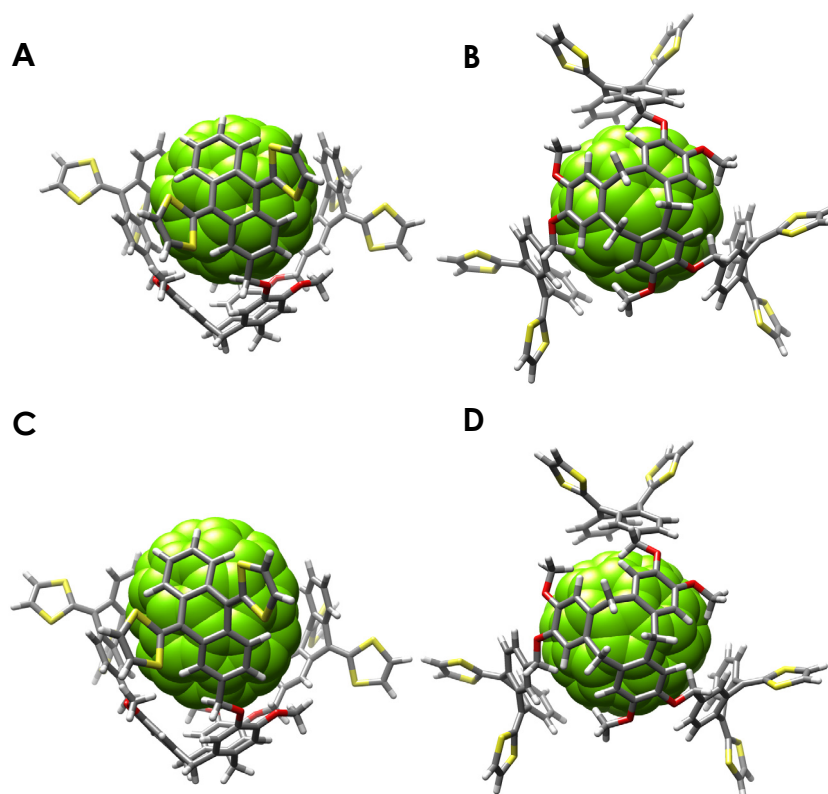


Figure 13: Energy-minimized structures (DFT) of a) $C_{60}@6$ side view, b) $C_{60}@6$ top view, c) $C_{70}@6$ side view, and d) $C_{70}@6$ top view.

The structures show that the fullerenes dwell deep into the cavity of the **6** host, with the CTV serving both as a bowl-shaped recognition element and

¹⁶ For a comprehensive comparative study of the performance of different DFT functionals for the evaluation of supramolecular systems, see: Zhao, Y.; Truhlar, D. G. *J. Chem. Theory Comput.* **2007**, 3, 289-300. The authors demonstrate that BH&H is reliable for systems dominated by dispersion interactions, such the one described in this chapter.

as a preorganizing scaffold for the exTTF subunits, which wrap almost completely around the surface of the fullerenes (Figure 13).

Deformation energies of the host, calculated as the difference between the energy of the host in the complex and the energy of the free **6** structure at both the BP86/TZP and BH&H/TZ2P levels gave convergent results. **6** requires 7 - 9 kcal·mol⁻¹ to adapt to C₆₀, whereas less deformation is needed to form the complex with C₇₀, only 1.5 - 2.5 kcal·mol⁻¹ (Table 2). The average angle between the centroids of two consecutive aromatic rings in the CTV and the linking methylene carbon in the C₆₀@**6** complex is 113.6°, and slightly larger, 114.0°, for C₇₀@**6** but quite similar to the one found for the free **6** (112.2°). The curvature of the exTTF units is also dependent on the guest. The average angle between the planes defined by the two aromatic rings of each exTTF subunit is 49.9° for C₆₀@**6** and 52.0° for C₇₀@**6**, being just 40.0° for the optimized free receptor. In addition, the dihedral angle between the atoms that link CTV and exTTF subunits is very similar for the C₇₀@**6** and the free **6** (153.4° and 154.0°, respectively) but smaller than the one found for the C₆₀@**6** (157.0°). The energy release to build up the complex starting from the two isolated units computed at the BH&H level nicely correlates with the binding constants reported above and with those of related systems.^{3b} For C₇₀@**6**, the interaction energy is -22.1 kcal·mol⁻¹, while for C₆₀@**6** we evaluated -15.0 kcal·mol⁻¹. These values also agree with the calculated tiny amount of charge transferred from host to the fullerene (0.31 for C₇₀, 0.25 for C₆₀) when forming the complex (Table 2).

As it can be seen in Table 2, the energy of the HOMO in the complex resembles the HOMO in the receptor that is located in the exTTF fragments, while the LUMO is located in the fullerene molecule (Figure 14). In addition, in both complexes the HOMO-LUMO gap is not very large, which facilitates the charge transfer from the receptor to the fullerene.

Table 2: Total energies for the host (H), the guest (G) and the complex (HG) at the geometry of the complex, and for the free host (H_f) at the BP86/TZP and at the BH&H/TZ2P levels. Energies of the HOMO, the LUMO, and Mulliken charges (BP86/TZP).

C₆₀@6 Complex						
	BP86/TZP	BH&H/TZ2P	HOMO	LUMO	Mulliken Charges	
	E (kcal mol⁻¹)	E (kcal mol⁻¹)	E (eV)	E (eV)	q H-HG	q G-HG
Host (H)	-24414.58	-36530.48	-4.166	-2.059		
Guest (G)	-11966.41	-17793.22	-6.238	-4.586		
Complex (HG)	-36369.38	-54347.38	-4.191	-3.646	0.25	-0.25
Free Host (H _f)	-24422.26	-36539.11				
Deformation (H)	7.7	8.6				
Binding Energy	+19.3	-15.0				
C₇₀@6 Complex						
	BP86/TZP	BH&H/TZ2P	HOMO	LUMO	Mulliken Charges	
	E (kcal mol⁻¹)	E (kcal mol⁻¹)	E (eV)	E (eV)	q H-HG	q G-HG
Host (H)	-24419.82	-36537.62	-4.104	-2.103		
Guest (G)	-14022.76	-20823.16	-6.252	-4.543		
Complex (HG)	-38426.79	-57384.40	-4.145	-3.567	0.31	-0.31
Free Host (H _f)	-24422.26	-36539.11				
Deformation (H)	2.4	1.5				
Binding Energy	+18.2	-22.1				

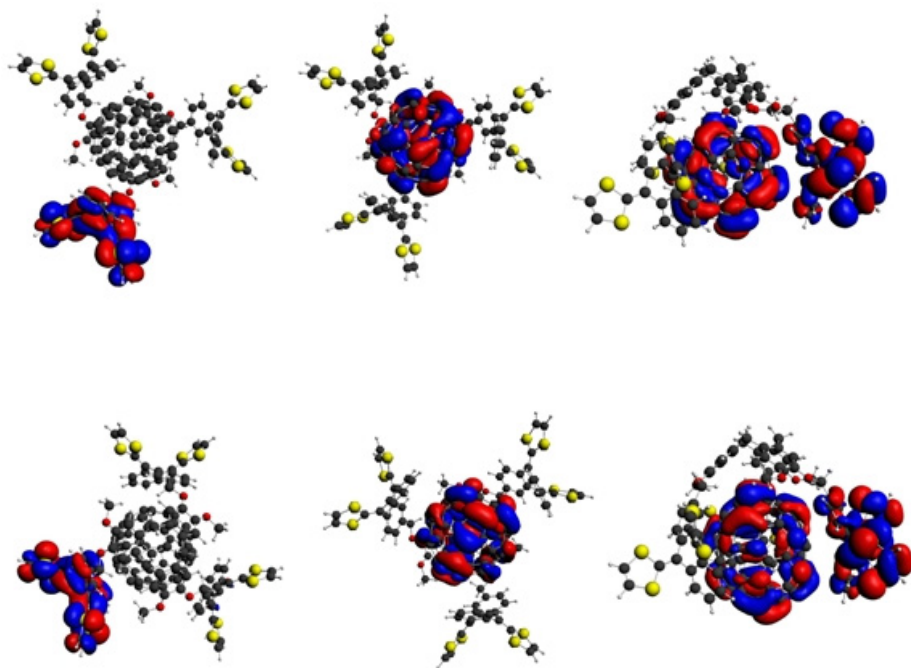


Figure 14: Representation of different views of the HOMO, the LUMO, and both orbitals (electron density contours 0.015 ebohr⁻³) in the complexes. Top: C₆₀@6 complex; bottom: C₇₀@6 complex.

Excitation energies were determined at the BP86/DZP level by means of the time-dependent DFT (TD-DFT) approach, in order to shed light on the electronic absorption spectra. A total number of 300 singlet-singlet excitations were included. The charge transfer band is very accurately reproduced by the calculations, with a calculated $\lambda_{\max} = 498$ nm (observed = 478 nm) for C₆₀ complex and $\lambda_{\max} = 484$ nm (observed = 472 nm) for C₇₀ complex (Figure 15).

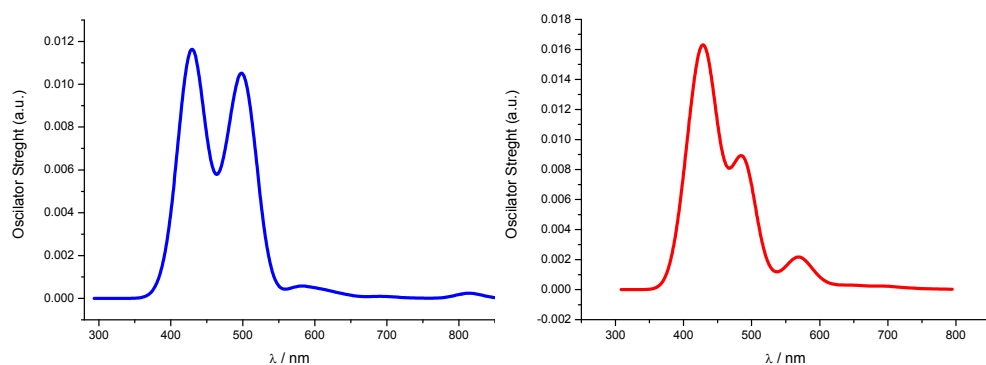


Figure 15: Simulated UV spectrum of C₆₀@6 (left) and C₇₀@6 (right) complexes (representation of molecular orbitals, as well as simulated electronic spectra were performed with ADFview 2007.01).

Calculations showing the electrostatic potential distribution of the fullerenes C₆₀ and C₇₀ and the host, respectively, were performed from the previously minimized structures. The electrostatic potential mapped onto an electronic charge density isosurface of the molecules is shown so that, from most negative values to most positive values, the range of colors is red, orange, yellow, green, light blue, dark blue, where green regions are the most neutral ones.

Figure 16 shows the mapping of the electrostatic potential for C₆₀ (left) and C₇₀ (right) fullerenes. In the representation, the whole surface is mostly positive, especially in the centre of the pentagonal and hexagonal rings.

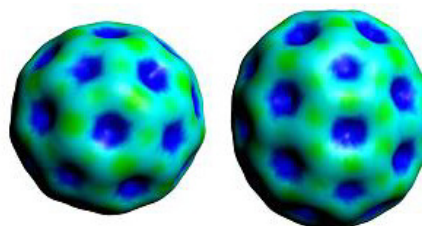


Figure 16: Mapping of the electrostatic potential onto an electron density isosurface of C_{60} and C_{70} (BP86/DZP).

In the case of receptor **6**, as can be seen in Figure 18, the entire molecule is mostly negative (red) and the most negative regions are found in the aromatic surfaces of cyclotrimeratriylene moiety as well as in the anthracene-like part in exTTF moiety (see inner and side views in Figure 17). That means that there is not only a perfect match between the concave shape of the receptor and the convex surface of the fullerene, but also an electronic match, as the more negative electrostatic potential inside the cavity attracts the positive electrostatic potential of the fullerene.

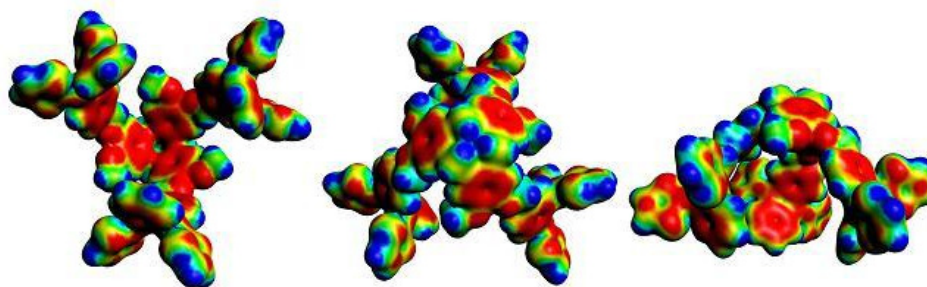


Figure 17: Mapping of the electrostatic potential onto an electron density isosurface of empty receptor (BP86/DZP). From left to right: inner, outer and side views of exTTF-CTV receptor **6**.

In the complexes (Figure 18), the electrostatic potential for fullerenes is no longer as positive as in the case of free fullerenes, which suggests that

either charge transfer or strong polarization occurred upon complexation. Indeed, analysis of the Mulliken atomic charges indicates clearly that the receptor and the fullerene moieties in the complex are slightly positively and negatively charged, respectively (see Table 2, charge analysis), as was pointed out above.

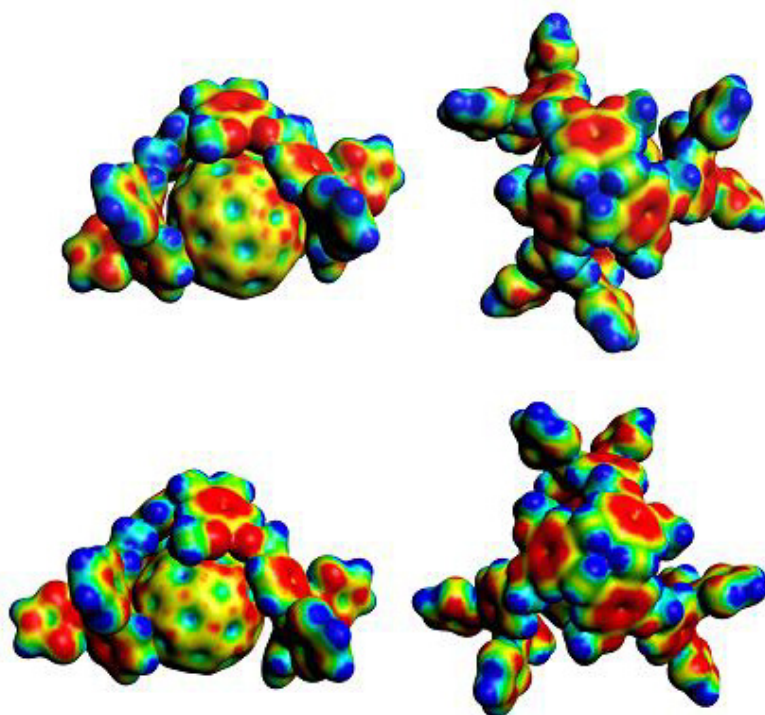


Figure 18: Mapping of the electrostatic potential onto an electron density isosurface of empty receptor (BP86/DZP) of the complexes $C_{70}@6$ (top) and $C_{60}@6$ (down).

IV.1.4 Homochiral Receptor

Given the chiral nature of the bowl-shaped trisubstituted CTV molecule, it was possible to separate and purify both enantiomers of **6**. The chiral HPLC profile obtained showed peaks at retention time 5.27 and 6.14 minutes for the first and the second enantiomer, respectively (Figure 19), preceded by

an impurity at retention time 4.40 min.

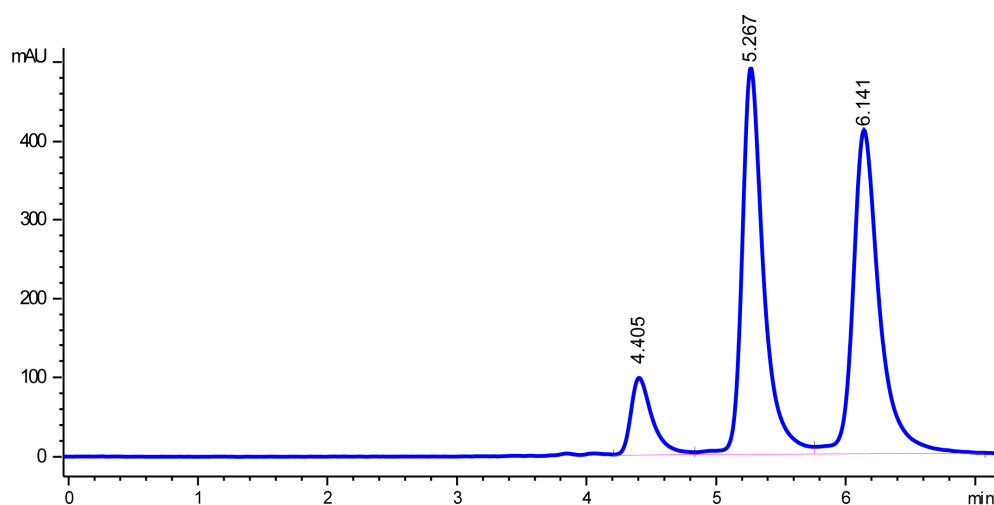


Figure 19: Chiral HPLC profile of **6** (Daicel Chiralpack IB, 250X4.6 mm, hexane/dichloromethane 40:60, flow 1 mL/min, $\lambda = 430$ nm).

The isolated enantiomers were characterized by circular dichroism (CD). As expected, the enantiomers show CD mirror images with a small Cotton effect despite their large UV absorbance (Figure 20). This molecule would be likely useful for the enantioselective recognition of the D_2 -isomers of the higher fullerenes C_{76} and/or C_{84} . These studies are currently under investigation.

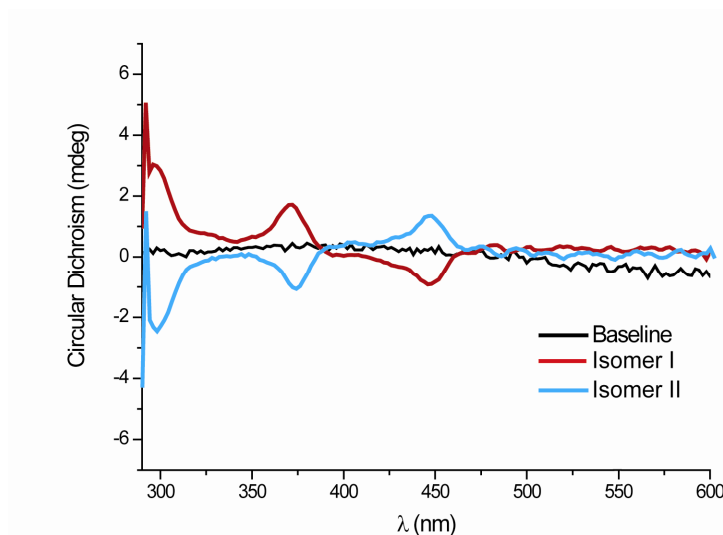


Figure 20: CD measurements of enantiomers of receptor **6** (1.7×10^{-5} M, chlorobenzene, 10 mm cuvette path-length).

IV.2 CONCLUSIONS

The exTTF-CTV based host **6** features the combination of two concave recognition fragments which results in a very effective association of C_{60} and C_{70} fullerenes.

The binding constants obtained for these complexes were comparable to the highest reported in the literature for metalloporphyrin-based receptors, and superior to any other receptor containing only purely organic fragments.

Taking into account the successful application of previous receptors - with binding constants two orders of magnitude smaller - to the construction of nanostructured electroactive materials,¹⁷ and the relatively simple

¹⁷ a) Fernández, G.; Sánchez, L.; Pérez, E. M.; Marín, N. *J. Am. Chem. Soc.* **2008**, *130*, 10674-10683; b) Fernández, G.; Pérez, E. M.; Sánchez, L.; Marín, N. *J. Am. Chem. Soc.*

Chapter IV

synthetic route that gives access to **6**, the utilization of this new host-guest system to similar goals becomes an interesting outcome of this research.

Finally, the easy access to the homochiral receptor opens the way to the enantioselective recognition of fullerenes.

2008, 130, 2410-2411; c) Fernández, G.; Pérez, E. M.; Sánchez, L.; Martín, N. *Angew. Chem. Int. Ed.* **2008**, 47, 1094-1097.

UNIVERSITAT ROVIRA I VIRGILI
SELF-ASSEMBLY BASED ON THE 2-UREIDO-4(1H)-PYRIMIDINONE MOTIF: FROM CYCLIC ARRAYS TO MOLECULAR CAPSULES
FOR FULLERENE SEPARATIONS
Elisa Huerta Martínez
DL:T.289-2012

CHAPTER V:
CARCERANDS FOR FULLERENES:
A MOLECULAR MARACA

UNIVERSITAT ROVIRA I VIRGILI
SELF-ASSEMBLY BASED ON THE 2-UREIDO-4(1H)-PYRIMIDINONE MOTIF: FROM CYCLIC ARRAYS TO MOLECULAR CAPSULES
FOR FULLERENE SEPARATIONS
Elisa Huerta Martínez
DL:T.289-2012

CHAPTER V: CARCERANDS FOR FULLERENES: A MOLECULAR MARACA

V.1 INTRODUCTION

Development of molecular containers and their complexes has opened a new and interesting research area. Molecular containers have inner phases just large enough to accommodate a single or multiple guest molecules. Since Donald J. Cram's first synthesis of a carcerand, which permanently entrapped a single guest molecule¹ (a carceplex, defined as an extreme form of complex stability), several containers such as hemicarcerands,² molecular lanterns,³ self-assembled capsules, and fullerenes⁴ have been synthesized and studied.⁵

¹ a) Cram, D. J. *Nature* **1992**, 356, 29-36. b) Cram, D. J. *Science* **1983**, 219, 1177-1183.

² Warmuth, R.; Yoon, J. *Acc. Chem. Res.* **2001**, 34, 95-105.

³ a) Watanabe, S.; Goto, K.; Kawashima, T.; Okazaki, R. *Tetrahedron Lett.* **1995**, 36, 7677-7680. b) Watanabe, S.; Goto, K.; Kawashima, T.; Okazaki, R. *J. Am. Chem. Soc.* **1997**, 119, 3195-3196.

⁴ a) Bethune, D. S.; Johnson, R. D.; Salem, J. R.; de Vries, M. S.; Yannoni, C. S. *Nature* **1993**, 366, 123-128. b) Edelman, F. T. *Angew. Chem. Int. Ed.* **1995**, 34, 981-985. c) Tellgmann, R.; Krawez, N.; Lin, S.-H.; Hertel, I. V.; Campbell, E. E. B. *Nature* **1996**, 382, 407-413. d) Saunders, M.; Jiménez-Vázquez, H. A.; Shimshi, R.; Khong, A. *Science* **1996**, 271, 1693-1697.

⁵ Warmuth, R. *J. Incl. Phenom. Macrocyclic Chem.* **2000**, 37, 1-38.

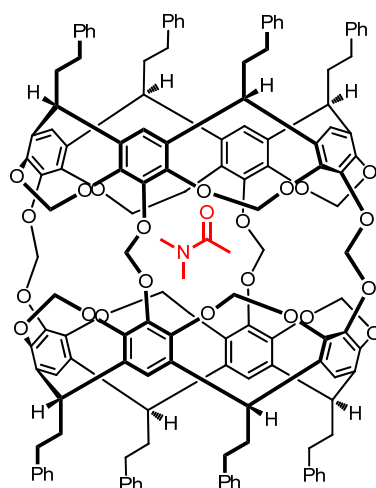


Figure 1: Cram's carcerand in which dimethylacetamide is incarcerated.

A variety of strategies have been successfully employed to create hosts that encapsulate smaller guest molecules. For example, the spherical or ellipsoid shells of fullerenes can be chemically opened in a controlled way, filled with metal ions, atomic nitrogen, or H_2 , and finally closed again by bond-forming reactions (molecular surgery).⁶ Tubular fullerenes⁷ (carbon nanotubes) can be filled with small simple molecules (e.g., KI , H_2 , N_2 , O_2 and H_2O) or with fullerenes (i.e., "nano-peapods").⁸ Containment lifetime can vary from rapid exchange with the surrounding environment - most ordinary complexes - to permanent entrapment where only rupture of covalent bonds can release the guests - carceplexes.⁹ Moreover, the templated

⁶ a) Mauser, H.; Hirsch, A.; van Eikerna-Hommes, N. J. R.; Clark, T.; Pietzak, B.; Weidinger, A.; Dunsch, L. *Angew. Chem. Int. Ed.* **1997**, *36*, 2835-2838. b) Komatsu, K.; Murata, M.; Murata, Y. *Science* **2005**, *307*, 238-240.

⁷ Meyer, R. R.; Sloan, J.; Dunin-Borkowski, R. E.; Kirkland, A. I.; Novotny, M. C.; Bailey, S. R.; Hutchison, J. L.; Green, M. L. H. *Science* **2000**, *289*, 1324-1326.

⁸ Hombaker, D. J.; Kahng, S.-J.; Misra, S.; Smith, B. W.; Johnson, A. T.; Mele, E. J.; Luzzi, D. E.; Yazdani, A. *Science* **2002**, *295*, 828-831.

⁹ Cram, D. J.; Cram, J. M. *Container Compounds and Their Guests*, *the Royal Society of Chemistry*, Cambridge, **1994**.

assembly process responsible for forming a permanent container can be assessed quantitatively because the template is permanently caught in the cage. These nanoscale systems have well-defined 3D structures, which facilitates their characterization.

Molecular containers constructed from two or more subunits held together by metal-ligand interactions,¹⁰ hydrogen bonding,¹¹ or covalent bonds⁹ have been reported. Rebek¹² and others have shown that resorcinarene/pyrogallolarene hexamers can encapsulate several guests or solvent molecules as well as a single large molecule.

Among the few examples of carceplexes so far reported, the largest

¹⁰ a) Kusukawa, T.; Fujita, M. *J. Am. Chem. Soc.* **1999**, *121*, 1397-1398. b) Yoshizawa, M.; Kusukawa, T.; Fujita, M.; Yamaguchi, K. *J. Am. Chem. Soc.* **2000**, *122*, 6311-6312. c) Yu, S.-Y.; Kusukawa, T.; Birada, K.; Fujita, M. *J. Am. Chem. Soc.* **2000**, *122*, 2665-2666. d) Jacopozi, P.; Dalcanale, E. *Angew. Chem. Int. Ed.* **1997**, *36*, 613-615. e) Fochi, F.; Jacopozi, P.; Wegelius, E.; Rissanen, K.; Cozzini, P.; Marastoni, E.; Fiscaro, E.; Manini, P.; Fokkens, R.; Dalcanale, E. *J. Am. Chem. Soc.* **2001**, *123*, 7539-7552. f) Cuminetti, N.; Ebbing, M. H. K.; Prados, P.; de Mendoza, J.; Dalcanale, E. *Tetrahedron Lett.* **2001**, *42*, 527-530. g) Fox, O. D.; Dalley, K.; Harrison, R. G. *J. Am. Chem. Soc.* **1998**, *120*, 7111-7112. h) Fox, O. D.; Leung, J. F.-Y.; Hunter, J. M.; Dalley, K.; Harrison, R. G. *Inorg. Chem.* **2000**, *39*, 783-790. i) Fox, D. O.; Dalley, N. K.; Harrison, R. G. *Inorg. Chem.* **1999**, *38*, 5860-5863. j) Yoshizawa, M.; Kusukawa, T.; Fujita, M.; Yamaguchi, K. *J. Am. Chem. Soc.* **2000**, *122*, 6311-6312.

¹¹ a) Hof, F.; Craig, S.; Nuckolls, C.; Rebek, J., Jr. *Angew. Chem. Int. Ed.* **2002**, *41*, 1488-1508. b) Rebek, J., Jr. *Acc. Chem. Res.* **1999**, *32*, 278-286. c) de Mendoza, J. *Chem. Eur. J.* **1998**, *4*, 1373-1377. d) Conn, M. M.; Rebek, J., Jr. *Chem. Rev.* **1997**, *97*, 1647-1668. e) Rebek, J., Jr. *Chem. Soc. Rev.* **1996**, 255-264.

¹² a) Shivanyuk, A.; Rebek, J., Jr. *Proc. Natl. Acad. Sci. U. S. A.* **2001**, *98*, 7662-7665. b) Shivanyuk, A.; Rebek, J., Jr. *Chem. Commun.* **2001**, 2424-2425. c) Yamanaka, M.; Shivanyuk, A.; Rebek, J., Jr. *J. Am. Chem. Soc.* **2004**, *126*, 2939-2943.

molecules incarcerated were described by Gibb *et al.*,¹³ in capsules made of two cavitand tetrols (deep-cavitands) covalently linked by methylene bridges. The efficiency of the dimerization process was closely related to the efficiency of the encapsulation-templation effect caused by the guest. They reported the incarceration of molecules such as steroids or adamantane dimers, although in low yield.

V.2 DESIGN CONSIDERATIONS AND CALCULATIONS

In this Chapter, we describe the synthesis of a carceplex based on the covalent post-modification of the hydrogen-bonded dimeric capsule described in Chapter III.

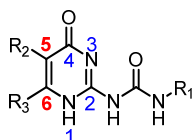


Figure 2: 2-ureido-4[1H]-pyrimidinone.

To this aim, a new CTV-UPy molecule, bearing a terminal double bond at position 5 or 6 of the pyrimidinone ring (Figure 2) was envisaged. The fullerene guest ensures formation of the dimeric capsule acting as a template,¹⁴ while the hydrogen bonding UPy units place the allyl groups in a favorable position¹⁵ for cross-metathesis (CM),¹⁶ leading to a unimolecular,

¹³ Srinivasan, K.; Gibb, B. C. *Chem. Commun.* **2008**, 4640-4642.

¹⁴ a) Sherman, J. C. *Chem. Commun.* **2003**, 1617-1623. b) Makeiff, D. A.; Sherman, J. C. *Chem. Eur. J.* **2003**, *9*, 3253-3262. c) Makeiff, D. A.; Sherman, J. C. *J. Am. Chem. Soc.* **2005**, *127*, 12363-12367.

¹⁵ a) Wang, L.; Vysotsky, M. O.; Bogdan, A.; Bolte, M.; Böhmer, V. *Science* **2004**, *304*, 1312-1314. b) Bogdan, A.; Vysotsky, M. O.; Ikai, T.; Okamoto, Y.; Böhmer, V. *Chem. Eur. J.* **2004**, *10*, 3324-3330.

permanently closed capsule, whose windows can open in polar solvents by disruption of the hydrogen-bonded framework.

The most favorable position of the lateral chain containing the double bond for the metathesis reaction, as well as its length, was evaluated computationally.

Geometry optimizations were done using Density Functional Theory (DFT). As previously shown (Chapter III, section III.3.4), most of the self-assembled capsules are homochiral, with an $A_{\beta}A_{\beta}$ conformation for the two-carbon linking chain. This geometry was taken as the initial one in our model studies. The bonds were constructed and the energies were minimized using the ADF code (Figure 3).¹⁷

¹⁶ a) Tronka, T. M.; Grubbs, R. H. *Acc. Chem. Res.* **2001**, *34*, 18-29. b) Kilbinger, A. F. M.; Cantrill, E. J.; Waltman, A. W.; Day, M. W.; Grubbs, R. H. *Angew. Chem. Int. Ed.* **2003**, *42*, 3281-3285.

¹⁷ Version 2007.01 BP86 (LDA) was used in all the cases as functional with a DZP basis set. See experimental part. a) Te Velde, G.; Bickelhaupt, F. M.; Baerends, E. J.; Fonseca Guerra, C.; Van Gisbergen, S. J. A.; Snijders, J. G.; Ziegler, T. J. *Comput. Chem.* **2001**, *22*, 931-967. b) Fonseca Guerra, C.; Snijders, J. G.; Te Velde, G.; Baerends, E. J. *Theor. Chem. Acc.* **1998**, *99*, 391-403.

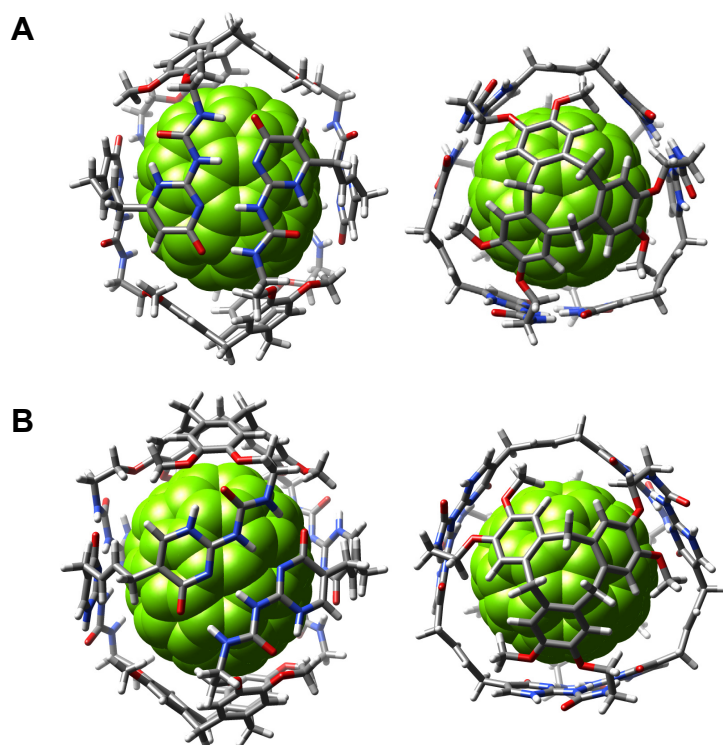


Figure 3: Side (left) and top (right) views of minimized structures (BP86/DZP) of carceplexes after metathesis bearing substitution at the 6-position (A) or 5-position (B) of the pyrimidinone ring.

The optimized structures look quite similar in geometry, depending on the position of the allyl group. The major differences arise from the bridging chain, as the top view representations highlight (Figure 3, right): a variation in the dihedral angle formed between the oxygen of the CTV, the two-carbon chain and the nitrogen of the urea is needed to accommodate the covalently-bonded pyrimidinones in the structure. These differences do not translate, however, in the calculated minimum energies, which are indeed very similar (-51923.8 kcal \cdot mol $^{-1}$ for the 6-substituted model and -51907.1 kcal \cdot mol $^{-1}$ for the 5-substituted one), probably due to the flexibility and adaptability of the entire system.

V.2.1 Synthetic Approach

Since both models seem to be suitable, the corresponding pyrimidinones bearing terminal double bonds were, therefore, synthesized in order to introduce them into the CTV-scaffold (Scheme 1). Thus, pyrimidinone **9g**, whose synthesis was depicted in Chapter II, was reacted with 1,1'-carbonyldiimidazole (CDI), affording blocked isocytosine **52a**.

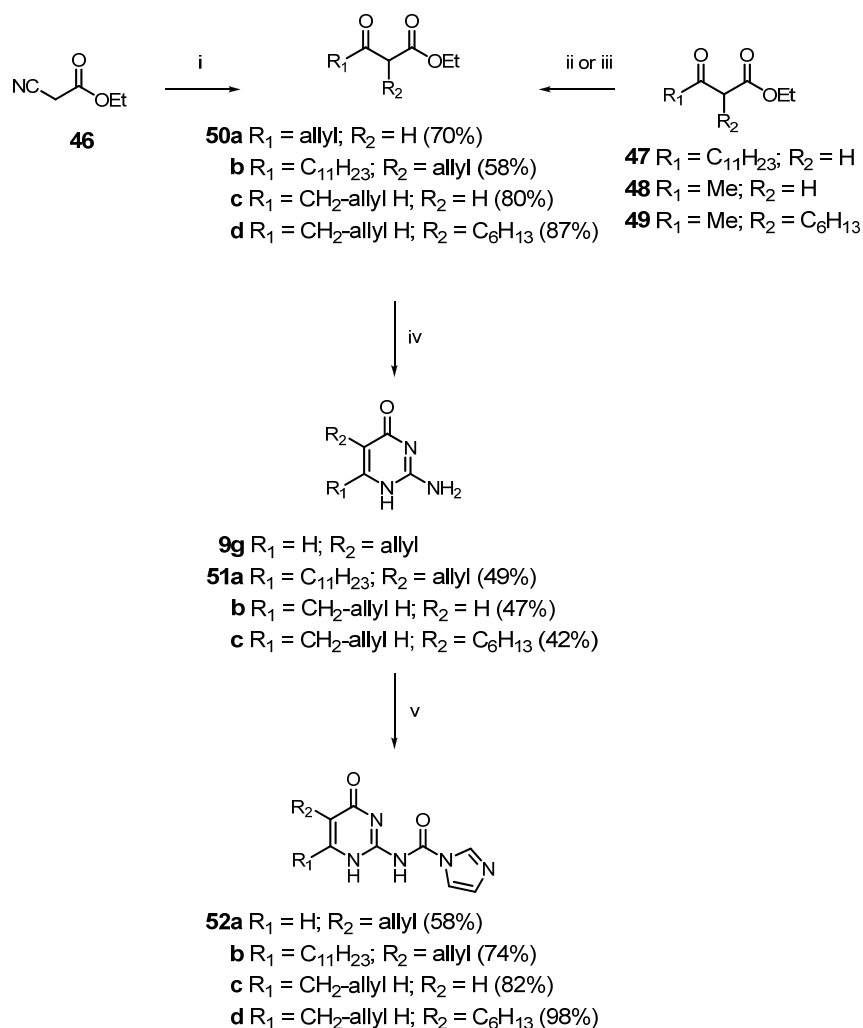
Given that pyrimidinone **9g** was almost insoluble, another derivative bearing an eleven carbon aliphatic chain in position 6 was synthesized (Scheme 1). β -ketoester **47**¹⁸ was alkylated in α position to introduce the allyl function,¹⁹ and compound **50b** was obtained in good yield. It was then treated with guanidinium carbonate to get pyrimidinone **51a**, which was activated as imidazolide (**52b**) with CDI in good yields.

The synthesis of the corresponding pyrimidinones with the allyl function in position 6 was also carried out. The first attempt started from the corresponding β -ketoester: ethyl cyanoacetate (**46**), was treated with a mixture of zinc and allyl bromide in the presence of $AlCl_3$ under Barbier-type reaction conditions,²⁰ affording allyl β -ketoester **50a** in a good yield after purification (Scheme 1). Unfortunately, the condensation reaction with guanidinium carbonate to get the corresponding pyrimidinone failed due to the fast isomerization of the double bond upon heating under basic media.

¹⁸ Keizer, H. M.; González, J. J.; Segura, M.; Prados, P.; Sijbesma, R. P.; Meijer, E. W.; de Mendoza, J. *Chem. Eur. J.* **2005**, *11*, 4602-4608.

¹⁹ a) Kenji, M.; Masaya, I. *Tetrahedron* **1987**, *43*, 45-58. b) Piva, O. *Tetrahedron* **1994**, *50*, 13687-13696.

²⁰ Lee, A. S.-Y.; Lin, L.-S. *Tetrahedron Lett.* **2000**, *41*, 8803-8806.



i) 1. Zn (dust), AlCl_3 , allyl bromide, 2. HCl 3M; ii) allyl bromide, NaOEt, THF, r.t., overnight; iii) 1. LDA/THF, 0 °C; 2. allyl bromide, overnight; iv) guanidinium carbonate, EtOH, reflux, overnight; v) CDI, DCM, r.t., overnight.

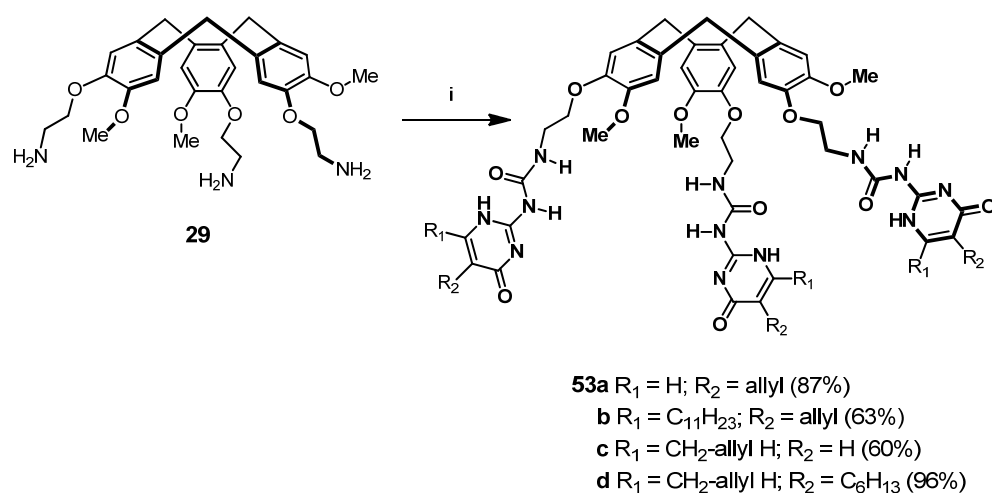
Scheme 1: Synthesis of blocked isocytosine precursors.

To avoid such isomerization, an extra carbon was introduced between the allyl group and the heterocycle. Ethyl acetoacetate (**48**) was alkylated in γ position under strong basic medium with allyl bromide. β -ketoester **50c** was obtained in good yield after flash chromatography and its treatment

with half equivalent of guanidinium carbonate gave pyrimidinone **51b**, which was subsequently reacted with CDI to yield the corresponding imidazolide **52c** (Scheme 1).

Analogously, a more soluble version of **51b** was prepared. Commercially available ethyl 2-acetyloctanoate (**49**) was reacted with allyl bromide in the presence of two equivalents of LDA to yield compound **50d**. This compound was subsequently reacted with guanidinium carbonate and pyrimidinone **51c** was formed. The corresponding imidazolide **52d** was obtained in excellent yield after reaction of **51c** in standard conditions (Scheme 1).

The reaction of three equivalents of imidazolides **52a-d** with triamino-functionalized CTV **29** at 60 °C in a 5:1 DCM/DMF mixture or in THF afforded the CTV-UPy receptors **53a-d** in yields from moderate to excellent (Scheme 2).

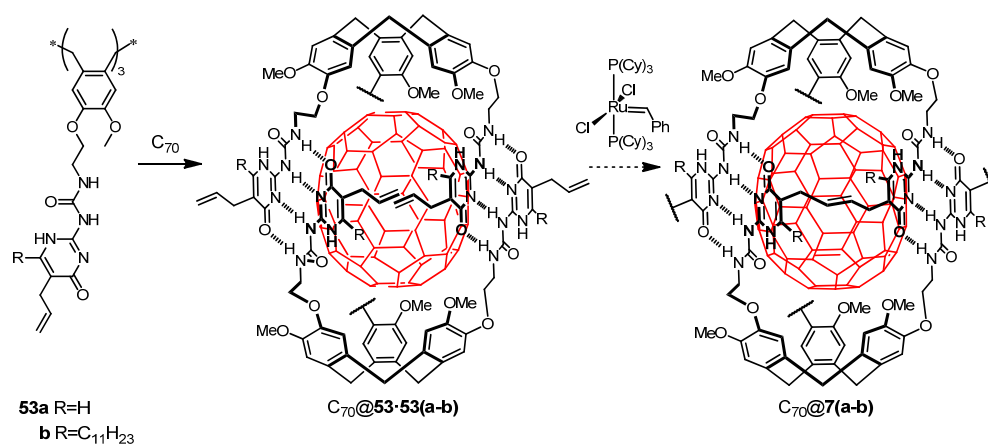


i) 5:1 DCM/DMF mixture (**52a**) or THF (**52b-d**), 50-60 °C, 2 days

Scheme 2: Synthesis of "maraca" precursors.

Thus, first generation Grubbs' catalyst was added to a mixture of CTV-host **53a** and fullerene C₇₀ in dichloromethane in a 2:1 ratio, under high dilution conditions (Scheme 3). After 4 days, the catalyst was removed and the crude mixture was subjected to mass spectrometry analysis. However,

the mass of the final compound was neither detected by MALDI-TOF nor ESI techniques, maybe due to the fact that compound **53a** was quite insoluble in solvents such as dichloromethane or chloroform, even in the presence of C_{70} which should facilitate the solubilization due to complex formation.



Scheme 3: Synthetic attempts to C_{70} carceplexes **7a-b**.

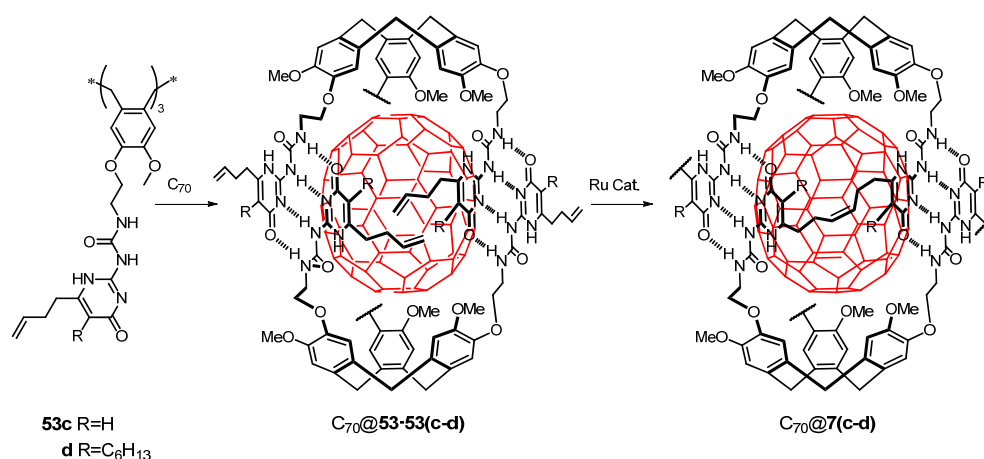
Alkene metathesis was then carried out with the soluble version receptor **53b** (Scheme 3) using once again C_{70} as template. Unlike **53a**, high dilution conditions were not required since the solubility of **53b** favored complex formation as was easily detected since the fast solubilization of C_{70} in the selected solvent. Unfortunately, although different conditions were tested (Table 1) the desired carceplex was not detected in any of the cases studied.

Table 1: Conditions tested in crossed metathesis of compound **53b** (15 mol% loading of catalyst was used in all cases).

Entry	Solvent (Conc.)	Temp. (°C)	Time
1	DCM (5.5x10 ⁻² mM)	r.t.	4 days
2	DCM (0.8 mM)	80*	3h
3	THF (0.8 mM)	80*	3h

* Microwave irradiation.

Although DFT calculations predicted structures with similar energies for both the 5-allyl or 6-allyl positions, the 5-allyl-substituted compound might be less favored to undergo a metathesis reaction, since the linker must rotate to bring the allyl groups at a productive distance. This does not occur when the allyl group is located at position 6 (see models in Figure 3).



Scheme 4: Syntheses of carceplexes **C₇₀@7c-d**.

Thus, compound **53c** was reacted with first generation Grubbs' catalyst (15 mol%) in dichloromethane in the presence of **C₇₀**, but no product was detected in the mass spectrometry analysis of the crude. However, the use

of a second generation Grubbs²¹ catalyst allowed the cross-metathesis to proceed, yielding the unimolecular, permanently closed capsule **7c**, as was indicated by MALDI-TOF mass spectrometry (Figure 4). However, besides the carceplex, different by-products were detected in the mass spectrum, such as unreacted starting material, alternative cross-metathesis adducts and free fullerenes.

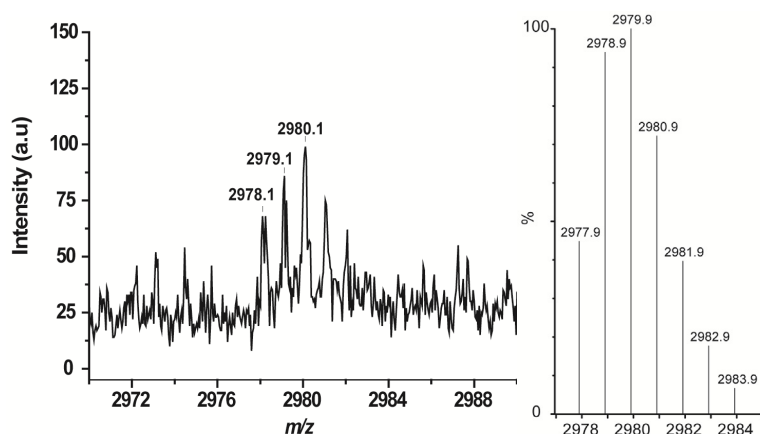


Figure 4: MALDI-TOF profile of the peak corresponding to compound $C_{70}@7c$ (left) and calculated isotopic distribution (right) for $C_{178}H_{120}N_{24}O_{24}$ (dithranol, dichloromethane).

Due to the poor solubility, the yield was low and **7c** could not be isolated from the crude mixture. Therefore, the reaction was carried out with compound **53d**, a more soluble version of the carcerand precursor.

The reaction was monitored by 1H NMR spectroscopy to find optimal conditions, using not only dichloromethane but also chloroform as solvents. In addition, the highly active Hoveyda-Grubbs catalyst was also

²¹ Scherman, O. A.; Ligthart, G. B. W. L.; Ohkawa, H.; Sijbesma, R. P.; Meijer, E. W. *Proc. Natl. Acad. Sci. U. S. A.* **2006**, *103*, 11850-11855.

employed.²²

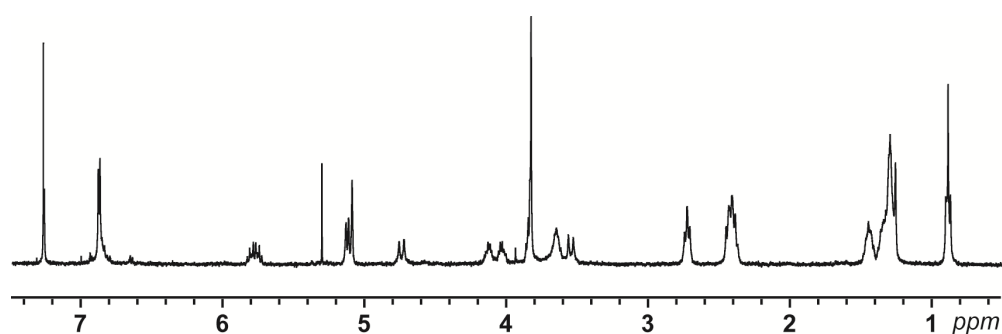


Figure 5: ¹H NMR spectrum of **53d** (CDCl₃ +TFA, 400 MHz).

Figure 5 displays the ¹H NMR pattern of receptor **53d**. A drop of TFA is needed to avoid broadening of the signals due to aggregation. The signals of the terminal double bond were present at 5.1 and 5.7 ppm. In CD₂Cl₂ or CDCl₃, in the presence of C₇₀, the resulting deep red solution showed the characteristic pattern of the quadruple hydrogen bond array (Figure 6) at downfield shift. In this case, signals appeared broadened, maybe as a consequence of the presence of a six-carbon chain in position 5 of the pyrimidinone.

²² Dimartino, G.; Wang, D.; Chapman, R. N.; Arora, P. S. *Org. Lett.* **2005**, *7*, 2389-2392.

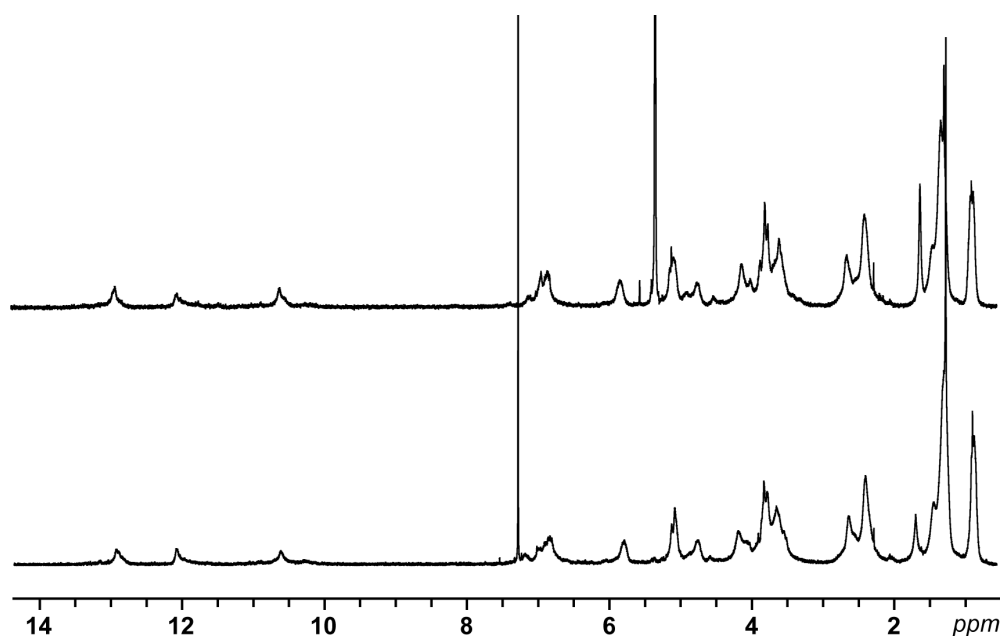


Figure 6: ^1H NMR spectra (400 MHz) of C_{70} complexes of **53d** in CD_2Cl_2 (top) and CDCl_3 (bottom).

Thus, reactions were carried out inside NMR tubes at room temperature and Table 2 summarizes the conditions tested.

Table 2: Cross-metathesis conditions.

Entry	Solvent	Conc. (mM)	Catalyst (loading)
1	CD_2Cl_2	2.5	Hoveyda-Grubbs (15 mol%)
2	CD_2Cl_2	2.5	2 nd Gen. Grubbs (15 mol%)
3	CDCl_3	2.5	Hoveyda-Grubbs (15 mol%)
4	CDCl_3	2.5	2 nd Gen. Grubbs (15 mol%)

The ^1H NMR spectra show how the signals corresponding to the terminal allyl groups disappear along the time (Figure 7). Hoveyda-Grubbs' catalyst works nicely, both in dichloromethane or chloroform, whereas second generation Grubbs' catalyst showed almost no reaction in dichloromethane but worked very well in chloroform.

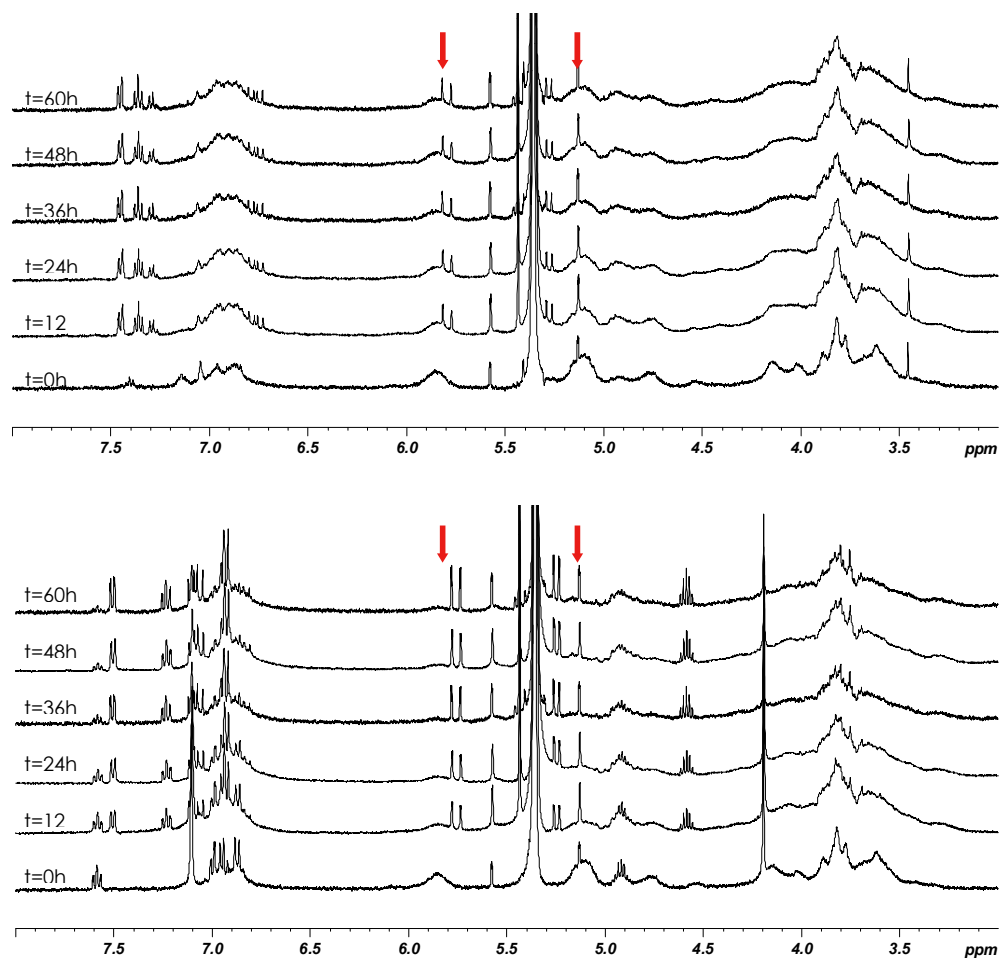


Figure 7: ^1H NMR (400MHz) monitoring experiment of cross-metathesis reaction of **53d** in the presence of C_{70} in CD_2Cl_2 using 2nd generation Grubbs (top) and Hoveyda-Grubbs (bottom) catalysts.

After reaction, the catalyst was removed and the crude was easily purified by flash chromatography in silica gel using a mixture of dichloromethane and 2% methanol, yielding about 50-70% of a deep red solid material. This material was subjected to mass spectrometry analysis by MALDI-TOF technique (Figure 8), showing two main peaks, one at $m/z = 3483.8$ which corresponds to the $[\text{M}]^+$ of carceplex **7d**, and another at $m/z = 2643.3$ corresponding to the empty carcerand $[\text{M}-\text{C}_{70}]^+$. A peak at $m/z = 840.1$ was also observed, which corresponds to free C_{70} fullerene.

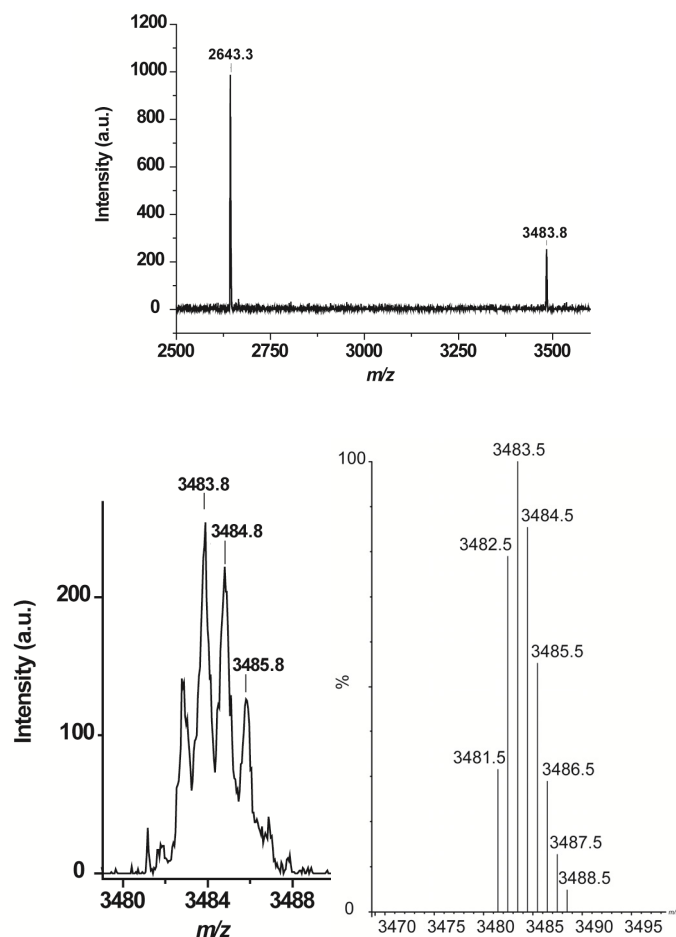


Figure 8: MALDI-TOF spectra of C_{70} carceplex **7d** (dichloromethane, dithranol, positive mode). Top: main peaks at $m/z=2643.3$ and 3483.8 . Bottom: detail of experimental (left) and calculated for $C_{214}H_{192}N_{24}O_{24}$ (right) $[M]^+$ peaks of carcerand **7d**.

Nevertheless, in the ESI-MS experiment (Figure 9), only the peaks corresponding to $[M+H]^+$, $[M+Na]^+$, $[M+H]^{2+}$ and/or $[M+Na]^{2+}$ were detected but neither the empty carcerand nor the free fullerene, even under negative mode. Thus, it can be concluded that the observed $[M-C_{70}]^+$ in the MALDI-TOF experiment is due to fragmentation in the spectrometer and that

the guest remains incarcerated even in the gas phase.²³ The absence of empty carcerand along the reaction could be explained by the high entropic and desolvation cost of generating a considerable empty space.

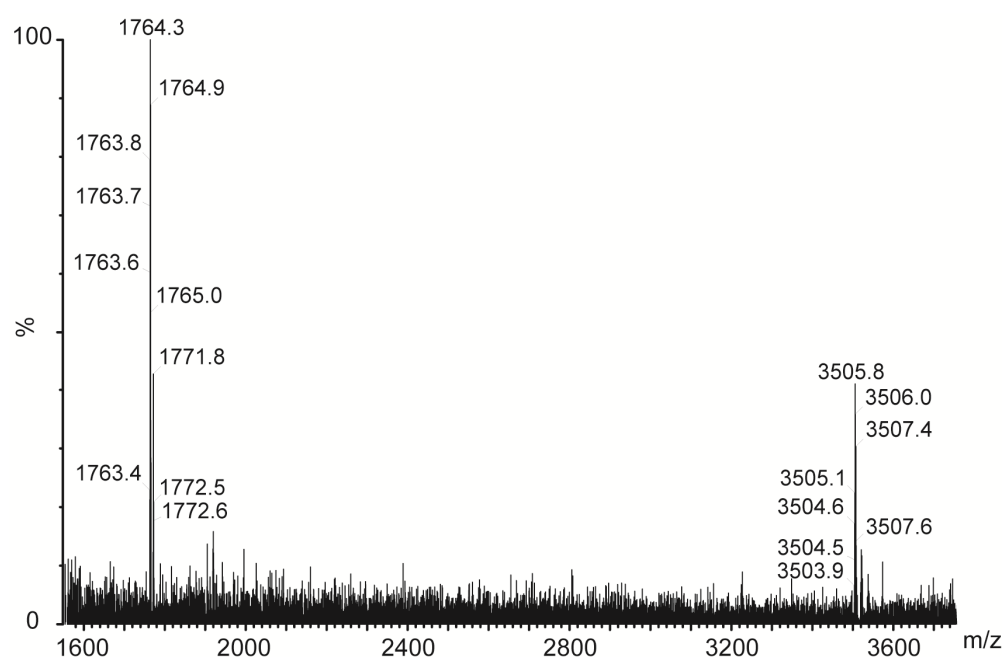


Figure 9: ESI⁺ mass spectrum of carceplex C₇₀@**7d** showing [M+Na]²⁺ (m/z: 1764.3) and [M+Na]⁺ (m/z: 3505.8) peaks.

On the other hand, the possible formation of the carcerand in the absence of guest was investigated. The reaction was carried out in chloroform using both catalysts mentioned and ¹H NMR monitoring experiments. After catalyst removal, the crude was subjected to mass spectrometry analysis. As expected, no empty carcerand was found, and the mass spectra were dominated mainly by unreacted material, as well as by non-productive by-products, such as two adjacent UPy moieties on the

²³ Nuwaysir, L. M.; Castoro, J. A.; Yang, C. L.-C.; Wilkins, C. L. *J. Am. Chem. Soc.* **1992**, *114*, 5748-5751.

same CTV covalently linked (ring-closing metathesis product) or dimers arising from the cross-metathesis of two UPy of different CTV units.²⁴

In the same way, the cross-metathesis was carried out with **53d** in the presence of a better guest such as C₈₄, yielding, after purification, 45% of a dark greenish material C₈₄@**7d**, using chloroform as solvent and either of the catalysts. The product was detected by MALDI-TOF mass spectrometry, both in positive and negative modes (Figure 10). Likewise as for the C₇₀ carceplex, the mass spectrum showed signals corresponding to the empty carcerand that do not appear in the ESI spectrum, which is dominated by the peaks corresponding to [M+Na]⁺ and [M+Na]²⁺.²⁴

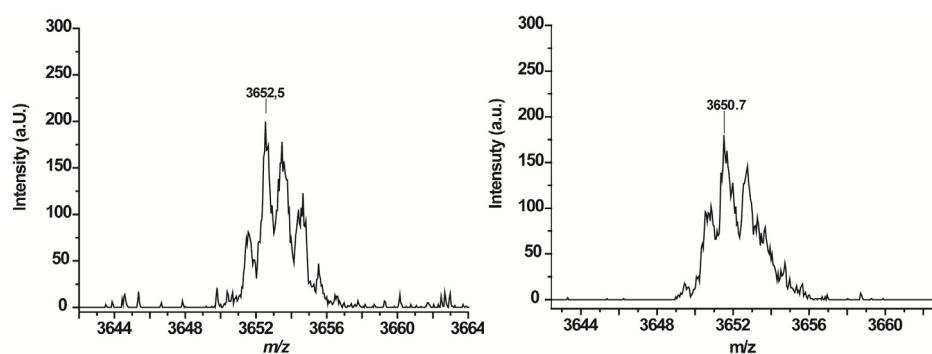


Figure 10: MALDI-TOF spectra of carceplex C₈₄@**7d** in dichloromethane and dithranol. Positive (M⁺, left) and negative (M-H, right) modes.

DFT calculations were performed for both C₇₀ and C₈₄ carceplexes to shed light on their structures (Figure 11). The UPy bridging chains remain perpendicular to the CTV plane and no torsions are needed to achieve the alkene metathesis. Remarkably, the angle between two hydrogen-bonded UPy units is very close to planarity in both cases, like for isolated UPy dimers.

²⁴ See appendix, Section VII.4

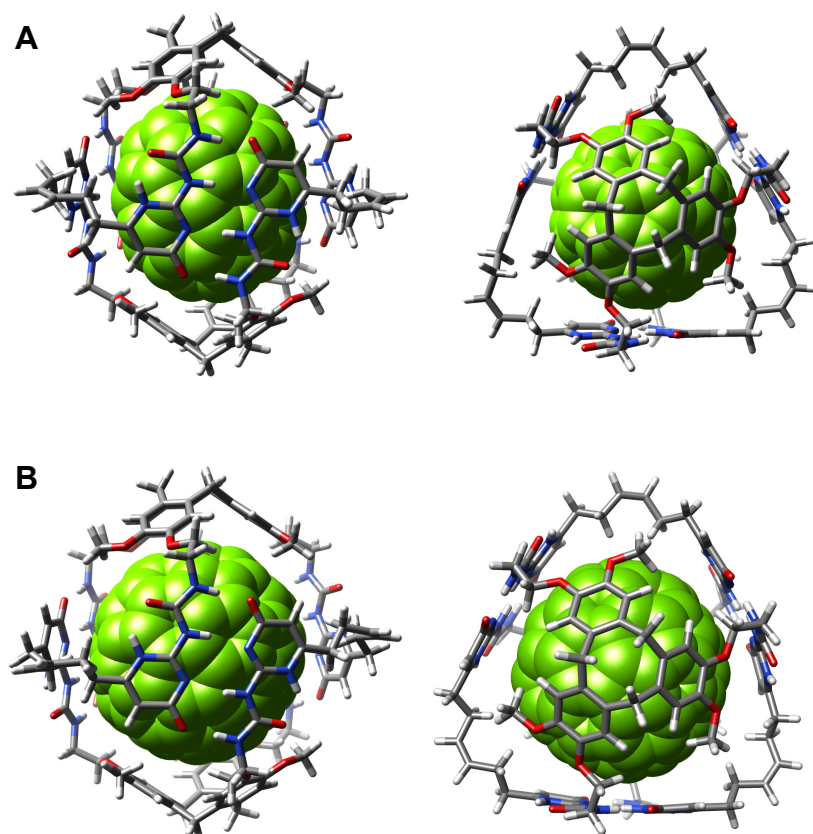


Figure 11: Side (left) and top (right) views of optimized models of carceplexes C₇₀@**7d** (A) and C₈₄@**7d** (B).

Finally, the reaction was carried out using fullerite and a 5% (w/w) of **53d**, 15 mol% Hoveyda-Grubbs catalyst in dry dichloromethane. After purification, C₈₄@**7d** carceplex was detected by MALDI-TOF mass spectrometry as expected, but only double-charged species of C₉₀@**7d** carceplex ($[M]^{2+}$ and $[M+Na]^{2+}$) were detected by ESI⁺ (Figure 12).

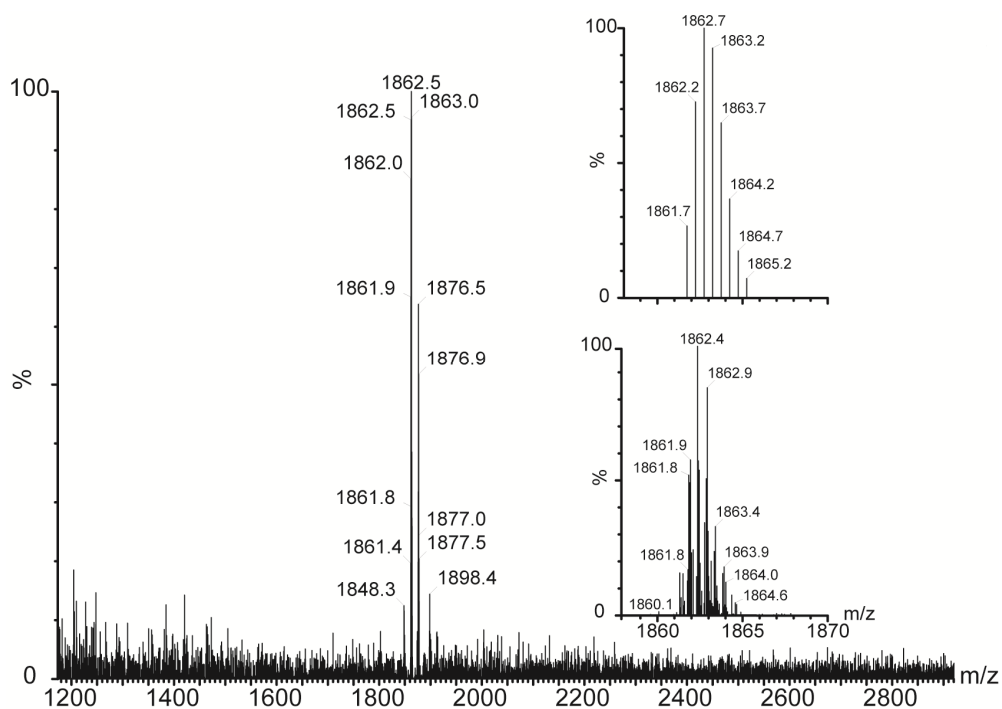


Figure 12: ESI⁺ profile of cross-metathesis in the presence of fullerite. Inner plots: zoom of experimental (bottom) and calculated (top) isotopic distribution for double charged C₉₀@**7d** (C₂₃₄H₁₉₂N₂₄O₂₄).

Since the reaction was not as clean as for pure fullerenes, optimization of the experimental conditions should be explored in the future to set-up a procedure for the preparation of carceplexes of higher fullerenes directly from fullerene mixtures.

V.2.2 Stability Studies and Properties of Incarcerated Fullerenes

The ^1H NMR spectra of carceplex **7d** showed complex signals for both C_{70} and C_{84} cases. These could arise from different factors, such as the stability of the hydrogen bonding network, the presence of chiral and meso forms, or of *cis/trans* isomers around each of the three double bonds (Figure 13).

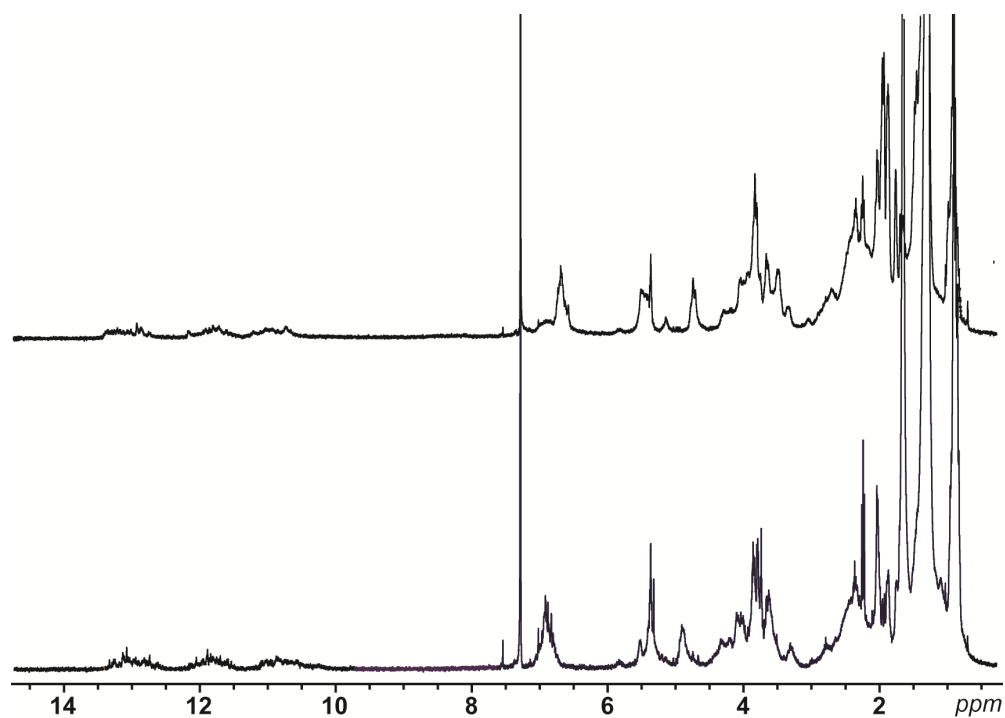


Figure 13: ^1H NMR (CDCl_3 , 400 MHz) spectra of $\text{C}_{84}@7\mathbf{d}$ (top) and $\text{C}_{70}@7\mathbf{d}$ (bottom) carceplexes.

Other signals were sharp, such as the NH's, the aromatic protons or those for the double bonds around 5.7 ppm. However, ^1H - ^1H COSY spectrum showed only one signal for the double bond, coupled with the neighboring methylene (Figure 14).

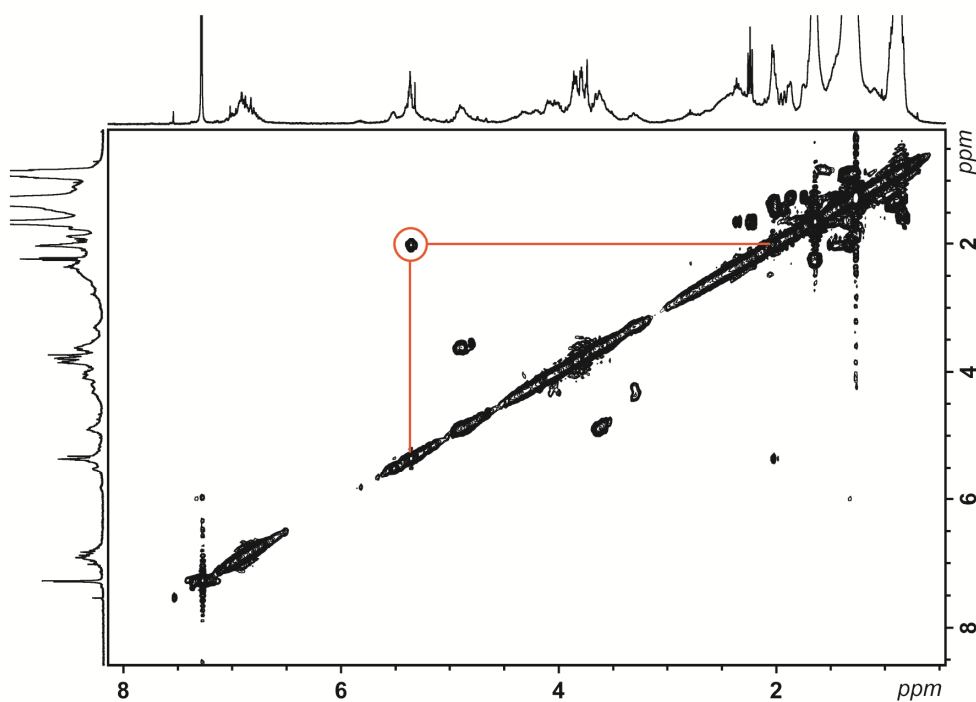


Figure 14: ^1H - ^1H COSY (CDCl_3 , 400 MHz) spectrum of $\text{C}_{70}@7\text{d}$.

Addition of a drop of TFA caused the hydrogen bonds to disrupt, simplifying the ^1H NMR spectra significantly (Figure 15). Thus, typical signals as the CTV methylene bridges became clearly differentiated. Based on the previously observed ratios of homochiral vs. *meso* capsules in the self-assembly of racemic precursors, a similar behavior could be anticipated for the carceplexes. The observed splitting of the methoxy signal accounts for this hypothesis. Moreover, addition of TFA did not cause the fullerene to precipitate, and the solution remained deeply red, unlike in the case of the self-assembled capsules already described.

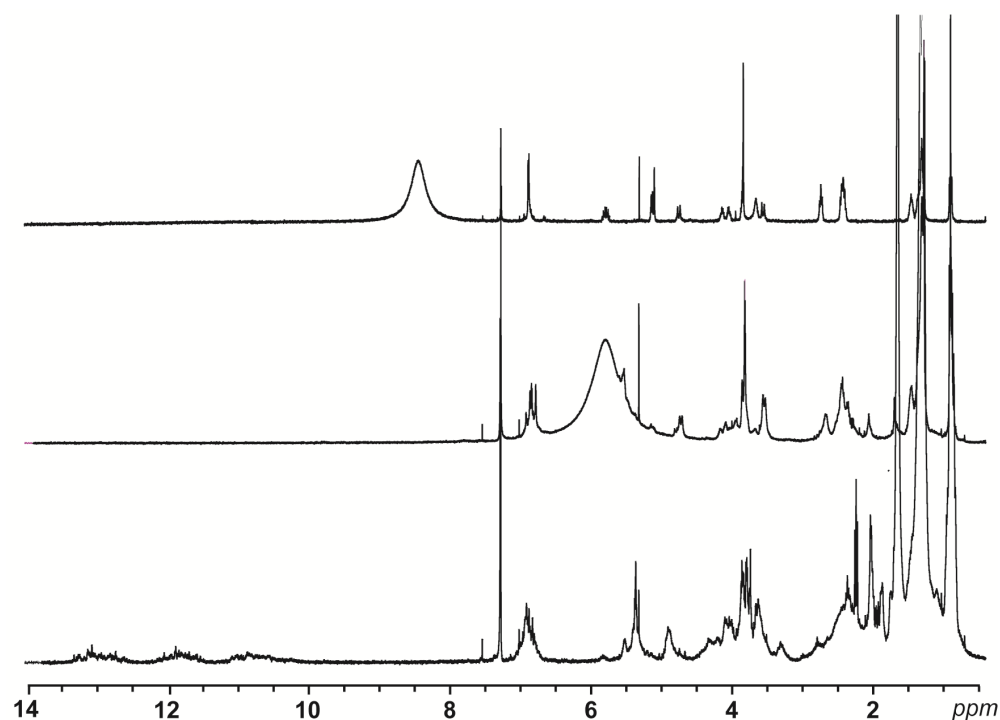


Figure 15: ¹H NMR (CDCl₃, 400 MHz) spectra of **53d** with TFA (top), $C_{70}@7d$ with TFA (middle), and $C_{70}@7d$ (bottom).

In addition, variable temperature experiments were carried out with $C_{70}@7d$ in tetrachloroethane. When the sample was heated up to 388 K, broadening occurred but none of the signals were shifted. On the contrary, when complex $C_{70}@53d$ **53d** was heated up to the same temperature, significant shifts were observed, especially at the NH region.²⁴

In addition, diffusion ordered spectroscopy (DOSY) experiments were performed in chloroform. Figure 16 shows that diffusion coefficients for the C_{84} carceplex (red spectrum) were somewhat smaller than those for $C_{70}@7d$ (black spectrum) as expected from the large size of the fullerene. Indeed, when TFA was added to the C_{70} carceplex solution (green spectrum), no significant changes in the diffusion rate were observed, which accounts once again for the permanent entrapment of the guest inside the carcerand.

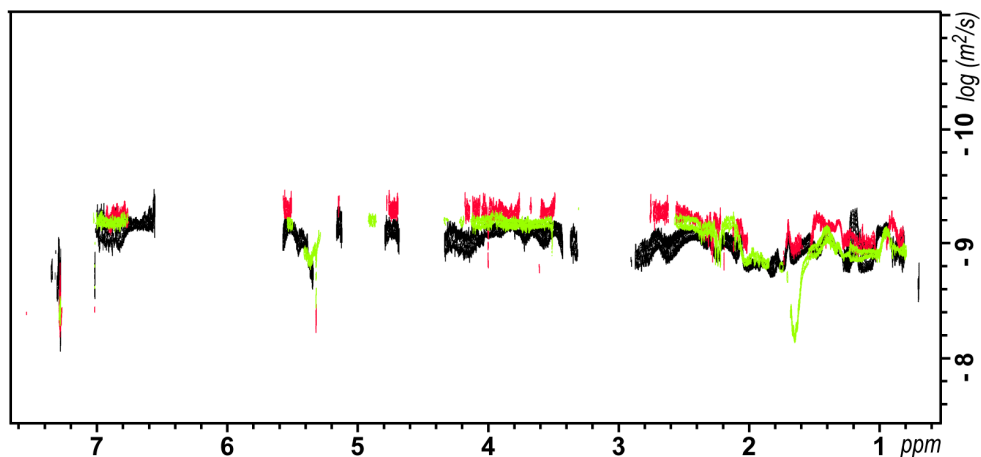


Figure 16: DOSY ($CDCl_3$, 400 MHz) experiments of $C_{70}@7d$ (black spectrum), $C_{84}@7d$ (red spectrum) and $C_{70}@7d$ with TFA (green spectrum).

Finally, $C_{70}@7d$ was checked by gel permeation chromatography (GPC). A Styragel HR-1 GPC column was used with THF as mobile phase and chromatograms were collected at 500 nm (Figure 17). Pure C_{70} was injected as reference, giving rise to a peak at retention time 18.5 min. When the carceplex was injected, a peak at retention time 7.5 min with a strong absorption in the visible region was observed. Moreover, when the sample was treated with variable amounts of TFA (0.2% and 0.5%), the peak was still observed at the same retention time, indicating that the fullerene was not released from the capsule despite the breaking of the hydrogen-bonded network.

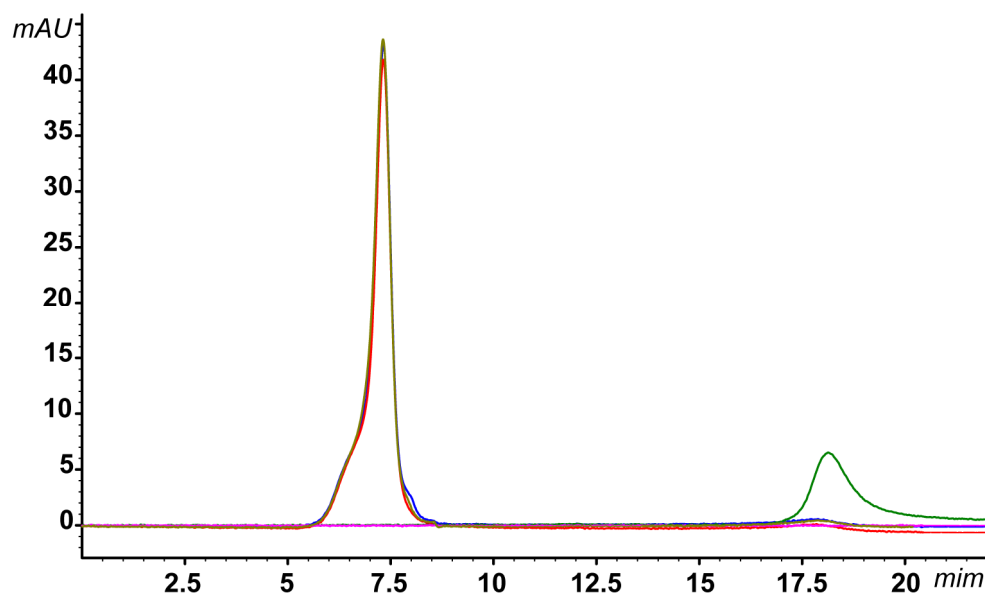


Figure 17: GPC profile (Styragel HR1, mobile phase: THF 1 mL/min, detection wavelength: 470 nm) of C₇₀@7d (blue line), C₇₀@7d with 0.2% v/v of TFA (red line), C₇₀@7d with 0.5% v/v of TFA (light green line) and C₇₀ standard (dark green line). THF/TFA blank injection (pink line).

The electrochemical properties of both carceplexes were studied through a series of cyclic voltammetry (CV) and differential pulse voltammetry (DPV) experiments, and compared with those obtained for pristine fullerenes.²⁵ A mixture of toluene and acetonitrile (5:1)²⁶ containing 0.1 M of Bu₄NPF₆ as supporting electrolyte was used as solvent for all samples. The working electrode was glassy carbon, the counter electrode was platinum and Ag/AgCl electrode was used as reference. All samples

²⁵ a) Echegoyen, L; Echegoyen, L. E. *Acc. Chem. Res.* **1998**, *31*, 593-601. b) Boulas, P. L.; Jones, M. T.; Ruoff, M. S.; Lorents, D. C.; Malhorta, R.; Tse, D. S.; Kadish, K. M. *J. Phys. Chem.* **1996**, *100*, 7573-7579. c) Boulas, P. M.; Jones, M. T.; Kadish, K. M.; Ruoff, M. S.; Lorents, D. C.; Tse, D. S. *J. Am. Chem. Soc.* **1994**, *116*, 9393-9394.

²⁶ a) Xie, Q.; Pérez-Cordero, E.; Echegoyen, L. *J. Am. Chem. Soc.* **1992**, *114*, 3978-3980. b) Allemand, P. M.; Koch, A.; Wuld, F.; Rubin, Y.; Diederich, F.; Álvarez, M. M.; Anz, S. J.; Whetten, R. L. *J. Am. Chem. Soc.* **1991**, *113*, 1050-1051.

were deoxygenated with an argon flow prior to measurement. In all cases, the concentration of the samples was 0.1 mM, except for pure C₈₄ for which, due to its poor solubility in the solvent of choice, a saturated solution of unknown concentration was used instead.

Cyclic voltammograms obtained for C₇₀ showed three well defined reduction waves and a less defined fourth peak between 0.0 and -2.0 V at different scan rates (50-100 mV/s), the process being electrochemically reversible (Figure 18, left). Meanwhile, not well-defined but still visible waves were obtained in the case of C₈₄ (Figure 18, right), due to the low sample concentration. CV of both carceplexes showed almost no response. For comparison, the CV of a 0.1 mM solution of a hydrogen-bonded complex formed by mixing two equivalents of the carcerand precursor **53d** and one equivalent of C₇₀ was also measured. The complex showed a very different behavior than the one observed for the carceplex.

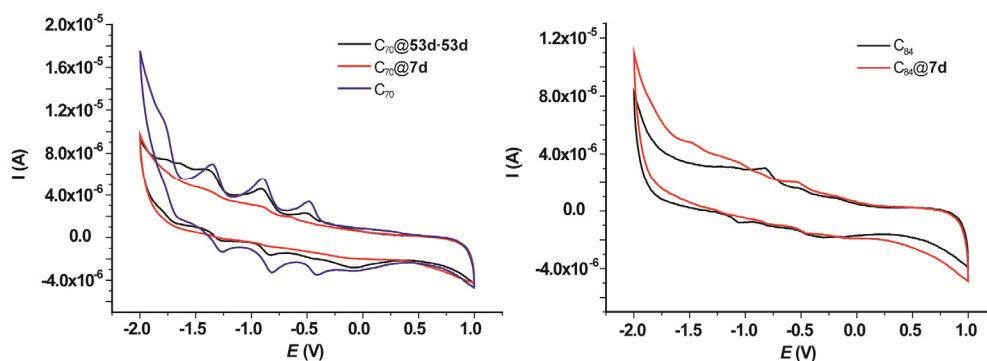


Figure 18: Cyclic voltammograms (CV) of left: pure C₇₀ (blue), C₇₀@**53d-53d** (black), C₇₀@**7d** (red) and right: pure C₈₄ (black) and C₈₄@**7d** (red). WE: glassy carbon; CE: Pt wire; RE: Ag/Ag⁺; Scan Rate: 100 mV/s.

The voltammograms obtained for C₇₀@**53d-53d** showed well defined waves corresponding to fullerene reductions. Compared with the free fullerene, the intensity of the waves is somehow reduced, probably because

encapsulation causes a decrease in the diffusion rate to the electrode.²⁷ Moreover, the electronic effect of the capsule over the fullerene is very small since there was almost no shifting of the waves upon encapsulation.²⁸

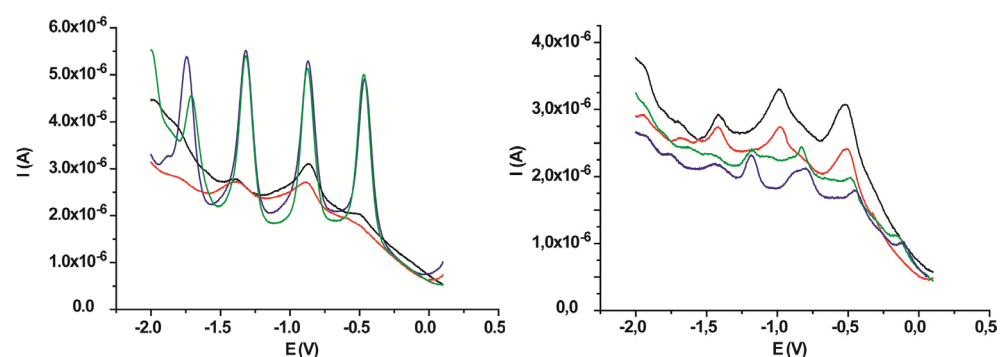


Figure 19: Differential pulse voltammograms (DPV) of left: pristine C_{70} (blue), pristine C_{70} + 1% MeOH (green), $C_{70}@7d$ (red), $C_{70}@7d$ + 1% MeOH (black) and right: pristine C_{84} (blue), pristine C_{84} + 1% MeOH (green), $C_{84}@7d$ (red), $C_{84}@7d$ + 1% MeOH (black). WE: glassy carbon; CE: Pt; RE: Ag/Ag⁺; Scan Rate: 50 mV/s, 25 mV pulse during 10 ms and 40 ms period.

DPV experiments were carried out as an alternative due to the higher sensitivity of this technique. Figure 19 shows the voltammograms obtained for C_{70} (left) and C_{84} (right) and their corresponding carceplexes. C_{70} showed again its four first characteristic reduction waves. Regarding the C_{70} carcerand, the low intensity of the waves could be ascribed to the shell around the fullerene, which does not allow a correct solvation of C_{70} anions. That means that the openings in the shell are very small and the electrolyte cannot contact the fullerene. Addition of a competitive solvent such as

²⁷ Iglesias-Sánchez, J. C.; Fragoso, A.; de Mendoza, J.; Prados, P. *Org. Lett.* **2006**, *8*, 2571-2574.

²⁸ Zhang, S.; Palker, A.; Fragoso, A.; Prados, P.; de Mendoza, J.; Echegoyen, L. *Chem. Mater.* **2005**, *17*, 2063-2068.

MeOH over the carceplex solution,²⁹ to induce hydrogen bonding disruption, did not cause any significant effect on its electrochemistry. This represents an additional evidence of no fullerene release.

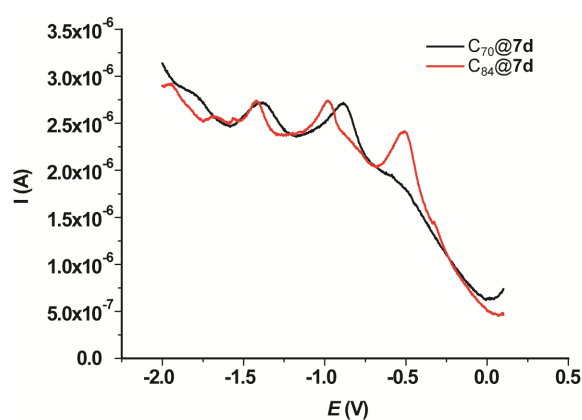


Figure 20: Stacked DPV of $C_{70}@7d$ (black) and $C_{84}@7d$ (red). WE: glassy carbon; CE: Pt; RE: Ag/Ag⁺; Scan Rate: 50 mV/s, 25 mV pulse during 10 ms and 40 ms period.

The case of C_{84} is more difficult to explain, since the waves observed in the carceplex are not comparable in intensity with those obtained for the free fullerene. DPV (Figure 19, right) showed waves for the carceplex at very different reduction potentials than C_{84} . Moreover, it must be noted that the commercially available C_{84} used in the reaction is a mixture of isomers, and the system does not seem to be selective for any of them. However, the waves obtained for the C_{84} carceplex showed intensities comparable with those measured for $C_{70}@7d$ (Figure 20). Therefore, the electrochemical behavior observed for the C_{70} carceplex might be extrapolated to the C_{84} carceplex.

²⁹ Addition in a control experiment of 1% methanol to the free C_{70} did not cause any electrochemical change.

Chapter V

V.3 CONCLUSIONS

An expeditious synthetic way has been developed to synthesize a new kind of carceplexes, using hydrogen bonding and template effects as the key step. This work constitutes the only example of fullerene carceplexes reported to date, which are the largest guests ever incarcerated.

Since calculations predicted quasi-degenerated structures, the position of the allyl group in the pyrimidinone ring is a critical question for a successful crossed metathesis reaction.

It has been demonstrated that the absence of guest does not produce an empty carcerand, only unreacted material and ring-closing metathesis products being mainly found. Moreover, the presence of multiple guests gave the capsule the opportunity to choose the best one. In this way, small quantities of higher fullerenes (C_{90}) carceplexes were isolated. Although this procedure must be optimized, it opens the way to new materials from otherwise hardly accessible fullerenes.

Carceplexes stability was studied through a collection of NMR, GPC and voltammetry experiments. It was proved that the fullerene remains inside the carcerand even if the hydrogen-bonded network is broken.

UNIVERSITAT ROVIRA I VIRGILI
SELF-ASSEMBLY BASED ON THE 2-UREIDO-4(1H)-PYRIMIDINONE MOTIF: FROM CYCLIC ARRAYS TO MOLECULAR CAPSULES
FOR FULLERENE SEPARATIONS
Elisa Huerta Martínez
DL:T.289-2012

CHAPTER VI: EXPERIMENTAL PART

UNIVERSITAT ROVIRA I VIRGILI
SELF-ASSEMBLY BASED ON THE 2-UREIDO-4(1H)-PYRIMIDINONE MOTIF: FROM CYCLIC ARRAYS TO MOLECULAR CAPSULES
FOR FULLERENE SEPARATIONS
Elisa Huerta Martínez
DL:T.289-2012

CHAPTER VI: EXPERIMENTAL PART

VI.1 GENERAL PRODECURES

All commercial reagents (Acros, Aldrich, Fluka, Panreac) were used without any additional purification. Solvents were dried and distilled using conventional methods¹ or using a Solvent Purification System (SPS).

Melting points were measured either on a Mettler Toledo DSC822e Differential Scanning Calorimeter, at a working temperature from ambient to 700 °C or or in a Büchi B-540 melting point apparatus. NMR spectra were performed on Bruker Advance 300 (¹H: 300 MHz, ¹³C: 75 MHz) 400 Ultrashield (¹H: 400 MHz, ¹³C: 100 MHz) and 500 Ultrashield (¹H: 500 MHz, ¹³C: 125 MHz) spectrometers. Deuterated solvents used are indicated in each case. Chemical shifts (δ) are expressed in ppm, and are referred to the residual peak of the solvent. Mass analysis was performed in Waters LCT Premier (ESI or APCI mode), Waters GCT (EI and CI ionization modes) or Bruker MALDI-TOF spectrometers. Elemental analyses were done on a Perkin Elmer 2400 CHN analyzer and are expressed in percentage (%). UV-vis measurements were done in a double beam UV-vis Shimadzu spectrophotometer (UV-2401PC model) with a thermostated Peltier (7-60 °C) sample holder (optical range from 190 to 1100 nm, variable slit). CD measurements were carried out in a Chirascan circular dichroism spectrometer from Applied Photophysics, with simultaneous measurement of UV-vis and CD spectra in the range 165 to 900 nm. The device is equipped with a Peltier thermal control unit (-40/+100 °C) with possibility of temperature ramp control. IR spectroscopy was done in a FTIR Bruker Tensor 27 spectrometer with an ATR accessory(spectral range from 4000 to 400 cm⁻¹). Electrochemistry was done

¹ Perrin, D. D.; Armarego, W. L. F.; Perrin, D. R. *Purification of Laboratory Chemicals*, 2nd Ed.; Pergamon Press: Oxford, **1980**.

in an Princeton Applied Research PARSTAT 2273 potentiostat offering compliance voltage up to $\pm 100\text{V}$ (available at the counter electrode), $\pm 10\text{ V}$ scan range and $\pm 2\text{ A}$ current range. Calorimetric measurements were performed in an isothermal titration microcalorimeter Microcal VP-ITC. The operating temperature range varies from $2\text{ }^\circ\text{C}$ up to $80\text{ }^\circ\text{C}$ with a noise level of 1 nanocal/sec (4 nanowatts). Vapor pressure osmometry (VPO) experiments were done in a KNAUER K-7000 osmometer with a cell working temperature range $20 - 130\text{ }^\circ\text{C}$.

Thin layer chromatography (TLC) was performed on Alugram Sil G-25/UV254-coated aluminium sheets (Macherey-Nagel) with detection by UV at 254 nm and/or phosphomolybdic acid (in EtOH or in a $\text{CeSO}_4/\text{H}_2\text{SO}_4/\text{H}_2\text{O}$ mixture), 2,4-dinitrophenyl hydrazine, ninhydrine and 50% solution of sulphuric acid in EtOH as stains. Flash chromatography was performed using silica gel Chromagel 60 AC.C ($40\text{-}60\text{ }\mu\text{m}$) and Chromagel 60 AC.C ($70\text{-}200\text{ }\mu\text{m}$), following the procedure described by W. C. Still.² High performance liquid chromatography (HPLC) analyses were carried out on an Agilent Technologies Serie 1100 apparatus, with UV-diode array, fluorescence and light scattering detectors. HPLC grade solvents were purchased from Scharlab and Carlo Erba and were used with no further purification. Conditions were indicated in each case.

Compounds 1,3-bis(benzyloxy)-5-(bromomethyl)benzene (**10**),³ 2-oxo-tetrahydro-2H-pyran-3-carbaldehyde (**16**),⁴ 2-carboethoxy-5 α -cholestan-3-one (**19**),⁵ ethyl 3-oxotetradecanoate (**21**),⁶ 2-amino-6-undecylpyrimidin-

² Still, W. C.; Kahn, M.; Mitra, A. *J. Org. Chem.* **1978**, *43*, 2923-2925.

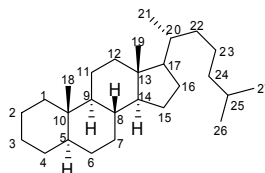
³ Andrus, M. B.; Liu, J.; Meredith, E. L.; Nartey, E. *Tetrahedron Lett.* **2003**, *44*, 4819-4822.

⁴ Harmon, A. D.; Hutchinson, R. *J. Org. Chem.* **1975**, *40*, 3474-3480.

⁵ Mikulás, M.; Möller, C.; Rust, S.; Wierchem, F.; Armhein, P.; Rück-Braun, K. *J. Prakt. Chem.* **2000**, *342*, 791-803.

4(1H)-one (**9j**),⁶ and 5-(*tert*-butyldimethylsilyloxy)pentan-2-one (**22**)⁷ were synthesized as described in literature. The synthesis of dendrimeric aminopyrimidinones **1n** and **1o**, has been described in a publication.⁸

Cholesteryl derivatives have been characterized by following this numbering:



General Procedure A: γ -Alkylation of β -ketoesters. To a solution of dry diisopropylamine (2 eq.) in dry THF, cooled to 0 °C, *n*-BuLi (2.2 M solution in hexanes, 2 eq.) was slowly added under an argon atmosphere and the mixture was stirred for 20 min. Then ethyl acetoacetate (1 eq.) was added dropwise and the reaction was stirred at 0 °C for 1 h. Finally, a solution of the corresponding alkylating agent (1 eq.) in dry THF was added dropwise and the reaction was stirred for 2 h at 0 °C. 10% aq. HCl was added and the organic phase was separated, dried (MgSO₄) and the solvent evaporated at reduced pressure. The crude was purified by flash chromatography as described below affording the desire compound.

General Procedure B: α -Alkylation of β -ketoesters. Ethyl acetoacetate (6 eq.) was added to a suspension of sodium ethoxyde (1.3 eq.) in dry THF and stirred at room temperature for 20 min. A solution of of the corresponding

⁶ Keizer, H. M.; González, J. J.; Segura, M.; Prados, P.; Sijbesma, R. P.; Meijer, E. W.; de Mendoza, J. *Chem. Eur. J.* **2005**, *11*, 4602-4608.

⁷ Chiarello, J.; Joullié, M. M. *Tetrahedron* **1988**, *44*, 41-48.

⁸ Hahn, U.; González, J. J.; Huerta, E.; Segura, M.; Eckert, J.-F.; Cardinali, F.; de Mendoza, J.; Nierengarten, J.-F. *Chem. Eur. J.* **2005**, *11*, 6666-6672.

alkylating agent (1 eq.) in THF was added and the mixture was refluxed for 3 h. Water was then added and the aqueous phase was extracted with EtOAc (x 3). The combined organic phases were washed with NH₄Cl and the solvent was evaporated under reduced pressure. The residual oil was distilled to remove the excess of ethyl acetoacetate and the residue purified by flash chromatography as indicated in each case.

General Procedure C: Synthesis of Pyrimidinones. A suspension of the corresponding β -ketoester (1 eq.) and guanidinium carbonate (0.5 eq.) in absolute ethanol was refluxed overnight. Solvent was partially evaporated and the reaction mixture was cooled to 4 °C. The precipitate was filtered off and washed with cold ethanol, yielding the pyrimidinone as a solid.

General Procedure D: Synthesis of Blocked Isocytosines (Imidazolides). A suspension of the corresponding pyrimidinones (1 eq.) and CDI (2 eq.) in dry THF or CH₂Cl₂ was stirred under an argon atmosphere for 3-8 h. The solvent was removed under reduced pressure and the residue was triturated in acetone. The solid was filtered off, washed and dried under air, affording the desire blocked isocytosine as a white solid.

General Procedure E: Synthesis of Ureidopyrimidinones from Isocyanates.

Method A: A mixture of the pyrimidinone (1 eq.) and the isocyanate (2 eq.) in a sealed tube was dissolved in a 2:1 mixture of THF/DFM (dry solvents) and the reaction was heated at 60-65 °C for 2 days. The solvent was removed until dryness and the solid residue was triturated in cold ethanol, the precipitate filtered off and washed with more ethanol, yielding the urea which was dried under air.

Method B: To a suspension of the pyrimidinone (1 eq.) in dry toluene, in a sealed tube, the isocyanate (7 eq.) and Et₃N (57 eq.) were added and the mixture was heated at 80-85 °C overnight. The solvent was removed under

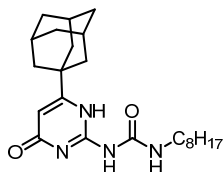
reduced pressure and the solid residue was triturated in cold ethanol. The precipitate was filtered off, washed with more ethanol and dried under air, affording the desired urea.

General Procedure F: Synthesis of Ureidopyrimidinones from Imidazolides. A suspension of the imidazolide (1 eq.) and the amine (1 eq.) in dry CH_2Cl_2 or CHCl_3 in a sealed tube was heated at 50-60 °C for 3-12 h. The solution was treated with 10% aq. HCl and extracted with CHCl_3 (x 3). The organic phase was washed with brine, dried (MgSO_4) and concentrated to dryness. The residue was triturated in EtOH, filtered off, washed with ethanol and dried under air, yielding the desired product.

General Procedure G: Synthesis of Carceplexes by Grubb's Metathesis. Reagents were dried at the high vacuum pump over a 6 hours period. The solvent was freshly degassed and the glassware was previously dried at high temperature (which one?) in the oven, cooled down into a desiccator under inert atmosphere. A solution of the Grubbs II or Hoveyda-Grubbs II catalysts (15 mol%) in dry and degassed solvent (DCM or chloroform) was added to a solution of the allyl substituted CTV-UPy and fullerene (0.5 mol·eq.) in DCM or CHCl_3 at concentration ca. 10^{-3} M. The mixture was stirred at room temperature under argon for 4 days. The solution was filtered through a bed of Celite to remove the catalyst. The filtrate was then evaporated and the solid residue was purified by flash chromatography (DCM/MeOH 0 to 2% was used in all cases).

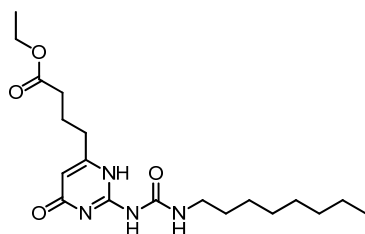
VI.2 SYNTHESIS CHAPTER II

1-(6-Adamantan-1-yl)-4-oxo-1,4-dihydropyrimidin-2-yl)-3-octylurea (**1a**).



Prepared by following the general procedure E (method A) from **9k** (30 mg, 0.12 mmol), octyl isocyanate (0.16 mL, 0.86 mmol) and Et₃N (0.97 mL, 6.97 mmol), affording **1a** (46 mg, 94%) as a white solid. Mp 179-180 °C ¹H NMR (400 MHz, CDCl₃): 13.40 (s, 2H, NH), 11.94 (br s, 2H, NH), 10.17 (s, 2H, NH), 5.87 (s, 2H, CH), 3.25 (q, *J* = 8.0 Hz, 4H, HNCH₂C₇H₁₅), 2.13 (br s, 6H, CHadam), 1.87-1.74 (m, 24H, CH₂adam), 1.62 (q, *J* = 5.2 Hz, 4H, HNCH₂CH₂C₆H₁₃), 1.37-1.23 (m, 20H, CH₂), 0.87 (t, *J* = 6.4 Hz, 6H, CH₃). ¹³C NMR (100 MHz, CDCl₃): 174.7 (C), 158.8 (C), 153.0 (C), 126.3 (C), 103.0 (CH), 100.0 (C), 40.1 (CH₂), 36.2 (CH₂), 31.8 (CH₂), 29.4 (CH₂), 29.3 (CH₂), 27.9 (CH), 27.0 (CH₂), 22.6 (CH₂), 14.1 (CH₃). MALDI-TOF MS (dithranol): *m/z* 802.0 [(2M+H)⁺], 401.1 [(M+H)⁺]. Elemental analysis calcd. (%) for C₂₃H₃₆N₄O₂ (400.3)•½EtOH: C 68.05, H 9.28, N 13.23; found C 68.67, H 9.08, N 13.11.

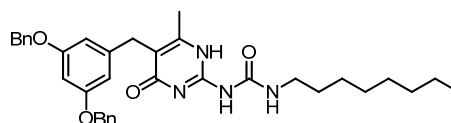
Ethyl 4-(2-(3-octylureido)-6-oxo-3,6-dihydropyrimidin-4-yl)butanoate (**1b**).



Prepared by following the general procedure E (method A) from **9l** (30 mg, 0.13 mmol), octyl isocyanate (0.15 mL, 0.93 mmol), affording **1b** (49 mg, 97%) as a white solid. Mp 279-280 °C. ¹H NMR (400 MHz, CDCl₃): 13.20 (s, 2H, NH), 11.81 (br s, 2H, NH), 10.03 (s, 2H, NH), 5.77 (s, 2H, CH), 4.09 (q, *J* = 7.2 Hz, 4H, CH₂CH₃), 3.17 (q, *J* = 6.1 Hz, 4H, HNCH₂C₇H₁₅), 2.47 (t, ³*J* = 7.6 Hz, 4H, COCH₂),

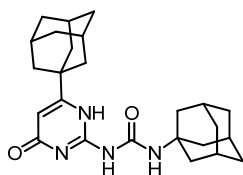
2.32 (t, $^3J = 7.0$ Hz, 4H, CCH₂), 1.92 (q, $^3J = 7.3$ Hz, 4H, CH₂), 1.56 (q, $^3J = 7.3$ Hz, 4H, HNCH₂CH₂C₆H₁₃), 1.32-1.18 (m, 26H, CH₂, CH₂CH₃), 0.80 (t, $^3J = 7.4$ Hz, 6H, CH₃). ¹³C NMR (100 MHz, CDCl₃): 173.0 (CO), 172.3 (CO), 156.6 (NCON), 151.3 (C), 148.2 (N₂C=N), 106.3 (CH), 60.7 (OCH₂), 40.1 (NCH₂), 32.9 (CH₂), 31.9 (CH₂), 30.1 (CH₂), 29.5 (CH₂), 29.4 (CH₂), 29.3 (CH₂), 29.2 (CH₂), 27.0 (CH₂), 22.6 (CH₂), 18.9 (CH₃), 14.1 (CH₃). ESI-MS (+ve): *m/z* 783.4 [(2M+Na)⁺], 761.4 [(2M+H)⁺], 403.2 [(M+Na)⁺], 381.2 [(M+H)⁺]. HRMS calcd. for C₁₉H₃₂N₄O₄ [(M+Na)⁺]: 403.2321, found: 403.2314.

1-(5-(3,5-Bis(benzyloxy)benzyl)-6-methyl-4-oxo-1,4-dihydropyrimidin-2-yl)-3-octylurea (1c).



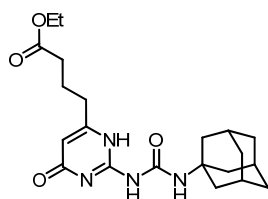
Prepared by following the general procedure E (method B) from **9c** (30 mg, 0.070 mmol), octyl isocyanate (0.089 mL, 0.49 mmol) and Et₃N (0.56 mL, 4.00 mmol), affording **1c** (40 mg, 97%) as a white solid. Mp 198-200 °C. ¹H NMR (400 MHz, CDCl₃): 12.87 (s, 2H, NH), 11.90 (br s, 2H, NH), 10.12 (s, 2H, NH), 7.36-7.24 (m, 20H, CHAr), 6.41 (s, 6H, CHAr), 4.95 (s, 8H, OCH₂Ar), 3.71 (s, 4H, CH₂), 3.19 (q, $^3J = 6.8$ Hz, 4H, HNCH₂), 2.05 (s, 6H, CH₃), 1.54 (q, $^3J = 7.2$ Hz, 4H, HNCH₂CH₂), 1.31-1.17 (m, 20H, CH₂), 0.78 (t, $^3J = 6.8$ Hz, 6H, CH₃). ¹³C NMR (100 MHz, CDCl₃): 159.9 (C), 153.0 (C), 137.0 (C), 128.5 (CH), 127.9 (CH), 127.5 (CH), 107.5 (CH), 99.8 (CH), 70.0 (CH₂), 40.0 (CH₂), 35.3 (CH₂), 31.8 (CH₂), 29.3 (CH₂), 29.2 (CH₂), 27.0 (CH₂), 22.6 (CH₂), 21.5 (CH₃), 14.1 (CH₃). MALDI-TOF MS (dithranol): *m/z* 1188.9 [(2M+Na)⁺], 1165.5 [(2M+H)⁺], 583.5 [(M+H)⁺]. Elemental analysis calcd. (%) for C₃₅H₄₂N₄O₄ (582.3): C 72.14, H 7.26, N 9.61; found C 70.14, H 7.36, N 9.34.

1-((3s,5s,7s)-Adamantan-1-yl)-3-(6-((3r,5r,7r)-adamantan-1-yl)-4-oxo-1,4-dihydropyrimidin-2-yl)urea (1d).



Prepared by following the general procedure E (method B) from **9k** (30 mg, 0.12 mmol), adamantyl isocyanate (44 mg, 0.24 mmol) and Et₃N (0.17 mL, 1.22 mmol), affording **1d** (49 mg, 95%) as a white solid (as a 90:10 mixture of *keto/enol* tautomers). Mp 296-297 °C. ¹H NMR (400 MHz, CDCl₃): 13.52 (s, 4H, NH *keto/enol*), 11.79 (br s, 2H, NH *keto*), 10.94 (s, 2H, NH *enol*), 9.82 (s, 2H, NH *enol*), 9.41 (s, 2H, NH *keto*), 6.17 (s, 2H, CH *enol*), 5.85 (s, 2H, CH *keto*), 2.11 (br s, 24H CHadam *keto/enol*), 1.85-1.65 (m, 96H, CH₂adam *keto/enol*). MALDI-TOF MS (dithranol): *m/z* 845.0 [(2M+H)⁺], 423.1 [(M+H)⁺]. Elemental analysis calcd. (%) for C₂₅H₃₄N₄O₂ (422.3)•½EtOH: C 70.08, H 8.37, N 12.57; found C 70.30, H 8.03, N 12.98.

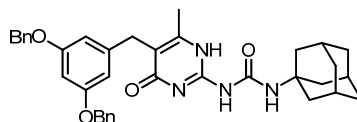
Ethyl 4-(2-(3-adamantan-1-yl)ureido)-6-oxo-3,6-dihydropyrimidin-4-yl)butanoate (1e).



Prepared by following the general procedure E (method A) from **9l** (30 mg, 0.13 mmol), adamantyl isocyanate (48 mg, 0.27 mmol), affording **1e** (37 mg, 63%) as a white solid. Mp 178-179 °C. ¹H NMR (400 MHz, CDCl₃): 13.20 (s, 2H, NH), 11.58 (br s, 2H, NH), 9.27 (s, 2H, NH), 5.78 (s, 2H, CH), 4.08 (q, ³J = 7.2 Hz, 4H, CH₂CH₃), 2.46 (t, ³J = 7.6 Hz, 4H, COCH₂), 2.31 (t, ³J = 7.0 Hz, 4H, CCH₂), 2.15-2.01 (br s, 24H, CH₂adam), 1.91 (q, ³J = 7.3 Hz, 4H, CH₂), 1.68-1.60 (m, 6H, CHadam), 1.21 (t, ³J = 7.3 Hz, 6H, CH₃). ¹³C NMR (100 MHz, CDCl₃): 172.9

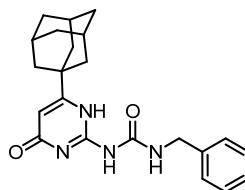
(CO), 172.4 (CO), 155.5 (NCON), 151.0 (C), 147.9 (N₂C=N), 106.0 (CH), 60.7 (OCH₂), 52.1 (C), 41.3 (CH₂), 36.4 (CH₂), 32.9 (CH₂), 31.8 (CH₂), 29.5 (CH), 22.1 (CH₂), 14.1 (CH₃). ESI-MS (+ve): *m/z* 827.4 [(2M+Na)⁺], 805.4 [(2M+H)⁺], 425.2 [(M+Na)⁺], 403.2 [(M+H)⁺]. HRMS calcd. for C₂₁H₃₁N₄O₄ [(M+H)⁺]: 403.2345, found: 403.2347.

1-(Adamantan-1-yl)-3-(5-(3,5-bis(benzyloxy)benzyl)-6-methyl-4-oxo-1,4-dihydropyrimidin-2-yl)urea (1f).



Prepared by following the general procedure E (method B) from **9c** (30 mg, 0.07 mmol), adamantyl isocyanate (25 mg, 0.14 mmol) and Et₃N (0.098 mL, 0.70 mmol), affording **1f** (41 mg, 94%) as a white solid. Mp 244-245 °C. ¹H NMR (400 MHz, CDCl₃): 13.52 (s, 2H, NH), 11.79 (br s, 2H, NH), 9.41 (s, 2H, NH), 7.35-7.27 (m, 20H, CHAr), 6.44 (s, 6H, CHAr), 4.97 (s, 8H, OCH₂Ar), 3.70 (s, 4H, CH₂), 2.15-2.01 (br s, 24H, CH₂adam), 1.68-1.60 (m, 12H, CHadam, CH₃). ¹³C NMR (100 MHz, DMSO-*d*₆): 159.9 (C), 159.7 (C_{Ar}), 144.2 (NCON), 143.1 (N₂C=N), 137.6 (C), 130.3 (C), 128.8 (CHPh), 128.2 (CHPh), 128.1 (CHPh), 107.6 (CHAr), 99.7 (CHAr), 69.6 (CH₂), 51.2 (C), 41.7 (CH₂), 36.3 (CH₂), 35.5 (CH₂), 29.6 (CH), 29.2 (CH₃). MALDI-TOF (dithranol): *m/z* 1209.7 [(2M+H)⁺], 605.3 [(M+H)⁺]. Elemental analysis calcd. (%) for C₃₇H₄₀N₄O₄ (604.3)•½EtOH: C 72.70, H 6.90, N 8.92; found C 73.03, H 6.81, N 9.09.

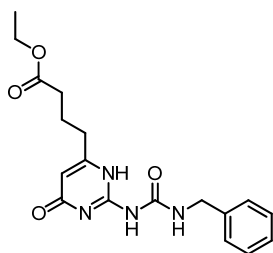
1-Benzyl-3-(6-adamantyl-4-oxo-1,4-dihydropyrimidin-2-yl)urea (1g).



Prepared by following the general procedure F from **24a** (50 mg, 0.174 mmol) and benzylamine (13.4 μL, 0.123 mmol), affording **1g** (55 mg, 83%) as

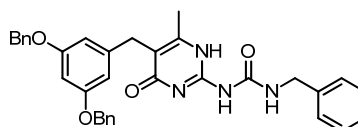
a white solid. Mp 278-279 °C. ¹H NMR (400 MHz, CDCl₃): 13.30 (s, 2H, NH), 12.10 (br s, 2H, NH), 10.84 (s, 2H, NH), 7.44-7.28 (m, 10H, CHAr), 5.85 (d, ⁴J = 1.86 Hz, 2H, CH), 4.48 (d, ³J = 5.8 Hz, 4H, CH₂), 2.13 (br s, 6H, CHadam), 1.87-1.74 (m, 24H, CH₂adam). ¹³C NMR (100 MHz, CDCl₃): 174.7 (C), 158.8 (C), 153.0 (C), 145.7 (C), 137.0 (C), 128.6 (CH), 128.0 (CH), 127.6 (CH), 106.2 (CH), 100.5 (CH), 70.1 (CH₂), 46.6 (CH₂), 29.4 (CH₂), 29.3 (CH₂), 27.9 (CH). ESI-MS (+ve): m/z 779.5 [(2M+Na)⁺], 757.4 [(2M+H)⁺], 401.2 [(M+Na)⁺], 379.2 [(M+H)⁺]. Elemental analysis calcd. (%) for C₂₂H₂₆N₄O₂ (378.2)•EtOH: C 67.90, H 7.60, N 13.20; found C 66.17, H 6.96, N 13.21.

Ethyl 4-(2-(3-benzylureido)-6-oxo-3,6-dihydropyrimidin-4-yl)butanoate (**1h**).



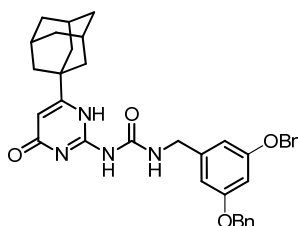
Prepared by following the general procedure F from **24b** (30 mg, 0.094 mmol) and benzylamine (21 μL, 0.19 mmol), affording **1h** (29 mg, 85%) as a white solid. Mp 125-126 °C. ¹H NMR (400 MHz, CDCl₃): 13.12 (s, 2H, NH), 12.03 (br s, 2H, NH), 10.76 (s, 2H, NH), 6.35 (m, 10H, CHAr); 5.83 (s, 2H, CH), 4.45 (d, ⁴J = 5.4 Hz, 4H, ArCH₂NH), 4.13 (q, ³J = 7.2 Hz, 4H, CH₂CH₃), 2.52 (t, ³J = 7.6 Hz, 4H, CH₂), 2.37 (t, ³J = 7.2 Hz, 4H, CH₂), 1.96 (q, ³J = 7.3 Hz, 4H, CH₂), 1.25 (t, ³J = 7.2 Hz, 6H, CH₃). ¹³C NMR (100 MHz, CDCl₃): 128.5 (CH), 127.4 (CH), 127.1 (CH), 106.2 (CH), 60.7 (CH₂), 43.5 (CH₂), 32.8 (CH₂), 31.6 (CH₂), 22.1 (CH₂), 14.2 (CH₃). ESI-MS (+ve): m/z 739.3 [(2M+Na)⁺], 717.3 [(2M+H)⁺], 381.1 (100) [(M+Na)⁺], 359.1 [(M+H)⁺]. Elemental analysis calcd. (%) for C₁₈H₂₂N₄O₄ (358.2)•½EtOH: C 59.83, H 6.61, N 14.69; found C 59.73, H 6.34, N 15.08.

1-Benzyl-3-(5-(3,5-bis(benzyloxy)benzyl)-6-methyl-4-oxo-1,4-dihydropyrimidin-2-yl)urea (1i).



Prepared by following the general procedure F from **24c** (30 mg, 0.058 mmol) and benzylamine (13 μ L, 0.115 mmol), affording **1i** (27 mg, 85%) as a white solid. Mp 223-225 $^{\circ}$ C. ^1H NMR (400 MHz, CDCl_3): 12.78 (s, 2H, NH), 12.06 (br s, 2H, NH), 10.87 (s, 2H, NH), 7.37-7.22 (m, 28H, CHAr), 7.15 (t, $^3J = 7.2$ Hz, 2H, CHAr), 6.46 (t, $^4J = 2.2$ Hz, 2H, CHAr), 6.42 (d, $^4J = 2.2$ Hz, 4H, CHAr), 4.96 (s, 8H, OCH_2Ar), 4.42 (d, $^3J = 6.0$ Hz, 4H, CH_2), 3.71 (s, 4H, CH_2), 2.07 (s, 6H, CH_3). ^{13}C NMR (100 MHz, CDCl_3): 128.5 (CH), 128.5 (CH), 127.9 (CH), 127.5 (CH), 127.0 (CH), 107.5 (CH), 99.8 (CH), 70.0 (CH_2), 43.6 (CH_2), 30.7 (CH_2), 19.3 (CH_3). ESI-MS (+ve): m/z 1143.4 [(2M+Na) $^+$], 1121.4 [(2M+H) $^+$], 583.2 [(M+Na) $^+$], 561.2 [(M+H) $^+$]. HRMS calcd. for $\text{C}_{34}\text{H}_{33}\text{N}_4\text{O}_4$ [(M+H) $^+$]: 561.2502, found: 561.2476.

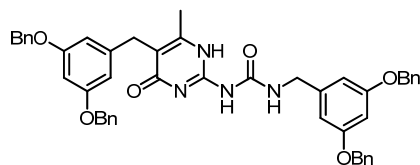
1-(3,5-Bis(benzyloxy)benzyl)-3-(6-adamantyl-4-oxo-1,4-dihydropyrimidin-2-yl)urea (1j).



Prepared by following the general procedure F from **24a** (25 mg, 0.074 mmol) and **2b** (24 mg, 0.074 mmol), affording **1j** (37 mg, 85%) as a white solid. Mp 200-202 $^{\circ}$ C. ^1H NMR (400 MHz, CDCl_3): 13.25 (s, 2H, NH), 12.08 (br s, 2H, NH), 10.75 (s, 2H, NH), 7.40-7.25 (m, 20H, CHAr), 6.65 (d, $^4J = 1.8$ Hz, 4H, CHAr), 6.47 (t, $^4J = 1.8$ Hz, 2H, CHAr), 5.81 (s, 2H, CH), 5.00 (s, 8H, OCH_2Ar), 4.42 (s, 4H, NCH_2Ar), 2.13 (br s, 6H, CHadam), 1.87-1.74 (m, 24H, CH_2adam). ^{13}C NMR (100 MHz, CDCl_3): 174.7 (C), 158.8 (C), 153.1 (C), 145.7 (C), 137.0

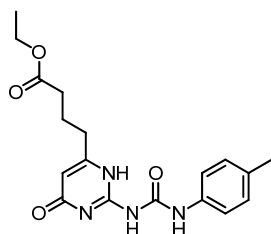
(C), 128.6 (CH), 128.0 (CH), 127.6 (CH), 106.2 (CH), 100.5 (CH), 70.1 (CH₂), 46.6 (CH₂), 29.4 (CH₂), 29.3 (CH₂), 27.9 (CH). MALDI-TOF (dithranol): *m/z* 1181.4 [(2M+H)⁺], 591.4 [(M+H)⁺]. Elemental analysis calcd. (%) for C₃₆H₃₈N₄O₄ (590.3)•½EtOH: C 72.41, H 6.73, N 9.13; found C 72.21, H 6.74, N 8.88.

1-(3,5-Bis(benzyloxy)benzyl)-3-(5-(3,5-bis(benzyloxy)benzyl)-6-methyl-4-oxo-1,4-dihydropyrimidin-2-yl)urea (1k).



Prepared by following the general procedure F from **24c** (30 mg, 0.058 mmol) and **26** (18 mg, 0.058 mmol), affording **1k** (27 mg, 60%) as a white solid. Mp 217-218 °C. ¹H NMR (400 MHz, CDCl₃): 12.73 (s, 2H, NH), 12.08 (br s, 2H, NH), 10.79 (s, 2H, NH), 7.34-7.22 (m, 40H, CHAr), 6.60 (s, 4H, CHAr), 6.43 (s, 2H, CHAr), 6.37 (s, 6H, CHAr), 4.91 (s, 8H, OCH₂Ar), 4.88 (s, 8H, OCH₂Ar), 4.34 (d, ³J = 6.4 Hz, 4H, CH₂), 3.68 (s, 4H, CH₂), 2.02 (s, 6H, CH₃). MALDI-TOF (dithranol): *m/z* 1545.8 [(2M+H)⁺], 773.5 [(M+H)⁺]. Elemental analysis calcd. (%) for C₄₈H₄₄N₄O₆ (772.3)•EtOH: C 73.33, H 6.15, N 6.84; found C 73.30, H 6.22, N 6.78.

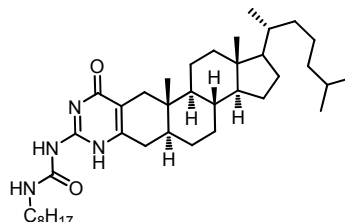
Ethyl 4-(6-oxo-2-(3-p-tolylureido)-3,6-dihydropyrimidin-4-yl)butanoate (1l).



Prepared by following the general procedure F from **24b** (30 mg, 0.094 mmol) and *p*-toluidine (10 mg, 0.094 mmol), affording **1l** (16 mg, 25%) as a white solid. Mp 174-175 °C. ¹H NMR (400 MHz, CDCl₃): 13.04 (s, 2H, NH), 12.90 (br s, 2H, NH), 12.03 (s, 2H, NH), 7.55 (d, ³J = 8.0 Hz, 4H, CHAr), 7.11 (d, ³J = 8.0

Hz, 4H, CHAR), 5.79 (s, 2H, CH), 4.13 (q, $^3J = 7.2$ Hz, 4H, CH₂CH₃), 2.30 (s, 6H, CH₃), 2.24 (m, 8H, CH₂), 1.84 (q, $^3J = 7.3$ Hz, 4H, CH₂), 1.25 (t, $^3J = 7.2$ Hz, 6H, CH₃). ¹³C NMR (100 MHz, CDCl₃): 172.3 (C), 154.7 (C), 154.4 (C), 135.7 (C), 133.4 (C), 129.4 (CH), 120.5 (CH), 106.1 (CH), 60.6 (CH₂), 32.9 (CH₂), 31.6 (CH₂), 21.6 (CH₂), 20.8 (CH₃), 14.2 (CH₃). ESI-MS (+ve): *m/z* 739.3 [(2M+Na)⁺], 717.3 [(2M+H)⁺], 381.1 [(M+Na)⁺], 359.1 [(M+H)⁺]. Elemental analysis calcd. (%) for C₁₈H₂₂N₄O₄ (358.2): C 60.32, H 6.19, N 15.63; found C 59.97, H 6.19, N 15.87.

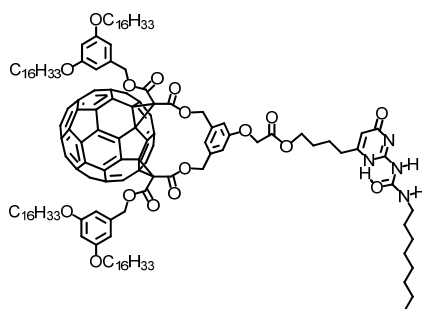
1-((3aS,3bR,5aS,11aS,11bS,13aR)-11a,13a-Dimethyl-1-((R)-6-methylheptan-2-yl)-10-oxo-2,3,3a,3b,4,5,5a,6,7,10,11,11a,11b,12,13,13a-hexadecahydro-1H-cyclopenta[5,6]naphtho[1,2-g]quinazolin-8-yl)-3-octylurea (1m).



Prepared by following the general procedure E (method B) from **9h** (27 mg, 0.059 mmol), octyl isocyanate (0.18 mL, 0.82 mmol) and Et₃N (0.098 mL, 0.70), affording **1m** (29 mg, 80%) as a white solid. Mp 240-242 °C. ¹H NMR (400 MHz, CDCl₃): 12.81 (s, 2H, NH), 11.85 (br s, 2H, NH), 10.15 (s, 2H, NH), 3.21 (m, 4H, HNCH₂), 2.54 (d, $^2J = 17.2$ Hz, 2H, H-1a), 2.35-0.78 (m, 80H, H-1b, H-4, H-5, H-6, H7, H-8, H-9, H-11, H-12, H-14, H-15, H-16, H-17, H-20, H-22, H-23, H-24, H-25, CH₂ octyl chain), 0.89 (d, $^3J = 6.0$ Hz, 6H, CH₃-21), 0.86 (d, $^3J = 6.7$ Hz, 12H, CH₃-26, C₇H₁₄CH₃), 0.83 (d, $^3J = 6.7$ Hz, 6H, CH₃-27), 0.71 (s, 6H, CH₃-19), 0.65 (s, 6H, CH₃-18). ¹³C NMR (100 MHz, CDCl₃): 152.2 (NCON), 113.3 (C-2), 55.4 (CH-17), 55.3 (CH-14), 52.7 (CH-9), 41.5 (C-13), 39.6 (CH-5), 39.1 (CH₂-12), 38.9 (CH₂-24), 38.5 (CH₂NH), 35.2 (CH₂-1), 35.0 (CH₂-22), 34.8 (CH-20), 34.5 (CH-8), 34.1 (C-10), 31.0 (CH₂), 30.4 (CH₂-4), 30.1 (CH₂-7), 28.5 (CH₂), 28.4 (CH₂), 28.3 (CH₂), 27.2 (CH₂-16), 27.1 (CH₂-6), 27.0 (CH-25), 26.1 (CH₂), 23.2 (CH₂-15), 22.9 (CH₂-23), 21.8 (CH₃-26), 21.7 (CH₂), 21.6 (CH₃-27), 20.2 (CH₂-11), 17.8 (CH₃-21),

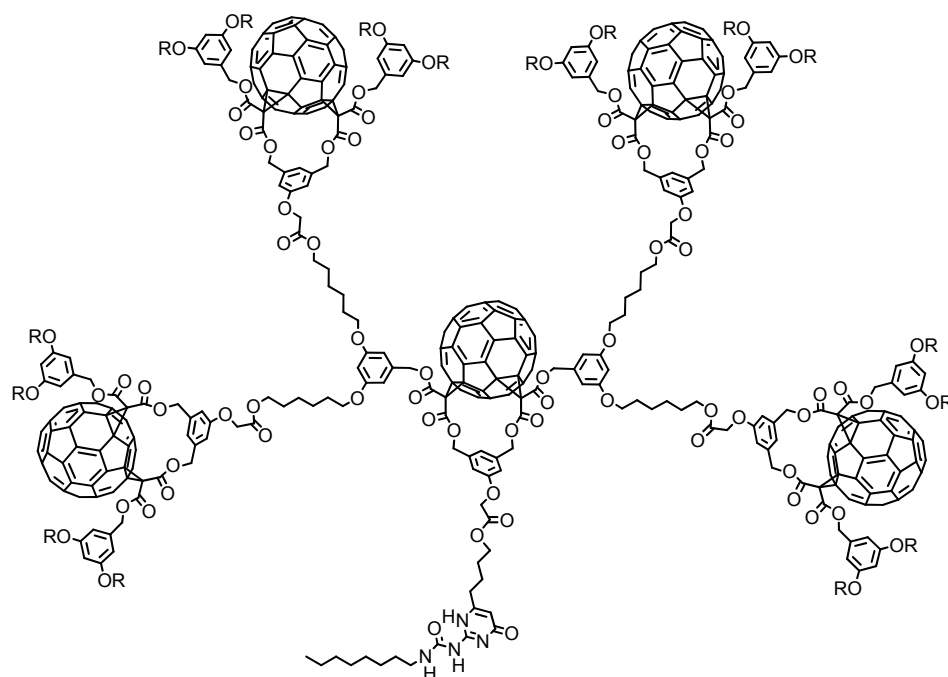
13.1 (CH₃), 11.0 (CH₃-18), 10.8 (CH₃-19). MALDI-TOF (dithranol): *m/z* 1218.4 [(2M+H)⁺], 609.3 [(M+H)⁺]. Elemental analysis calcd. (%) for C₃₈H₆₄N₄O₂ (608.5)•EtOH: C 73.35, H 10.77, N 8.55; found C 73.14, H 10.48, N 8.87.

Compound 1n:



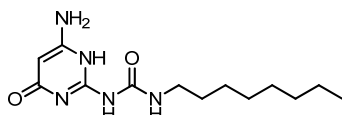
Prepared by following general procedure E, method B from **9m** (24 mg, 0.010 mmol) and purified by column chromatography on silica gel (hexanes/EtOAc, 7:2 to EtOAc) to give **1n** (12 mg, 48%) as a glassy, dark orange product. ¹H NMR (500 MHz, CHCl₃): 13.23 (br s, 2H), 11.81 (br s, 2H), 10.06 (br s, 2H), 7.12 (s, 2H), 6.78 (s, 4H), 6.43 (d, ⁴J = 2.0 Hz, 4H), 6.32 (t, ⁴J = 2.0 Hz, 2H), 5.79 (s, 2H), 5.71 (d, ²J = 13.0 Hz, 4H), 5.25 (s, 8H), 5.04 (d, ²J = 13.0 Hz, 4H), 4.67 (s, 4H), 4.23 (t, ³J = 6.0 Hz, 4H), 3.81 (t, ³J = 6.0 Hz, 16H), 3.19 (q, ³J = 8.0 Hz, 4H), 2.47 (t, ³J = 7.0 Hz, 4H), 1.27 (m, 108H), 0.89 (t, ³J = 6.0 Hz, 24H). UV/Vis (CH₂Cl₂): λ_{max} (ε) = 260 (256000), 438 (7200), 463 nm (6800 mol⁻¹m³cm⁻¹). MALDI-TOF (dithranol): *m/z* 5126.0 [(2M+H)⁺], 2564.7[(M+H)⁺]. HRMS: *m/z* calcd. for C₁₇₁H₁₈₁N₄O₁₇ [(M+H)⁺]: 2564.2834, found: 2564.4042.

Compound 1o:



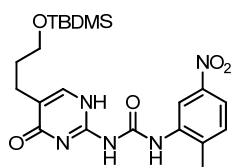
Prepared by following general procedure E, method B from **9n** (45 mg, 0.004 mmol) affording 38 mg (87%) of **1o** as a dark orange-brown solid. $^1\text{H NMR}$ (500 MHz, CDCl_3): 13.25 (br s, 2H), 11.86 (br s, 2H), 10.12 (br s, 2H), 7.12 (s, 10H), 6.78 (s, 16 H), 6.70 (s, 4H), 6.45 (m, 40H), 6.35 (m, 20H), 5.74 (d, $^2J = 13.0$ Hz, 20H), 5.59 (s, 2H), 5.29 (s, 40H), 5.05 (d, $^2J = 13.0$ Hz, 20H), 4.65 (s, 20H), 4.23 (m, 20H), 3.82 (m, 80H), 2.26 (m, 4H), 1.71 (m, 100H), 1.48–1.20 (m, 896H), 0.88 (t, $^3J = 7.0$ Hz, 102H). UV/Vis (CH_2Cl_2): λ_{max} (ϵ) = 261 (980000), 437 (35300), 464 nm (33200 $\text{mol}^{-1}\text{m}^3\text{cm}^{-1}$). MALDI-TOF (dithranol): m/z 21932 $[(2M+H)^+]$, 10964 $[(M+H)^+]$.

1-(6-Amino-4-oxo-1,4-dihydropyrimidin-2-yl)-3-octylurea (**1p**).



Prepared by following the general procedure E (method A) from 2,4-diamino-6-hydroxypyrimidine (500 mg, 3.80 mmol) and octyl isocyanate (1.20 mL, 5.71 mmol), affording **1p** (975 mg, 94%) as a yellow solid. Mp 209-212 °C. ¹H NMR (400 MHz, DMSO-*d*₆): 10.61 (s, 1H, NH), 9.16 (s, 1H, NH), 7.96 (s, 1H, NH), 6.46 (s, 2H, NH₂), 4.73 (s, 1H, CH), 3.10 (m, 2H, CH₂), 1.45 (m, 2H, CH₂), 1.26 (m, 10H, CH₂), 0.85 (t, ³J = 7.7 Hz, 3H, CH₃). ¹³C NMR (400 MHz, DMSO-*d*₆): 163.9 (C), 154.3 (C), 153.8 (C), 79.1 (CH), 31.2 (CH₂), 29.2 (CH₂), 28.6 (CH₂), 28.6 (CH₂), 28.6 (CH₂), 26.3 (CH₂), 22.1 (CH₂), 13.9 (CH₃). HRMS calcd. for C₁₃H₂₄N₅O₂ [(M+H)⁺]: 282.1930, found: 282.1935.

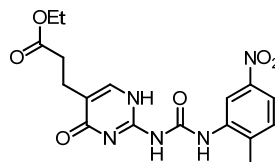
1-(5-(3-((*tert*-Butyldimethylsilyloxy)propyl)-4-oxo-1,4-dihydropyrimidin-2-yl)-3-(2-methyl-5-nitrophenyl)urea (**1q**).



Prepared following general procedure E, method A from aminopyrimidinone **9o** (164 mg, 0.61 mmol), 2-methyl-5-nitrophenyl isocyanate (127 mg, 0.70 mmol) and triethyl amine (1.0 mL, 7.31 mmol) affording **1q** (220 mg, 81%) as a beige solid. ¹H NMR (400 MHz, CDCl₃): 12.81 (s, 2H, NH), 12.35 (s, 2H, NH), 12.15 (s, 2H, NH), 8.39 (s, 2H, CHAr), 7.93 (dd, ⁴J = 1.8 Hz, ³J = 8.4 Hz, 2H, CHAr), 7.32 (d, ³J = 8.4 Hz, 2H, CHAr), 3.64 (t, ³J = 6.2 Hz, 4H, CH₂), 2.49 (t, ³J = 7.5 Hz, 4H, CH₂), 2.45 (s, 6H, CH₃), 1.77 (quint., ³J = 7.5 Hz, 4H, CH₂), 0.88 (s, 18H, CH₃), 0.03 (s, 12H, SiCH₃). ¹³C NMR (100 MHz, DMSO-*d*₆): 146.5 (C), 138.0 (C), 136.2 (C), 131.7 (CH), 131.5 (CH), 129.3 (C), 118.4 (CH), 114.8 (CH), 62.4 (CH₂), 31.2 (CH₂), 26.3 (CH₃), 23.6 (CH₂), 18.6 (CH₃), 18.4 (CH₃), -4.9 (CH₃).

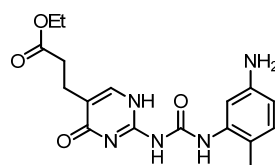
Elemental analysis calcd. (%) for $C_{17}H_{19}N_5O_6$ (389.4) $\cdot \frac{1}{2}H_2O$: C 51.25, H 5.06, N 17.58; found C 51.70, H 4.79, N 17.60.

Ethyl 3-(2-(3-(2-methyl-5-nitrophenyl)ureido)-4-oxo-1,4-dihydropyrimidin-5-yl)propanoate (1r).



Prepared following general procedure E, method A from **9e** (50 mg, 0.30 mmol), 2-methyl-5-nitrophenyl isocyanate (63 mg, 0.35 mmol) and triethyl amine (0.5 mL, 3.63 mmol) affording **1q** (94 mg, 90%) as a white solid. 1H NMR (400 MHz, $DMSO-d_6$): 8.89 (s, 1H, CHAr), 7.88 (dd, $^4J = 2.7$ Hz, $^3J = 8.7$ Hz, 1H, CHAr), 7.68 (br s, 1H, CHAr), 7.52 (d, $^3J = 8.7$ Hz, 1H, CHAr), 4.05 (q, $^3J = 7.2$ Hz, 2H, CH_2), 2.41 (br s, 4H, CH_2), 1.17 (t, $^3J = 7.3$ Hz, 3H, CH_3). ^{13}C NMR (100 MHz, $DMSO-d_6$): 172.8 (C), 162.7 (C), 149.9 (C), 146.6 (C), 138.0 (C), 136.7 (C), 131.7 (CH), 131.6 (CH), 129.3 (C), 118.5 (CH), 114.8 (CH), 60.4 (CH_2), 32.5 (CH_2), 23.1 (CH_2), 18.7 (CH_3), 14.6 (CH_3). ESI-MS (+ve): m/z 801.3 $[(2M+Na)^+]$, 412.1 $[(M+Na)^+]$, 390.2 $[(M+H)^+]$. Elemental analysis calcd. (%) for $C_{17}H_{19}N_5O_6$ (389.4) $\cdot \frac{1}{2}H_2O$: C 51.25, H 5.06, N 17.58; found C 51.70, H 4.79, N 17.60.

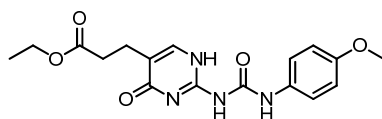
Ethyl 3-(2-(3-(5-amino-2-methylphenyl)ureido)-4-oxo-1,4-dihydropyrimidin-5-yl)propanoate (1s).



To a suspension of **1r** (30 mg, 0.077 mmol) and palladium black (5.74 mg, 0.054 mmol) in dry DMF (20 mL) a balloon containing hydrogen gas was attached at room temperature. The reaction mixture was stirred 48 h and the mixture was filtered through a bed of Celite. Solvent was removed at reduced pressure to give the crude product, which was subsequently

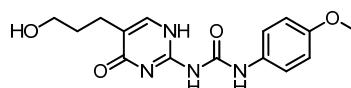
washed with ethanol and hexane before drying to give **1s** (27 mg, 97%) as a beige solid. ¹H NMR (400 MHz, DMSO-*d*₆): 9.62 (br s, 2H, NH₂), 7.67 (s, 1H, CH), 7.16 (s, 1H, CHAr), 6.85 (d, ³J = 8.1 Hz, 1H, CHAr), 6.27 (dd, ⁴J = 2.3 Hz, ³J = 8.1 Hz, 1H, CHAr), 4.05 (q, ³J = 7.2 Hz, 2H, CH₂), 2.52-2.55 (m, 4H, CH₂), 2.10 (s, 3H, CH₃), 1.17 (t, ³J = 7.2 Hz, 3H, CH₃). ¹³C NMR (100 MHz, DMSO-*d*₆): 172.7 (C), 161.6 (C), 151.4 (C), 147.5 (C), 136.6 (C), 130.9 (CH), 118.8 (C), 115.0 (C), 110.5 (CH), 107.8 (CH), 60.3 (C), 32.6 (CH₂), 23.0 (CH₂), 17.3 (CH₃), 14.6 (CH₃). HRMS calcd. for C₁₇H₂₂N₅O₄ 360.1672 [(M+H)⁺], found: 360.1688.

Ethyl 3-(2-(3-(4-methoxyphenyl)ureido)-4-oxo-1,4-dihydropyrimidin-5-yl)propanoate (1t).



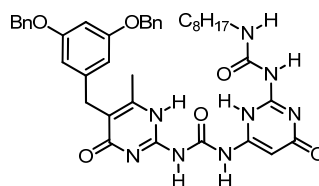
Prepared by following the general procedure F from **24e** (53 mg, 0.173 mmol) and *p*-anisidine (20 mg, 0.160 mmol), affording **1t** (52 mg, 93%) as a white solid. Mp 233 °C. ¹H NMR (400 MHz, CDCl₃): 12.99 (d, ³J = 4.8 Hz, 2H, NH), 12.1 (s, 2H, NH), 12.04 (s, 2H, NH), 7.63 (d, ³J = 9.2 Hz, 4H, CHAr), 7.30 (d, ³J = 4.8 Hz, 2H, CH), 6.92 (d, ³J = 9.2 Hz, 4H, CHAr), 4.15 (q, ³J = 7.2 Hz, 4H, OCH₂CH₃), 3.81 (s, 6H, CH₃), 2.74 (t, ³J = 6.0 Hz, 4H, CH₂), 2.68 (t, ³J = 6.0 Hz, 4H, CH₂), 1.27 (t, ³J = 7.2 Hz, 6H, OCH₂CH₃). ¹³C NMR (400 MHz, CDCl₃): 173.0 (CO), 171.9 (CO), 156.2 (CH), 154.5 (N₂C=N), 154.1 (NCON), 134.5 (CAr), 131.4 (C), 122.0 (CHAr), 119.9 (CAr), 114.1 (CHAr), 60.5 (OCH₂), 55.5 (OCH₃), 32.1 (CH₂), 23.4 (CH₂), 14.3 (CH₃). ESI-MS (+ve): *m/z* 743.2 [(2M+Na)⁺], 721.2 [(2M+H)⁺], 383.1 [(M+Na)⁺], 361.1 [(M+H)⁺]. Elemental analysis calcd. (%) for C₁₇H₂₀N₄O₅ (360.1)•EtOH: C 56.66, H 5.59, N 15.55; found C 56.18, H 5.59, N 15.33.

1-(5-(3-Hydroxypropyl)-4-oxo-1,4-dihydropyrimidin-2-yl)-3-(4-methoxyphenyl)urea (1u).



To a suspension of **1t** (50 mg, 0.144 mmol) in dry CH₂Cl₂ (5 mL) under an argon atmosphere, a solution of DIBAL-H (1M in CH₂Cl₂, 718 μL, 0.718 mmol) was added dropwise and the reaction was stirred at -78 °C for 5 h and allowed to warm to room temperature overnight. 10% HCl (10 mL) was added and the mixture was strongly stirred for 30 min. Solvent was evaporated at reduced pressure and the residue extracted with CH₂Cl₂ in a Soxhlet system for a week. The solution was concentrated until dryness, yielding **1u** (30 mg, 59%) as a white solid. Mp 197 °C. ¹H NMR (400 MHz, DMSO-*d*₆): 9.72 (br s, 1H, NH), 7.56 (s, 1H, CH), 7.39 (d, ³J = 8.6 Hz, 2H, CHAr), 6.91 (d, ³J = 8.6 Hz, 2H, CHAr), 4.43 (br s, 1H, OH), 3.71 (m, 3H, CH₃), 3.37 (m, 2H, OCH₂), 2.30 (m, 2H, CH₂), 1.59 (m, 2H, CH₂). ¹³C RMN (100 MHz, CDCl₃): 163.3 (CO), 155.8 (CAr), 155.0 (CH), 152.3 (N₂C=N), 151.0 (NCON), 120.2 (CAr), 115.04 (CHAR), 114.5 (CHAR), 60.6 (CH₂), 55.7 (CH₃), 32.3 (CH₂), 23.4 (CH₂). ESI-MS (MeOH): *m/z* 1294.8 [(4M+Na)⁺], 1272.7 [(4M)⁺], 977.0 [(3M+Na)⁺], 659.1 [(2M+Na)⁺], 637.0 [(2M+H)⁺], 341.2 [(M+Na)⁺], 319.2 [(M+H)⁺]. HRMS calcd. for C₁₅H₁₈N₄O₄Na [(M+Na)⁺]: 341.1226, found: 341.1226.

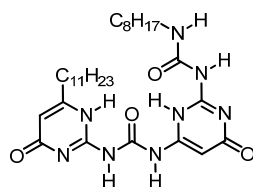
1-(5-(3,5-Bis(benzyloxy)benzyl)-6-methyl-4-oxo-1,4-dihydropyrimidin-2-yl)-3-(2-(3-octylureido)-6-oxo-3,6-dihydropyrimidin-4-yl)urea (2a).



A suspension of **1p** (50 mg, 0.18 mmol) and **24c** (93 mg, 0.18 mmol) in CH₂Cl₂ (15 mL) was refluxed for 2 h. Then DMF (10 mL) was added and the mixture

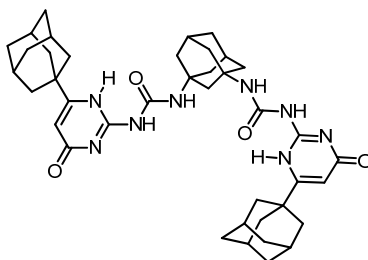
was heated at 65 °C for 2 h. The reaction was diluted with CH₂Cl₂ (10 mL) and the organic phase was washed with 10% HCl and brine, dried (MgSO₄) and the solvent was evaporated at reduced pressure. The residue was triturated with MeOH, the precipitate was filtered off and washed with MeOH, affording **2a** (99 mg, 76%) as a white solid. Mp > 410 °C. ¹H NMR (400 MHz, DMSO-*d*₆): 7.40-7.37 (m, 10H, CHAr), 6.48-6.42 (m, 3H, CHAr), 6.38 (s, 1H, CH), 5.01 (s, 4H, OCH₂Ar), 3.65 (m, 2H, HNCH₂), 3.56 (s, 2H, CH₂Ar), 1.95 (s, 3H, CH₃), 1.45-1.25 (m, 12H, CH₂), 0.84 (m, 3H, CH₃). ESI-MS: *m/z* 735.4 [(M+H)⁺]. HRMS calcd. for C₄₀H₄₇N₈O₆ [(M+H)⁺]: 735.8512, found: 735.8532.

1-(2-(3-Octylureido)-6-oxo-3,6-dihydropyrimidin-4-yl)-3-(4-oxo-6-undecyl-1,4-dihydropyrimidin-2-yl)urea (2b).



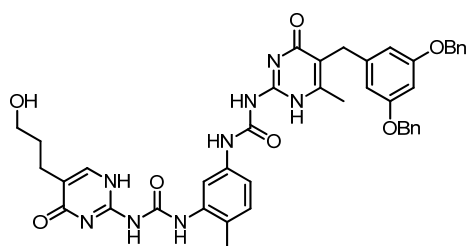
A suspension of **24d** (64 mg, 0.18 mmol) and **1p** (50 mg, 0.18 mmol) in CH₂Cl₂ (20 mL) was refluxed for 2 h. Then DMF (10 mL) was added and the mixture was heated at 65 °C for 2 h. The reaction was diluted with CH₂Cl₂ (10 mL) and the organic phase was washed with 10% HCl and brine, dried (MgSO₄) and the solvent was evaporated at reduced pressure. The residue was triturated with MeOH, the precipitate was filtered off and washed with MeOH, affording **2b** (91 mg, 89%) as a white solid. Mp > 410 °C. ¹H NMR (400 MHz, DMSO-*d*₆): 10.57 (br s, 2H, NH), 6.43 (br s, 2H, CH), 3.12 (m, 2H, HNCH₂), 2.22 (t, ³J = 7.9 Hz, 2H, CH₂C₁₀H₂₁), 1.51-1.48 (m, 4H, CH₂), 1.32-1.20 (m, 26H, CH₂), 0.86 (m, 6H, CH₃). MALDI-TOF (negative mode): *m/z* 571.2 [(M-H)⁺]. MALDI-TOF (positive mode): 1166.0 [(2M+Na)⁺].

1,1'-(Adamantane-1,3-diyl)-bis-[3-(6-adamantyl-4-oxo-1,4-dihydropyrimidin-2-yl)urea] (3b).



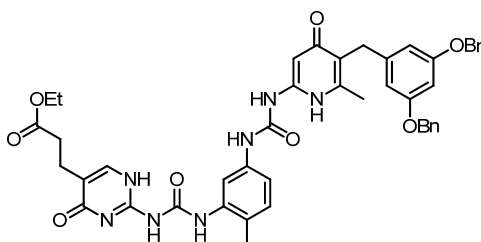
To a suspension of 1,3-adamantanedicarboxylic acid (50 mg, 0.22 mmol) in toluene (15 mL), Et₃N (61 μL, 0.44 mmol) and DPPA (93 μL, 0.44 mmol) were added and the reaction was heated at 40 °C for 1 h and at 80 °C for 3 h. Then **6k** (107 mg, 0.44 mmol) was added and the mixture was heated at 80 °C for 2 days. Toluene was evaporated under reduced pressure and the residue was triturated with MeOH. The precipitate was filtered off affording **3b** (133 mg, 85%) as a white solid (as a 94:6 mixture of *keto/enol* tautomers). Mp 317-318 °C. ¹H NMR (400 MHz, CDCl₃): 13.46 (m, 1H, NH *keto*), 13.45 (s, 1H, NH *enol*), 11.74 (m, 1H, NH *keto*), 10.92 (s, 1H, NH *enol*), 9.73 (m, 1H, NH *keto*), 9.32 (s, 1H, NH *enol*), 6.11 (s, 1H, CH *enol*), 5.83 (s, 1H, CH *keto*), 2.53-1.27 (m, 44H, CH_{adam}, CH_{2adam} *keto/enol*). ¹³C NMR (100 MHz, DMSO-*d*₆): 152.7 (NCON), 129.3 (N₂C=N), 109.5 (CH), 57.0 (C), 52.3 (C), 48.8 (CH₂), 43.7 (CH₂), 38.6 (CH₂), 36.9 (CH₂), 36.6 (CH₂), 28.4 (CH), 28.2 (CH). MALDI-TOF: *m/z* 3542.1 [(5M)⁺], 2833.6 [(4M)⁺], 2125.2 [(3M)⁺], 1416.8 [(2M)⁺], 708.4 [(M)⁺]. HRMS calcd. for C₄₀H₅₂N₈O₄Na [(M+Na)⁺]: 731.4009, found: 731.4009.

1-(5-(3-(5-(3,5-Bis(benzyloxy)benzyl)-6-methyl-4-oxo-1,4-dihydropyridin-2-yl)ureido)-2-methylphenyl)-3-(5-(3-hydroxypropyl)-4-oxo-1,4-dihydropyrimidin-2-yl)urea (4a).



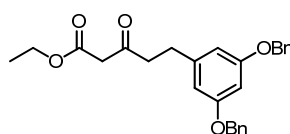
Compound **4c** (42.0 mg, 0.05 mmol) was dissolved in dry DCM (5 mL) under argon atmosphere. Solution was then cooled down to $-78\text{ }^{\circ}\text{C}$ and DIBAL-H solution 1M in toluene (258 μL , 0.26 mmol) was carefully added. The reaction mixture was stirred at $-78\text{ }^{\circ}\text{C}$ for 2h and at room temperature overnight. Then, 0.5 mL of HCl (3M) were added, solution was stirred for 15 minutes and filtered through Celite. Solvent was evaporated under reduced pressure. The solid material was triturated in MeOH, filtered and dried under air. **4a** was obtained as an off-white solid (29 mg, 73%). Mp $> 400\text{ }^{\circ}\text{C}$. ^1H NMR (400 MHz, DMSO- d_6): 8.09 (s, 1H, CH), 7.64 (s, 1H, CH), 7.44-7.29 (m, 10H, CHAr), 7.23 (d, $^3J = 7.9\text{ Hz}$, 1H, CHAr), 7.18 (d, $^3J = 8.0\text{ Hz}$, 1H, CHAr), 6.50 (t, $^4J = 1.9\text{ Hz}$, 1H, CHAr), 6.43 (d, $^4J = 2.0\text{ Hz}$, 1H, CHAr), 5.04 (s, 4H, CH₂), 3.66 (s, 2H, CH₂), 3.43 (t, $^3J = 6.7\text{ Hz}$, 2H, CH₂), 2.33 (t, $^3J = 6.7\text{ Hz}$, 2H, CH₂), 2.24 (s, 3H, CH₃), 2.12 (s, 3H, CH₃), 1.63 (quint., $^3J = 6.7\text{ Hz}$, 2H, CH₂). ^{13}C NMR (100 MHz, DMSO- d_6): 172.5 (C), 172.1 (C), 167.1 (C), 166.0 (C), 159.3 (C), 143.0 (C), 137.6 (C), 136.7 (C), 131.8 (CH), 131.0 (CH), 128.7 (CH), 128.7 (CH), 128.1 (CH), 127.8 (CH), 118.9 (C), 115.0 (CH), 114.7 (C), 112.9 (CH), 107.6 (CH), 99.6 (CH), 69.7 (CH₂), 60.5 (CH₂), 30.2 (CH₂), 23.6 (CH₂), 17.9 (CH₃), 17.2 (CH₃), 16.2 (CH₂). MALDI-TOF (dithranol, DCM, MeOH): m/z 1541.9 ([2M+H]⁺), 771.2 ([M+H]⁺). ESI-MS (MeOH, HCOOH): m/z 2311.3 ([3M+H]⁺), 1541.6 ([2M+H]⁺), 771.3 ([M+H]⁺). HRMS calcd. for C₄₂H₄₃N₈O₇ 771.3255 ([M+H]⁺), found: 771.3264.

Ethyl 3-(2-(3-(5-(3-(5-(3,5-bis(benzyloxy)benzyl)-6-methyl-4-oxo-1,4-dihydropyridin-2-yl)ureido)-2-methylphenyl)ureido)-4-oxo-1,4-dihydropyrimidin-5-yl)propanoate (4c).



Prepared by following general procedure F from **1s** (25 mg, 0.07 mmol) and **24c** (37 mg, 0.07 mmol) in DMF (5 mL) at 65 °C. Compound **4a** (51 mg, 89%) was obtained as an off-white solid. ¹H NMR (400 MHz, DMSO-*d*₆): 8.08 (s, 1H, CHAr), 7.68 (br s, 1H, CH), 7.42-7.29 (m, 10H, CHAr), 7.23 (d, ³J = 8.6 Hz, 1H, CHAr), 7.17 (d, ³J = 8.7 Hz, 1H, CHAr), 6.49 (t, ⁴J = 1.6 Hz, 1H, CHAr), 6.43 (d, ⁴J = 1.5 Hz, 2H, CHAr), 5.03 (s, 4H, OCH₂Ar), 4.05 (q, ³J = 7.0 Hz, 2H, OCH₂), 3.66 (s, 2H, CH₂), 3.33 (br s, 3H, NH), 2.51-2.48 (m, 4H, CH₂), 2.23 (s, 3H, CH₃), 2.12 (s, 3H, CH₃), 1.17 (t, ³J = 6.7 Hz, 3H, CH₃). ¹³C NMR (125 MHz, DMSO-*d*₆): 172.8 (C), 172.2 (C), 166.0 (C), 165.9 (C), 159.9 (C), 159.7 (C), 143.0 (C), 137.6 (C), 136.7 (C), 131.8 (CH), 131.0 (CH), 128.7 (CH), 128.7 (CH), 128.1 (CH), 127.8 (CH), 118.9 (C), 115.0 (CH), 114.7 (C), 112.9 (CH), 107.6 (CH), 99.6 (CH), 69.7 (CH₂), 60.1 (CH₂), 32.9 (CH₂), 30.2 (CH₂), 23.0 (CH₂), 21.7 (CH₃), 18.0 (CH₃), 14.3 (CH₃). MALDI-TOF (dithranol, DCM, MeOH): *m/z* 2439.1 ([3M+H]⁺), 1626.0 ([2M+H]⁺), 813.4 ([M+H]⁺). ESI-MS (MeOH, HCOOH): *m/z* 2438.9 ([3M+H]⁺), 1626.6 ([2M+H]⁺), 813.3 ([M+H]⁺). HRMS calcd. for C₄₄H₄₅N₈O₈ 813.3360 ([M+H]⁺), found: 813.3327.

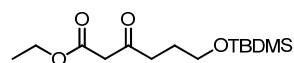
5-(3,5-Bis-benzyloxyphenyl)-3-oxopentanoic acid ethyl ester (8a).



Prepared by following the general procedure A from **10** (4.77 g, 12.45

mmol), purification by flash chromatography (hexane/EtOAc, 9:1 → 8:2) afforded **8a** (3.50 g, 65%) as a yellow oil. ¹H NMR (200 MHz, CDCl₃): 7.42-7.32 (m, 10H, CHAr), 6.49-6.44 (m, 3H, CHAr), 5.01 (s, 4H, CH₂Ar), 4.19 (q, *J* = 6.1 Hz, 2H, OCH₂), 3.42 (s, 2H, COCH₂CO), 2.87 (s, 4H, CH₂), 1.27 (t, *J* = 6.1 Hz, 3H, CH₃). ¹³C NMR (75 MHz, CDCl₃): 201.8 (CO), 167.1 (CO), 160.0 (C), 142.9 (C), 136.9 (C), 128.6 (CHPh), 127.9 (CHPh), 127.5 (CHPh), 107.5 (CHAr), 99.8 (CHAr), 70.0 (CH₂Ph), 61.4 (CH₂Ph), 49.4 (OCH₂), 44.2 (CH₂CO), 29.6 (CH₂Ar), 14.1 (CH₃). FAB-MS: *m/z* 432.3 [M⁺]. HRMS calcd. for C₂₇H₂₈O₅ [M⁺]: 432.1937, found: 432.1945.

6-*tert*-Butyldimethylsilyloxy-3-oxohexanoic acid ethyl ester (**8b**).

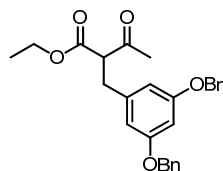


Method A: Prepared by following the general procedure A from **11** (1.21 g, 5.09 mmol), purification by flash chromatography (hexane/EtOAc, 95:5) yielded **5b** (224 mg, 16%) as a yellow oil.

Method B: NaH (60% dispersion in mineral oil, 130 mg, 3.25 mmol) was suspended in dry THF (5 mL) and the mixture was refluxed. A solution of **22** (703 mg, 3.25 mmol) in THF (2 mL) was added dropwise and the mixture was refluxed for 30 min. A solution of diethyl carbonate (600 μL, 4.88 mmol) in THF (3 mL) was added and the reaction was refluxed overnight. The mixture was cooled to room temperature, sat. aq. NH₄Cl (20 mL) was added and the aqueous phase was extracted (2 x 20 mL) with Et₂O. The organic phase was dried (MgSO₄) and concentrated to dryness. The residual oil was purified by flash chromatography (hexane/Et₂O, 95:5), affording **8b** (252 mg, 27%) as a yellow oil. ¹H NMR (300 MHz, CDCl₃): 4.19 (q, ³*J* = 7.4 Hz, 2H, CH₂CH₃), 3.62 (t, ³*J* = 6.7 Hz, 2H, OCH₂CH₂), 3.45 (s, 2H, COCH₂CO), 2.62 (t, ³*J* = 6.7 Hz, 2H, CH₂OTBDMS), 1.81 (quint., ³*J* = 6.7 Hz, 2H, CH₂), 1.28 (t, ³*J* = 7.4 Hz, 3H, CH₂CH₃), 0.88 (s, 9H, ^tBu), 0.04 (s, 6H, CH₃). ¹³C NMR (75 MHz, CDCl₃): 202.7 (CO), 167.2 (CO), 61.9 (OCH₂CH₃), 61.3 (OCH₂CH₂), 49.4 (COCH₂CO), 39.4

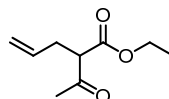
(OCH₂CH₂CH₂), 29.3 (C, ^tBu), 26.6 (OCH₂CH₂), 25.9 (CH₃, ^tBu), 14.1 (OCH₂CH₃), -2.8 (SiCH₃). EI-MS: *m/z* 231.0 [(M-^tBu)⁺], 157.0 [(M-OTBDMS)⁺]. HRMS calcd. for C₁₄H₂₉O₄Si [(M+H)⁺]: 289.1835, found: 289.1843.

Ethyl 2-(3,5-bis(benzyloxy)benzyl)-3-oxobutanoate (**8c**).



Prepared by following the general procedure B from **10** (2.66 g, 6.96 mmol), purification by flash chromatography (hexane/EtOAc, 9:1) afforded **8c** (1.78 g, 60%) as a yellow oil. ¹H NMR (CDCl₃, 400 MHz): 7.45-7.32 (m, 10H, CHAr), 6.51 (t, ⁴J = 2.2 Hz, 1H, CHAr), 6.46 (d, ⁴J = 2.2 Hz, 2H, CHAr), 5.04 (s, 4H, OCH₂Ar), 4.17 (q, ³J = 8.1 Hz, 2H, CH₂CH₃), 3.78 (t, ³J = 7.7 Hz, 1H, CH), 3.12 (d, ³J = 7.7 Hz, 2H, ArCH₂), 2.19 (s, 3H, CH₃), 1.24 (t, ³J = 8.1 Hz, 3H, CH₂CH₃). ¹³C NMR (100 MHz, CDCl₃): 202.4 (CO), 169.2 (CO), 160.2 (CAr), 140.8 (CAr), 137.0 (CPh), 128.7 (CHPh), 128.1 (CHPh), 127.6 (CHPh), 108.1 (CHAr), 100.6 (CHAr), 70.1 (OCH₂Ph), 61.6 (OCH₂), 61.1 (CHCO), 34.4 (CH₂Ar), 29.8 (COCH₃), 14.2 (CH₃). HRMS calcd. for C₂₇H₂₉O₅ [(M+H)⁺]: 433.2015, found: 433.2028.

Ethyl 2-acetylpent-4-enoate (**5d**).

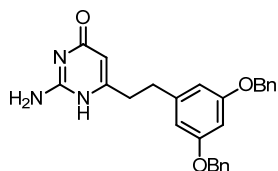


Prepared by following the general procedure B from a solution of **12** (1.40 g, 18.2 mmol) in THF (5 mL), purification by flash chromatography (hexane/CH₂Cl₂, 98:2) afforded **8d** (0.48 g, 15%) as a yellow oil, which showed the same spectroscopic properties as those previously reported.⁹ ¹H

⁹ a) Kenji, M.; Masaya, I. *Tetrahedron* **1987**, *43*, 45-58. b) Piva, O. *Tetrahedron* **1994**, *50*, 13687-13696.

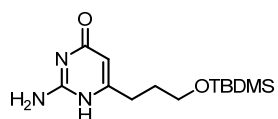
NMR (CDCl₃, 400 MHz): 5.76 (m, 1H, CH₂=CH), 5.08 (m, 2H, CH₂=CH), 4.20 (q, ³J = 10.0 Hz, 2H, OCH₂), 3.53 (t, ³J = 8.0 Hz, 1H, CH), 2.58 (t, ³J = 8.0 Hz, 2H, CH₂), 2.24 (s, 3H, CH₃), 1.27 (t, 3H, ³J = 10.0 Hz, CH₃).

2-Amino-6-(3,5-bis(benzyloxy)phenethyl)pyrimidin-4(1H)-one (9a).



Prepared by following the general procedure C from **8a** (803 mg, 1.98 mmol), yielding **9a** (717 mg, 85%) as a white solid. Mp 88-89 °C. ¹H NMR (300 MHz, DMSO-*d*₆): 7.52-7.32 (m, 10H, CHAr), 6.44-6.42 (m, 3H, CHAr), 5.76 (br s, 3H, NH, NH₂), 5.59 (s, 1H, CH), 4.95 (s, 4H, CH₂Ph), 2.82 (m, 2H, CH₂), 2.61 (m, 2H, CH₂). ¹³C NMR (125 MHz, DMSO-*d*₆): 169.2 (CNH), 163.3 (CO), 159.9 (CAr), 156.0 (CNH₂), 144.2 (CAr), 137.6 (CAr), 128.9 (CHBn), 128.6 (CHBn), 128.2 (CHBn), 107.9 (CHAr), 100.4 (CH), 99.9 (CHAr), 69.7 (CH₂Bn), 38.8 (CH₂), 34.2 (CH₂). ESI-MS (MeOH + 0.1% TFA, 90v): *m/z* 428.1 [(M+H)⁺]. Elemental analysis calcd. (%) for C₂₆H₂₅N₃O₃ (427.2): C 73.05, H 5.89, N 9.83; found C 73.38, H 6.00, N 9.85.

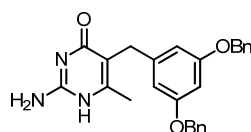
2-Amino-6-(3-((tert-butyl)dimethylsilyloxy)propyl)pyrimidin-4(1H)-one (9b).



Prepared by following the general procedure C from **8b** (90 mg, 0.313 mmol), yielding **9b** (48 mg, 55%) as a white solid. Mp 216-217 °C. ¹H NMR (500 MHz, CDCl₃): 6.42 (br s, 3H, NH, NH₂), 5.61 (s, 1H, CH), 3.64 (t, ³J = 5.6 Hz, 2H, OCH₂), 2.45 (t, ³J = 7.0 Hz, 2H, CH₂OTBMS), 1.83 (t, ³J = 7.0 Hz, 2H, CH₂), 0.88 (s, 9H, ^tBu), 0.04 (s, 6H, CH₃). ¹³C NMR (125 MHz, DMSO-*d*₆): 168.8 (CNH), 165.0 (CO), 156.9 (CNH₂), 99.6 (CHAr), 62.1 (OCH₂), 33.5 (CH₂), 31.9 (CH₂), 26.0 (CH₃, ^tBu), 18.1 (C, ^tBu), -3.7 (SiCH₃). EI-MS (4000v): *m/z* 566.9 [(2M+H)⁺], 284.1

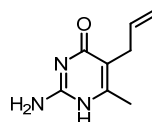
[(M+H)⁺], 152.2 [(M-OTBDMS)⁺]. HRMS calcd. for C₁₃H₂₆N₃O₂Si [(M+H)⁺]: 284.1795, found: 284.1791.

2-Amino-5-(3,5-bis(benzyloxy)benzyl)-6-methylpyrimidin-4(1H)-one (**9c**).



Prepared by following the general procedure C from **8c** (1.30 g, 3.00 mmol), yielding **9c** (1.21 g, 94%) as a white solid. Mp 223-225 °C. ¹H NMR (400 MHz, DMSO-*d*₆): 7.43-7.31 (m, 10H, CHAr), 6.46 (t, ⁴J = 2.2 Hz, 1H, CHAr), 6.41 (d, ⁴J = 2.2 Hz, 2H, CHAr), 6.30 (s, 1H, NH), 5.01 (s, 4H, OCH₂Ar), 3.55 (s, 2H, CH₂), 3.35 (br s, 2H, NH₂), 1.95 (s, 3H, CH₃). ¹³C NMR (100 MHz, DMSO-*d*₆): 159.3 (C), 143.7 (C), 137.1 (C), 128.3 (CH), 127.7 (CH), 127.7 (CH), 109.9 (C), 107.1 (CH), 99.0 (CH), 69.1 (CH₂), 30.0 (CH₂), 21.5 (CH₃). HRMS calcd. for C₂₆H₂₆N₃O₃ [(M+H)⁺]: 428.1974, found: 428.1972.

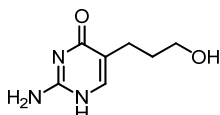
5-Allyl-2-amino-6-methylpyrimidin-4(1H)-one (**9d**).



Prepared by following the general procedure C from **8d** (481 mg, 2.83 mmol), yielding **9d** (266 mg, 57%) as a white solid, which showed the same spectroscopic properties as those previously reported.¹⁰ ¹H NMR (400 MHz, DMSO-*d*₆): 10.75 (br s, 1H, NH), 6.28 (br s, 2H, NH₂), 5.74 (ddt, ³J_{cis} = 10.0 Hz, ³J_{trans} = 16.8 Hz, ³J = 6.0 Hz, 1H, CH₂=CH), 4.95-4.90 (m, 2H, CH₂=CH), 3.06 (d, ³J = 6.0 Hz, 2H, CH₂), 2.01 (s, 3H, CH₃).

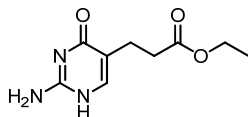
¹⁰ Yoshimoto, M.; Hansch, C. J. *Med. Chem.* **1976**, *19*, 71-98.

2-Amino-5-(3-hydroxypropyl)pyrimidin-4(1H)-one (**9e**).



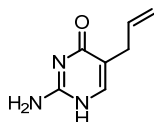
Prepared by following the general procedure C from **16** (585 mg, 4.57 mmol), affording **9e** (434 mg, 56%) as a white solid. Mp 178 °C. ¹H NMR (300 MHz, CDCl₃): 11.06 (br s, 1H, NH), 7.36 (s, 1H, CH), 6.47 (s, 2H, NH₂), 4.40 (br s, 1H, OH), 3.34 (t, ³J = 6.4 Hz, 2H, OCH₂), 2.19 (t, ³J = 7.3 Hz, 2H, CH₂Py), 1.54 (dt, ³J = 6.4 Hz, ³J = 7.3 Hz, 2H, CH₂). ¹³C NMR (75 MHz, CDCl₃): 163.9 (CO), 155.2 (CH), 151.9 (CNH₂), 114.5 (CCH₂), 60.4 (CH₂OH), 32.0 (CH₂), 23.2 (CH₂). ESI-MS (MeOH + 0.1% TFA, 60v): *m/z* 169.1 [(M)⁺]. HRMS calcd. for C₇H₁₂N₃O₂ [(M+H)⁺]: 170.0630, found: 170.0930.

Ethyl 3-(2-amino-4-oxo-1,4-dihydropyrimidin-5-yl)propanoate (**9f**).



Prepared by following the general procedure C from **17** (1.02 g, 4.7 mmol), affording **9f** (479 mg, 51%) as a white solid. Mp 216 °C. ¹H NMR (500 MHz, DMSO-*d*₆): 10.86 (s, 1H, NH), 7.40 (s, 1H, CH), 6.34 (s, 2H, NH), 4.04 (q, ³J = 7.0 Hz, 2H, OCH₂CH₃), 2.47-2.42 (m, 4H, CH₂), 1.16 (t, ³J = 7.0 Hz, 3H, CH₃). ¹³C NMR (125 MHz, DMSO-*d*₆): 172.9 (CO), 162.8 (CO), 155.6 (CNH₂), 154.1 (CH), 113.1 (C), 72.7 (OCH₂), 33.3 (CH₂CO), 23.1 (CH₂), 14.6 (CH₃). ESI-MS (MeOH + 0.1% TFA, 4000v): *m/z* 844.6 [(4M)⁺], 633.8 [(3M)⁺], 422.9 [(2M)⁺], 212.1 [(M+H)⁺], 166.1 [(M-EtOH)⁺]. Elemental analysis calcd. (%) for C₉H₁₃N₃O₃ (211.1): C 51.18, H 6.20, N 19.89; found C 50.87, H 6.14, N 19.88.

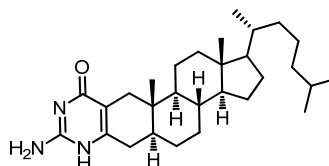
5-Allyl-2-aminopyrimidin-4(1H)-one (**9g**).



Prepared by following the general procedure C from **18** (1.65 g, 10.6 mmol),

affording **9g** (450 mg, 28% as a mixture of 70:30 *keto/enol*) as a white solid. Mp 182 °C. ¹H NMR (400 MHz, DMSO-*d*₆): 7.65 (t, ⁴J = 0.8 Hz, 1H, CH *enol*), 7.45 (br s, 1H, OH *enol*), 7.37 (t, ⁴J = 0.8 Hz, 1H, CH *keto*), 6.63 (br s, 1H, NH *keto*), 5.99-5.82 (m, 1H, CH₂=CH *keto/enol*), 5.13 (ddt, ³J_{trans} = 17.2 Hz, ⁴J = 2.0 Hz, 1H, CH₂=CH *enol*), 5.07 (ddt, ³J_{cis} = 9.2 Hz, ⁴J = 1.6 Hz, 1H, CH₂=CH *enol*), 5.02 (ddt, ³J_{trans} = 17.2 Hz, ⁴J = 2.0 Hz, 1H, CH₂=CH *keto*) 4.98 (ddt, ³J_{cis} = 9.2 Hz, ⁴J = 1.6 Hz, 1H, CH₂=CH *enol*), 3.36 (br s, 2H, NH₂), 3.03 (dq, ³J = 6.4 Hz, ⁴J = 1.6 Hz, 2H, CH₂ *enol*), 2.94 (dq, ³J = 6.4 Hz, ⁴J = 1.6 Hz, 2H, CH₂ *keto*). ¹³C NMR (100 MHz, DMSO-*d*₆): 181.0 (C *enol*), 156.1 (C *keto*), 137.3 (CH₂=CH *keto/enol*), 136.0 (CH *keto*), 135.3 (CH *enol*), 119.8 (CNH₂ *keto*), 118.5 (CNH₂ *keto*), 117.0 (C *enol*), 115.6 (CH₂=CH *keto/enol*), 112.9 (C *keto*), 31.9 (CH₂ *enol*), 31.0 (CH₂ *keto*). HRMS calcd. for C₇H₁₀N₃O [(M+H)⁺]: 152.0824, found: 152.0823.

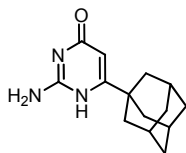
(3aS,3bR,5aS,11aS,11bS,13aR)-8-Amino-11a,13a-dimethyl-1-((R)-6-methylheptan-2-yl)-3,3a,3b,4,5,5a,6,7,11,11a,11b,12,13,13a-tetradecahydro-1H-cyclopenta[5,6]naphtho[1,2-g]quinazolin-10(2H)-one (9h).



Prepared by following the general procedure C from **19** (300 mg, 0.65 mmol), affording **9h** (243 mg, 82%) as a white solid. Mp > 300 °C. ¹H NMR (400 MHz, DMSO-*d*₆): 6.16 (br s, 1H, NH), 3.35 (br s, 2H, NH₂), 2.40 (d, ²J_{gem} = 16.4 Hz, 1H, H-1a), 2.13 (dd, ²J_{gem} = 17.6 Hz, ³J = 4.4 Hz, 1H, H-4a), 2.02-1.96 (m, 2H, H-4b, H-12a), 1.84-1.72 (m, 1H, H-16a), 1.65-1.62 (m, 2H, H-1b, H-7a), 1.59-0.73 (m, 22H, H-5, H-6, H-7b, H-8, H-9, H-11, H-12b, H-14, H-15, H-16b, H-17, H-20, H-22, H-23, H-24, H-25), 0.99 (d, ³J = 6.0 Hz, 3H, CH₃-21), 0.85 (d, ³J = 6.8 Hz, 3H, CH₃-26), 0.84 (d, ³J = 6.8 Hz, 3H, CH₃-27), 0.66 (s, 3H, CH₃-19), 0.64 (s, 3H, CH₃-18). ¹³C NMR (100 MHz, DMSO-*d*₆): 159.5 (CO), 158.8 (C-3), 158.1 (CNH₂), 106.7 (C-2), 56.5 (CH-14 or CH-17), 56.2 (CH-14 or CH-17), 53.9 (CH-9), 42.6 (C-13), 41.7 (CH-5), 40.1 (CH₂-12), 39.9 (CH₂-4), 39.4 (CH₂-24), 36.9 (CH₂-1),

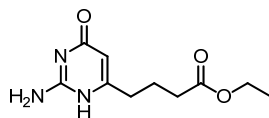
36.1 (CH₂-22), 35.8 (CH-20), 35.6 (CH-8), 34.9 (C-10), 31.8 (CH₂-7), 28.6 (CH₂-16), 28.3 (CH₂-6), 27.9 (CH-25), 24.4 (CH₂-15), 23.7 (CH₂-23), 23.2, 22.9 (CH₃-26, CH₃-27), 21.3 (CH₂-11), 19.0 (CH₃-21), 12.3 (CH₃-18), 12.1 (CH₃-19). ESI-MS: *m/z* 476.3 [(M+Na)⁺], 454.3 [(M+H)⁺]. HRMS calcd. for C₂₉H₄₈N₃O [(M+H)⁺]: 454.3997, found: 454.3803.

6-(Adamantan-1-yl)-2-aminopyrimidin-4(1H)-one(9k).



Prepared by following the general procedure C from **23a** (9.00 g, 36.00 mmol), affording **9k** (8.10 g, 92%) as a white solid, which showed the same spectroscopic properties as those previously reported.¹¹ ¹H NMR (400 MHz, DMSO-*d*₆): 10.52 (s, 1H, NH), 6.32 (s, 2H, NH₂), .5.35 (s, 1H, CH), 2.00 (br s, 3H, CH_{adam}), 1.81 (br s, 6H, CH_{2adam}), 1.68 (m, 6H, CH_{2adam}).

Ethyl 4-(2-amino-6-oxo-3,6-dihydropyrimidin-4-yl)butanoate (9l).

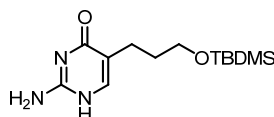


Prepared by following the general procedure C from **23b** (2.00 mL, 8.01 mmol), yielding **9l** (919 mg, 51%) as a white solid. Mp 146-147 °C. ¹H NMR (500 MHz, DMSO-*d*₆): 6.47 (br s, 3H, NH₂, NH), 5.36 (s, 1H, CH), 4.04 (q, ³J = 7.1 Hz, 2H, CH₂CH₃), 2.27 (q, ³J = 7.5 Hz, 4H, CH₂), 1.79 (q, ³J = 7.5 Hz, 2H, CH₂), 1.17 (t, ³J = 7.1 Hz, 3H, CH₃). ¹³C NMR (125 MHz, DMSO-*d*₆): 174.8 (C), 173.1 (C), 156.2 (C), 100.4 (CH), 60.2 (CH₂), 33.4 (CH₂), 33.4 (CH₂), 23.3 (CH₂), 14.6 (CH₃). ESI-MS (CH₃CN/H₂O, 0.1% formic acid): *m/z* 226.1 [(M+H)⁺]. HRMS calcd. for

¹¹ Orzeszko, B.; Kazimierczuk, Z.; Maurin, J. K.; Laudy, A. E.; Starosciak, B. J.; Vilpo, J.; Vilpo, L.; Balzarini, J.; Orzeszko, A. *Il Farmaco* **2004**, *59*, 929-937.

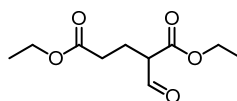
$C_{10}H_{16}N_3O_3$ [(M+H)⁺]: 226.1192, found: 226.1188.

2-Amino-5-(3-((*tert*-butyldimethylsilyloxy)propyl)pyrimidin-4(1H)-one (9o).



A solution of TBDMSCl (245 mg, 1.63 mmol), imidazole (222 mg, 3.26 mmol) and **9e** (250 mg, 1.48 mmol) in DMF (6 mL) was heated at 60 °C in a sealed tube for 24 h. The solvent was removed in vacuo and water was added to the residue. The precipitate was filtered off and washed with cold Et₂O, yielding **9o** (350 mg, 83%) as a white solid. Mp 218 °C. ¹H NMR (500 MHz, DMSO-*d*₆): 7.43 (s, 1H, CH), 6.23 (br s, 3H, NH), 3.63 (t, ³J = 6.3 Hz, 2H, OCH₂), 2.39 (t, ³J = 7.0 Hz, 2H, CH₂OTBDMS), 1.72 (t, ³J = 6.3 Hz, 2H, CH₂), 0.89 (s, 9H, ^tBu), 0.05 (s, 6H, CH₃). ¹³C NMR (125 MHz, DMSO-*d*₆): 172.3 (CO), 154.9 (CH), 153.0 (CNH₂), 114.0 (C), 61.9 (OCH₂), 31.4 (CH₂), 25.8 (CH₃), 23.0 (CH₂), 17.9 (SiC), -5.3 (CH₃). EI-MS (MeOH, 4000v): *m/z* 567.3 [(2M+H)⁺], 284.3 [(M+H)⁺], 152.2 [(M-OTBDMS)⁺]. Elemental analysis calcd. (%) for C₁₃H₂₅N₃O₂Si (283.2): C 55.09, H 8.89, N 14.82; found C 54.64, H 8.70, N 15.11.

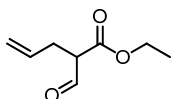
Diethyl 2-formylpentanedioate (17).



A mixture of **14** (5.00 g, 26.6 mmol) and ethyl formate (1.97 g, 26.6 mmol) in 15 mL of dry Et₂O was added dropwise to a suspension of NaH (60% dispersion in mineral oil, 1.23 g, 30.8 mmol) in dry Et₂O. EtOH (0.2 mL) was added as an activator for the reaction and the mixture was stirred overnight under an argon atmosphere. The reaction was quenched with sat. aq. NH₄Cl (100 mL) and the aqueous phase was extracted with Et₂O (3 x 50 mL). The organic phase was dried (MgSO₄) and the solvent was evaporated under reduced pressure. The residual oil was purified by flash chromatography (hexane/EtOAc, 9:1), affording **17** (3.16 g, 55%) as a

colorless oil (as a 80:20 mixture of *enol/keto* tautomers), which showed the same spectroscopic properties as those previously reported.¹² ¹H NMR (400 MHz, CDCl₃): 11.07 (d, ³J = 12.6 Hz, 1H, OH), 9.35 (s, 1H, CHO), 6.78 (d, ³J = 11.6 Hz, 1H, CHOH), 3.89 (q, ³J = 7.2 Hz, 2H, OCH₂), 3.73 (q, ³J = 7.2 Hz, 2H, OCH₂), 3.11 (t, ³J = 8.7 Hz, 1H, CHCO), 2.13 (q, ³J = 8.7 Hz, 2H, CH₂ keto), 2.04 (m, 4H (keto), 2H (enol), CH₂), 0.98-0.70 (m, 6H, CH₃).

Ethyl 2-formylpent-4-enoate (**18**).



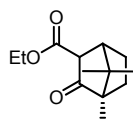
A solution of LDA in THF/*n*-heptane (2M, 25.4 mL, 50.8 mmol) was diluted in THF (300 mL) at -78 °C and stirred for a few minutes. Compound **15** (6.00 g, 45.4 mmol) was added through a cannula and the solution was stirred for 10 min. Then ethyl formate (3.80 g, 50.8 mmol) was added and the reaction mixture was stirred at -78 °C for 1.5 h and allowed to warm to room temperature. The solvent was evaporated under reduced pressure and CH₂Cl₂ and 3M HCl were added. The organic layer was removed and the aqueous phase was extracted with CH₂Cl₂ (x 3). The organic layer was washed with brine, dried (MgSO₄) and concentrated to dryness. The crude mixture was purified by distillation (80 °C, 2 mbar), yielding **18** (4.10 g, 58%) as light yellow oil (as a 75:25 mixture of *enol/keto* tautomers), which showed the same spectroscopic properties as those previously reported.¹³ ¹H NMR (400 MHz, CDCl₃): 11.42 (d, ³J = 11.6 Hz, 1H, OH), 9.66 (s, 1H, CHO), 6.95 (d, ³J = 11.6 Hz, 1H, CHOH), 5.75 (m, 1H, CH₂=CH keto/enol), 5.03 (m, 2H, CH₂=CH keto/enol), 4.18 (q, ³J = 7.2 Hz, 2H, OCH₂), 3.33 (t, ³J = 6.8 Hz, 1H, CHCO), 2.76 (d, ³J = 7.6 Hz, 2H, CH₂ enol), 2.57 (t, ³J = 7.6 Hz, 2H, CH₂ keto), 1.24 (t, ³J = 7.2

¹² Wrigglesworth, R.; Inglis, W. D.; Livingstone, D. B.; Suckling, C. J.; Wood, H. C. S. *J. Chem. Soc., Perkin Trans. 1* **1984**, 959-963.

¹³ Durrwachter, J. R.; Wong, C.-H. *J. Org. Chem.* **1988**, 53, 4175-4181.

Hz, 3H, CH₃).

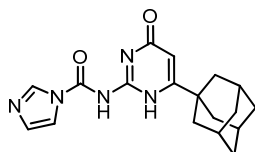
(4R)-Ethyl-4,7,7-trimethyl-3-oxobicyclo[2.2.1]heptane-2-carboxylate (20).



A suspension of NaH (60% dispersion in mineral oil, 1.54 g, 38.6 mmol) in 150 mL of dry THF was refluxed under an argon atmosphere. Then, a solution of (1R)-(+)-camphor (5.00 g, 32.2 mmol) in 40 mL of dry THF was added dropwise through an addition funnel for 30 min. The reaction was refluxed for 30 min and another solution of diethyl carbonate (4.7 mL, 38.6 mmol) in 10 mL of dry THF was added dropwise in the same way. The reaction was refluxed overnight. The solvent was removed under reduced pressure; the residue was dissolved in CH₂Cl₂ and washed with sat. aq. NH₄Cl. The aqueous phase was extracted with CH₂Cl₂ (3 x 50 mL), the organic phase was dried (Na₂SO₄) and the solvent was evaporated under reduced pressure. The crude was purified by flash chromatography (hexane/EtOAc, 9:1), affording compound **20** (3.10 g, 43%) as a yellow oil (as a 80:20 mixture of *endo/exo* isomers), which showed the same spectroscopic properties as those previously reported.¹⁴ ¹H NMR (400 MHz, CDCl₃): 4.11 (q, ³J = 7.2 Hz, 2H, OCH₂ *endo*), 4.09 (q, ³J = 7.2 Hz, 2H, OCH₂ *exo*), 3.24 (ddd, ³J = 4.8 Hz, ⁴J = 2.0 Hz, ⁴J = 0.7 Hz, 1H, CH *endo*), 2.79 (s, 1H, CH *exo*), 2.56 (d, ³J = 4.3 Hz, 1H, CH bridge *exo*), 2.34 (t, ³J = 4.8 Hz, 1H, CH bridge *endo*), 1.85-1.74 (m, 1H, CH_{eq}CH bridge *endo/exo*), 1.66-1.58 (m, 1H, CH_{eq}CCH₃ *endo/exo*), 1.52-1.41 (m, 2H, CH_{ax} *endo/exo*), 1.20 (t, ³J = 7.2 Hz, 3H, CH₃ *exo*), 1.19 (t, ³J = 7.2 Hz, 3H, CH₃ *endo*), 0.93 (s, 3H, CH₃ *endo*), 0.90 (s, 3H, CH₃ *exo*), 0.87 (s, 3H, CH₃ *exo*), 0.86 (s, 3H, CH₃ *endo*), 0.79 (s, 3H, CH₃ *endo*), 0.70 (s, 3H, CH₃ *exo*).

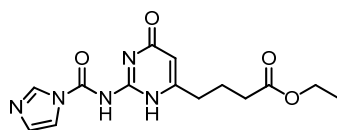
¹⁴ a) Paquette, L. A.; Dahnke, K.; Doyon, J.; He, W.; Wyant, K.; Friedrich, D. *J. Org. Chem.* **1991**, *56*, 6199-6205. b) Shumway, W. W.; Dalley, N.; Birney, D. M. *J. Org. Chem.* **2001**, *66*, 5832-5839.

***N*-(6-(Adamantan-1-yl)-4-oxo-1,4-dihydropyrimidin-2-yl)-1H-imidazole-1-carboxamide (**24a**).**



Prepared by following the general procedure D from **9k** (1.00 g, 4.10 mmol), affording **24a** (1.25 g, 90%) as a white solid. Mp 247-249 °C. ¹H NMR (400 MHz, CDCl₃): 8.61 (s, 1H, NCHN), 7.71 (s, 2H, NH), 7.58 (s, 1H, CHN), 7.13 (s, 1H, CHN), 5.88 (s, 1H, CH), 2.18 (br s, 3H, CH), 1.90 (br s, 6H, CH₂), 1.81 (m, 6H, CH₂). ¹³C NMR (100 MHz, CDCl₃): 175.4 (C), 174.7 (C), 166.3 (C), 161.5 (C), 137.8 (CH), 129.5 (CH), 116.9 (CH), 102.3 (CH), 40.0 (CH₂), 36.6 (C), 36.0 (CH₂), 27.8 (CH). MALDI-TOF (dithranol): *m/z* 340.2 [(M+H)⁺]. Elemental analysis calcd. (%) for C₁₈H₂₁N₅O₂ (339.4): C 63.70, H 6.24, N 20.64; found C 63.88, H 6.33, N 20.57.

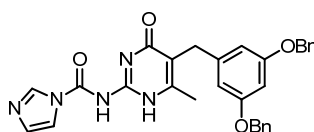
Ethyl 4-(2-(1H-imidazole-1-carboxamido)-6-oxo-3,6-dihydropyrimidin-4-yl)butanoate (24b**).**



Prepared by following the general procedure D from **9l** (227 mg, 1 mmol), affording **24b** (299 mg, 93%) as a white solid. Mp > 300 °C (dec.). ¹H NMR (400 MHz, CDCl₃): 9.83 (s, 1H, NCHN), 7.65 (s, 1H, CHN), 7.05 (s, 1H, NCH), 5.82 (s, 1H, CH), 4.16 (q, ³J = 7.0 Hz, 2H, CH₂CH₃), 2.74 (t, ³J = 7.6 Hz, 2H, COCH₂), 2.46 (t, ³J = 7.0 Hz, 2H, CCH₂), 2.10 (q, ³J = 7.4 Hz, 2H, CH₂), 1.27 (t, ³J = 7.0 Hz, 3H, CH₃). ¹³C NMR (100 MHz, CDCl₃): 174.8 (C), 160.4 (C), 156.8 (C), 156.4 (C), 137.7 (CH), 127.6 (CH), 117.5 (CH), 104.0 (CH), 60.6 (CH₂), 32.7 (CH₂), 31.6 (CH₂), 22.3 (CH₂), 14.6 (CH₃). MALDI-TOF: *m/z* 342.8 [(M+Na)⁺]. ESI-MS (CH₂Cl₂/MeOH, 0.1% formic acid): *m/z*: 284.1 [(M+H-imidazole+MeOH)⁺], 226.1 [(M+H-imidazole-CO)⁺]. Elemental analysis calcd. (%) for C₁₄H₁₇N₅O₄

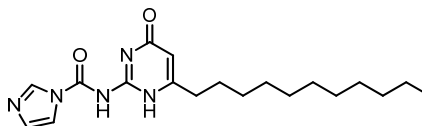
(319.3) • C₃H₄N₂: C, 52.71; H, 5.46; N, 25.31; found C, 52.22; H, 5.80; N, 25.08.

N-(5-(3,5-Bis(benzyloxy)benzyl)-6-methyl-4-oxo-1,4-dihydropyrimidin-2-yl)-1H-imidazole-1-carboxamide (24c).



Prepared by following the general procedure D from **9c** (708 mg, 1.90 mmol), affording **24c** (969 mg, 98%) as a white solid. Mp 252 °C. ¹H NMR (400 MHz, DMSO-*d*₆): 7.71 (s, 1H, NCHN), 7.42-7.30 (m, 10H, CHAr), 7.05 (s, 2H, CHN), 6.46 (t, ⁴J = 2.2 Hz, 1H, CHAr), 6.41 (d, ⁴J = 2.2 Hz, 2H, CHAr), 6.31 (s, 2H, NH), 5.01 (s, 4H, OCH₂), 3.56 (s, 2H, CH₂), 1.95 (s, 3H, CH₃). ¹³C NMR (100 MHz, DMSO-*d*₆): 163.5 (C), 159.3 (C), 153.4 (C), 143.7 (C), 142.3 (C), 137.0 (C), 135.1 (CH), 128.3 (CH), 127.7 (CH), 127.7 (CH), 121.6 (CH), 110.0 (C), 107.1 (CH), 99.3 (CH), 69.1 (CH₂), 30.0 (CH₂), 21.2 (CH₃). MALDI-TOF (DCM): *m/z* 544.1 [(M+Na)⁺], 522.1 [(M+H)⁺], 454.1 [(M+H-imidazole)⁺]. Elemental analysis calcd. (%) for C₃₀H₂₇N₅O₄ (521.2): C 69.08, H 5.22, N 13.43; found C 68.95, H 5.27, N 13.58.

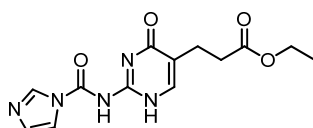
N-(4-Oxo-6-undecyl-1,4-dihydropyrimidin-2-yl)-1H-imidazole-1-carboxamide (24d).



Prepared by following the general procedure D from **9j** (800 mg, 1.89 mmol), affording **24d** (638 mg, 94%) as a white solid. Mp 179 °C. ¹H NMR (400 MHz, CDCl₃): 8.88 (s, 1H, NCHN), 7.67 (s, 1H, CHN), 7.04 (s, 1H, CHN), 5.83 (s, 1H, CH), 2.67 (t, ³J = 7.6 Hz, 2H, CH₂), 1.78 (q, ³J = 7.6 Hz, 2H, CH₂), 1.51-1.21 (m, 16H, CH₂), 0.90 (t, ³J = 7.7 Hz, 3H, CH₃). ¹³C NMR (125 MHz, DMSO-*d*₆): 161.0 (C), 157.2 (C), 156.7 (C), 135.0 (CH), 122.0 (CH), 117.6 (CH), 103.5 (CH), 32.9 (CH₂), 31.9 (CH₂), 29.6 (CH₂), 29.4 (CH₂), 29.3 (CH₂), 29.2 (CH₂), 29.0 (CH₂),

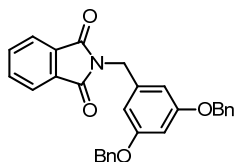
27.5 (CH₂), 22.7 (CH₂), 14.1 (CH₃). HRMS calcd. for C₁₆H₂₆N₃O₂ [(M+H-imidazole)⁺]: 292.2025, found: 292.2025. Elemental analysis calcd. (%) for C₁₉H₂₉N₅O₂ (359.2): C 63.48, H 8.13, N 19.48; found C 63.51, H 8.14, N 19.43.

Ethyl 3-(2-(1H-imidazole-1-carboxamido)-4-oxo-1,4-dihydropyrimidin-5-yl)propanoate (24e).



Prepared by following the general procedure D from **9f** (50 mg, 0.237 mmol), affording **24e** (57 mg, 76%) as a white solid. Mp 142 °C. ¹H NMR (500 MHz, CDCl₃): 8.83 (s, 1H, NCHN), 7.77 (s, 1H, NH), 7.66 (s, 1H, CHN), 7.50 (s, 1H, CHN), 7.17 (s, 1H, CH), 7.12 (s, 1H, NH), 4.18 (q, ³J = 7.1 Hz, 2H, OCH₂CH₃), 2.78 (t, ³J = 6.6 Hz, 2H, COCH₂), 2.70 (t, ³J = 6.6 Hz, 2H, CH₂), 1.29 (t, ³J = 7.1 Hz, 3H, CH₃). ¹³C-RMN (125 MHz, CDCl₃): 172.8 (CO), 161.8 (CO), 157.0 (C), 156.2 (CH), 138.0 (C), 135.0 (C), 128.5 (CH), 118.0 (CH), 117.5 (CH), 60.6 (CH₂), 32.0 (CH₂), 22.7 (CH₂), 14.2 (CH₃). MALDI-TOF (dithranol/CH₂Cl₂, +ve): *m/z* 306.2 [(M+H)⁺], 238.1 [(M-imidazole)⁺]. Elemental analysis calcd. (%) for C₁₃H₁₅N₅O₄ (305.1): C 51.14, H 4.95, N 22.94; found C 51.09, H 5.09, N 22.80.

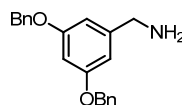
2-(3,5-Bis(benzyloxy)benzyl)isoindoline-1,3-dione (25).



A suspension of potassium phthalimide (0.99 g, 5.22 mmol) and **10** (1.00 g, 2.61 mmol) in DMF (15 mL) in a sealed tube was heated at 80 °C for 2 days. The mixture was cooled to room temperature and water (100 mL) was added. The emulsion was extracted with CH₂Cl₂ (3 x 100 mL) and the combined organic layers were washed with 2M HCl (3 x 100 mL), dried (MgSO₄) and concentrated to dryness. The residue was purified by

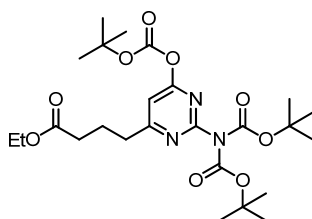
crystallization in a mixture of hexane/Et₂O. The solid was filtered off and dried under vacuum, affording **25** (906 mg, 77%) as a beige solid. ¹H NMR (400 MHz, CDCl₃): 7.74 (m, 2H, CHAr), 7.65 (m, 2H, CHAr), 7.34-7.19 (m, 10H, CHAr), 6.59 (d, ⁴J = 2.3 Hz, 2H, CHAr), 6.44 (t, ⁴J = 2.3 Hz, 1H, CHAr), 4.92 (s, 4H, OCH₂), 4.70 (s, 2H, NCH₂). ¹³C NMR (100 MHz, CDCl₃): 168.0 (C), 160.1 (C), 138.6 (C), 136.7 (C), 134.0 (CH), 132.1 (C), 128.6 (CH), 128.0 (CH), 127.6 (CH), 123.4 (CH), 107.4 (CH), 101.4 (CH), 70.1 (CH₂), 41.6 (CH₂). HRMS calcd. for C₂₉H₂₃NO₄Na [(M+Na)⁺]: 472.1525; found: 472.1509.

3,5-Bis(benzyloxy)phenylmethanamine (**26**).



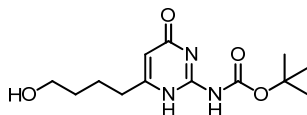
A suspension of **25** (775 mg, 1.72 mmol) in EtOH (40 mL) was refluxed and then hydrazine monohydrate (1.42 g, 27.55 mmol) was added. The mixture was refluxed for 2 h and then it was cooled to room temperature. 20% aq. KOH (20 mL) was added and the aqueous phase was extracted with CH₂Cl₂ (3 x 50 mL). The combined organic phases were washed with water and brine, dried (MgSO₄) and the solvent was evaporated under reduced pressure, yielding **26** (548 mg, 99%) as a brown-yellow oil. ¹H NMR (400 MHz, CDCl₃): 7.48-7.36 (m, 10H, CHAr), 6.64 (d, ⁴J = 1.8 Hz, 2H, CHAr), 6.56 (t, ⁴J = 1.8 Hz, 1H, CHAr), 5.08 (s, 4H, OCH₂), 3.85 (s, 2H, NCH₂), 1.80 (br s, 2H, NH₂). ¹³C NMR (100 MHz, CDCl₃): 160.2 (C), 145.7 (C), 137.0 (C), 128.6 (CH), 128.0 (CH), 127.6 (CH), 106.2 (CH), 100.5 (CH), 70.1 (CH₂), 46.6 (CH₂). HRMS calcd. for C₂₁H₂₂NO₂ [(M+H)⁺]: 320.1651, found: 320.1639

Compound 27.



A mixture of **91** (637 mg, 2.83 mmol), Boc₂O (2.60 g, 11.89 mmol), triethylamine (0.6 mL, 4.25 mmol) and a catalytic amount of DMAP in THF (20 mL) was stirred at 40 °C for two days. The solvent was evaporated and the residue was purified by column chromatography on silica gel (hexane/EtOAc, 5:2), yielding **27** (694 mg, 47%) as a pale yellow oil. ¹H NMR (300 MHz, CDCl₃): 6.94 (s, 1H, CHAr), 4.12 (q, ³J = 7.0 Hz, 2H, CH₂), 2.83 (t, ³J = 8.0 Hz, 2H, CH₂), 2.35 (t, ³J = 8.0 Hz, 2H, CH₂), 2.05 (quint., ³J = 8.0 Hz, 2H, CH₂), 1.54 (s, 9H, CH₃), 1.41 (s, 18H, CH₃), 1.23 (t, ³J = 7.0 Hz, 3H, CH₃). ¹³C NMR (75 MHz, CHCl₃): 174.6 (C), 172.8 (C), 166.0 (C), 158.1 (C), 150.1 (C), 149.0 (C), 108.5 (CH), 85.1 (C), 83.3 (C), 60.4 (CH₂), 36.5 (CH₂), 33.2 (CH₂), 27.8 (CH₃), 27.5 (CH₃), 23.5 (CH₂), 14.2 (CH₃). ESI-MS: *m/z* 526.3 [(M+H)⁺], 426.2 [(M+H-Boc)⁺], 326.2 [(M+H-2Boc)⁺], 226.1 [(M+H-3Boc)⁺]. HRMS calcd. for C₂₅H₄₀N₃O₉ [M+H]: 526.2765, found: 526.2753.

tert-Butyl (6-(4-hydroxybutyl)-4-oxo-1,4-dihydropyrimidin-2-yl)carbamate (**28**).

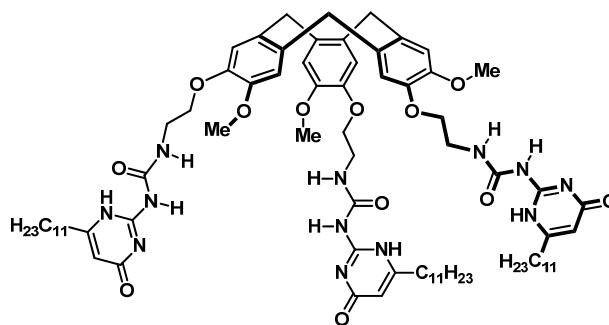


A solution of DIBAL-H (1M in CH₂Cl₂, 6.6 mL, 6.60 mmol) was added dropwise to a solution of **27** (694 mg, 1.32 mmol) in dry CH₂Cl₂ (6 mL) at -78 °C under argon. The reaction mixture was stirred at -78 °C for 5 h and then allowed to warm to room temperature overnight. The mixture was diluted with CH₂Cl₂, washed with sat. aq. NH₄Cl and brine, dried (MgSO₄) and the solvent was evaporated. Purification by column chromatography on silica gel

(hexane/EtOAc, 7:3) gave **28** (208 mg, 56%) as a pale greenish oil. The final product is a mixture of ~25:75 *enol/keto* (as determined by NMR analysis). ^1H NMR (500 MHz, CDCl_3): 5.90 (s, 1H, CH *keto*), 5.60 (s, 1H, CH *enol*), 3.62 (t, $^3J = 8.0$ Hz, 2H, CH_2), 2.44 (m, 2H, CH_2), 1.67 (m, 2H, CH_2), 1.58 (m, 2H, CH_2), 1.50 (s, 9H, CH_3). ^{13}C NMR (125 MHz, CDCl_3): 174.2 (C), 168.6 (C), 161.8 (C), 155.9 (C), 152.8 (C), 152.7 (C), 150.1 (C), 106.7 (CH), 100.2 (CH), 84.3 (C), 62.2 (CH_2), 60.4 (CH_2), 36.7 (CH_2), 32.0 (CH_2), 31.8 (CH_2), 29.7 (CH_2), 28.1 (CH_2), 28.0 (CH_3), 24.4 (CH_3), 24.2 (CH_3). ESI-MS: m/z 284.1 [(M+H) $^+$]. HRMS calcd. for $\text{C}_{13}\text{H}_{22}\text{N}_3\text{O}_4$ [(M+H) $^+$]: 284.1610, found: 284.1620.

VI.3 SYNTHESIS CHAPTER III

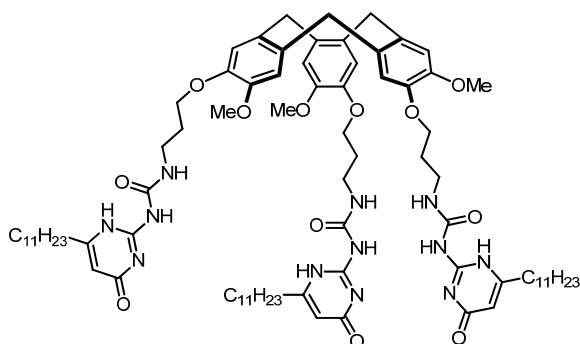
1,1',1''-(((3,8,13-Trimethoxy-10,15-dihydro-5H-tribenzo[*a,d,g*]cyclononene-2,7,12-triyl)tris(oxy))tris(ethane-2,1-diyl)tris(3-(4-oxo-6-undecyl-1,4-dihydropyrimidin-2-yl)urea) (**5a**).



A suspension of imidazolide **24d** (200 mg, 0.56 mmol) and CTV-triamino **29** (100 mg, 0.19 mmol) in 10 mL of CH_2Cl_2 was stirred at 50 °C in a sealed tube for 2 days. The reaction mixture was subsequently added to 25 mL of methanol under vigorous stirring to result in a white solid. After sonicating the suspension for 1 minute, the solid was allowed to decant. The solvent was removed and the remaining solid was washed three times following the same procedure. The resulting white solid was dried under air to yield **5a** (247 mg, 94%). Mp 140-142 °C. ^1H NMR (400 MHz, $\text{DMSO}-d_6$): 11.48 (s, 3H, NH), 9.79 (s, 3H, NH), 7.66 (s, 3H, NH), 7.13 (s, 3H, CHAr), 7.08 (s, 3H, CHAr), 5.75 (s, 3H,

CH), 4.68 (d, $^2J = 13.2$ Hz, 3H, ArCH₂Ar), 3.50 (d, $^2J = 13.2$ Hz, 3H, ArCH₂Ar), 4.03 (m, 6H, OCH₂), 3.69 (s, 9H, OCH₃), 3.47 (m, 6H, CH₂NH), 2.30 (t, $^3J = 7.6$ Hz, 6H, CCH₂), 1.51 (m, 6H, CCH₂CH₂), 1.18 (m, 48H, CH₂), 0.83 (t, $^3J = 6.8$ Hz, 9H, CH₃). ¹³C NMR (125 MHz, DMSO-*d*₆): 161.2 (C), 154.6 (C), 151.0 (C), 147.8 (C), 146.1 (C), 132.6 (C), 131.9 (C), 117.1 (C), 116.2 (CH), 114.4 (CH), 103.5 (CH), 67.9 (CH₂), 55.8 (CH₃), 35.8 (CH₂), 34.7 (CH₂), 30.7 (CH₂), 28.4 (CH₂), 28.3 (CH₂), 28.2 (CH₂), 28.1 (CH₂), 27.9 (CH₂), 26.7 (CH₂), 21.5 (CH₂), 13.2 (CH₃). ESI-MS: *m/z* 1412 [(M+H)⁺]. Elemental analysis calcd. (%) for C₇₈H₁₁₄N₁₂O₁₂ (1411.8): C 66.36, H 8.14, N 11.91; found C 66.27, H 8.47, N 11.73.

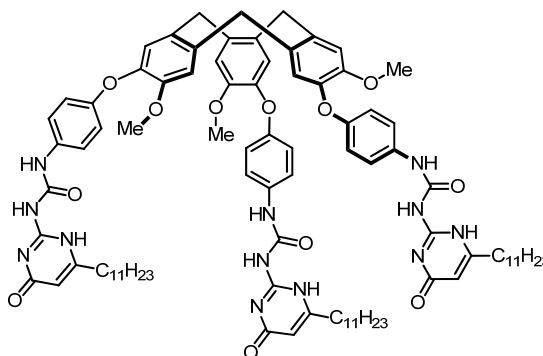
1,1',1''-(((3,8,13-Trimethoxy-10,15-dihydro-5H-tribenzo[*a,d,g*]cyclononene-2,7,12-triyl)tris(oxy))tris(propane-3,1-diyl))tris(3-(4-oxo-6-undecyl-1,4-dihydropyrimidin-2-yl)urea) (5b).



CTV-NH₂ **31** (25 mg, 0.04 mmol) and **24d** (45 mg, 0.12 mmol) were reacted following general procedure F to yield compound **5b** (45 mg, 75%) as a white solid. Mp > 400 °C. ¹H NMR (500 MHz, DMSO-*d*₆+CDCl₃): 9.73 (br s, 3H, NH), 7.02 (s, 3H, CHAR), 6.99 (s, 3H, CHAR), 4.68 (d, $^2J_{\text{gem}} = 13.9$ Hz, 3H, ArCH₂Ar), 4.02 (m, 3H, CH₂), 3.94 (m, 3H, CH₂), 3.70 (s, 9H, CH₃), 3.50 (d, $^2J_{\text{gem}} = 13.9$ Hz, 3H, ArCH₂Ar), 2.26, (m, 6H, CH₂), 1.90 (m, 6H, CH₂), 1.50 (m, 6H, CH₂), 1.22 (m, 54H, CH₂), 0.84 (t, $^3J = 7.0$ Hz, 9H, CH₃). ¹³C NMR (125 MHz, DMSO-*d*₆): 168.8 (C), 161.8 (C), 155.3 (C), 151.7 (C), 148.5 (C), 147.1 (C), 132.8 (C), 132.2 (C), 115.8 (CH), 114.2 (CH), 104.6 (CH), 66.6 (CH₂), 55.9 (CH₃), 36.8 (CH₂), 35.8 (CH₂), 31.9 (CH₂), 29.6 (CH₂), 29.5 (CH₂), 29.4 (CH₂), 29.3

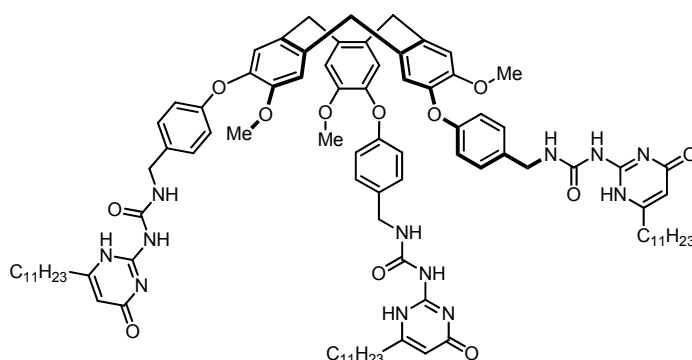
(CH₂), 29.2 (CH₂), 27.1 (CH₂), 22.7 (CH₂), 14.3 (CH₃). ESI-MS: *m/z* 1454.1 [(M+H)⁺]. Elemental analysis calcd. (%) for C₈₁H₁₂₀N₁₂O₁₂•CH₂Cl₂ (1452.9): C 64.00, H 7.99, N 10.92; found C 64.45, H 8.32, N 11.08.

1,1'-(((3,8,13-Trimethoxy-12-(4-(3-(6-oxo-4-undecyl-3,6-dihydropyridin-2-yl)ureido)phenoxy)-10,15-dihydro-5H-tribenzo[a,d,g]cyclononene-2,7-diyl)bis(oxy))bis(4,1-phenylene))bis(3-(4-oxo-6-undecyl-1,4-dihydropyrimidin-2-yl)urea) (5c).



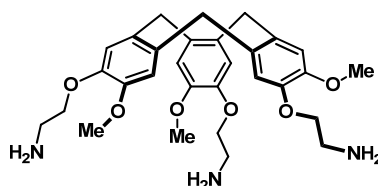
Prepared by following general procedure F from CTV-NH₂ **33** (30 mg, 0.043 mmol) and **24d** (46 mg, 0.13 mmol) in a DCM/DMF 5:2 mixture. Compound **5c** (55 mg, 88%) was obtained as a yellowish solid. Mp > 400 °C. ¹H NMR (DMSO-*d*₆, 400 MHz): 7.32 (d, ³J = 8.7 Hz, 2H, CHAr), 7.17 (s, 1H, CHAr), 7.04 (s, 1H, CHAr), 6.74 (d, ³J = 8.7 Hz, 2H, CHAr), 6.34 (br s, 1H, NH), 5.74 (s, 1H, CH), 4.70 (d, ²J_{gem} = 13.0 Hz, 1H, ArCH₂Ar), 3.56 (s, 3H, OCH₃), 3.53 (d, ²J_{gem} = 13.0 Hz, 1H, ArCH₂Ar), 1.50 (m, 2H, CH₂), 1.17-1.14 (br s, 18H, CH₂), 0.75 (m, 3H, CH₃). ¹³C NMR (100 MHz, DMSO-*d*₆): 161.2 (C), 154.9 (C), 153.0 (C), 148.9 (C), 142.3 (C), 135.9 (C), 132.0 (C), 131.8 (C), 121.5 (CH), 120.2 (CH), 118.4 (C), 116.3 (CH), 114.3 (CH), 114.1 (C), 55.3 (CH₃), 30.5 (CH₂), 28.2 (CH₂), 28.2 (CH₂), 28.1 (CH₂), 28.1 (CH₂), 28.0 (CH₂), 27.9 (CH₂), 27.2 (CH₂), 26.7 (CH₂), 26.5 (CH₂), 21.3 (CH₂), 13.1 (CH₃). ESI-MS: *m/z* 1412.3 [(M+H)⁺]. Elemental analysis calcd. (%) C₉₀H₁₁₄N₁₂O₁₂•CH₂Cl₂ (1554.9): C 66.61, H 7.38, N 10.24; found C 66.21, H 7.55, N 10.71.

1,1',1''-((((3,8,13-Trimethoxy-10,15-dihydro-5H-tribenzo[a,d,g]cyclononene-2,7,12-triyl)tris(oxy))tris(benzene-4,1-diyl))tris(methylene))tris(3-(4-oxo-6-undecyl-1,4-dihydropyrimidin-2-yl)urea) (5d).



Compound **35** (44 mg, 0.06 mmol) and **24d** (66 mg, 0.18 mmol) were reacted following general procedure F, yielding CTV-UPy **5d** (81 mg, 83%) as a white solid as a 70:30 mixture of *keto/enol* isomers. Mp > 400 °C. ¹H NMR (500 MHz, DMSO-*d*₆): 7.23-7.10 (m, 6H, CHAr), 7.04 (s, 3H, CHAr), 6.97 (s, 3H, CHAr), 6.81-6.79 (s, 6H, CHAr), 6.36 (br s, 3H, NH), 5.71 (s, 1H, CH *keto*), 5.42 (s, 3H, CH *enol*), 4.75 (d, ²J_{gem} = 12.9 Hz, 3H, ArCH₂Ar), 4.29 (s, 6H, CH₂ *keto*), 4.13 (s, 6H, CH₂ *enol*), 3.76-3.52 (m, 12H, ArCH₂Ar, OCH₃), 2.32 (t, ³J = 7.7 Hz, 6H, CH₂ *keto*), 2.21 (t, ³J = 7.3 Hz, CH₂ *enol*), 1.60-1.47 (m, 12H, CH₂), 1.23-1.12 (m, 42H, CH₂), 0.88-0.78 (m, 9H, CH₃). ¹³C NMR (125 MHz, DMSO-*d*₆): 170.2 (C), 167.0 (C), 161.6 (C), 156.1 (C), 153.5 (C), 150.3 (C), 129.1 (CH), 123.2 (CH), 116.8 (CH), 114.9 (CH), 104.7 (CH), 100.8 (CH), 56.2 (CH₃), 42.4 (CH₂), 37.3 (CH₂), 36.8 (CH₂), 35.3 (CH₂), 31.8 (CH₂), 29.6 (CH₂), 29.5 (CH₂), 29.4 (CH₂), 29.3 (CH₂), 29.2 (CH₂), 28.7 (CH₂), 28.0 (CH₂), 27.7 (CH₂), 22.6 (CH₂), 14.3 (CH₃). ESI-MS: *m/z* 1454.1 [(M+H)⁺]. Elemental analysis calcd. (%)C₉₃H₁₂₀N₁₂O₁₂ •H₂O(1596.9): C 69.12, H 7.61, N 10.40; found C 68.84, H 7.87, N 10.11.

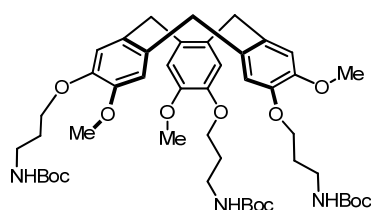
2,2',2''-((3,8,13-Trimethoxy-10,15-dihydro-5H-tribenzo[a,d,g]cyclononene-2,7,12-triyl)tris(oxy))triethanamine (29).



((3,8,13-trimethoxy-10,15-dihydro-5H-tribenzo[a,d,g]cyclononene-2,7,12-triyl)tris(oxy))tris(ethane-2,1-diyl) trimethanesulfonate (CTV-OMs)¹⁵ (1.20 g, 1.55 mmol) was dissolved in DMF (10 mL) and NaN₃ (2.00 g, 30.00 mmol) was added. The suspension was stirred overnight at 50 °C. The mixture was poured into 400 mL of ice-water. The off-white precipitate was filtered and washed several times with cold water. A small portion of this material was dried *in vacuo* over P₂O₅ and characterized by ¹H NMR (300 MHz, CDCl₃): 6.93 (s, 3H, CHAr), 6.85 (s, 3H, CHAr), 4.73 (d, ²J = 13.0 Hz, 3H, ArCH₂Ar), 4.14 (m, 6H, OCH₂), 3.83 (s, 9H, OCH₃), 3.56-3.52 (m, 9H, CH₂N and ArCH₂Ar). The still wet azide intermediate was then treated with triphenylphosphine (2.46 g, 9.30 mmol) in THF (50 mL) for 2 h. Concentrated ammonia (1 mL) was added and the solution was stirred overnight at r.t.. The solvent was evaporated and the product was precipitated by addition of Et₂O (500 mL), filtered off and thoroughly washed with Et₂O. Recrystallization from hot methanol afforded pure triamine **29** (0.74 g, 89%) as a white solid: ¹H NMR (300 MHz, MeOH-*d*₄): 6.92 (s, 3H, CHAr), 6.90 (s, 3H, CHAr), 4.53 (d, ²J = 13.6 Hz, 3H, ArCH₂Ar), 3.91 (m, 6H, OCH₂), 3.74 (s, 9H, OCH₃), 3.35 (d, ²J = 13.6 Hz, 3H, ArCH₂Ar), 2.86 (t, 9H, CH₂N). ¹³C NMR (75 MHz, MeOH-*d*₄): 147.6 (CH), 146.3 (C), 132.2 (CH), 131.9 (CH), 115.3 (C), 113.8 (CH), 71.0 (OCH₂), 55.6 (OCH₃), 40.7 (CH₂N), 34.9 (ArCH₂Ar). FAB-MS: *m/z* 538.0 ([M+H]⁺).

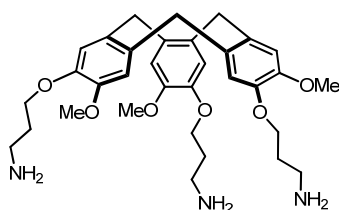
¹⁵ Vériot, G.; Dutasta, J. P.; Matouzenko, G.; Collet, A. *Tetrahedron* **1995**, *51*, 389-400.

Tri-tert-butyl **(((3,8,13-trimethoxy-10,15-dihydro-5H-tribenzo[a,d,g]cyclononene-2,7,12-triyl)tris(oxy))tris(propane-3,1-diyl))tricarbamate (30).**



A suspension of CTV-triphenol¹⁵ (250 mg, 0.61 mmol), *tert*-butyl-*N*-(3-bromopropyl)carbamate (610 mg, 2.50 mmol) and Cs₂CO₃ (1.20 g, 3.70 mmol) was stirred in CH₃CN (15 mL) for 18 h at 55 °C. The solvent was removed under reduced pressure and the residue was taken up in CHCl₃ (50 mL). The precipitate was filtered off over Celite and the solvent was removed under reduced pressure. The oily residue obtained was dried at high vacuum to yield compound **30** (486 mg, 90%) as a foam, which showed the same spectroscopic properties as those previously reported.¹⁶ ¹H NMR (400 MHz, CDCl₃): 6.85 (s, 3H, CHAr), 6.83 (s, 3H, CHAr), 5.44 (br s, 3H, NH), 4.77 (d, ²J_{gem} = 13.7 Hz, 3H, ArCH₂Ar), 4.06 (m, 6H, OCH₂), 3.85 (s, 9H, OCH₃), 3.55 (d, ²J_{gem} = 13.7 Hz, 3H, ArCH₂Ar), 3.33 (m, 6H, NCH₂), 1.97 (m, 6H, CH₂), 1.46 (s, 18H, O^tBu).

3,3',3''-((3,8,13-Trimethoxy-10,15-dihydro-5H-tribenzo[a,d,g]cyclononene-2,7,12-triyl)tris(oxy))tris(propan-1-amine) (31):

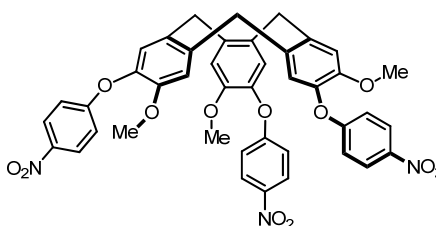


Compound **30** (325 mg, 0.37 mmol) was dissolved in dichloromethane (2 mL)

¹⁶ Dam, H. H.; Reinhoudt, D. N.; Verboom W. *New J. Chem.* **2007**, 31, 1620-1632.

and trifluoroacetic acid (1 mL) was added. The mixture was stirred for two hours at room temperature. Solvent was removed and the residue was taken up with dichloromethane (30 mL) and washed with NaOH (6M, 30 mL). The aqueous phase was extracted with DCM (3 x 50 mL). Organic layer was dried with MgSO₄ and solvent eliminated under reduced pressure. The residue was triturated with hexane and the solid was filtered and dried under air. Compound **31** was isolated (150 mg, 70%) as a white solid which showed the same spectroscopic properties as those previously reported.¹⁶ ¹H NMR (CDCl₃, 400 MHz): 6.84 (s, 3H, CHAr), 6.79 (s, 3H, CHAr), 4.70 (d, ²J_{gem} = 13.2 Hz, 3H, ArCH₂Ar), 4.05 (m, 6H, OCH₂), 3.79 (s, 9H, OCH₃), 3.49 (d, ²J_{gem} = 13.2 Hz, 3H, ArCH₂Ar), 2.87 (t, ³J = 8.4 Hz, 6H, NCH₂), 1.92 (m, 6H, CH₂), 1.78 (br s, 6H, NH₂).

2,7,12-Trimethoxy-3,8,13-tris(4-nitrophenoxy)-10,15-dihydro-5H-tribenzo[a,d,g]cyclononene (32).

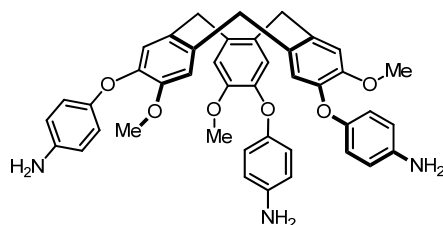


CTV-triphenol¹⁵ (500 mg, 1.22 mmol), 4-fluoronitrobenzene (1.04 g, 7.34 mmol) and K₂CO₃ (846 mg, 6.12 mmol) were suspended in dry DMF, placed into a sealed tube and warmed at 70 °C over 2 days. DMF was removed under reduced pressure and the solid residue was dissolved in DCM and washed with HCl 10%. Solvent was eliminated and the residue was then triturated with MeOH affording compound **32** (846 mg, 97%) as a yellow solid, which showed the same spectroscopic properties as those previously reported.¹⁷ ¹H NMR (400 MHz, CDCl₃): 8.15 (d, ³J = 9.2 Hz, 6H, CHAr), 7.12 (s,

¹⁷ Arduini, A.; Calzavacca, F.; Demuru, D.; Pochini, A.; Secchi A. *J. Org. Chem.* **2004**, *69*, 1386-1388.

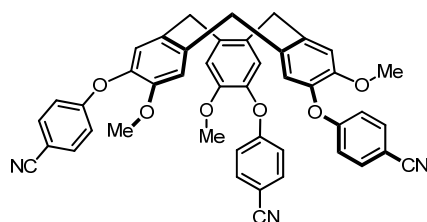
3H, CHAr), 6.92 (d, $^3J = 9.2$ Hz, 6H, CHAr), 6.88 (s, 3H, CHAr), 4.84 (d, $^2J_{gem} = 14.0$ Hz, 3H, ArCH₂Ar), 3.69 (s, 9H, OCH₃), 3.67 (d, $^2J_{gem} = 14.0$ Hz, 3H, ArCH₂Ar).

4,4',4''-((3,8,13-Trimethoxy-10,15-dihydro-5H-tribenzo[a,d,g]cyclononene-2,7,12-triyl)tris(oxy))trianiline (33).



CTV-triphenol¹⁵ (50 mg, 0.07 mmol), palladium on activated charcoal (10%, 3.5 mg, 3.7 μ L) and hydrazine monohydrate (13.7 μ L, 0.28 mmol) were dissolved in 40 mL of ethanol. The resulting mixture was refluxed overnight into a sealed tube and then Pd catalyst was removed by filtration over Celite under nitrogen atmosphere. The filtrate was concentrated under vacuum and the resulting oily residue was dissolved in CH₂Cl₂ and washed with water to eliminate hydrazine residues. Compound **33** (30 mg, 63%) was obtained as a white solid after evaporation of the organic phase. This compound showed the same spectroscopic properties as those previously reported.¹⁷ ¹H NMR (400 MHz, CDCl₃): 6.98 (s, 3H, CHAr), 6.83 (d, $^3J = 8.8$ Hz, 6H, CHAr), 6.73 (s, 3H, CHAr), 6.63 (d, $^3J = 8.8$ Hz, 6H, CHAr), 4.65 (d, $^2J_{gem} = 13.7$ Hz, 3H, ArCH₂Ar), 3.73 (s, 9H, OCH₃), 3.42 (d, $^2J_{gem} = 13.7$ Hz, 3H, ArCH₂Ar).

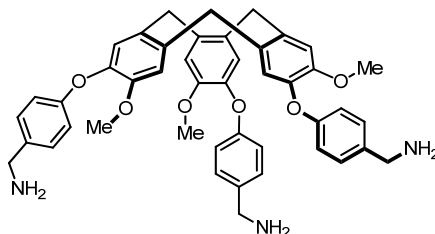
4,4',4''-((3,8,13-Trimethoxy-10,15-dihydro-5H-tribenzo[a,d,g]cyclononene-2,7,12-triyl)tris(oxy))tribenzonitrile (34).



A suspension of CTV-triphenol¹⁵ (610 mg, 1.49 mmol), 4-fluorobenzonitrile

(1.10 g, 8.96 mmol) and K_2CO_3 (1.03 g, 7.47 mmol) in dry DMF (10 mL) was placed into a sealed tube and stirred at 100 °C overnight. DMF was removed under reduced pressure and the solid residue was dissolved in DCM and washed with HCl 10%. The organic phase was dried over Na_2SO_4 , the solvent was evaporated and the residue was then triturated with MeOH. The resulting suspension was filtered and the solid was washed with fresh MeOH affording **34** as a beige solid (939 mg, 88%), which showed the same spectroscopic properties as those previously reported.¹⁷ 1H NMR (400 MHz, $CDCl_3$): 7.54 (d, $^3J = 8.8$ Hz, 6H, CHAr), 7.09 (s, 3H, CHAr), 6.90 (d, $^3J = 8.8$ Hz, 6H, CHAr), 6.88 (s, 3H, Ar), 4.82 (d, $^2J_{gem} = 14.0$ Hz, 3H, ArCH₂Ar), 3.71 (s, 9H, OCH₃), 3.65 (d, $^2J_{gem} = 14.0$ Hz, 3H, ArCH₂Ar).

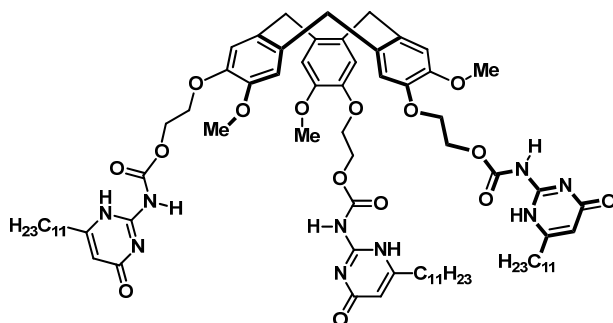
(((3,8,13-Trimethoxy-10,15-dihydro-5H-tribenzo[a,d,g]cyclononene-2,7,12-triyl)tris(oxy))tris(benzene-4,1-diyl))trimethanamine (35).



To a solution of compound **34** (230 mg, 0.32 mmol) in dry THF (50 mL), a 1M solution of B_2H_6 in THF (1.6 mL, 1.60 mmol) was added. The resulting mixture was refluxed overnight, cooled to room temperature, quenched with small portions of water and finally extracted with CH_2Cl_2 (50 mL). The separated organic layer was then washed with brine until the aqueous washings were neutral, dried over anhydrous Na_2SO_4 and evaporated to dryness under reduced pressure. The residue was triturated with hexane and filtered, affording the triamine **35** (133 mg, 57%) as a beige solid, which showed the same spectroscopic properties as those previously reported.¹⁷ 1H NMR (400 MHz, $CDCl_3$): 7.27 (d, $^3J = 9.0$ Hz, 6H, CHAr), 6.94 (s, 3H, CHAr), 7.92 (d, $^3J = 9.0$ Hz, 6H, CHAr), 6.75 (s, 1H, CHAr), 4.74 (d, $^2J_{gem} = 14.0$ Hz, 3H, ArCH₂Ar), 4.63 (s,

6H, CH₂N), 3.69 (s, 9H, OCH₃), 3.53 (d, ²J_{gem} = 14.0 Hz, 3H, ArCH₂Ar).

((3,8,13-Trimethoxy-10,15-dihydro-5H-tribenzo[a,d,g]cyclononene-2,7,12-triyl)tris(oxy))tris(ethane-2,1-diyl)tris((4-oxo-6-undecyl-1,4-dihydropyrimidin-2-yl)carbamate) (36).



A suspension of imidazolide **24d** (140 mg, 3.88 mmol) and 2,2',2''-((3,8,13-trimethoxy-10,15-dihydro-5H-tribenzo[a,d,g]cyclononene-2,7,12-triyl)tris(oxy))triethanol¹⁵ (60 mg, 1.11 mmol) in 5 mL of dry CH₂Cl₂ was stirred at 50 °C in a sealed tube for 6 h. The solvent was then removed under reduced pressure and the solid residue was sonicated with methanol, filtered and washed with cold methanol. The resulting solid was dried under vacuum affording **36** (145 mg, 92%) as a white solid. Mp 158-160 °C. ¹H NMR (400 MHz, CDCl₃): 6.81 (d, ³J = 6.4 Hz, 6H, CHAr), 5.92 (s, 3H, CH), 4.65 (d, ²J_{gem} = 14.0 Hz, 3H, ArCH₂Ar), 4.50 (m, 6H, OCH₂), 4.16 (m, 6H, OCH₂), 3.78 (s, 9H; OCH₃), 3.48 (d, ²J_{gem} = 14.0 Hz, 3H, ArCH₂Ar), 2.39 (t, ³J = 7.2 Hz, 6H, CCH₂), 1.56 (m, 2H, CH₂), 1.24 (m, 48H, CH₂), 0.86 (t, ³J = 7.7 Hz, 12H, CH₃). ¹³C NMR (100 MHz, CDCl₃): 148.5 (C), 146.5 (C), 133.4 (C), 132.1 (C), 116.7 (CH), 114.2 (CH), 106.3 (CH), 67.4 (CH₂), 64.9 (CH₂), 56.4 (CH₃), 36.3 (CH₂), 31.9 (CH₂), 29.7 (CH₂), 29.6 (CH₂), 29.5 (CH₂), 29.4 (CH₂), 29.3 (CH₂), 29.1 (CH₂), 27.6 (CH₂), 22.6 (CH₂), 14.3 (CH₃). ESI-MS: *m/z* 1436.1 [M+Na]⁺. Elemental analysis calcd. (%) for C₇₈H₁₁₁N₉O₁₅ (1414.8): C 66.22, H 7.91, N 8.91; C 66.57, H 7.99, N 8.01.

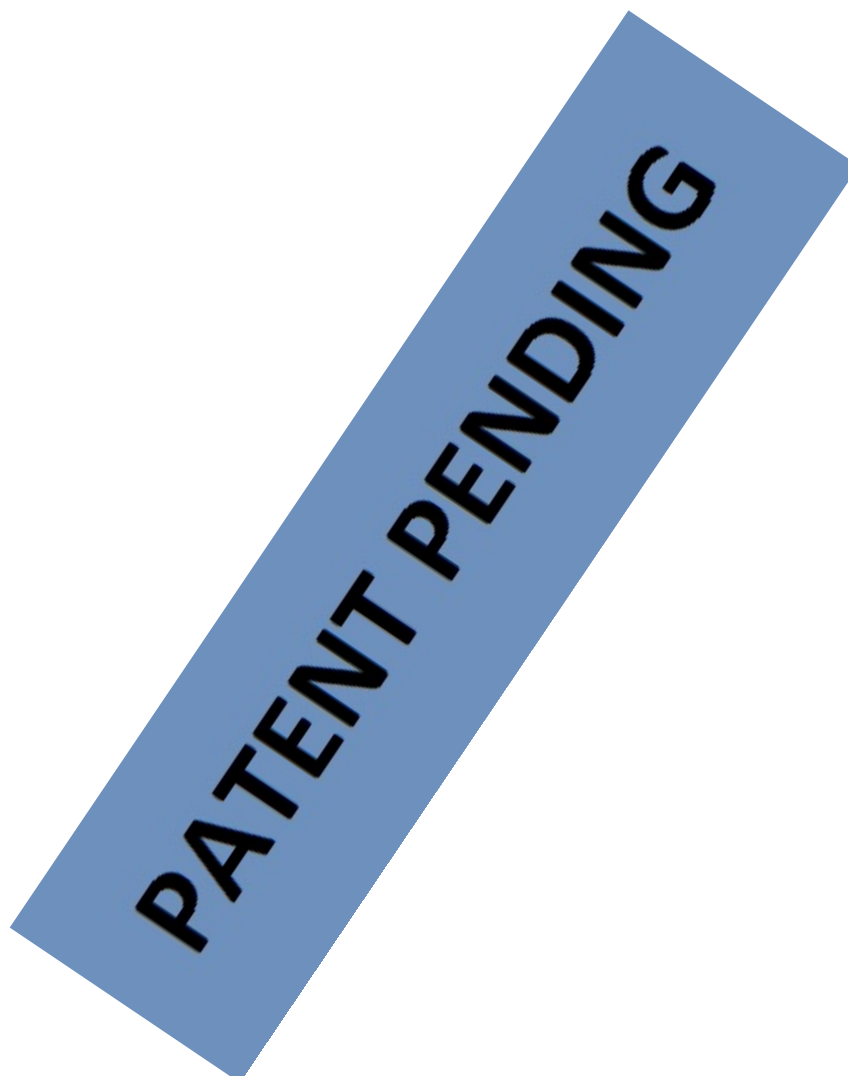
PATENT PENDING

PATENT PENDING

PATENT PENDING

PATENT PENDING

PATENT PENDING



VI.3.1 Methods for Fullerene Extractions and Extracts Analysis

C₇₀ Extraction Procedure and HPLC Samples Preparation with Receptor 5a:

Pure fullerenes or fullerene mixtures were suspended in the appropriate amount of a 1.2×10^{-3} M solution of CTV-UPy **5a** in THF in each case (Table 1) and diluted until 1 mL with pure THF. The mixtures were stirred over 15 minutes. No sonication or heat was used in the extraction. The mixtures were filtered and 400 μ L of solution were diluted in 500 μ L of toluene and 10 μ L of TFA. Then, the samples were injected in HPLC.

Table 1

Mixture [C₆₀/C₇₀/5a₂]	C₆₀ (μg)	C₇₀ (μg)	CTV solution (μL)
[1:1:1]	350	420	830
[1:1:0.5]	490	550	545
[1:12:12]	60	490	890
[6:1:1]	1680	330	655

Fullerite Extraction-Precipitation-Extraction Procedure for C₇₀ purification: A solution of 3.8 mg of **5a** in THF (2 mL) was added to 20.9 mg of solid fullerite. The mixture was stirred for 15 minutes at 22 °C and was filtered to eliminate the solid residue. An aliquot was analyzed by HPLC. The first extraction gives an 84:16 C₇₀/C₆₀ mixture. The solution was treated with 50 μL of trifluoroacetic acid to break the hydrogen bonds and leads the fullerenes precipitated, and centrifuged (5 min, 4500 rpm). Liquid was removed and the solid residue was washed with fresh THF and dried in vacuum. The solid was re-extracted with 1.60 mg of CTV as described above.

Soot Extraction: Direct soot extraction was performed in the same way as with the fullerite from 34.2 mg of solid soot and 1 mg of **5a** in 5 mL of THF. The extract was analyzed by HPLC.

MASS SPECTROMMETRY ANALYSIS OF FULLERENE EXTRACTIONS

The technique employed in this case was MALDI-TOF (–ve), without matrix, and the ionization method was electron capture, which provides low fragmentation of the samples.

Sample Preparation For Qualitative Fullerene Determination: A solution of approximately 1 mg/mL of fullerene mixture was prepared in dichlorobenzene. Approximately 1 μL of this solution was then spotted onto a MALDI plate (3 spots / sample). The plate was leaved to dry, covering with box lid or similar.

Sample Preparation For Quantitative Experiments: Each sample must contain 1 equivalent (with respect to the maximum possible quantity of fullerene to be determined) of internal standard for shot-to-shot intensity corrections. The fullerene closest in mass to that which is to be determined must be used.

The general strategy to follow is the standard addition. 5 additions up to a maximum of 20% of the maximum possible concentration of the measured fullerene must be performed. The internal standard concentration must be constant across all solutions within a single determination.

Example of Quantification of C₇₀ in Fullerite (approx. 80% C₆₀, 20% C₇₀)

A solution of 1 mg/mL of fullerite in dichlorobenzene was prepared (Solution **A**). If we considered that the amount of C₇₀ is 20% of the total mass of fullerite, the solution must contain up to 200 µg/mL of C₇₀.

A solution of similar concentration of internal standard was prepared in DCB: 217.1 µg/mL of C₇₆ (Solution **B**). A new solution of 0.2 mL 1:1 mixture of **A** and **B** was made (Solution **C**) and finally a solution of 40 µg/mL of C₇₀ (Solution **D**; 20% of the maximum possible concentration of the measured fullerene) was prepared to perform the addition as follows:

Addition (1): with DCB	20 µL (C)			Made up to 70 µL
Addition (2): with DCB	20 µL (C)	+	10 µL (D)	Made up to 70 µL
Addition (3): with DCB	20 µL (C)	+	20 µL (D)	Made up to 70 µL
Addition (4): with DCB	20 µL (C)	+	30 µL (D)	Made up to 70 µL

Addition (5): 20 μ L (C) + 40 μ L (D) Made up to 70 μ L
with DCB

Addition (6): 20 μ L (C) + 50 μ L (D)

Each determination was spotted 5 times (1 μ L) onto the MALDI plate. At the moment, a maximum of 12 determinations may be performed on 1 plate.

Soot Extraction Procedure and Sample Preparation for Qualitative Mass

Analyses: Compound **5a** was dissolved in THF and the solution was added over the solid soot samples, then THF was added to the mixture to complete the final volume (10 mL, see table 2). The mixtures were stirred overnight. No sonication or heat was used during the extraction. The resulting suspension was filtered. To 2 mL of the solution containing the **5a₂**:fullerene complexes, 10 μ L of TFA were added and solvent was then removed. The solid residue was redissolved in 0.5 mL of o-dichlorobenzene and subjected to the mass analysis.

Table 2

Entry	% w/w 5a	5a (mg)	Soot (mg)	THF (mL)
1	1%	0,16	155	10
2	2%	0,25	123	10
3	5%	0,72	144	10
4	10%	1,21	121	10
5	15%	1,85	123	10
6	20%	2,52	126	10
7	40%	5,74	144	10
8	60%	7,64	127	10

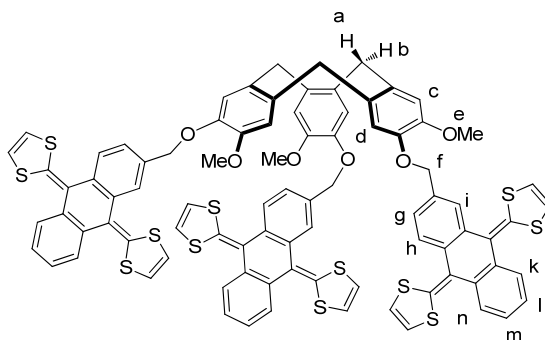
UNIVERSITAT ROVIRA I VIRGILI
SELF-ASSEMBLY BASED ON THE 2-UREIDO-4(1H)-PYRIMIDINONE MOTIF: FROM CYCLIC ARRAYS TO MOLECULAR CAPSULES
FOR FULLERENE SEPARATIONS
Elisa Huerta Martínez
DL:T.289-2012

UNIVERSITAT ROVIRA I VIRGILI
SELF-ASSEMBLY BASED ON THE 2-UREIDO-4(1H)-PYRIMIDINONE MOTIF: FROM CYCLIC ARRAYS TO MOLECULAR CAPSULES
FOR FULLERENE SEPARATIONS
Elisa Huerta Martínez
DL:T.289-2012

UNIVERSITAT ROVIRA I VIRGILI
SELF-ASSEMBLY BASED ON THE 2-UREIDO-4(1H)-PYRIMIDINONE MOTIF: FROM CYCLIC ARRAYS TO MOLECULAR CAPSULES
FOR FULLERENE SEPARATIONS
Elisa Huerta Martínez
DL:T.289-2012

VI.4 SYNTHESIS CHAPTER IV

Compound 6.

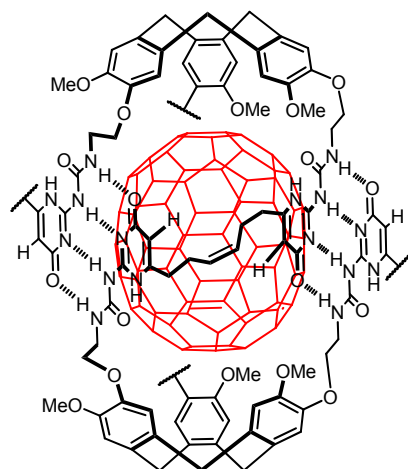


CTV-triphenolREF (25 mg, 0.06 mmol), exTTF methylene alcohol²¹ (88 mg, 0.21 mmol) and PPh₃ (57 mg, 0.21 mmol) were mixed together, dissolved in dry DCM into a round bottom flask and stirred at 0 °C. DIAD (44 μL, 0.21 mmol) was then added and the mixture was allowed to reach room temperature and was stirred for 4 days. Solvent was taken up and the residue was purified by flash chromatography in CHCl₃/MeOH (1%). Compound **6** was isolated as a yellow solid (45 mg, 46%). ¹H NMR (500 MHz, chlorobenzene-*d*₅, 353 K): 8.09 (br s, 3H, H_i), 7.97 (s, 6H, H_k + H_n), 7.93 (d, *J* = 8.2 Hz, 3H, H_h), 7.53 (br d, *J* = 8.2 Hz, 3H, H_g), 7.44 (hidden under solvent signal, 6H, H_l + H_m), 7.31 (s, 3H, H_c), 7.12 (s, 3H, H_d), 6.06 (m, 12H, H_j), 5.36 (m, 6H, H_f), 4.92 (d, *J* = 14.0 Hz, 3H, H_a), 3.84 (s, 9H, H_e), 3.73 (d, *J* = 14.0 Hz, 3H, H_b). HPLC-MS analysis (Sunfire C18, MeCN, 1 mL/min, λ=254 nm): 95% purity. APCI(+) MS: *m/z* 1584.1 [M]⁺. ESI-MS (+ve): *m/z* 1548.2 [M]⁺, 792.7 [M]²⁺. MALDI-TOF: 1584.2 [M]⁺.

²¹ Marshallsay, G. J.; Bryce, M. R. J. *Org. Chem.* **1994**, *59*, 6847-6849.

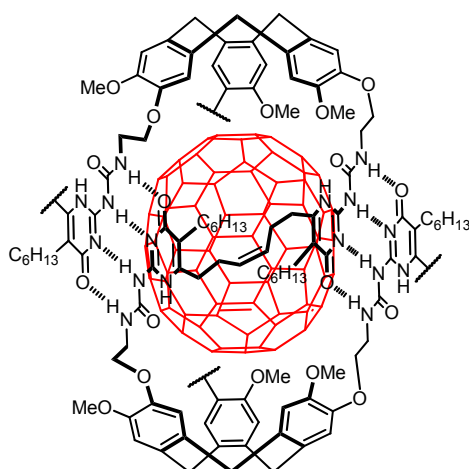
VI.5 SYNTHESIS CHAPTER V

Compound C₇₀@7c.



It was synthesized by following general procedure G from **53c** (25.0 mg, 0.022 mmol) and C₇₀ (9.5 mg, 0.011 mmol) in dry DCM (10 mL) and Grubbs II catalyst (15 mol%). Compound C₇₀@**7c** was detected in MALDI-TOF mass spectrometry (dithranol/DCM): *m/z* 2980.1 [(M+H)⁺], 2139.0 [(M-C₇₀+H)⁺].

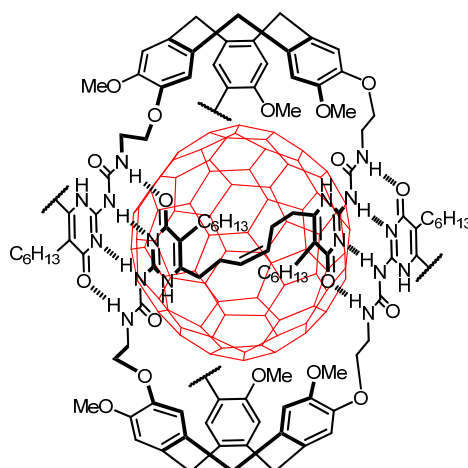
Compound C₇₀@7d.



It was synthesized by following general procedure G from **53d** (20.0 mg, 0.015 mmol) and C₇₀ (6.2 mg, 0.008 mmol) in dry chloroform (10 mL) and

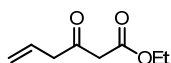
Hoveyda-Grubbs catalyst (15 mol%). Compound **C₇₀@7d** was isolated as a deep red solid (35.7 mg, 70%). ¹H NMR (400 MHz, CDCl₃): 13.37-12.59 (m, 6H, NH), 12.18-12.99 (m, 6H, NH), 11.15-10.31 (m, 6H, NH), 7.09-6.72 (m, 12H, CHAr), 5.47-5.28 (m, 6H, CH), 4.98-4.79 (m, 6H, ArCH₂Ar), 4.67-3.26 (m, 48H, ArCH₂Ar, CH₂, OCH₃), 2.80-1.05 (m, 84H, CH₂), 0.99-0.81 (m, 18H, CH₃). MALDI-TOF (dithranol): *m/z* 3483.8 [(M)⁺], 2643.3 [(M-C₇₀)⁺]. ESI-MS (DCM/MeOH): 3505.8 [(M+Na)⁺], 1764.3 [(M+Na)²⁺].

Compound **C₈₄@7d**.



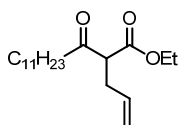
It was synthesized by following general procedure G from **53d** (10.0 mg, 0.008 mmol) and **C₈₄** (3.8 mg, 0.004 mmol) in dry chloroform (5 mL) and Hoveyda-Grubbs catalyst (15 mol%). Compound **C₈₄@7d** was isolated as a deep red solid (12.2 mg, 46%). ¹H NMR (400 MHz, CDCl₃): 13.44-12.66 (m, 6H, NH), 12.20-11.43 (m, 6H, NH), 11.26-10.72 (m, 6H, NH), 7.08-6.59 (m, 12H, CHAr), 5.53-5.40 (m, 6H, CH), 4.77-4.71 (m, 6H, ArCH₂Ar), 4.35-3.36 (m, 48H, ArCH₂Ar, CH₂, OCH₃), 2.90-1.20 (m, 84H, CH₂), 1.03-0.82 (m, 18H, CH₃). MALDI-TOF (pyrene/DCM, negative mode): *m/z* 3650.7 [(M-H)⁻]. MALDI-TOF (dithranol/DCM, positive mode): *m/z* 3652.6 [(M)⁺], 3643.7 [(M-C₈₄)⁺]. ESI-MS (DCM/MeOH): 3674.1 [(M+Na)⁺], 1848.7 [(M+Na)²⁺].

Ethyl 3-oxohex-5-enoate (50a):



Allyl bromide (8.6 g, 70.4 mmol), ethyl cyanoacetate (5.0 mL, 46.9 mmol) and Zn (dust) (12.5 g, 187.6 mmol) were suspended in tetrahydrofuran (250 mL). After stirring 10 min at 0 °C, AlCl₃ (2.5 g, 18.8 mmol) was added. The mixture was stirred at room temperature and the reaction was followed by TLC (hexane/EtOAc 9:1). When complete, HCl 3M (150 mL) was added and the mixture was stirred for additional 30 minutes. The reaction was filtered through cotton and extracted with dichloromethane (3 x 150 mL). Organic layer was washed with brine (150 mL), dried over MgSO₄ and the solvent was taken up under reduced pressure. The oily residue was purified by flash chromatography in hexane/EtOAc (10:1). Compound **5a** was obtained as yellowish oil (5.13 g, 70%) which showed the same spectroscopic properties as those previously reported.²² GC-MS: R.t: 3.47 min. EI-MS: *m/z* 156 [M⁺]; 115 [M⁺- allyl].

Ethyl 2-allyl-3-oxotetradecanoate (50b):

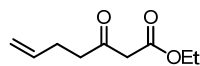


Sodium ethoxide (1.0 g, 13.9 mmol) was added over a THF solution (30 mL) of ethyl 3-oxodecanoate⁶ (4.9 g, 18.0 mmol) and stirred at room temperature over a 30 min period. Allyl bromide (1.4 g, 11.4 mmol) was dissolved in 8 mL of THF and added dropwise over the mixture. The reaction was refluxed overnight. Water was added to quench the reaction, organic phase was separated and the aqueous layer was extracted twice with EtOAc (30 mL). Combined organic layers were washed with ammonium chloride (50 mL), dried over magnesium sulphate and the solvent was taken

²² Bennett, F.; Knight, D. W.; Fenton G. J. *Chem. Soc., Perkin Trans. 1*, **1991**, 133–140.

up at reduced pressure. The crude was purified by flash chromatography (hexane/EtOAc 10:1) to afford **50b** as a colorless oil (2.46 g, 70%). ¹H NMR (400 MHz, CDCl₃): 5.70 (ddt, ³J_{cis} = 10.0 Hz, ³J_{trans} = 17.2 Hz, ³J = 6.8 Hz, 1H, CH₂=CH), 5.04 (dd, ³J_{cis} = 10.0 Hz, ³J_{trans} = 17.2 Hz, 2H, CH₂=CH), 4.16 (q, ³J = 8.8 Hz, 2H, OCH₂), 3.50 (t, ³J = 7.2 Hz, 1H, CH), 2.56 (t, ³J = 7.2 Hz, 2H, CH₂CO), 2.51-1.46 (m, 2H, CH₂-allyl), 1.57-1.54 (m, 2H, CH₂), 1.25-1.21 (m, 16H, CH₂), 0.85 (t, ³J = 6.4 Hz, 3H, CH₃). ¹³C NMR (400 MHz, CDCl₃): 204.6 (CO), 169.2 (CO), 134.4 (=CH), 117.3 (=CH₂), 61.3 (OCH₂), 58.6 (CH), 42.1 (CH₂), 32.2 (CH₂), 31.8 (CH₂), 29.7 (CH₂), 29.5 (CH₂), 29.4 (CH₂), 29.3 (CH₂), 29.2 (CH₂), 29.0 (CH₂), 23.3 (CH₂), 22.6 (CH₂), 14.0 (CH₃), 14.0 (CH₃). EI-MS: 310.2 [(M)⁺]. HRMS: *m/z* calcd. for C₁₉H₃₄O₃Na [(M+Na)⁺]: 333.2406, found: 333.2410.

Ethyl 3-oxohept-6-enoate (**50c**):

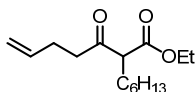


All the glassware used was previously dried at high temperature in the oven, cooled down into a desiccator under inert atmosphere. Freshly distilled diisopropyl amine (7.1 mL, 51.0 mmol) was dissolved in dry THF (20 mL) under argon atmosphere at -78 °C. *n*-Butyllithium (2.5 M in hexane, 20.4 mL, 50.97 mmol) was added and the mixture was stirred over 15 minutes. Ethyl acetoacetate (2.8 mL, 22.2 mmol) was dissolved in 180 mL of dry tetrahydrofuran and placed in a round bottom flask under argon atmosphere at 0 °C. The previously prepared LDA was carefully added over ethyl acetoacetate solution and the mixture was stirred 1h at 0 °C under argon. Then, allyl bromide (4.5 mL, 51.0 mmol) was added to the reaction and was allowed to reach room temperature overnight. Reaction was treated with HCl 3M (100 mL) and aqueous layer was extracted twice with dichloromethane (75 mL). The combined organic layers were washed with brine (100 mL), dried over MgSO₄ and solvent was eliminated under reduced pressure. The crude was purified by flash chromatography (hexane/EtOAc 9:1) affording **50c** (3.06 g, 80%) as an orange oil which

showed the same spectroscopic properties as those previously reported.²³

¹H NMR (400 MHz, CDCl₃): 5.78 (ddt, ³J_{cis} = 10.4 Hz, ³J_{trans} = 17.2 Hz, ³J = 6.4 Hz, 1H, CH₂=CH), 5.00 (dd, ³J_{cis} = 10.4 Hz, ³J_{trans} = 17.2 Hz, 2H, CH₂=CH), 4.17 (q, ³J = 7.2 Hz, 2H, OCH₂), 3.42 (s, 1H, CH), 2.64 (t, ³J = 7.2 Hz, 2H, CH₂CO), 2.34 (q, ³J = 7.2 Hz, 2H, CH₂-allyl), 0.85 (t, ³J = 7.2 Hz, 3H, CH₃). GC-MS: R.t: 5.01 min, EI-MS: m/z 170 [M⁺].

Ethyl 2-(pent-4-enoyl)octanoate (**50d**).

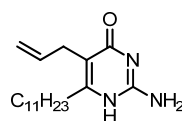


A solution of LDA (2M in hexane, 22.9 mL, 42.8 mmol) was added over a solution of ethyl acetoacetate (5 mL, 20.8 mmol) in THF (150 mL) under argon atmosphere at 0 °C. After 20 minutes, allyl bromide (3.6 mL, 41.7 mmol) were added and the reaction was allowed to reach room temperature overnight. Reaction was quenched with HCl 3M (100 mL) and aqueous layer was extracted twice with DCM (75 mL). The organic phase was washed with brine, dried over MgSO₄ and solvent was eliminated under reduced pressure. The product was purified by flash chromatography (hexane/EtOAc 9:1) and **50d** was isolated as a yellowish oil (4.8 g, 87%) as a 70:30 mixture of *keto/enol* isomers. ¹H NMR (400 MHz, CDCl₃): 15.19 (s, 1H, OH), 5.79 (ddt, ³J_{cis} = 10.0 Hz, ³J_{trans} = 17.2 Hz, ³J = 6.8 Hz, 1H, CH₂=CH *keto*), 5.5961-5.58 (m, 1H, CH₂=CH *enol*), 5.08-5.06 (m, 2H, CH₂=CH *enol*), 5.01 (dd, ³J_{cis} = 10.0 Hz, ³J_{trans} = 17.2 Hz, 2H, CH₂=CH *keto*), 4.18 (q, ³J = 7.6 Hz, 2H, OCH₂), 3.42 (t, ³J = 7.3 Hz, 1H, CH *keto*), 2.62 (m, 2H, CH₂), 2.34 (q, ³J = 7.2 Hz, 2H, CH₂), 1.85-1.83 (m, 2H, CH₂), 1.27-1.25 (m, 9H, CH₂, CH₃), 0.88 (t, ³J = 7.0 Hz, 3H, CH₃). ¹³C NMR (100 MHz, CDCl₃): 204.7 (C *enol*), 202.9 (C *keto*), 169.9 (C *keto*), 169.2 (C *enol*), 134.4 (CH), 117.5 (CH₂), 61.3 (CH₂), 58.5 (CH), 42.3 (CH₂), 32.2 (CH₂), 29.5 (CH₂), 29.4 (CH₂), 29.3 (CH₂), 28.9 (CH₂), 23.6 (CH₂),

²³ Nguyen, V. T. H.; Bellur, E.; Langer, P. *Tetrahedron Lett.* **2005**, 47, 113-116.

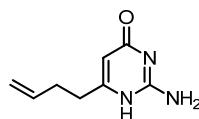
14.1 (CH₃). GC-MS: R.t.: 6.23 min. EI-MS: *m/z* 254.0 [(M)⁺].

5-Allyl-2-amino-6-undecylpyrimidin-4(1H)-one (51a):



Prepared by following general procedure C from compound **50b** (2.00 g, 6.4 mmol) and guanidinium carbonate (586 mg, 3.2 mmol). Compound **51a** was obtained as a white solid (967 mg, 49%). Mp: 201-203 °C. ¹H NMR (400 MHz, DMSO-*d*₆): 10.75 (br s, 1H, NH), 6.28 (br s, 2H, NH₂), 5.74 (ddt, ³*J*_{cis} = 10.0 Hz, ³*J*_{trans} = 16.8 Hz, ³*J* = 6.0 Hz, 1H, CH₂=CH), 4.95-4.91 (m, 2H, CH₂=CH), 3.03 (d, ³*J* = 6.0 Hz, 2H, CH₂), 2.49-2.46 (m, 2H, CH₂-allyl), 1.57-1.55 (m, 2H, CH₂), 1.25-1.21 (m, 16H, CH₂). ¹³C NMR (100 MHz, DMSO-*d*₆): 156.1 (C keto), 137.4 (CH₂=CH), 119.8 (CNH₂ keto), 115.6 (CH₂=CH), 112.9 (=C), 31.1 (CH₂), 29.8 (CH₂), 42.1 (CH₂), 32.2 (CH₂), 31.8 (CH₂), 29.7 (CH₂), 29.5 (CH₂), 29.4 (CH₂), 29.3 (CH₂), 29.2 (CH₂), 29.0 (CH₂), 23.3 (CH₂), 22.6 (CH₂), 14.0 (CH₃), 14.0 (CH₃). ESI-MS: *m/z* 611.0 [(2M+H)⁺], 328.0 [(M+Na)⁺], 306.0 [(M+H)⁺].

2-Amino-6-(but-3-enyl)pyrimidin-4(1H)-one (51b):

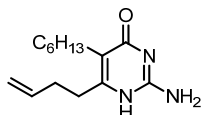


Prepared by following general procedure C from compound **50c** (3.1 g, 17.9 mmol) and guanidinium carbonate (1.7 g, 9.0 mmol). A white solid **51b** was obtained (1.4 g, 47%) which showed the same spectroscopic properties as those previously reported.²⁴ ¹H NMR (400 MHz, DMSO-*d*₆): 10.75 (br s, 1H, NH), 6.55 (br s, 2H, NH₂), 5.81 (ddt, ³*J*_{cis} = 12.4 Hz, ³*J*_{trans} = 18.8 Hz, ³*J* = 6.4 Hz, 1H, CH₂=CH), 5.41 (s, 1H, CH), 5.00 (dd, ³*J*_{cis} = 12.4 Hz, ³*J*_{trans} = 18.8 Hz, 2H,

²⁴ Hirschberg, H. K. K.; Beijer, F. H.; van Aert, H. A.; Magusin, P. C. M. M.; Sijbesma, R. P.; Meijer E. W. *Macromolecules*, **1999**, 32, 2696-2705.

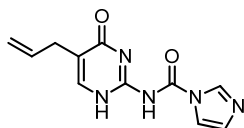
CH₂=CH), 2.34-2.31 (m, 4H, CH₂). ¹³C NMR (100 MHz, DMSO-*d*₆): 168.9 (CO), 164.2 (C), 156.6 (C), 138.5 (CH₂=CH), 115.7 (CH₂=CH), 100.4 (CH), 36.8 (CH₂), 32.2 (CH₂).

2-Amino-6-(but-3-en-1-yl)-5-hexylpyrimidin-4(1H)-one (51c).



Prepared by following general procedure C from compound **50d** (4.2 g, 18.0 mmol) and guanidinium carbonate (1.6 g, 9.0 mmol). Compound **51c** was obtained (1.9 g, 42%) as a white solid. Mp 241-243 °C. ¹H NMR (400 MHz, DMSO-*d*₆): 10.76 (br s, 1H, NH), 6.26 (br s, 2H, NH₂), 5.84 (ddt, ³J_{cis} = 13.1 Hz, ³J_{trans} = 17.1 Hz, ³J = 6.2 Hz, 1H, CH₂=CH), 4.99 (dd, ³J_{cis} = 13.1 Hz, ³J_{trans} = 17.1 Hz, 2H, CH₂=CH), 2.41-2.38 (m, 2H, CH₂), 2.73-2.70 (m, 4H, CH₂), 1.32-1.275 (m, 8H, CH₂), 0.86 (t, ³J = 7.0 Hz, 3H, CH₃). ¹³C NMR (100 MHz, DMSO-*d*₆): 207.8 (C), 160.2 (C), 153.7 (C), 138.8 (CH), 115.4 (CH₂), 112.2 (C), 32.7 (CH₂), 31.6 (CH₂), 29.7 (CH₂), 29.3 (CH₂), 24.9 (CH₂), 22.5 (CH₂), 14.4 (CH₃). ESI-MS: *m/z* 499.1 [(2M+H)⁺], 250.1 [(M+H)⁺]. Elemental analysis calcd. (%)C₁₄H₂₃N₃O•½ EtOH (249.3): C 66.14, H 9.62, N 16.85; found C 66.19, H 9.82, N 17.19.

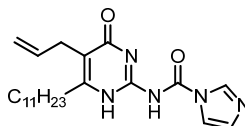
N-(5-Allyl-4-oxo-1,4-dihydropyrimidin-2-yl)-1H-imidazole-1-carboxamide (52a):



Prepared by following the general procedure D from **9g** (47 mg, 0.31 mmol), affording **52a** (41 mg, 58%) as a white solid. Mp 156-158 °C. ¹H NMR (400 MHz, DMSO-*d*₆): 7.77 (s, 1H, CH), 7.36 (s, 1H, CHNH), 7.03 (s, 1H, CH), 7.02 (s, 1H, CH), 6.34 (br s, 1H, NH), 5.86 (ddt, ³J = 6.4 Hz, ³J_{cis} = 10.0 Hz, ³J_{trans} = 16.4 Hz, 1H, CH₂=CH), 4.97 (dd, ³J_{cis} = 10.0 Hz, ³J_{trans} = 16.4 Hz, 2H, CH₂=CH), 2.94 (dq, ⁴J = 1.6 Hz, ³J = 6.4 Hz, 2H, CH₂). ¹³C NMR (100 MHz, DMSO-*d*₆): 155.6 (C), 137.2

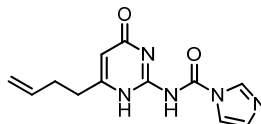
(CH), 136.0 (CH), 128.2 (CH), 122.8, (CH) 115.7 (CH₂), 113.1 (C), 31.0 (CH₂).
ESI-MS (MeOH): *m/z* 210.1 [(M-imidazol+MeOH)⁺].

***N*-(5-Allyl-4-oxo-6-undecyl-1,4-dihydropyrimidin-2-yl)-1*H*-imidazole-1-carboxamide (52b):**



Prepared by following the general procedure D from **51a** (100 mg, 0.33 mmol), affording **52b** (97 mg, 74%) as a white solid. Mp 162-165 °C ¹H NMR (400 MHz, DMSO-*d*₆): 8.16 (s, 1H, CH), 7.46 (s, 1H, CH), 6.95 (s, 2H, NH), 6.84 (s, 1H, CH), 5.76 (ddt, ³*J* = 6.0 Hz, ³*J*_{cis} = 10.0 Hz, ³*J*_{trans} = 16.8 Hz, 1H, CH₂=CH), 4.87 (dd, ³*J*_{cis} = 10.0 Hz, ³*J*_{trans} = 16.8 Hz, 2H, CH₂=CH), 3.05 (d, ³*J* = 6.0 Hz, 2H, CH₂), 2.30-2.26 (m, 2H, CH₂), 1.50 (q, ³*J* = 6.0 Hz, 2H, CH₂), 1.31-1.15 (m, 16H, CH₂), 0.81 (t, ³*J* = 6.0 Hz, 3H, CH₃). ¹³C NMR (100 MHz DMSO-*d*₆): 163.9 (C), 157.2 (C), 153.9 (C), 136.8 (CH), 135.1 (CH), 128.9 (CH), 121.8 (C), 117.1 (CH), 114.0 (CH₂), 109.5 (C), 34.0 (CH₂), 31.8 (CH₂), 29.6 (CH₂), 29.5 (CH₂), 29.4 (CH₂), 29.3 (CH₂), 29.2 (CH₂), 28.8 (CH₂), 28.4 (CH₂), 22.6 (CH₂), 14.2 (CH₃). ESI-MS (MeOH): 445.2 [(M-imidazol+TFA)⁺], 305.1 [(M-imidazol-CO)⁺].

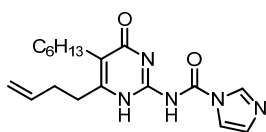
***N*-(6-(But-3-enyl)-4-oxo-1,4-dihydropyrimidin-2-yl)-1*H*-imidazole-1-carboxamide (52c):**



Carbonyl diimidazole (607 mg, 3.63 mmol) and compound **51b** (300 mg, 1.82 mmol) were placed into a sealed tube, suspended in dry THF (15 mL) and stirred initially at 50 °C during 30 minutes. Temperature was then dropped down to 30 °C and stirred overnight. Solvent was eliminated and the solid residue was triturated in acetone, filtered and washed. A white solid **52c** was obtained (385 mg, 82%). Mp: 249-250 °C. ¹H NMR (400 MHz, CDCl₃): 13.80 (br

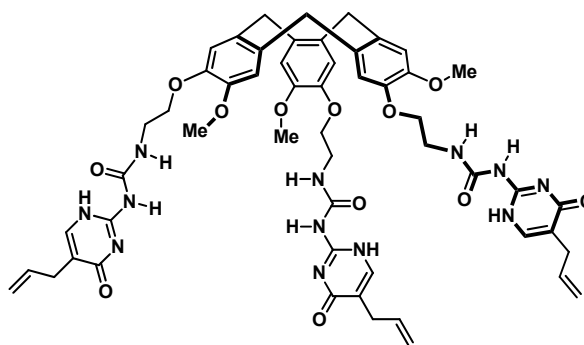
s, 1H, NH), 12.33 (br s, 1H, NH), 8.87 (s, 1H, CH), 7.63 (s, 1H, CH), 7.01 (s, 1H, CH), 5.89 (ddt, $^3J = 6.4$ Hz, $^3J_{cis} = 10.4$ Hz, $^3J_{trans} = 27.3$ Hz, 1H, CH₂=CH), 5.81 (s, 1H, CHCO), 5.20-5.15 (m, 2H, CH₂=CH), 2.76 (t, $^3J = 7.2$ Hz, 2H, CH₂), 2.52 (q, $^3J = 6.4$ Hz, 2H, CH₂). ¹³C NMR (100 MHz, DMSO-*d*₆): 168.8 (C), 163.7 (C), 156.3 (C), 138.5 (CH), 135.6 (CH), 122.2 (CH), 115.3 (CH₂), 100.3 (CH), 36.6 (CH₂), 32.0 (CH₂). ESI-MS (MeOH): 224.1 [(M-imidazol+MeOH)⁺]. Elemental analysis calcd. (%)C₁₂H₁₃N₅O₂ (259.1): C 55.59, H 5.05, N 27.01; found C 55.85, H 5.29, N 26.87.

***N*-(6-(But-3-en-1-yl)-5-hexyl-4-oxo-1,4-dihydropyrimidin-2-yl)-1*H*-imidazole-1-carboxamide (52d).**



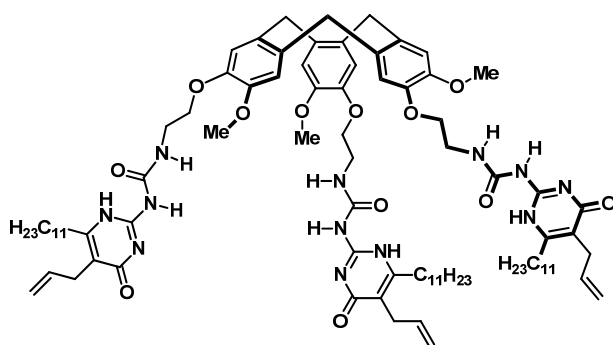
Prepared by following the general procedure D from **51c** (200 mg, 0.80 mmol), affording **52c** (199 mg, 74%) as a white solid. Mp: 233-235 °C. ¹H NMR (400 MHz, CDCl₃): 13.39 (br s, 1H, NH), 12.26 (br s, 1H, NH), 8.86 (s, 1H, CH), 7.63 (s, 1H, CH), 7.03 (s, 1H, CH), 5.90 (ddt, $^3J = 6.8$ Hz, $^3J_{cis} = 10.5$ Hz, $^3J_{trans} = 16.6$ Hz, 1H, CH₂=CH), 5.15 (dd, $^3J_{cis} = 10.5$ Hz, $^3J_{trans} = 16.6$ Hz, 2H, CH₂=CH), 2.80 (t, $^3J = 7.7$ Hz, 2H, CH₂), 2.53-2.42 (m, 4H, CH₂), 1.50 (q, $^3J = 7.7$ Hz, 2H, CH₂), 1.39-1.29 (m, 8H, CH₂), 0.89 (t, $^3J = 7.0$ Hz, 3H, CH₃). ¹³C NMR (100 MHz, CDCl₃): 168.8 (C), 163.7 (C), 156.3 (C), 138.5 (CH), 135.6 (CH), 122.2 (CH), 115.3 (CH₂), 100.3 (CH), 36.6 (CH₂), 32.0 (CH₂). ESI-MS (MeOH/TFA): 389.1 [(M-imidazol+TFA)⁺].

1,1',1''-(((3,8,13-Trimethoxy-10,15-dihydro-5H-tribenzo[a,d,g]cyclononene-2,7,12-triyl)tris(oxy))tris(ethane-2,1-diyl))tris(3-(5-allyl-4-oxo-1,4-dihydropyrimidin-2-yl)urea) (53a).



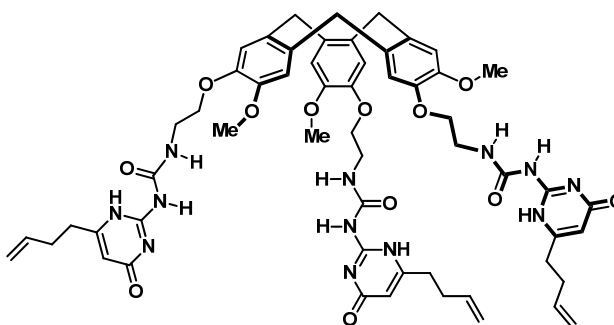
CTV-NH₂ **29** (25 mg, 0.47 mmol) and **52a** (35 mg, 0.14 mmol) were reacted following general procedure F to yield compound **53a** (43 mg, 87%) as a white solid. Mp >300 °C. ¹H NMR (400 MHz, DMSO-*d*₆): 9.60 (br s, 3H, NH), 7.52 (s, 3H, CHNH), 7.15 (s, 3H, CHAr), 7.10 (s, 3H, CHAr), 5.87 (ddt, ³J = 6.7 Hz, ³J_{cis} = 10.2 Hz, ³J_{trans} = 16.9 Hz, 3H, CH₂=CH), 5.03 (dd, (ddt, ³J_{cis} = 10.2 Hz, ³J_{trans} = 16.9 Hz, CH₂=CH), 6H, CH=CH₂), 4.69 (d, ²J = 13.2 Hz, 3H, ArCH₂Ar), 4.00 (m, 6H, CH₂), 3.71 (s, 9H, OCH₃), 3.52 (d, ²J = 13.2 Hz, 3H, ArCH₂Ar), 3.51-3.46 (m, 6H, CH₂), 3.00 (d, ³J = 6.0 Hz, 6H, CH₂). ¹³C NMR (100 MHz, DMSO-*d*₆): 170.8 (C), 168.9 (C), 160.2 (C), 159.8 (C), 148.1 (CAr), 146.5 (CAr), 136.2 (CHAR), 133.2 (CAr), 132.5 (CAr), 116.6 (CH₂), 115.9 (CH), 114.5 (CH), 67.9 (CH₂), 55.3 (CH₃), 39.1 (CH₂), 35.5 (CH₂). ESI-MS: *m/z* 1113.0 [(M+Na)⁺], 1091.1 [(M+H)⁺]. Elemental analysis calcd. (%) C₅₀H₆₀N₁₂O₁₂ (1069.1): C 60.60, H 5.66, N 12.72; found C 59.62, H 5.74, N 12.83.

1,1',1''-(((3,8,13-Trimethoxy-10,15-dihydro-5H-tribenzo[a,d,g]cyclononene-2,7,12-triyl)tris(oxy))tris(ethane-2,1-diyl))tris(3-(5-allyl-4-oxo-6-undecyl-1,4-dihydropyrimidin-2-yl)urea) (53b).



CTV-NH₂ **29** (36 mg, 0.067 mmol) and compound **52b** (80 mg, 0.20 mmol) were reacted following general procedure F to yield compound **53b** (64 mg, 63%) as a white solid. Mp 211-213 °C. ¹H NMR (400 MHz, DMSO-*d*₆): 10.71 (br s, 3H, NH), 7.21 (s, 3H, CHAr), 7.10 (s, 3H, CHAr), 5.77 (ddt, ³J = 6.9 Hz, ³J_{cis} = 11.3 Hz, ³J_{trans} = 16.7 Hz, 3H, CH₂=CH), 4.92 (m, 6H, CH₂=CH), 4.68 (s, ²J = 13.6 Hz, 3H, ArCH₂Ar), 3.91 (t, ³J = 5.8 Hz, 3H, CH₂), 3.69 (s, 9H, OCH₃), 3.50 (d, ²J = 13.6 Hz, 3H, ArCH₂Ar), 3.03 (d, ³J = 6.0 Hz, 6H, CH₂), 2.27 (t, ³J = 8.0 Hz, 6H, CH₂), 1.51 (q, ³J = 7.5 Hz, 6H, CH₂), 1.30-1.24 (m, 54H, CH₂), 0.86 (t, ³J = 7.0 Hz, 9H, CH₃). ¹³C NMR (100 MHz, DMSO-*d*₆): 166.2 (C), 154.0 (C), 148.0 (C), 146.7 (C), 137.6 (CH), 129.9 (C), 115.2 (CH), 114.3 (CH), 114.2 (CH₂), 68.0 (CH₂), 56.1 (CH₃), 39.1 (CH₂), 35.8 (CH₂), 34.5 (CH₂), 31.8 (CH₂), 29.5 (CH₂), 29.4 (CH₂), 29.3 (CH₂), 29.1 (CH₂), 28.9 (CH₂), 28.3 (CH₂), 22.6 (CH₂), 14.4 (CH₃). ESI-MS: 1555.1 [(M+Na)⁺].

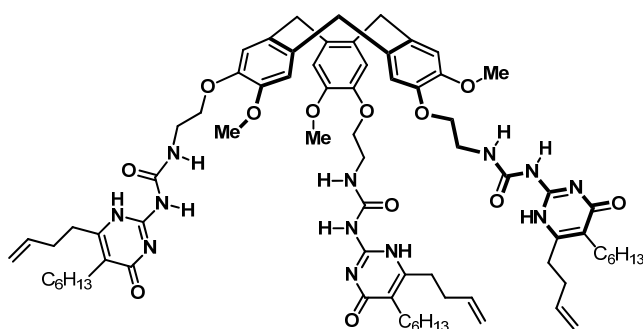
1,1',1''-(((3,8,13-Trimethoxy-10,15-dihydro-5H-tribenzo[a,d,g]cyclononene-2,7,12-triyl)tris(oxy))tris(ethane-2,1-diyl))tris(3-(6-(but-3-en-1-yl)-4-oxo-1,4-dihydropyrimidin-2-yl)urea) (53c).



CTV-NH₂ **29** (78 mg, 0.15 mmol) and compound **52c** (113 mg, 0.44 mmol) were reacted following general procedure F to yield compound **53c** (94 mg, 60%) as a white solid. Mp >300 °C. ¹H NMR (400 MHz, DMSO-*d*₆): 9.73(br s, 3H, NH), 7.17 (s, 3H, CHAr), 7.07 (s, 3H, CHAr), 5.71-5.65 (m, 3H, CH₂=CH), 5.63 (s, 3H, CH), 4.87 (dd, ³J_{cis} = 10.5 Hz, ³J_{trans} = 17.7 Hz, 6H, CH₂=CH), 4.66 (d, ²J_{gem} = 12.9, 3H, ArCH₂Ar), 4.00-3.83 (m, 6H, CH₂), 3.73-3.43 (m, 18H, OCH₃, CH₂, ArCH₂Ar), 2.36-2.32 (m, 6H, CH₂), 2.26-2.19(m, 6H, CH₂). ¹³C NMR (100 MHz, CDCl₃): 163.0 (C), 155.9 (C), 148.2 (C), 138.3 (C), 138.3 (C), 133.1 (CH), 132.4 (C), 116.5 (CH), 115.4 (CH), 104.2 (CH), 68.4 (CH₂), 56.7 (CH₃), 36.8 (CH₂), 35.9 (CH₂), 35.5 (CH₂), 31.9 (CH₂). MALDI-TOF: *m/z* 1111.5 [M]⁺. Elemental analysis calcd. (%)C₅₇H₆₆N₁₂O₁₂•½ CHCl₃ (1111.2): C 58.98, H 5.72, N 14.35; found C 58.50, H 5.87, N 14.51.

Chapter VI

1,1',1''-(((3,8,13-Trimethoxy-10,15-dihydro-5H-tribenzo[a,d,g]cyclononene-2,7,12-triyl)tris(oxy))tris(ethane-2,1-diyl))tris(3-(6-(but-3-en-1-yl)-5-hexyl-4-oxo-1,4-dihydropyrimidin-2-yl)urea) (53d).



CTV-NH₂ **29** (39 mg, 0.07 mmol) and compound **52d** (75 mg, 0.22 mmol) were reacted following general procedure F to yield compound **53d** (96 mg, 96%) as a beige solid. Mp >300 °C. ¹H NMR (400 MHz, DMSO-*d*₆): 9.61 (br s, 3H, NH), 7.66 (br s, 3H, NH), 7.14 (s, 3H, CHAr), 7.08 (s, 3H, CHAr), 5.76 (ddt, ³J_{cis} = 10.3 Hz, ³J_{trans} = 17.4 Hz, ³J = 6.5 Hz, 3H, CH₂=CH), 4.93 (dd, ³J_{cis} = 10.3 Hz, ³J_{trans} = 17.4 Hz, 6H, CH₂=CH), 4.70 (d, ²J = 12.8 Hz, 3H, ArCH₂Ar), 4.03-3.98 (m, 6H, CH₂), 3.70 (s, 9H, CH₃), 3.53-3.44 (m, 9H, ArCH₂Ar, CH₂), 2.34-2.22 (m, 12H, CH₂), 1.41-1.21 (m, 30H, CH₂), 0.85 (t, ³J = 6.2 Hz, 9H, CH₃). ¹³C NMR (100 MHz, DMSO-*d*₆): 175.1 (C), 162.1 (C), 148.9 (C), 146.5 (C), 138.1 (CH), 133.2 (C), 132.4 (C), 115.9 (CH), 115.6 (C), 114.3 (CH), 68.0 (CH₂), 56.3 (CH₃), 35.5 (CH₂), 33.2 (CH₂), 32.3 (CH₂), 31.6 (CH₂), 29.1 (CH₂), 24.9 (CH₂), 24.8 (CH₂), 22.5 (CH₂), 14.4 (CH₃). ESI-MS (-ve) (MeOH/HCOOH): 1362.4 [(M)-]. Elemental analysis calcd. (%)C₇₅H₁₀₂N₁₂O₁₂•EtOH (1363.7): C 65.60, H 7.72, N 11.92; found C 65.30, H 7.62, N 11.56.

CHAPTER VII: APPENDIX

UNIVERSITAT ROVIRA I VIRGILI
SELF-ASSEMBLY BASED ON THE 2-UREIDO-4(1H)-PYRIMIDINONE MOTIF: FROM CYCLIC ARRAYS TO MOLECULAR CAPSULES
FOR FULLERENE SEPARATIONS
Elisa Huerta Martínez
DL:T.289-2012

Chapter VII

CHAPTER VII: APPENDIX

VII.1 2D Molecular Architectures Based on the 2-Ureido-4(1H)-pyrimidinone Dimeric Motif

VPO Calibration Curves

Working temperature in vapor pressure osmometry (VPO) experiments was 35°C. Standards and samples were prepared gravimetrically using ethanol-free chloroform as solvent. Solvent zero was periodically checked.

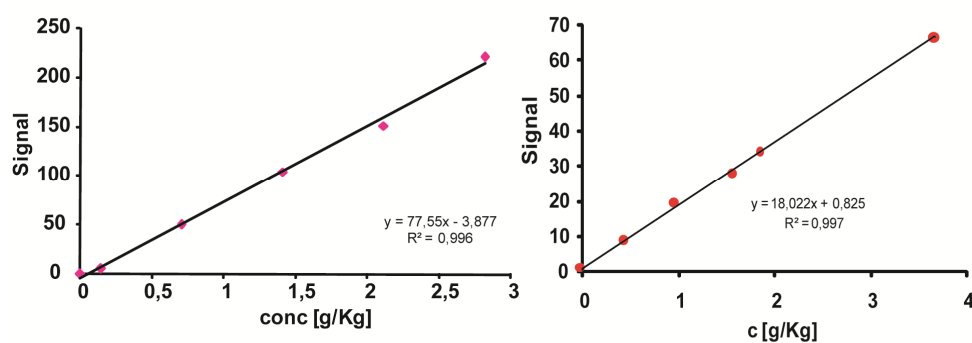


Figure 1: Graphical representation of the values obtained for calibration with bezil standard (left) and PS1000 standard (right).

Table 1: Calibration constant (K_{cal}) values obtained for each standard.

Standard	MW (g/mol)	K_{cal} (Kg/mol)
Benzil	210	16303.3
PS 1000	990	17481.8

Chapter VII

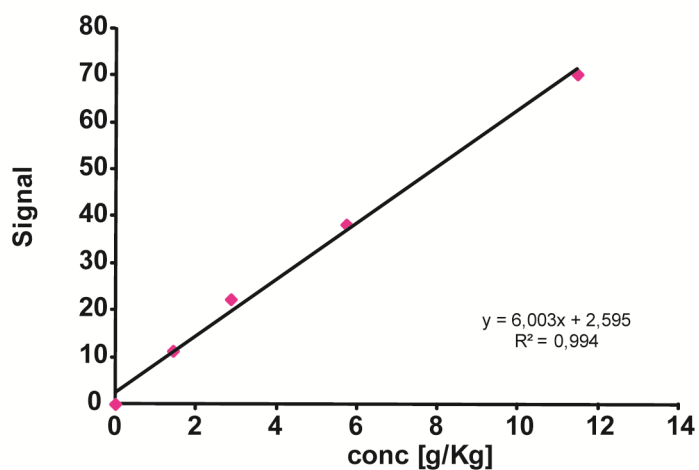


Figure 2: Plot of the VPO signals obtained for **2a** at different concentrations fitted to a lineal model.

Table 2: Average molecular weight calculated for **2a** determined as a function of the standard used in calculations.

Standard	Benzil	PS 1000
MW _n (g/mol)	2715.6	2911.9
N° Monomers	3.7	4.0

Chapter VII

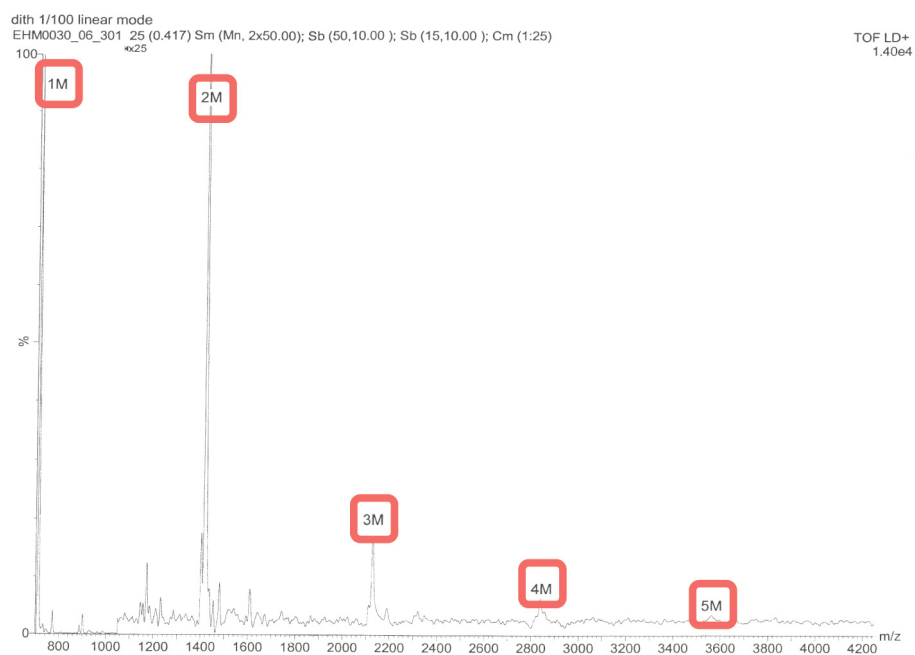


Figure 2: MALDI-TOF spectrum of compound 3b

VII.2 Fullerene Recognition and Separation by Encapsulation

Method for Quantification of C₇₀ Extractions

C ₆₀ Conc. (M)	Area (mUxs)	C ₇₀ Conc. (M)	Area (mUxs)
7,10 x 10 ⁻⁴	15081,20	7,35 x 10 ⁻⁴	19404,77
2,37 x 10 ⁻⁴	5297,32	2,45 x 10 ⁻⁴	6874,81
1,42 x 10 ⁻⁴	2868,27	1,47 x 10 ⁻⁴	3963,79
7,10 x 10 ⁻⁵	1424,08	7,35 x 10 ⁻⁵	1985,38
2,37 x 10 ⁻⁵	479,97	2,45 x 10 ⁻⁵	677,91
1,78 x 10 ⁻⁵	334,53	1,84 x 10 ⁻⁵	488,25
1,18 x 10 ⁻⁵	219,19	1,23 x 10 ⁻⁵	320,45
8,88 x 10 ⁻⁶	184,64	9,19 x 10 ⁻⁶	253,80
7,10 x 10 ⁻⁶	131,62	7,35 x 10 ⁻⁶	189,98
7,10 x 10 ⁻⁷	13,62	7,35 x 10 ⁻⁷	19,52

Chapter VII

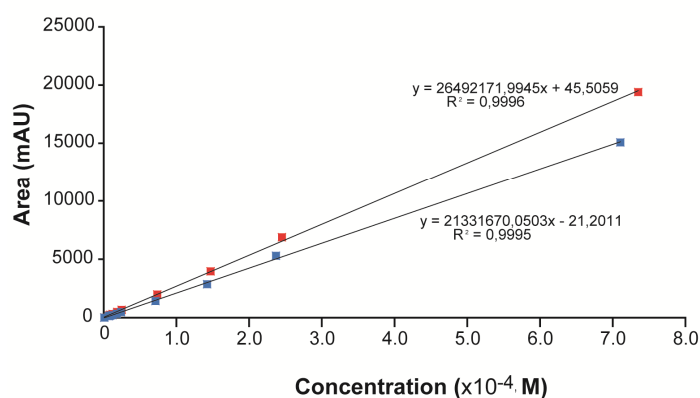


Figure 3: Calibration curves for a) C_{70} (red square) and b) C_{60} (blue square).

Method for Quantification of C_{84} Extractions

Standard	Concentration (M)		
	C_{60}	C_{70}	C_{84}
1	9.77×10^{-4}	1.04×10^{-3}	1.78×10^{-4}
2	7.67×10^{-4}	7.96×10^{-4}	1.48×10^{-4}
3	4.89×10^{-4}	5.22×10^{-4}	8.92×10^{-5}
4	2.44×10^{-4}	2.61×10^{-4}	4.46×10^{-5}
5	1.22×10^{-4}	1.30×10^{-4}	2.23×10^{-5}
6	6.11×10^{-5}	6.52×10^{-5}	1.12×10^{-5}
7	3.05×10^{-5}	3.26×10^{-5}	5.58×10^{-6}
8	1.53×10^{-5}	1.63×10^{-5}	2.79×10^{-6}
9	7.63×10^{-6}	8.15×10^{-6}	1.39×10^{-6}
10	3.8×10^{-6}	4.08×10^{-6}	6.97×10^{-6}
11	1.9×10^{-6}	2.04×10^{-6}	3.49×10^{-7}
12	9.54×10^{-7}	1.02×10^{-6}	1.74×10^{-7}

^aConcentrations of C_{84} below 5×10^{-5} M were not quantifiable by UV-vis

Chapter VII

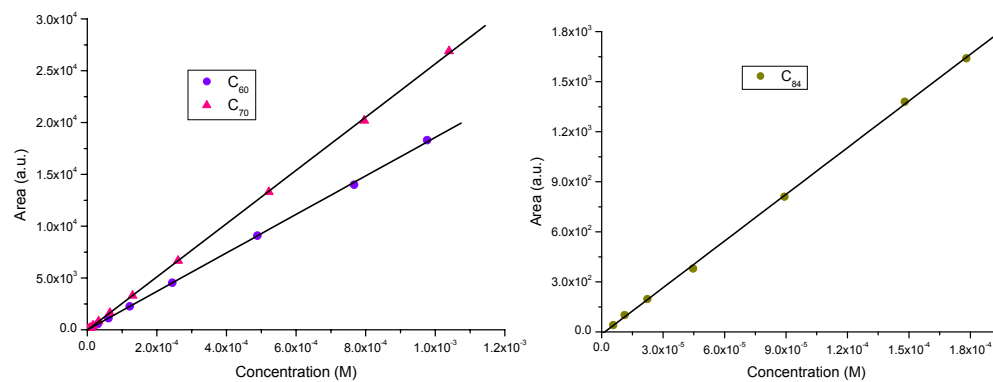


Figure 4: Calibration curves for C₆₀, C₇₀ (left) and C₈₄ (right).

Characterization of Homochiral Capsules

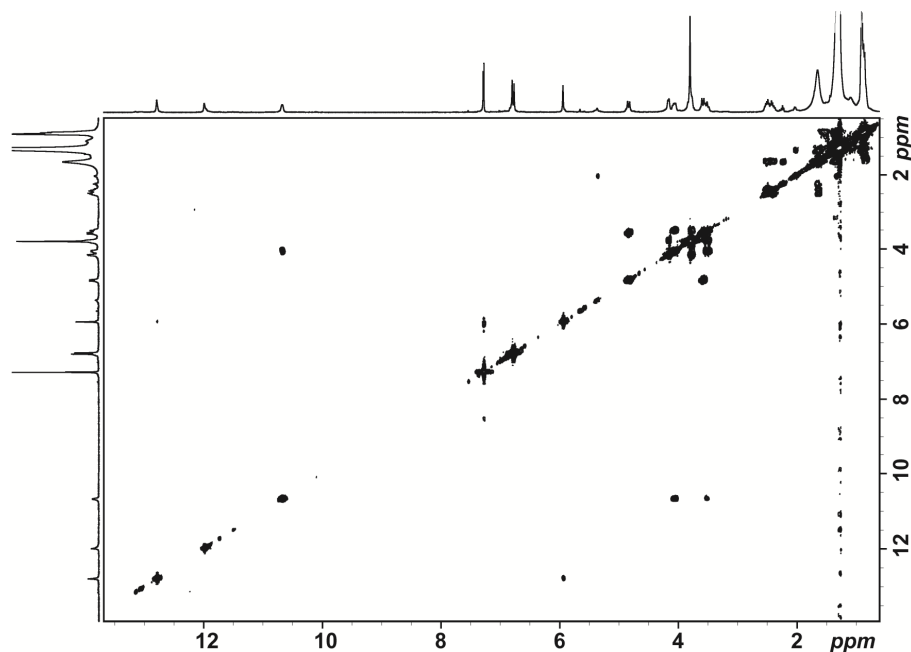


Figure 5: ¹H-¹H COSY NMR (400 MHz, CDCl₃) of homochiral C₇₀@5b 5b.

Chapter VII

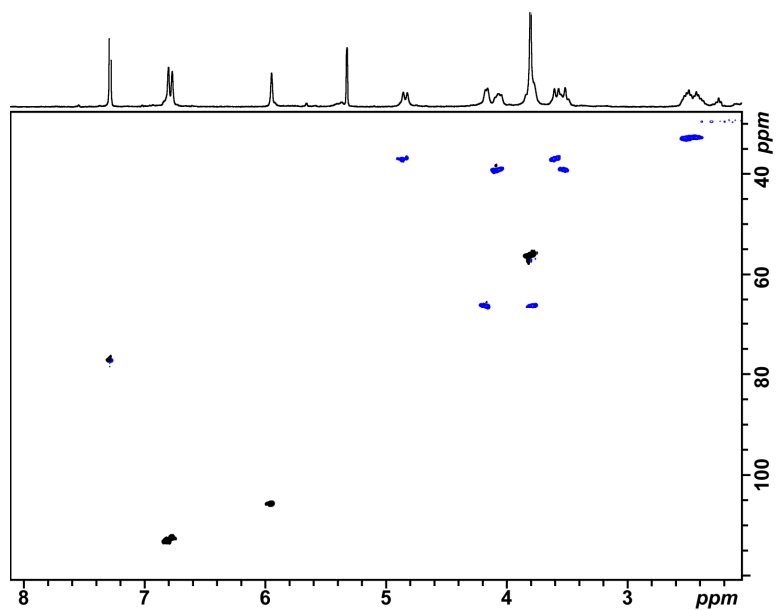


Figure 6: Phase dependent HSQC NMR (400 MHz, CDCl_3) of homochiral $\text{C}_{70}@5\mathbf{b}-5\mathbf{b}$.

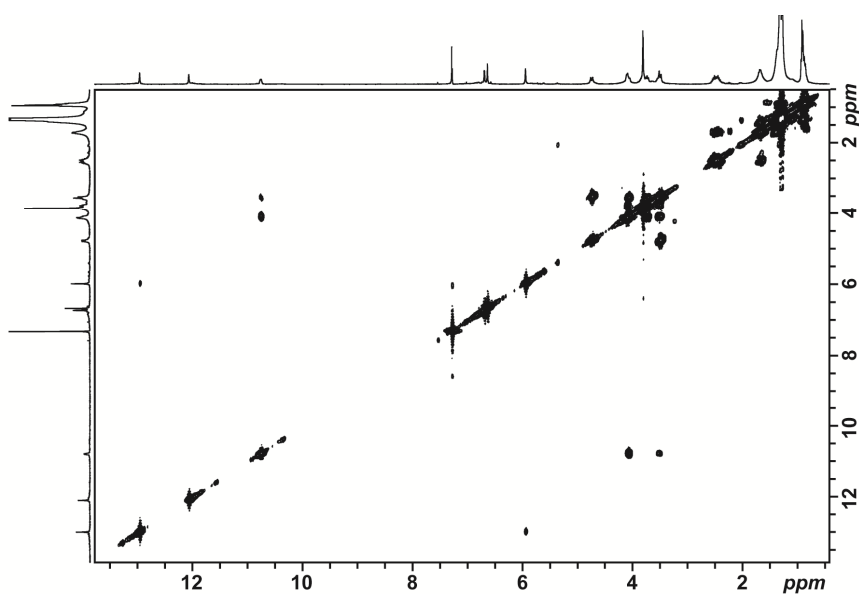


Figure 7: $^1\text{H}-^1\text{H}$ COSY NMR (400 MHz, CDCl_3) of $\text{C}_{76}@5\mathbf{b}-5\mathbf{b}$ (both in racemic form).

Chapter VII

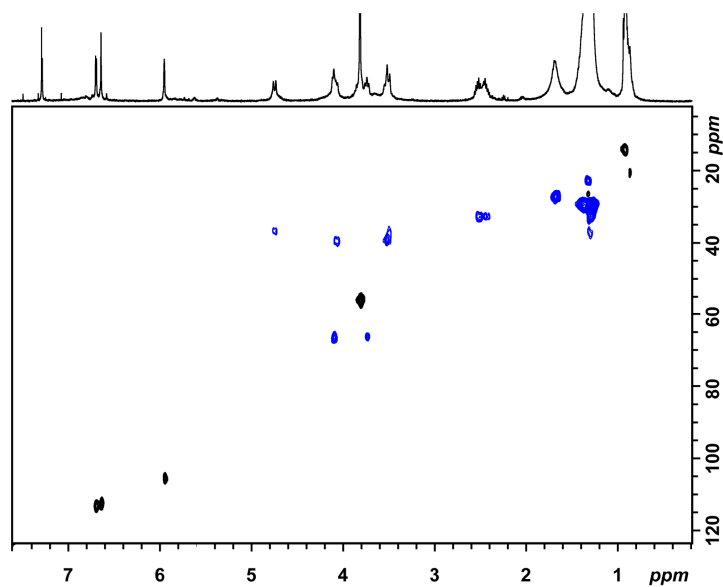


Figure 8: Phase dependent HSQC NMR (400 MHz, CDCl₃) C₇₆@**5b-5b** (both in racemic form).

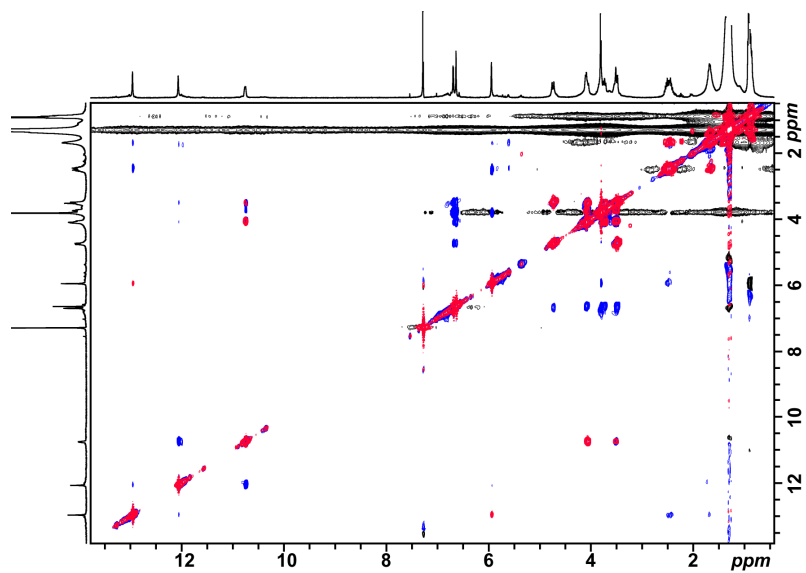


Figure 9: NOESY NMR (400 MHz, CDCl₃) C₇₆@**5b-5b** (both in racemic form, blue). Corresponding COSY signals (red) have been overloaded for clarity.

Chapter VII

Fitting of CD-data to a first order kinetic

The first order kinetic corresponds to the following equations:



$$\frac{d[CTV^\pm]}{dt} = k_v [CTV^\pm]^a \quad (2)$$

Where $[CTV]$ corresponds to the measured specie (in this case homochiral CTV-UPy), t is time (s), k_v is the velocity constant and a is the kinetic's order. If $a = 1$, then:

$$\frac{1}{[CTV^\pm]} d[CTV^\pm] = k_v dt \quad (3)$$

$$\int_0^t \frac{1}{[CTV^\pm]} d[CTV^\pm] = k_v \int_0^t dt \quad (4)$$

$$\ln[CTV^\pm]^t - \ln[CTV^\pm]^0 = k_v t \quad (5)$$

$$\ln\left(\frac{[CTV^\pm]^t}{[CTV^\pm]^0}\right) = k_v t \quad (6)$$

If t is represented against $\ln(f/f_0)$, where f is the signal measured for the homochiral specie present and f_0 is the signal of the racemic specie, the slope of the curve is the value of k_v .

Chapter VII

Racemization of CTV-UPy 5a

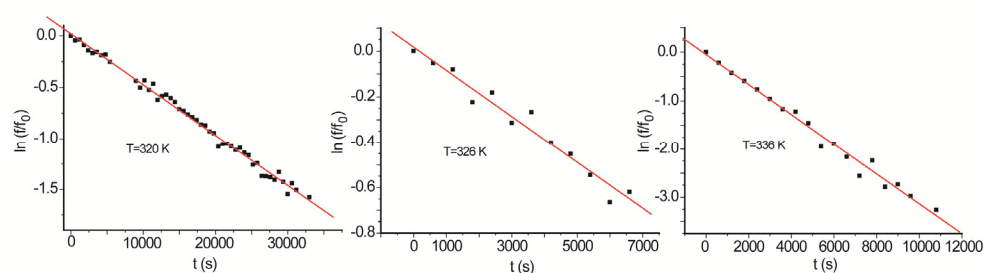


Figure 10: Plot of CD-signal (280 nm) vs time at 320 (left), 326 (middle) and 336 K (right) of racemization of CTV-UPy in tetrachloroethane.

Racemization of C₆₀ complex

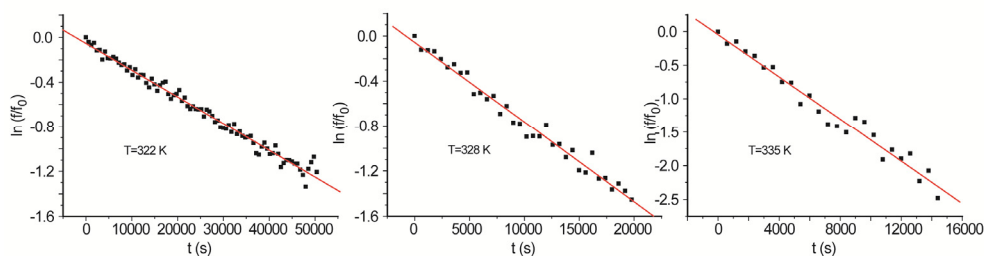


Figure 11: Plot of CD-signal (300 nm) vs time at 322 (top, right), 328 (top, left) and 335 K (down) of racemization of C₆₀@(CTV-UPy)₂ in tetrachloroethane.

Racemization of C₇₀ complex

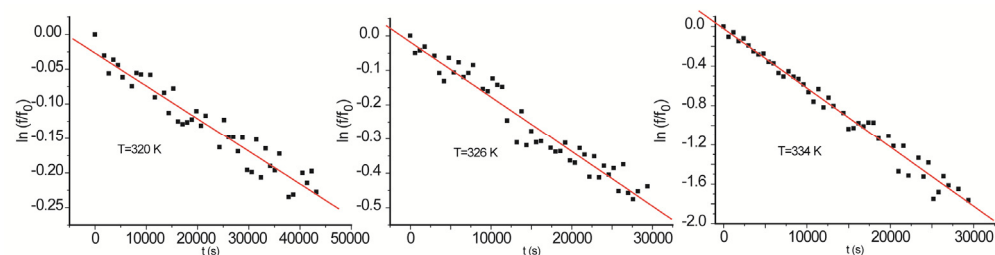


Figure 12: Plot of CD-signal (370 nm) vs time at 320 (top, right), 326 (top, left) and 334 K (down) of racemization of C₇₀@(CTV-UPy)₂ in tetrachloroethane.

Chapter VII

Racemization of C₈₄ complex

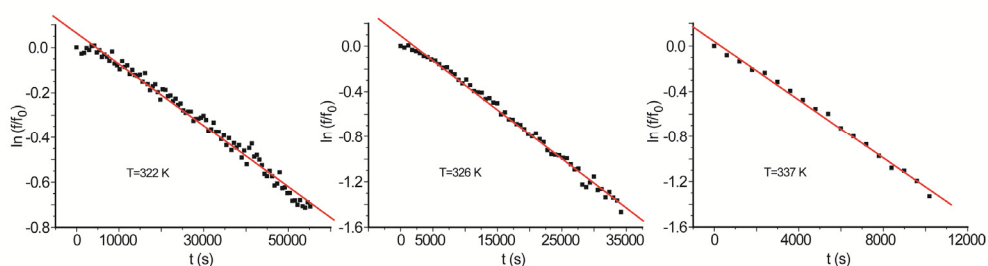


Figure 13: Plot of CD-signal (276 nm) vs time at 322 (top, right), 326 (top, left) and 337 K (down) of racemization of C₈₄@(CTV-UPy)₂ in tetrachloroethane.

When racemization is followed at different temperatures, Eyring equations can be used to calculate thermodynamic parameters in the transition state by representing the temperature (x) vs the values obtained for k_v (y). The enthalpy is then calculated for the slope of the linear fitting and the entropy from the origin ordinate.

$$\Delta H^\ddagger = -m \times R$$

$$b = \ln \frac{k_b}{h} + \frac{\Delta S^\ddagger}{R}$$

where R is the Gas Constant, h is Plank's Constant and k_b is Boltzman Constant.

Chapter VII

VII.3 Fullerene Recognition by Donor-Acceptor Interactions

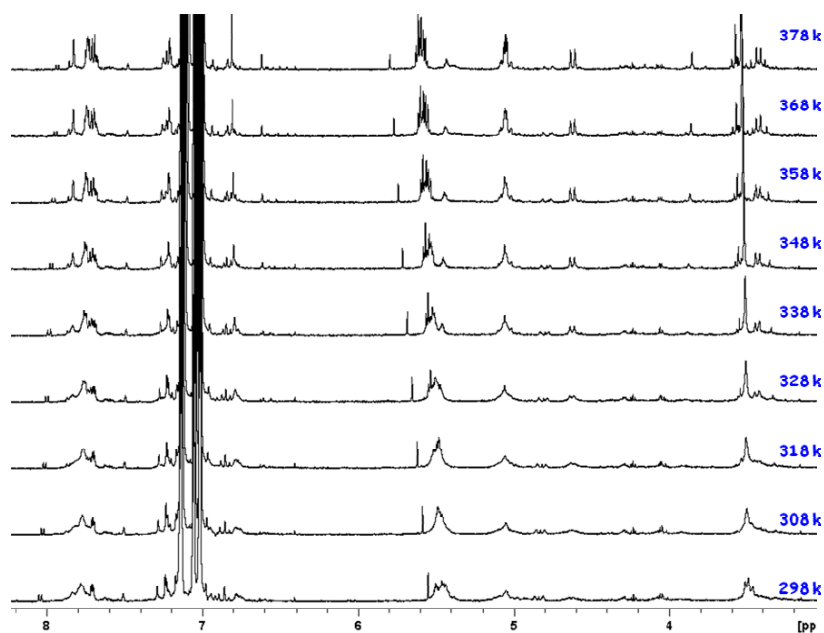


Figure 14: Variable temperature ¹H-NMR experiment (from 398 to 378 K) of compound C₆₀@6 in toluene (500 MHz).

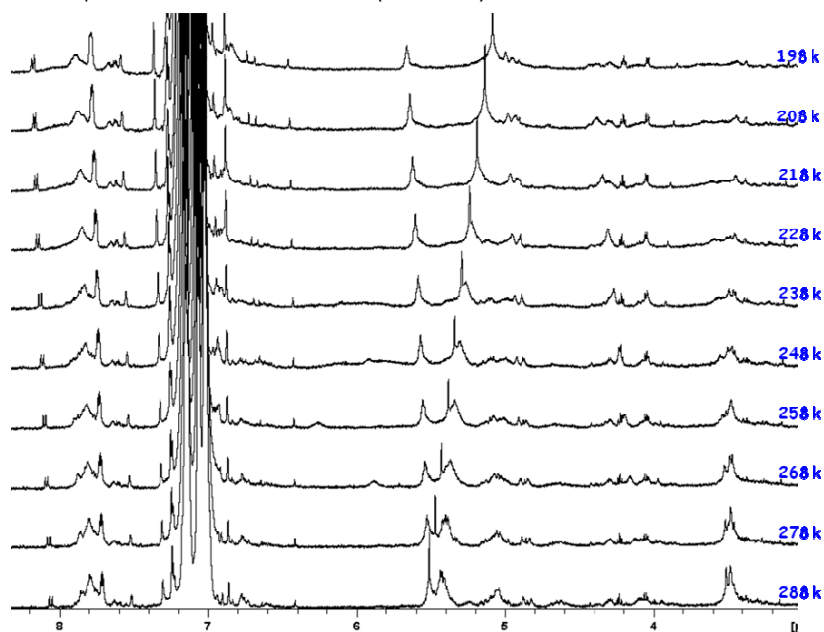


Figure 15: Variable temperature ¹H-NMR experiment (from 288 to 198 K) of compound C₆₀@6 in toluene (500 MHz).

Chapter VII

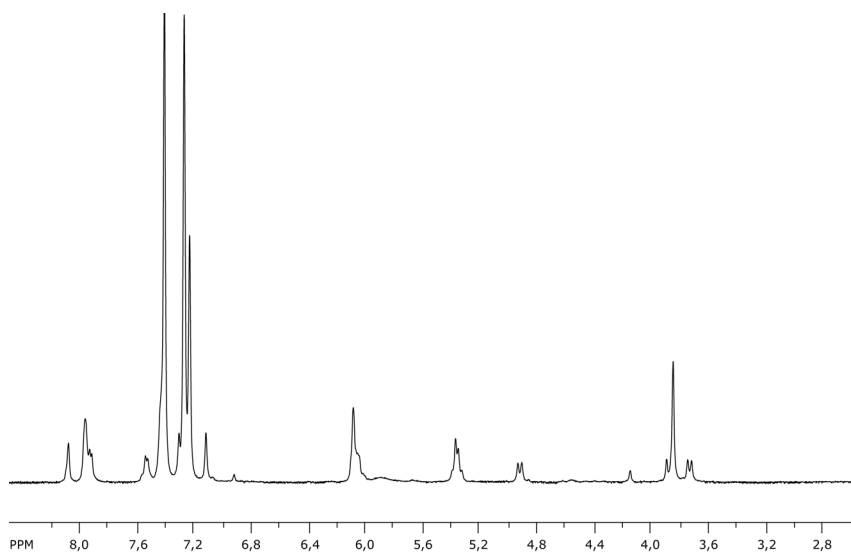


Figure 16: ^1H NMR (500 MHz, chlorobenzene- d_5 , 353 K) of **6**.

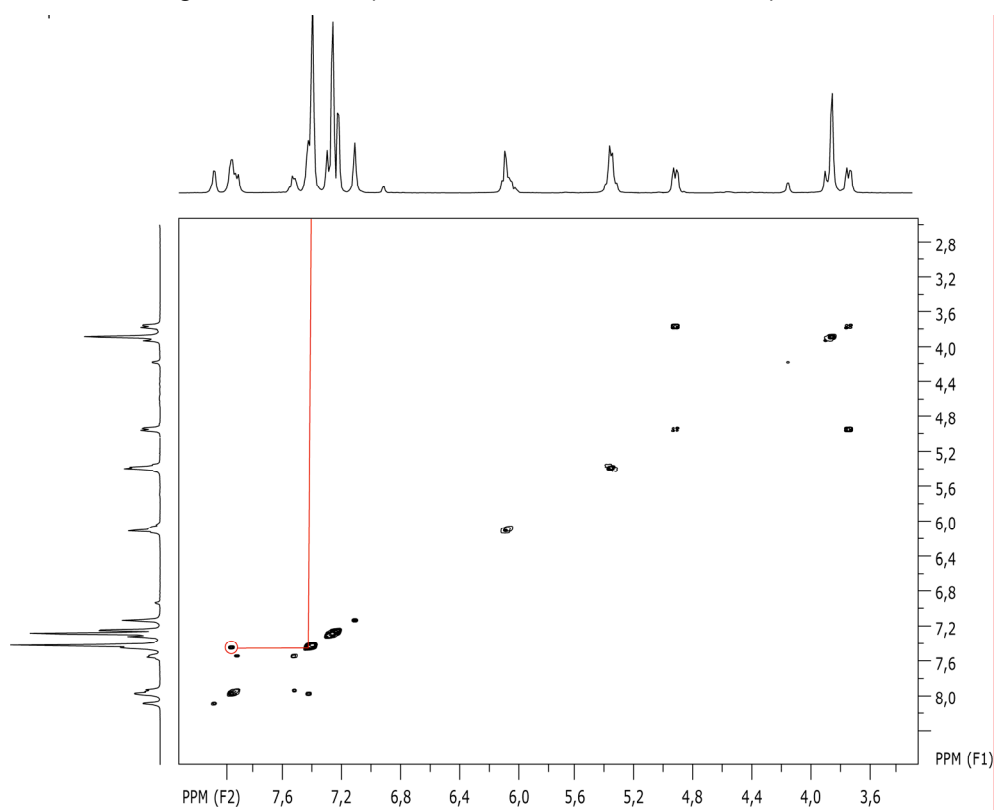


Figure 17: HH COSY (500 MHz, chlorobenzene- d_5 , 353 K) of **6**.

Chapter VII

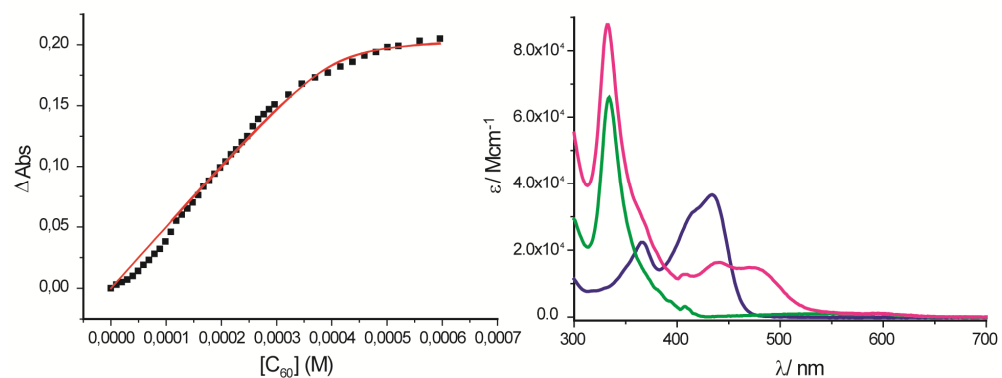


Figure 18: Binding isotherm (left) and calculated ϵ (right, pink) for the $C_{60}@6$.

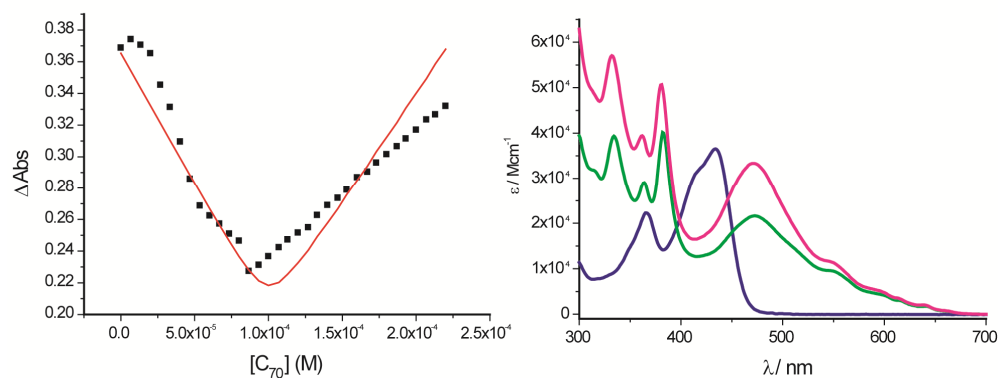


Figure 19: Binding isotherm (left) and calculated ϵ (right, pink) for the $C_{70}@6$.

Chapter VII

VII.4 Carcerands Based on the UPy Motif

C₇₀ Metathesis Reaction in Chloroform Monitored by NMR

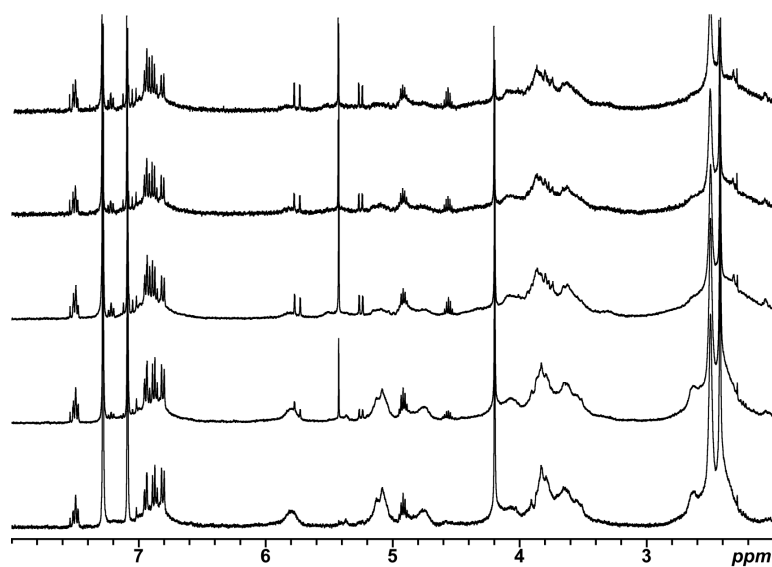


Figure 20: Using Hoveyda-Gurbbs' Catalyst.

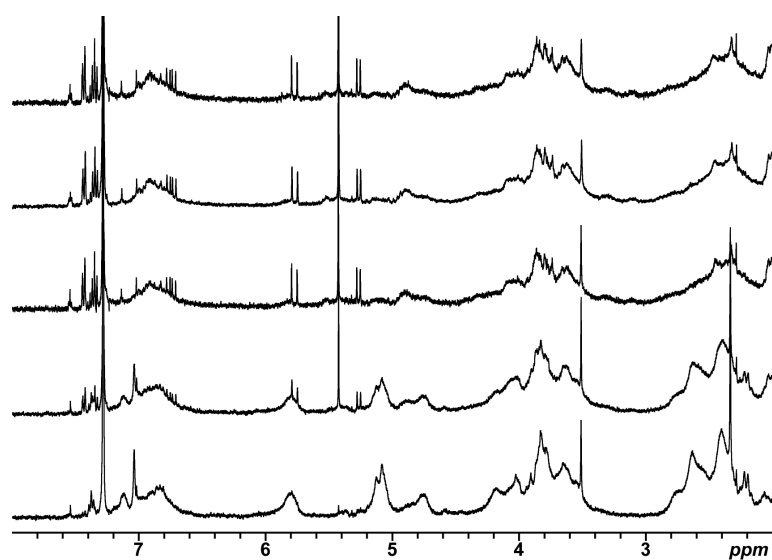


Figure 21: Using 2nd generation-Gurbbs' Catalyst.

Chapter VII

No Fullerene Metathesis Reaction in Chloroform Monitored by NMR

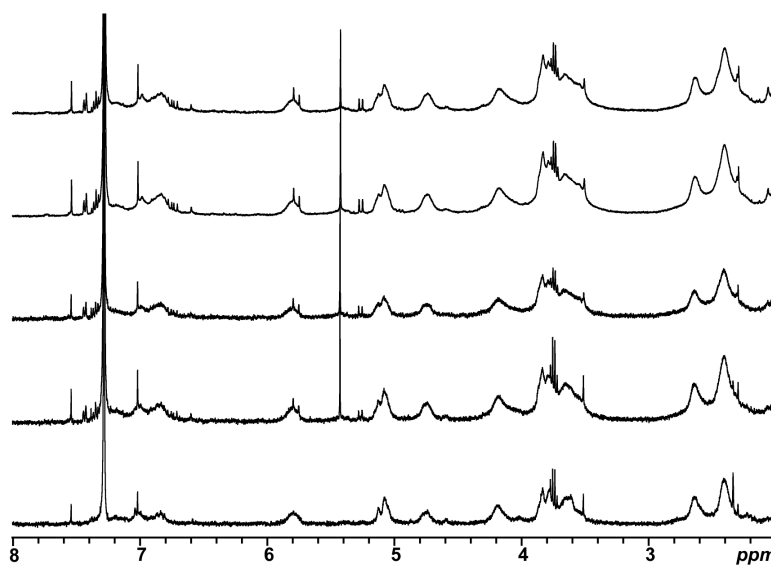


Figure 22: Methathesis reaction in the absence of fullerene using 2nd generation Grubbs' catalyst.

ESI+ Spectrum of No Fullerene Metathesis Reaction

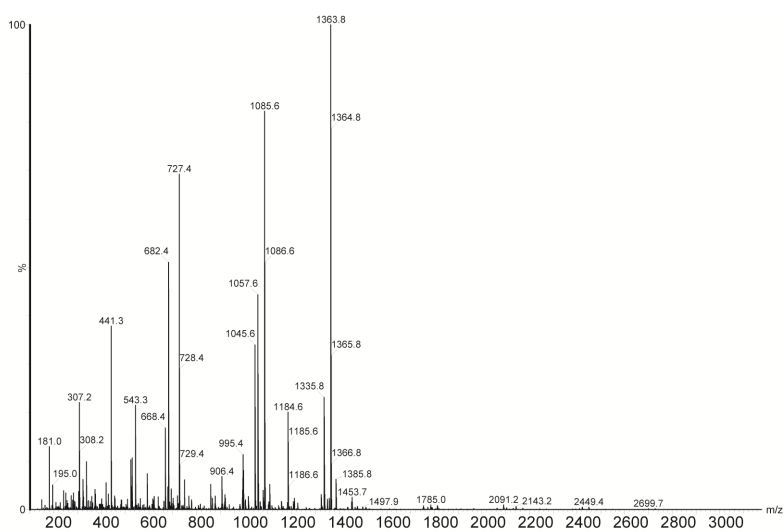


Figure 23: ESI-MS (+) of methathesis reaction of compound **53d** using 2nd generation Grubbs' catalyst.

Chapter VII

C₈₄ Metathesis Reaction in chloroform Monitored by NMR

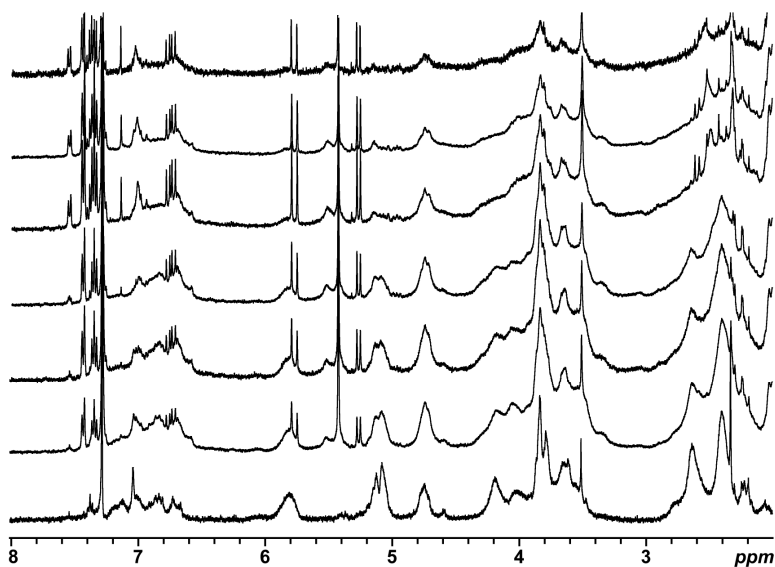


Figure 24: Using 2nd generation-Gurbbbs' Catalyst.

C₈₄@7d ESI+ Spectrum

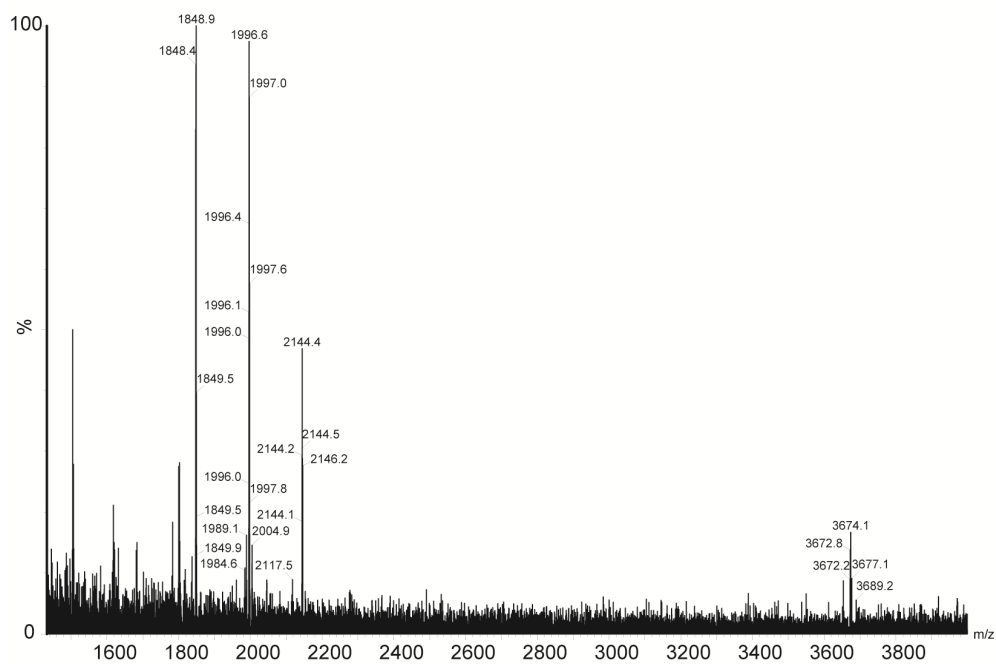


Figure 25: ESI-MS (+) spectrum of C₈₄@7d showing [(M+H)⁺] at m/z 3674.1 and [(M+Na)²⁺] at m/z 1848.9.

Chapter VII

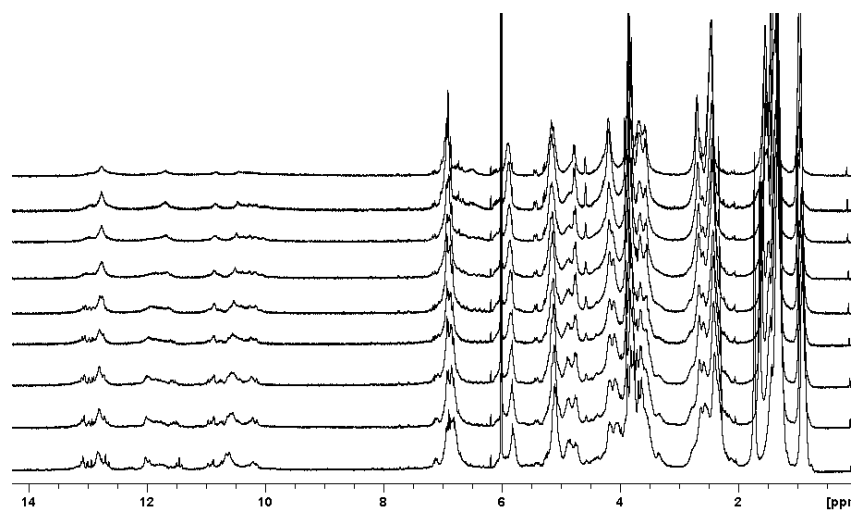


Figure 26: VT ¹H NMR (500 MHz, TCE-d₂) of C₇₀@53d-53d

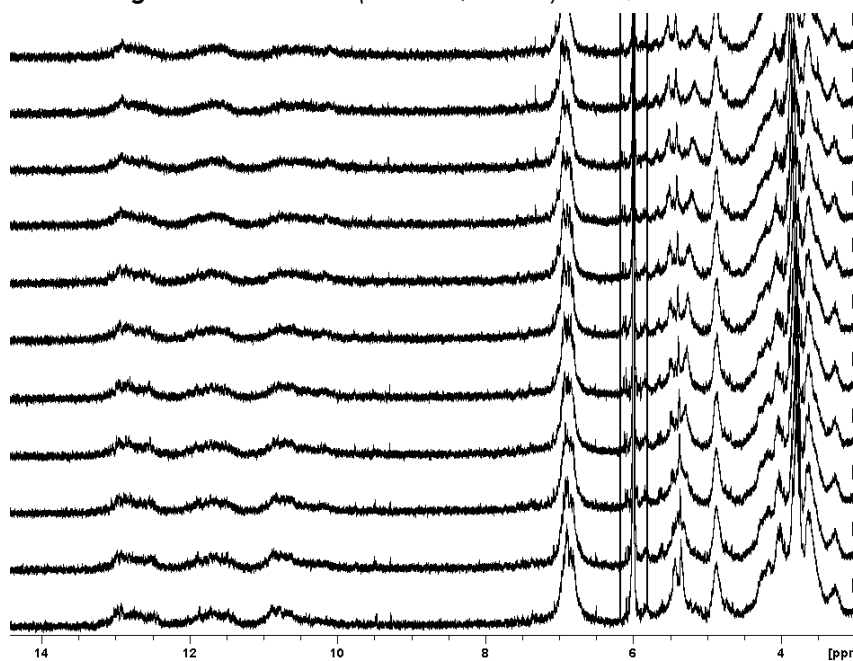


Figure 27: VT ¹H NMR (500 MHz, TCE-d₂) of C₇₀@7d.

RESUMEN

UNIVERSITAT ROVIRA I VIRGILI
SELF-ASSEMBLY BASED ON THE 2-UREIDO-4(1H)-PYRIMIDINONE MOTIF: FROM CYCLIC ARRAYS TO MOLECULAR CAPSULES
FOR FULLERENE SEPARATIONS
Elisa Huerta Martínez
DL:T.289-2012

RESUMEN

El trabajo de investigación de la presente tesis doctoral se ha basado en la síntesis y el estudio de las propiedades de arquitecturas 2D y 3D auto-asociadas mediante enlaces de hidrógeno. Para ello, se ha seleccionado la unidad de 2-ureido-4(1H)-pirimidinona¹ (en adelante, UPy) por su capacidad para dimerizar espontáneamente en disolventes apolares mediante la formación de cuatro enlaces de hidrógeno. Las UPys están en equilibrio entre distintos tautómeros, de los cuales sólo dos son complementarios y capaces de auto-asociarse formando dímeros. De ellos, el dímero DDAA formado por el tautómero 4-(1H)-pirimidinona es el más fuerte, debido a que la disposición de grupos dadores (D) y aceptores (A) favorece las interacciones secundarias de tipo atractivo (Figura 1).

¹ Beijer, F. H.; Sijbesma, R. P.; Kooijman, H.; Speck, A. L.; Meijer, E. W. *J. Am. Chem. Soc.* **1998**, *120*, 6761-6769. b) Folmer, B. J. B.; Sijbesma, R. P.; Kooijman, H.; Spek, A. L.; Meijer, E. W. *J. Am. Chem. Soc.* **1999**, *121*, 9001-9007. c) Söntjens, S. H. M.; Sijbesma, R. P.; van Genderen, M. H. P.; Meijer, E. W. *J. Am. Chem. Soc.* **2000**, *122*, 7487-7493.

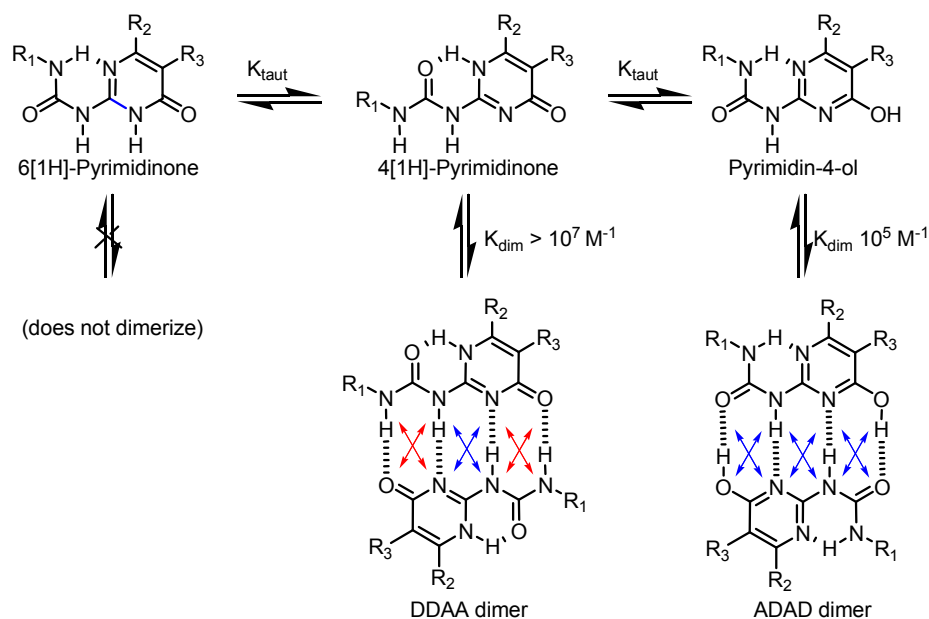


Figura 1: Representación del equilibrio tautomérico de las ureidopirimidinonas y sus formas diméricas.

Es en este contexto en el que se ha desarrollado, por una parte, la síntesis de derivados de ciclotriveratrilenos (CTV),² triplemente funcionalizados con UPys (Figura 2), capaces de auto-asociarse formando cápsulas, altamente flexibles y adaptables, en cuyo interior pueden alojarse fulerenos de distintos tamaños (tales como C₆₀, C₇₀ o C₈₄), siendo el complejo formado por éste último el más estable. Aprovechando la diferencia de estabilidad de cada complejo, se ha desarrollado y puesto a punto un método rápido y sencillo para la purificación de fulerenos, evitando el uso de cromatografía, mediante extracciones sólido-líquido que permite, además, el reciclaje de la cápsula. Utilizando un protocolo de

² a) Vériot, G.; Dutasta, J. P.; Matouzenko, G.; Collet, A. *Tetrahedron* **1995**, *51*, 389 - 400. b) Steed, J. W.; Junk, P. C.; Atwood, J. L.; Barnes, M. J.; Raston, C. L.; Burkhalter, R. S. *J. Am. Chem. Soc.* **1994**, *116*, 10346-10347.

extracción/reextracción, se han obtenido purezas del 97% para C₇₀, y hasta del 85% para C₈₄ en una única extracción a partir de mezclas complejas de fulerenos con un 15% y un 2-5% de C₇₀ y C₈₄, respectivamente, además de otros fulerenos. Esto constituye la primera aplicación práctica de cápsulas auto-asociadas para un proceso de separación selectiva, susceptible de ser empleado industrialmente. El proceso ha sido objeto de una patente en Estados Unidos.

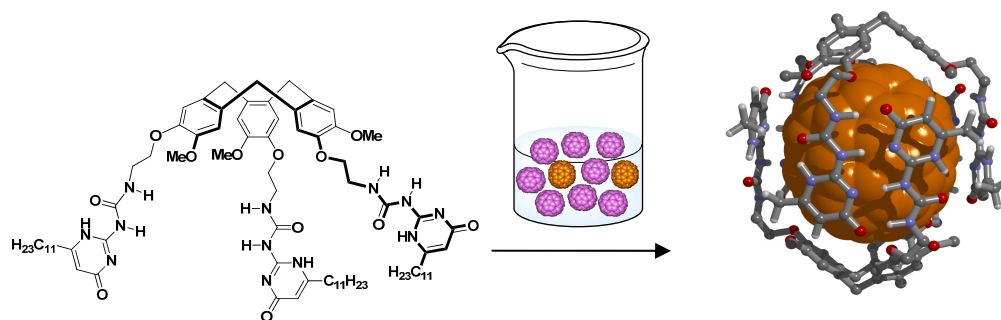


Figura 2: Estructura del receptor sintetizado basado en una plataforma de CTV y representación esquemática del proceso de extracción selectiva de fulerenos de mezclas complejas.

Por otro lado, a partir de estructuras como la descrita, se han conseguido sintetizar carcerandos³ capaces de encapsular un fullereno de forma permanente (maraca molecular), utilizando para ello metodología de Grubbs⁴ para la unión covalente de la cápsula. Este es, hasta la fecha, el único ejemplo de carcerando con un fullereno como huésped, sintetizado usando un doble efecto de plantilla: por un lado, el fullereno que preforma la cápsula y, por otro, los enlaces de hidrógeno que mantienen

³ a) Cram, D. J. *Molecular Nature* **1992**, 356, 29-36. b) Cram, D. J. *Science* **1983**, 219, 1177-1183.

⁴ Wang, L.; Vysotsky, M. O.; Bogdan, A.; Bolte, M.; Böhmer, V. *Science* **2004**, 304, 1312-1314.

unidas las dos mitades y posicionan los grupos alilo terminales en la dirección correcta para la reacción de metátesis. Así, el uso de diferentes fulerenos puros, como C_{70} o C_{84} permite la obtención de los correspondientes carceplejos de C_{70} y C_{84} (Figura 3). El uso de mezclas de fulerenos (fulerita) como plantilla para la formación del complejo y posterior reacción de metátesis, ha permitido también la obtención de un carceplejo de C_{90} .

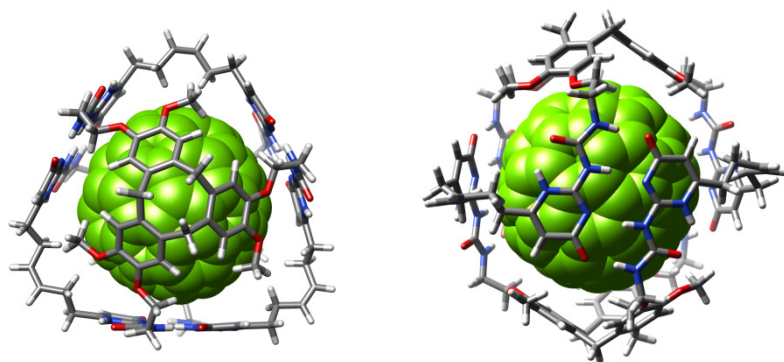


Figura 3: Vistas frontal y lateral de la estructura optimizada del carceplejo de C_{84} .

Además, se ha desarrollado un nuevo tipo de receptores para fulerenos, empleando la plataforma cóncava del CTV y tres unidades de tetratriafulvaleno extendido⁵ (Figura 4), en colaboración con el grupo del Prof. Nazario Martín (UCM), y que presentan interesantes propiedades con potencial aplicación en dispositivos fotovoltaicos.

⁵ a) Pérez, E. M.; Sánchez, L.; Fernández, G.; Martín, N. *J. Am. Chem. Soc.* **2006**, *128*, 7172. b) Pérez, E. M.; Capodilupo, A. L.; Fernández, G.; Sánchez, L.; Viruela, P. M.; Viruela, R.; Ortí, E.; Bietti, M.; Martín, N. *Chem. Commun.* **2008**, 4567. c) Gayathri, S. S.; Wielopolski, M.; Pérez, E. M.; Fernández, G.; Sánchez, L.; Viruela, R.; Ortí, E.; Guldí, D. M.; Martín, N. *Angew. Chem., Int. Ed.* **2009**, *48*, 815.

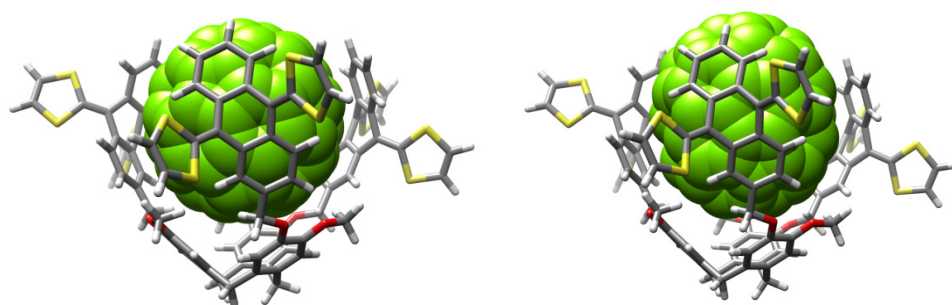


Figura 4: Geometrías optimizadas de los complejos C_{60} @CTV-exTTF (izquierda) y C_{70} @CTV-exTTF (derecha).

Finalmente, se ha trabajado en la síntesis de agregados bidimensionales cíclicos basados en bis-UPys no simétricas con el objetivo de crear materiales porosos,⁶ cuyas propiedades puedan ser moduladas mediante la funcionalización apropiada. Así, en colaboración con el grupo del Prof. J.-F. Nierengarten (Universidad de Estrasburgo), se han sintetizado dendrímeros globulares de fullereno,⁷ con una unidad central de UPy para su dimerización y que contienen hasta 5 unidades de C_{60} por monómero (Figura 5).

⁶ a) Söntjes, S. H. M.; Sijbesma, R. P.; Van Genderen, M. H. P.; Meijer, E. W. *Macromolecules* **2001**, *34*, 3815-3818. b) Keizer, H. M.; Ramzi, A.; Sijbesma, R. P.; Meijer, E. W. *Polymer Preprints* **2003**, *44*, 596-597.

⁷ Nierengarten, J. F. *Chem. Eur. J.* **2000**, *6*, 3667-3670.

RESUMEN

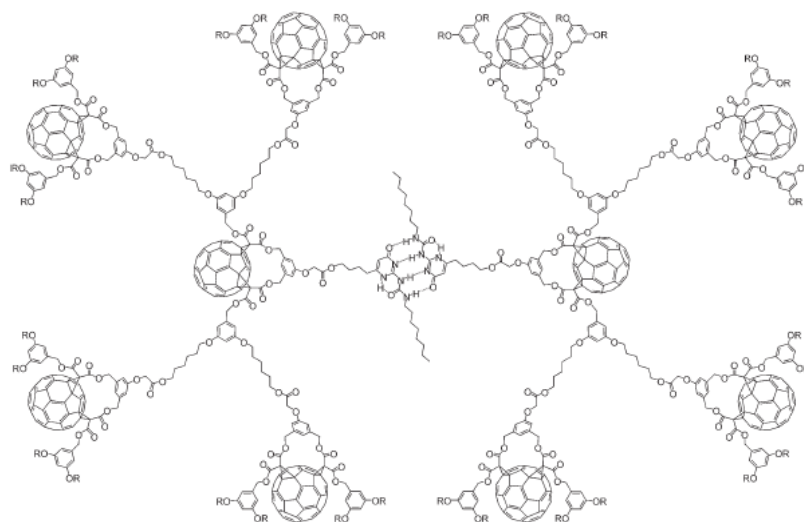


Figura 5: Dímero autoasociado del dendrímero globular con 5 unidades de fulereno ($R = C_{60}H_{30}$).

UNIVERSITAT ROVIRA I VIRGILI
SELF-ASSEMBLY BASED ON THE 2-UREIDO-4(1H)-PYRIMIDINONE MOTIF: FROM CYCLIC ARRAYS TO MOLECULAR CAPSULES
FOR FULLERENE SEPARATIONS
Elisa Huerta Martínez
DL:T.289-2012